UNIVERSITA' DEGLI STUDI DI MILANO-BICOCCA

Facoltà di Scienze Matematiche, Fisiche e Naturali

Scuola di Dottorato in Biologia, ciclo XXIV

THE LPT MULTIPROTEIN MACHINERY FOR LPS TRANSPORT IN GRAM-NEGATIVE BACTERIA: MOLECULAR DETAILS OF THE LPT INTERACTOME

(BIO/19)

Tesi di dottorato di:

Riccardo VILLA

Matr. N° 039688

Docente guida: Prof.ssa Alessandra POLISSI

Coordinatore del dottorato: Prof. Enzo WANKE

Anno Accademico 2011/2012

The Lpt Multiprotein Machinery for LPS Transport in Gram-negative Bacteria: Molecular Details of the Lpt Interactome

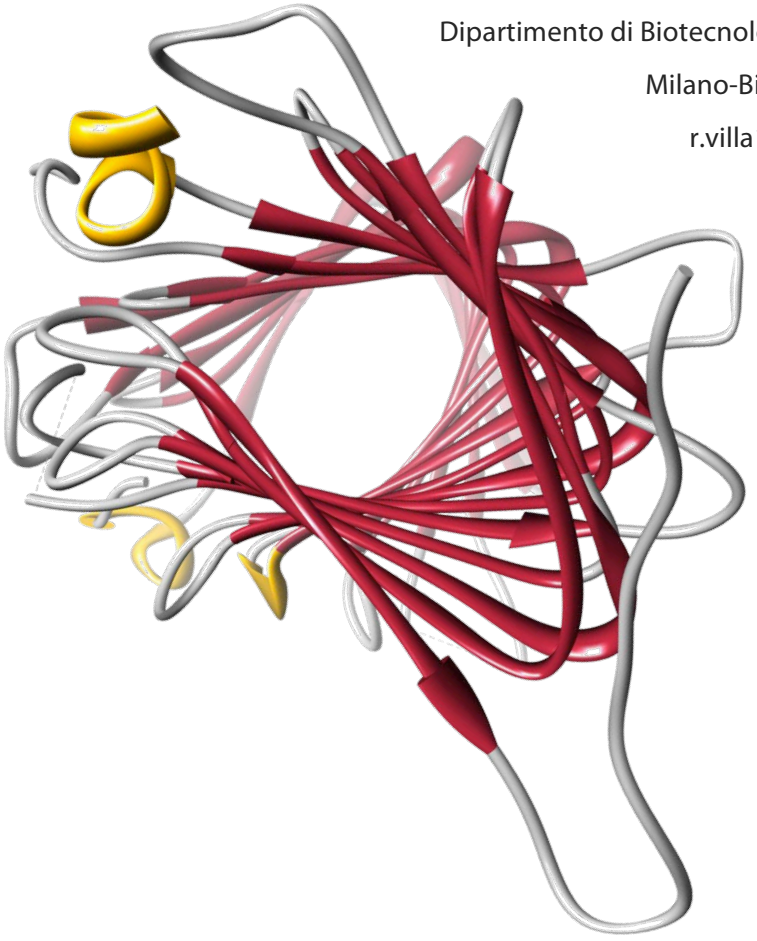

Dipartimento di Biotecnologie e Bioscienze, Università degli Studi di Milano-Bicocca, 20126 Milan, Italy.

r.villa11@campus.unimib.it

UNIVERSITA' DEGLI STUDI DI MILANO-BICOCCA

Dipartimento di Biotecnologie e Bioscienze

Facoltà di Scienze Matematiche, Fisiche e Naturali

Scuola di Dottorato in Biologia, ciclo XXIV

In collaboration with

HARVARD UNIVERSITY, CAMBRIDGE (MA)

Department of Chemistry and Chemical Biology

TABLE OF CONTENTS

- **PAPER 1** — Sperandeo, P., **Villa, R.**, Martorana, A. M., Samalikova, M., Grandori, R., Deho, G., & Polissi, A. (2011). "New Insights into the Lpt Machinery for Lipopolysaccharide Transport to the Cell Surface: LptA-LptC Interaction and LptA Stability as Sensors of a Properly Assembled Transenvelope Complex. *Journal of bacteriology*, *193*(5), 1042–1053. doi:10.1128/JB.01037-10.
- **PAPER 2** — **Villa, R.,** Martorana,. A. M., Gourlay, L. J. Sperandeo, M. Bolognesi, P., Kahne, D., & Polissi, A. (2012). Characterization of Functional Domains in LptC, a Conserved Membrane Protein Implicated in LPS Export Pathway in *Escherichia coli*. Paper draft.

ABSTRACT

The Lpt Multiprotein Machinery for LPS Transport in Gram-negative Bacteria: Molecular Details of The Lpt Interactome

Riccardo Villa

Dipartimento di Biotecnologie e Bioscienze, Università degli Studi di Milano-Bicocca, 20126 Milano, Italy.

r.villa11@campus.unimib.it

Key Words

LPS, membrane proteins, Lpt machinery, bacterial envelope, Gram-negative.

Abstract

The hallmark of Gram-negative bacteria is their cell envelope, which is composed of two membranes, the inner or cytoplasmic membrane (IM), and the outer membrane (OM), separated by a compartment (the periplasm) that contains a thin peptidoglycan layer.

Lipopolysaccharide (LPS) is the major component of the OM, and it acts as a selective barrier together with the OM proteins (OMPs), preventing the entry of many toxic molecules into the cell. Despite the structure and composition of OM have been elucidated in pivotal studies in the 50s and in the 70s, the factors required for the assembly of this organelle have only recently been identified.

LPS, once it is synthesized in the cytoplasm, has to be translocated through out the

cell envelope. Seven essential proteins cooperate in a unique fashion to extract the macromolecule from the IM and deliver it in the outer leaflet of the OM. LptBCFG form the IM complex that empowers the translocation process by ATP hydrolysis (Narita and Tokuda, 2009), LptDE constitute a complex embedded in the OM that finally flips LPS across the OM and deliver it to its final destination (Chng *et al*., 2010a; Freinkman *et al*., 2011), and LptA is a periplasmic protein that contacts both the IM and OM complexes (Sperandeo *et al*. 2007; Tran *et al.,* 2008).

Notably, LptC is single-pass IM protein with a large periplasm-protruding region.

LptC single mutants were obtained in this work by random-mutagenesis, and used *in vivo* and *in vitro* experiments to characterize two regions of the protein that distinctly interact with LptA and the IM protein complex LptBFG, respectively.

Chimera versions of LptC, either missing the transmembrane (TM) sequence, or with the IM anchor substituted by a heterologous sequence, were additionally constructed to this purpose.

Moreover, Both LptA and LptC were previously demonstrated to bind LPS *in vitro*, here it is presented a rapid bioinformatic tool which has been implemented to discover the molecular determinants of LptA for the interaction with Lipid A, the main component of LPS.

Genetic evidences previously obtained in our laboratory together with the presented data strongly support the LPS transport machinery model defined as the trans-envelope complex by Chng and coworkers (Chng *et al*., 2010a): indeed LptA interacts both with the IM and the OM protein complexes (LptBCFG and LptDE respectively), bridging them together. In support of this model, a phylogeny and structural motif conservation analysis of the Lpt components suggests that the unique structural domain retained in these proteins—despite the low sequence similarity—is the key to make possible the interaction between all the Lpt components.

ABBREVIATIONS

ABBREVIATIONS

ABC (Transporter): ATP Binding Casette Transporter

amp: Ampicilline

ara: Arabinose

cam: Chloramphenicol

EDTA: Ethylene diamino tetraacetic acid

IM: Inner Membrane

IMPs: Inner Membrane Proteins

IPTG: Isopropil-β-D-*manno*-octulosonic acid

kan: Kanamicine

Kdo: 3-deoxy-D-manno-ottulosonato

LPS: Lipopolysaccharide

NAD(P)H: Reduced nicotinamide adenine dinucleotide (phospate)

GlNAC: N-acetylglucosamine

MurNAc: N-acetylmuramic acid

OM: Outer Membrane

OMPs: Outer Membrane Proteins

ORF: Open Reading Frame

PPIase: peptidil-prolil-cis-trans-isomerases

TM: TransMembrane Domain

BACKGROUND

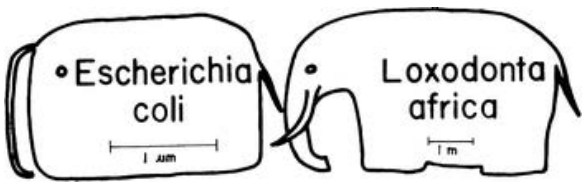

Anything that is true of E. coli must be true of elephant

(J. Monod)

Bacteria are our progenitors, our inventors, and our keepers. A few of them occasionally become our adversaries, or killers. They might even make us fat. The bacterial cell is defined as prokaryote, lacking well-defined nucleus and membrane-bound organelles, and with chromosomes composed of a single closed DNA circle. They come in many shapes and sizes, from minute spheres, cylinders and spiral threads, to flagellated rods, and filamentous chains. They are found everywhere on Earth and live in some of the most unusual and seemingly inhospitable places.

We are only the recent intruders into their well-established and self-developed world. They appeared on Earth about 3,5 billion years ago, just 1 brief thousand millennia after the planet formed. We—*Homo sapiens*—appeared only a little over 100,000 years ago.

But bacteria did much more than arrive first. They fundamentally changed the chemistry of the planet in many ways, rendering it hospitable enough for us to evolve and exist. They produced the atmospheric oxygen we breathe as well as the chemical forms of nitrogen essential for the plants and animals we eat. And bacteria continue to maintain our environment in life-sustaining balance in spite of our massive assaults on it.

They solved all the fundamental problems of life first—genetic, metabolic, and structural: we stand at the end of a long evolutionary trail they began to blaze.

But bacteria does not share all their talents: only microbes, fore example, can fix nitrogen, return gaseous nitrogen to replenish the atmosphere, and degrade cellulose, the major structural component of plant cells and the most abundant organic nutrient on Earth.

Some of them harm us: that is the problem. They damage our crops, harm our domesticated animals, spoil our food, cause disease, and sometimes kill us.

Vibrio cholerae, which causes epidemics of deadly cholera, and *Alivibrio fischeri*, which does nothing more threatening than lighting up parts of certain marine animals, appear to be identical—both are rod-shaped cells with a flagellum at one end. Notwithstanding pathogenic *cholerae* strains are able to produce an

enterotoxin: an oligomeric protein entering the intestinal epithelial cells via receptor-mediated endocytosis that allows the constitutive secretion of H_2O, Na^+, K^+, Cl^-, and HCO_3^- into the lumen of the small intestine resulting in rapid dehydration.

During the nineteenth century, the French scientist Louis Pasteur and the German physician Robert Koch demonstrated the role of bacteria as pathogens (causing disease). The twentieth century saw numerous advances in bacteriology, indicating their diversity, ancient lineage, and general importance. The discovery that some bacteria produced compounds lethal to other bacteria led to the development of antibiotics, which revolutionized the field of medicine.

Selman Waksman is the microbiologist who purified a compound from the soil bacterium *Streptomyces griseus* able to kill a wide spectrum of bacteria, including *Mycobacterium tuberculosis*. In his speech at the Nobel Banquet in December 1952, he said "The Great White Plague (i.e. *M. tuberculosis*), which only 10 years ago was thought to be immune to drug therapy, is gradually being eliminated [...] the antibiotic streptomycin pointed a way". Although the discovery of streptomycin proved that a bacterium was the cause of the disease and led to almost miraculous responses in patients infected with tuberculosis (TB), strains of *M. tuberculosis* that were resistant to the drug were discovered within a few months of intense use. To date TB claims a life every 10 seconds and global mortality rates are increasing despite the use of chemotherapy.

Infectious diseases are actually cause of death in 19.8% of the cases, second only to the non-transmissible, preventable, cardiovascular diseases (WHO, 2002).

As a matter of fact, defeating the antibiotic resistance is unavoidably struggling against the other side of the coin of evolution: the capacity to acquire resistance against toxic compounds is nothing more than the marked ability to mutate genome in order to survive against the new changes —adaptation. Pasteur notably said "Gentlemen, it is the microbes who will have the last word."

Merely, the struggle against antibiotic resistance is a war we will never win, but we still do have a chance to hold it back.

1.1The Battle Against Antibiotic Resistance

Despite the advent of the antibiotic era, followed by the promise of the genomic revolution to deliver new drug leads, the control of infectious diseases with antibiotics is still perilously fragile. Indeed, infectious diseases retain their preeminent position as major causes of morbidity and mortality worldwide (Infectious Diseases Society of America, www.idsociety.org/badbugsnodrugs.html, 2004). Drug resistance has emerged in an escalating number of bacterial genera within hospitals and in the community at large, making some infections difficult if not impossible to treat.

Of greatest concern is the departure of many large pharmaceutical companies from antibacterial drug discovery and their decreasing investment in this area of research (Spellberg *et al*., 2004). The length of time (~10 to 15 years) and huge costs (U.S. $800 million on average) associated with the taking of a new drug from the discovery phase to market (DiMasi *et al.,* 2006, Payne *et al.* 2003), combined with the perceived failure of whole-genome sequence-based approaches to spur a second golden age of novel antibacterial drug classes, has led many companies to prioritize other areas of research (Fernandes *et al.* 2006). For many reasons, investment in the discovery of antibacterials is not as attractive to companies as research into other novel therapeutic drugs. First, the success rate for the discovery of drugs in other therapeutic areas is four to five times higher than that for antibacterial discovery, according to the GlaxoSmithKline screening metrics (14 high-throughput screening runs are required to obtain one lead compound) (Payne *et al*., 2003). It is more cost-efficient to develop drugs that will be used by patients for life—such as insulin for diabetes—as compared with antibacterials, which are required only transiently (Infectious Diseases Society of America, ibidem).

Similarly, although the discovery of narrow-spectrum rather than broad-spectrum antibacterials should be encouraged to avoid the rapid emergence of resistant organisms, broad-spectrum drugs are currently the only ones that are likely to provide sufficient returns on investment in the current economic and regulatory environment.

Now, more than ever, there is an urge to create robust research networks of industry, academia, and health-related governmental institutions that can address the issues raised by the current level of antibacterial resistance and generate programs that prevent the emergence of future resistance (Bragonzi, 2010).

1.2 A Superbug is Born: Drug Resistance up-to-date

Antibiotic resistance is the acquired ability of a pathogen to withstand an antibiotic that kills off its sensitive counterparts. It originally arises from random mutations in existing genes or from intact genes that already serve a similar purpose. Exposure to antibiotics and other antimicrobial products, whether in the human body, in animals, or the environment, applies selective pressure that encourages resistance to emerge favoring both "naturally resistant" strains and strains which have "acquired resistance." Horizontal gene transfer, where genetic information is passed between different bacteria, allows resistance determinants to spread within harmless environmental or commensal microorganisms and pathogens, thus creating a reservoir of resistance. Resistance is also spread by the replication of bacteria that carry resistance genes, a process that produces genetically identical (or clonal) progeny (Bragonzi, 2010) (Fig. 1.1).

Unprecedented human air travel and migration allow bacterial strains to be transported rapidly between continents. Much of this dissemination is undetected, with resistant clones carried in the normal human flora and only becoming evident when they are the source of endogenous infections.

β-Lactams are a broad class of antibiotics, consisting of all agents that contain a β-lactam nucleus. These include penicillin derivatives, cephalosporins, monobactams, and carbapenems. β-Lactam antibiotics work by inhibiting cell wall synthesis by the bacterial organism and are the most widely used group of antibiotics.

On the other hand, β-lactamases are enzymes produced by some bacteria and are responsible for their resistance to β-Lactam antibiotics. The CTX-M-15 extended-spectrum β-lactamase (ESBL) encoded by the gene $bla_{\text{CTX-M-15}}$ was first reported in India in the mid-1990s (Hawkey, 2008). The gene jumped from the chromosome of its natural hosts, *Kluyvera* spp, to plasmids that have subsequently spread widely, establishing CTX-M-15 as the globally-dominant ESBL and the primary cause of acquired resistance to third-generation cephalosporins in Enterobacteriaceae (Canton *et al*., 2006; Livermore *et al*., 2007).

Recent surveys have identified ESBLs in 70–90% of Enterobacteriaceae in India (Livermore *et al*., 2007). Rates of cephalosporin resistance are lower in other countries but the growing prevalence of ESBL producers is sufficient to drive a greater reliance on carbapenems. Consequently, there is selection pressure for carbapenem

resistance in Enterobacteriaceae, and its emergence is a worldwide public health concern since there are few antibiotics in reserve beyond carbapenems (Livermore *et al*., 2009). Already *Klebsiella pneumoniae* clones with KPC carbapenemase are a major problem in the USA, Greece, and Israel, and plasmids encoding the VIM metallo-carbapenemase have disseminated among *K. pneumoniae* in Greece (Nordmann *et al*., 2009).

A new type of carbapenem resistance gene was reported in December 2009 (Yong *et al.,* 2010; Kumarasamy *et al.,* 2010), coding for the so-called New Delhi metallo-β-lactamase 1 (NDM-1) enzyme as several Indian hospitals were colonized by *K. pneumoniae* and *Escherichia coli* with bla_{NDM-1} on plasmids of varying size, which readily transferred between bacterial strains *in vitro*.

Escherichia coli is a Gram-negative, facultative anaerobic, intestinal bacterium belonging to the Enterobacteriaceae, which are taxonomically placed within the gamma subdivision of the Proteobacteria phylum (Fig. 1.5).

E. coli K-12 strain is one of the most widely studied organisms in modern research: its biochemical behavior and structure are well known, having been studied for much of this century. This plethora of information has made *E. coli* indispensable as the bacterial model system for biochemical, behavioral and structural studies.

It is also the most encountered bacterium in clinical laboratories, being the primary cause of human urinary tract infections. Pathogenic *E. coli* strains are responsible for pneumonia, meningitis and traveler's diarrhea. As part of the normal flora of the intestinal tract, *E. coli* is beneficial—it constitutes approximately 0.1% of the total bacterial amount. It is crucial in the digestion of food, and is our principle source of vitamin K and B-complex vitamins.

The most harmful type of *E. coli* is the strain called O157:H7. Researchers surmise that it arose when a harmless *E. coli* clone was infected by a Shiga-like toxin expressing virus. This toxin is able to destroy cells in the intestinal tract and, if it enters the bloodstream, can cause kidney and liver failures. Damage to organs can be permanent or even lethal in children and elderly people.

Very recently, in May 2011 an outbreak of haemolytic uraemic syndrome and bloody diarrhoea was caused by a virulent *E. coli* strain O104:H4 in Germany (Fig. 1.2). Virulence profiles and relevant phenotypes of outbreak isolate LB226692 were analysed by Bielaszewska and co-workers (Bielaszewsk *et al*., 2011).

The researchers showed that all the isolates belong to a clone (HUSEC041) previously isolated in Germany from a patient with haemolytic uraemic syndrome in 2001.

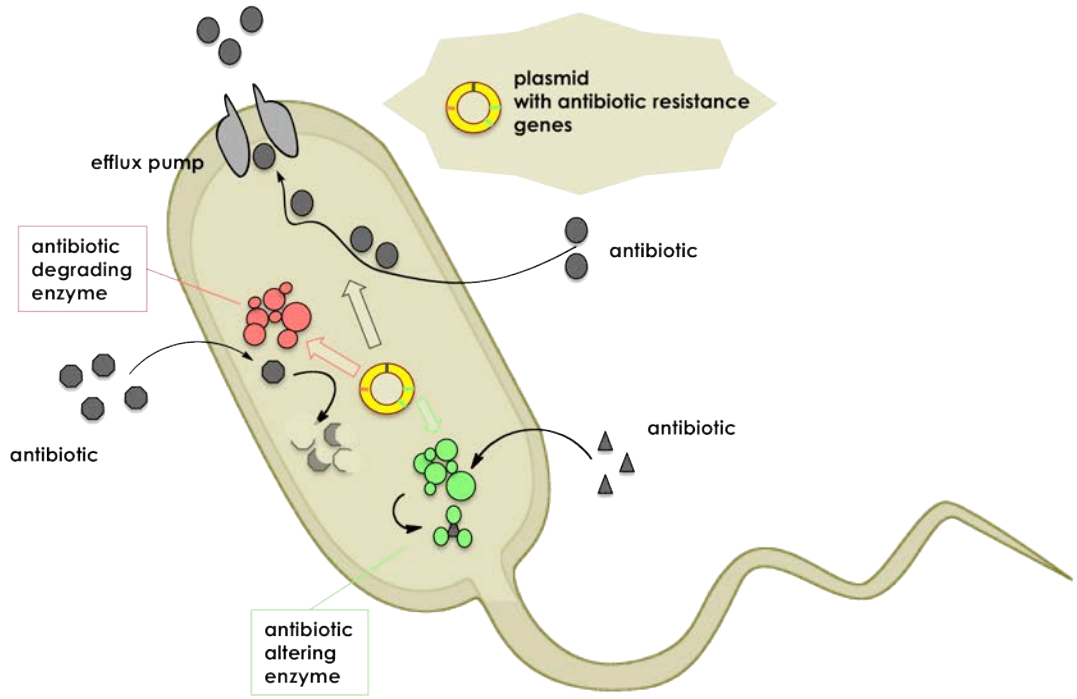

Figure 1.1 | Antibiotic Reistance is arising. Main mechanisms of resistance are shown. Plasmid can confer resistance to antibiotics thanks to the expression of degrading/altering enzymes or cellular pumps that extrude toxic agents.

This clone has a virulence profile that combines those of two different enteropathogenic strains: enterohaemorrhagic and enteroaggregative *E. coli*. They produce the Shiga toxin typical of the former, and have the so-called stacked-brick aggregative adherence typical of the latter. The outbreak isolates (but not the 2001 strain) also displayed an extended spectrum β-lactamase (ESBL) antibiotic resistance profile.

About 1000 symptomatic Shiga-toxin-producing *E. coli* infections and 60 cases of haemolytic uraemic syndrome are notified in Germany every year. But by June 20 2011, the numbers notified were 2684 and 810 respectively (See Fig. 1.2 for

details).

This outbreak demonstrates that blended virulence profiles in enteric pathogens introduced into susceptible populations, can have extreme consequences for infected people, by the way undergoing rapid genetic mutations is nothing new in bacterial world.

Modern genetics techniques have been successful in obtaining the sequence of several *E. coli* genomes: Blattner and colleagues published the genome sequence of strain K–12 in 1997. The genome was discovered to have approximately 4300 protein coding regions making up about 88% of the bacterial chromosome. In 2001, Perna and co-workers obtained the O157:H7 pathogenic strain genome sequence. These strains share a common ancestor, but in contrast to K-12, much of the genome of O157:H7 codes for unique proteins—over 1,300, some of which may be involved in disease causing traits. Many of these genes have been acquired from other microorganisms by lateral transfer as mentioned above.

This should be strongly taken into account when new antibiotics are designed: as strategies to combat problems caused by one strain of *E. coli* might not be universally successful. Bacteria carrying such genes are often referred to in the news media as "superbugs", since infections with these bacteria are very hard to treat successfully as decleared by the United Kingdom Health Protection Agency (Health Protection Report, HPA, July 2009).

A strategy to be developed is targeting generally conserved mechanisms essential to the cell to survive. The complex architecture that characterizes the Gram-negative cell envelope would be a target congenial to this purpose. Knowledge of the genetic organization and protein pathways that rule out the assembly of the bacterial envelope will enable more selective strategies to be developed to combat *E. coli* infections.

A

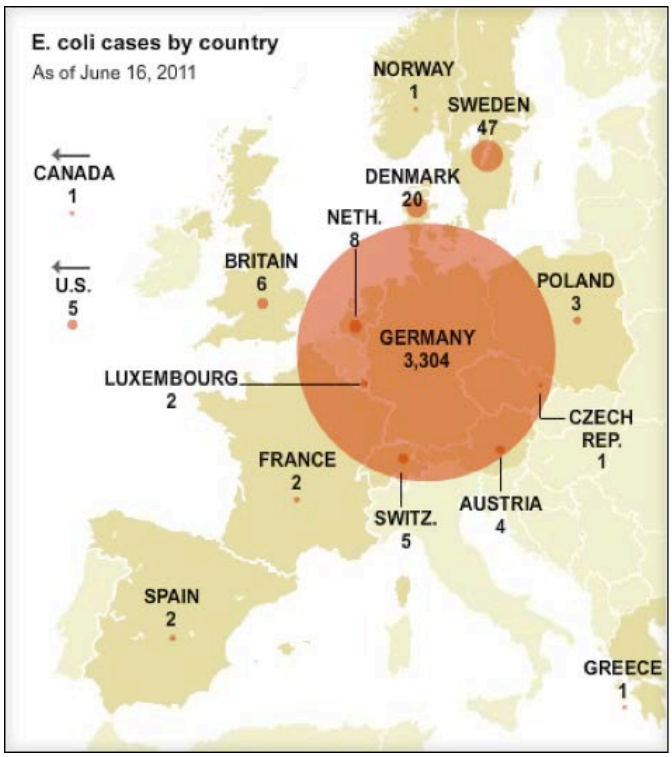

B

***E. coli* infections and deaths**

As of June 16, 2011

	CASES	HUS *	DEATHS
Total	3,412	825	39
24% HUS	3,412 total cases		

C

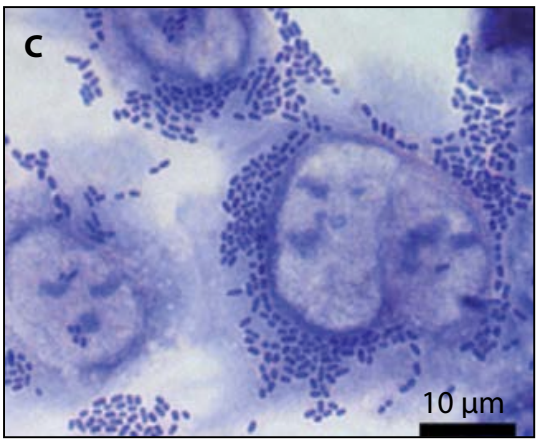

Figure 1.2 | June 2011: ***E. coli* outbreak in Europe. A** food poisoning outbreak in Germany and several other European countries has sickened more than 3400 people. It was caused by a O104:H4 *E. coli* strain that poses a pandemic potential. (Image copyright of AP Associate Press, from CBSnews.com) **B** Statistic of O104:H4 *E. coli* outbreak in Europe: more then 20% of infected people developed HUS: (*) Hemolytic uremic syndrome (HUS) is a dangerous complication present in nearly a quarter of the cases that consists in a variable combination of renal impairment, thrombocytopaenia, haemolytic anaemia, and myocardial damage. **C** Aggregative, so called, stacked-brick adherence to cultured intestinal epithelial cells by *E. coli* O104:H4 isolate LB226692 (Bielaszewsk *et al.*, 2011).

1.3 Targeting the Enemy Lines: The LPS Biogenesis

Scientists are facing many challenges in the quest for novel antibacterials. A major limitation in antibiotic development has been the difficulty associated with the identification of new structures that display the same low cytotoxicity for the host characteristic of conventional antibiotics and at the same time have a broad spectrum. No new classes of antibiotics were produced in the 37 years that elapsed

between the introduction of nalidixic acid (a bacteriostatic quinolone marketed in 1962) and that of linezolid (Zyvox; Pfizer) (an agent used to treat infections caused by multidrug-resistant Gram-positive bacteria marketed in 2000), which was followed by daptomycin (Cubicin; Cubist) in 2003 (Leeb *et al.,* 2004) and, more recently, by retapamulin (Altabax/Altargo; GlaxoSmithKline) (Coates *et al.,* 2002). All of the antibacterial agents that entered the market during this period were modifications of existing molecules (Boucher *et al.,* 2009).

Hence, physicians urgently need in their arsenals elusive antibiotics with novel structures and/or modes of action.

Lipopolysaccharide (LPS, or endotoxin) is an essential Gram-negative peculiar macromolecule that forms a strong and protective sheath around the bacterial cell, making up 1% of its volume, with 6 X 10^5 copies per cell (*E. coli* Statistics by CyberCell Database CCDB, University of Alberta). LPS by itself can be extraordinary potent, stimulating host responses to as few as 100 invading bacteria, corresponding to fmol of endotoxin. This sensitivity facilitates prompt mobilization of host defenses before invading bacteria have time to multiply and potentially overwhelm mobilized host defenses. Variations in endotoxin structure may contribute to bacterial virulence either by dampening early innate immune defense responses to infection, or by exacerbating systemic inflammatory response that ensue when local infection is not contained as in Gram-negative bacterial sepsis (reviewed by Gioannini *et al*., 2007).

At present days scientific search engines (such as PubMed and Google Scholar) detect more than ten new publications weekly deciphering, step by step, the labyrinthine pathways triggered by LPS in the host. Interests for the potential therapeutic effects of this molecules and for the complex molecular dynamics LPS is able to trigger in the host, are growing exponentially (see Fig. 1.3 for details).

On the contrary much less is known about the way this potent immuno-modulator is translocated through the bacterial envelope. As LPS constitutes a fundamental component of the bacterial cell, the proteinaceous LPS transport machinery illustrated from here on in, can be pointed out as a brand new target to counteract the multidrug resistance phenomenon.

Moreover, at the present time peptidomimetic strategies developed on studies how human anti-LPS factors are able to sequester the endotoxin seems promising, although the benefits of therapies targeting LPS remain to be elucidated (Nahra *et al.,* 2008). Investigation on LPS transport proteins may reveal common

molecular determinants implicated in LPS interaction both in bacterial cells and in LPS-binding proteins in the host immune cells.

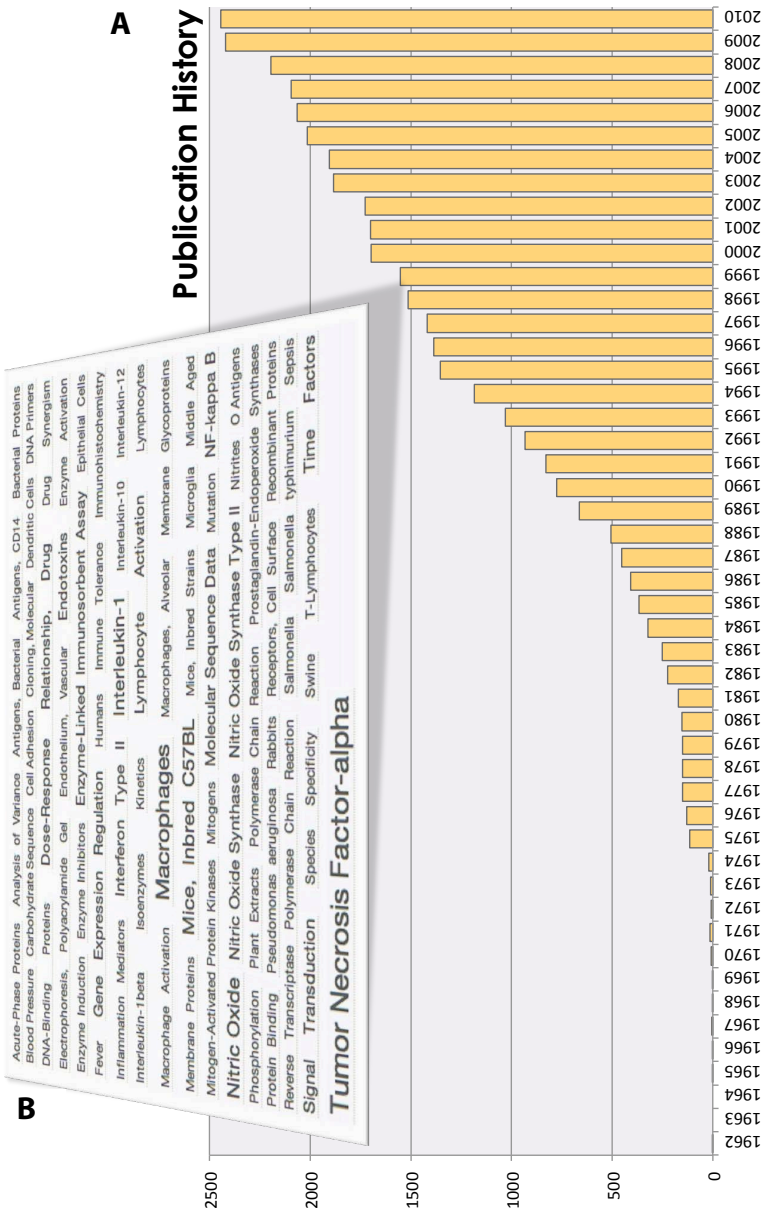

Figure 1.3 | LPS publication history. A LPS publication history shows a rapid increasing trend in publication from 1962 to 2010: LPS tag appears in 39,636 articles on line. **B** LigerCat (http://ligercat.ubio.org/articles) aggregates articles searched in PubMed, combining the associated LPS-related tag descriptors into a cloud, weighted by frequency, eventually showing a trend in this field.

1.4 The *Escherichia coli* Cell Envelope

All living cells are surrounded by the cytoplasmic membrane, a unit membrane whose overall architecture (a fluid lipid bilayer with integral and peripheral membrane proteins) is conserved among the three domains of life. Nevertheless, the chemical composition of the lipid bilayer poses a divide between *Archaea*, whose membrane lipids consist of isoprenoid hydrocarbon chains linked to glycerol-1-phosphate through an ether linkage, and both *Bacteria* and *Eukarya*, which contain glycerol-3-phosphate diesters of linear fatty acids (De Rosa *et al*., 1991; Wachtershauser, 2003).

Outside of the universally conserved cytoplasmic membrane, most prokaryotes have developed complex and varied peripheral architectures, collectively named the cell wall, that provide additional strength and protection against environmental insults and contribute to the cell shape determination (Beveridge, 1999; Ellen *et al*., 2010; Silhavy *et al*., 2010). The great majority of *Bacteria* is surrounded by an additional lipid bilayer, the outer membrane (OM), and is thus described as diderm bacteria; the OM is not present in monoderm bacteria, which possess the cytoplasmic membrane as the unique lipid membrane (Gupta, 1998; Sutcliffe, 2011; Desvaux *et al.,* 2009).

The prototypical OM has been characterized in great detail over the last half century in *Proteobacteria*, particularly in *Enterobacteriaceae*, and it is characterized by a peculiar glycolipid, the lipopolysaccharide (LPS), that forms the outer leaflet of the lipid bilayer, whereas the inner leaflet is composed of phospholipids. OM proteins (OMPs) and lipoproteins are also embedded and anchored, respectively, in the OM.

The architecture of *Proteobacteria* cell envelope that emerged from these studies has long since been considered the standard for all Gram-negative bacteria. It consists of the inner (cytoplasmatic) membrane (IM) and the LPS-containing OM that delimit a periplasmic space with a thin layer of murein.

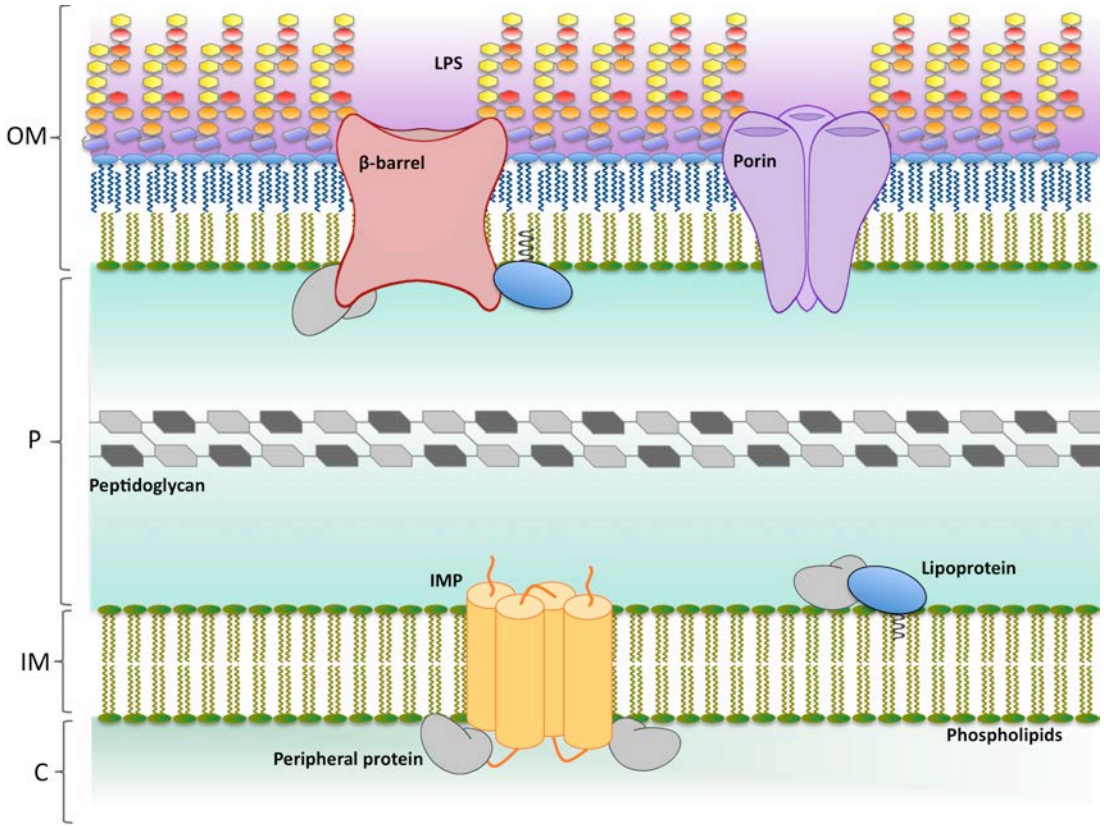

Figure 1.4 | Structure of *Escherichia coli* cell envelope. The envelope is composed of an inner membrane (IM), the periplasm (P) and an outer membrane (OM). The IM is a symmetric lipid bilayer composed of phospholipids, integral proteins (IMP) that span the membrane by α-helical transmembrane domains, and peripheral proteins associated to the inner leaflet of the IM. The periplasm (P) is hydrophilic gel-like compartment located between IM and OM and containing a layer of peptidoglycan. The OM is an asymmetric bilayer composed of phospholipid in the inner leaflet and Lipopolysaccharide (LPS) towards the outside. The OM also contains integral proteins folded in β-barrel conformation and trimeric proteins forming channels known as porins. Both IM and OM contain lipoproteins anchored to their periplasmic faces. Transenvelope secretory machines (see Fig. 1.11 as an example) are not shown (Sperandeo *et al*., 2012 in press).

Conversely, both low and high G+C% Gram-positive bacteria (*Firmicutes* and *Actinobacteria*, respectively) have been traditionally considered as monoderms. However, it is now recognized that different non-LPS OM architectures can be found in both Gram-negative and Gram-positive bacteria (Sutcliffe, 2010). For example, the Gram-negative *Thermotogae* appear to be surrounded by an OM not containing LPS (Plotz *et al*., 2000; Sutcliffe, 2010), whereas a mycolic acid-based OM is present in the *Corynebacterineae*, a suborder of Gram-positive bacteria that comprises mycobacteria and other genera such as *Corynebacterium*, and *Nocardia* (Minnikin, 1991; Zuber *et al*., 2008; Niederweis *et al.,* 2010). This latter example, in particular, suggests that functionally analogous OM architectures may have independently evolved in bacteria, thus highlighting the functional relevance of an additional outer lipid bilayer for bacterial adaptation. On the other hand, the Gram-negative *Chloroflexi* appear to be monoderms (Sutcliffe, 2011); thus, the Gram-positive *vs*. Gram-negative classification of *Bacteria* does not coincide with the monoderm *vs*. diderm grouping and neither criterion should be taken as a discriminating phylogenetic character (Fig. 1.5).

The presence of a highly structured OM poses several problems as of its biogenesis. Both lipid and protein components not only must be synthesized in the cytoplasm and/or at the IM level and translocated across the IM lipid bilayer, but also must traverse the aqueous periplasmic space and be assembled at the amphypathic final destination. The cell compartments external to the IM are devoid of ATP and other high energy carriers. As a consequence the energy to build up periplasmic and OM structures is either provided by exergonic reactions (thus involving substrates that have been energized before their translocation across the IM) or transduced by devices (usually protein machines) connected to the IM and capable to exploit the energy released by ATP hydrolysis in the cytoplasm or the proton motive force.

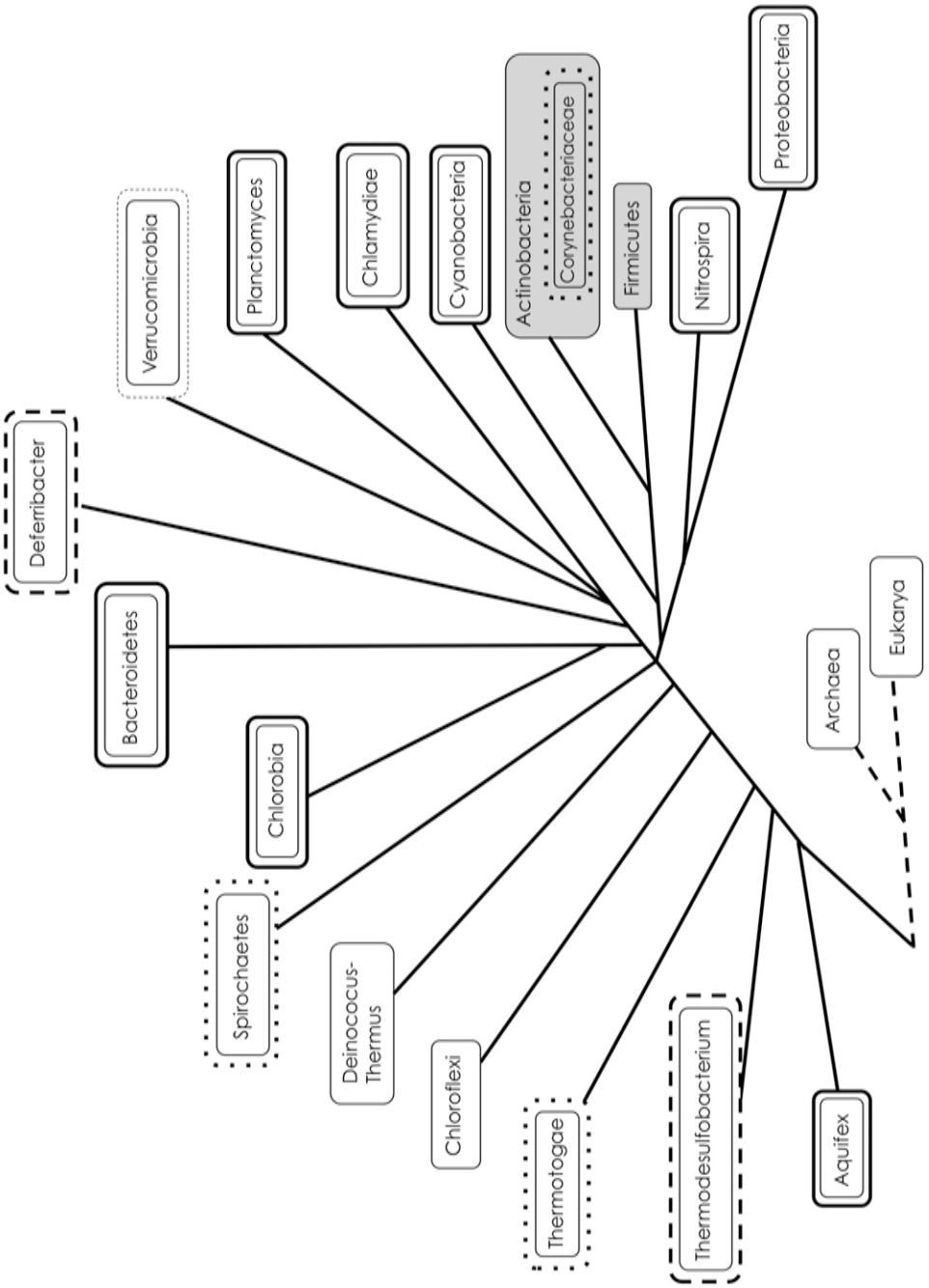

Figure 1.5 | Distribution of monoderm and diderm cells within the universal phylogenetic tree. Major lineages of Bacteria are shown. A gray box indicates Gram-positive bacteria. Monoderm cells are surrounded by a single line, whereas an additional outer line identifies the OM of diderm bacteria as follows: thick continuous line, OM with LPS; thick dashed line, LPS predicted but not experimentally demonstrated; thick dotted line, OM with different lipid composition; thin dashed line, data not available (Data from Sutcliffe, 2010; Figure from Sperandeo *et al*., 2012 in press).

1.5 An Overview of OM Structure, Functions and Evolution

The topography of the bacterial cell wall was made possible by the development of electron microscopy techniques. Early studies in the 1960's convincingly showed that the basic structure surrounding Gram-negative bacteria is composed by an inner and an outer membrane, both seemingly "unit membranes", separated by intermediated layers, including the peptidoglycan layer (Bladen and Mergenhagen, 1964). In Gram-positive bacteria, on the other hand, the OM was missing and a thicker peptidoglycan layer was present (reviewed by Glauert and Thornley, 1969). The striking correlation between cell wall structure and Gram staining was rationalized much later when it was shown that upon ethanol treatment the crystal violet-potassium iodide precipitate is retained within the cell by the thick peptidoglycan layer of Gram-positive bacteria, whereas it is washed away through the thinner murein sacculus of Gram-negatives that are thus decolorized (Beveridge and Davies, 1983).

Assessing a detailed chemical composition of the OM was facilitated by the different buoyant densities of the two membranes (approximately 1.22 and 1.15 for the OM and IM, respectively), which could therefore be fractionated by equilibrium centrifugation in sucrose density gradients and analyzed separately.

Our present understanding of the OM structure and composition is diagrammed in Figure 1.4, in the context of the Gram-negative cell envelope. This picture emerges from studies mainly performed on model Gram-negative bacteria, especially *Proteobacteria*, such as *Escherichia coli*, *Salmonella enterica* serovar Typhimurium and other *Enterobacteriaceae*, *Pseudomonas aeruginosa*, *Neisseria meningitidis* and others, whereas for other phyla information is less complete.

Several structural and functional aspects differentiate the OM from the plasma membrane. The most striking structural difference is the asymmetry of the OM bilayer. Whereas the periplasmic side is made by a layer of the same type of phospholipids that compose both leaflets of the IM, LPS paves the OM layer facing the environment outside the cell. This was first observed by immuno-electron microscopy (Muhlradt and Golecki, 1975) and then demonstrated by Kamio and Nikaido (1976) who showed that in intact cells of *S. enterica* serovar Thyphimurium phospholipids could not be chemically modified by an OM-impermeable

macromolecular reagent. The unique chemical structure and properties of LPS, as discussed below, are mainly responsible of the peculiar properties of the OM. This second lipid bilayer with an additional external hydrophilic region of long polysaccharide chains, endows Gram-negative bacteria with a strong additional diffusion barrier, which accounts for the generally higher resistance of Gram-negative bacteria, as compared to most Gram-positives, to many toxic chemicals such as antibiotics and detergents (e.g. bile salts) and to survive hostile environments such as the gastrointestinal tracts of mammals, encountered during host colonization or infection (Nikaido, 2003; Gunn, 2000).

Cell-environment exchanges across the OM are thus ensured by OM proteins, that are implicated in several functions such as nutrients uptake, transport and secretion of various molecules (proteins, polysaccharides, drugs), assembly of proteins or proteinaceous structures at the OM, and other types of interactions with the external environment and the underlaying cell compartments. Typical OM integral proteins (OMPs) are β-barrel proteins, whereas OM-associated proteins are generally lipoproteins that are anchored to the periplasmic side of the OM via a lipid tail attached to an N-terminal cystein residue (Sankaran and Wu, 1994). Bacterial lipoproteins are mostly OM associated, but IM lipoproteins are also known. The role of lipoproteins is little understood; the best known is Lpp (or Braun's protein), the most abundant protein in *E. coli* that anchors the peptidoglycan layer to the OM (Braun, 1975).

Many OMPs associate as trimeric pores or channels that allow passive diffusion across the OM of small hydrophilic molecules such as mono or oligosaccharides, aminoacids, ions and/or catabolism waste products, with various degrees of specificity, whereas other proteins are part of energy consuming active transport systems, especially for the transport of larger molecules (efflux pumps, TonB-dependent high affinity receptors, ABC transporters) that are connected to IM proteins to form transenvelope machines energized by ATP hydrolysis in the cytoplasm or by the IM proton gradient. Other OM proteins are devoted to secretion of proteins (with their final destination outside the OM or in the OM itself), either in concert with or independently of the main SecA-dependent secretory system as illustrated in Figure 1.12. For this energy costly secretion process, proteins may be first translocated in the periplasm in an energized form and then pass through the specific OMP transporter consuming the accumulated energy, or may be transported by transenvelope machines (Nikaido, 2003; Knowles *et al*., 2009; Karuppiah *et al*., 2011). The panoply of secretion systems that have evolved in bacteria meets the needs of a vast variety

protein structures and final destinations, including the intracellular milieu of eukaryotic cells (Holland, 2010).

OM creates the unique organelle of diderm bacteria: the periplasmic space, a viscous hydrophilic compartment lying between the IM and OM. Several processes that are crucial for cell viability occur in this compartment. Proteins residing in the periplasmic space fulfill important functions in the detection, processing and transport of nutrients into the cell, including periplasmic chaperones—which promote the biogenesis of periplasmic, outer membrane, and external appendages proteins such as pili and fimbriae—detoxifying enzymes (such as β–lactamases) preserve the cell from obnoxious chemicals (Oliver, 1996).

One of the major cell processes occurring in the periplasm is the synthesis of the peptydoglycan layer, the largest cell polymer that surrounds the bacterial cell forming the seamless murein sacculus (Gan *et al.,* 2008; Vollmer and Seligman, 2010). This cellular exoskeleton is the main structure responsible for the cell shape and the mechanical strength and elasticity of the bacterial envelope, which can withstand turgor pressure up to three atmospheres (Koch, 1998). Biosynthesis of the murein sacculus must be very carefully coordinated with that of IM and OM during cell growth and division. Understanding formation of the cell septum that separates two newborn bacterial cells at the biochemical, structural and topologycal levels remains one of the unresolved problems of the bacterial cell biology, although impressive advances have been obtained in this field in the last years (Margolin, 2009).

Electron microscopy observations of adhesion regions between OM and IM known as Bayer's bridges (Bayer, 1968) have been thought of for some time as potential sites for lipid trafficking and possibly protein transport between the two membranes. The idea of intermembrane adhesion zones was later considered an artifact and abandoned (Kellenberger, 1990). However, as mentioned above, protein machines that cross the periplasmic space and the murein layer are now well documented and, as we will see in the next paragraphs, appear to be implicated in LPS transport. Thus Bayer's bridges could be reevaluated as proteinaceous structure connecting the two envelope membranes.

It may be proposed that the LPS-containing OM is a primary feature of *Bacteria* and that a modified non-LPS OM may have evolved the some diderm phyla. Alternatively, an ancestral OM might not have contained LPS, which could thus be a subsequent specialization of the OM. In this scenario, monoderm bacteria such as Gram-positives could have lost OM as a secondary adaptation, compensating the

lack of OM with a more complex murein wall. Ironically, a subgroup of Gram-positives (*Corynebacteriaceae*) reinvented an outer lipid bilayer unrelated to LPS.

1.6 LPS Structure and Biosynthesis

LPS is a unique glycolipid present in Gram-negative bacteria. Immunological, genetics and biochemical studies have contributed to the determination of LPS chemical structure. The availability of several so called "rough (R) mutants" in *Salmonella* that showed a typical distinct colony morphology compared to the wild type "smooth (S)" strain, provided a powerful tool for initial LPS structural analysis. In fact compared to the wild type S strain, R mutants were sensitive to infection by the P22 phage: they showed different serological properties and did not contain rhamnose and mannose residues (Nikaido *et al*., 1964; Beckmann *et al*., 1964; Subbaiah and Stocker, 1964)—later demonstrated to be specific of the *O*-antigen portion (Luederitz *et al*., 1965). More recently biochemical and genetic approaches have fully elucidated the biosynthesis of this complex molecule. Also in the last few years a lot of progress has been made in determining the exact chemical structure not only of *Enterobacteria* LPS, but also of an increasing number of *Proteobacteria* (Muszynski *et al*., 2011; Mistretta *et al*., 2010; Holst *et al*., 2009; Carillo *et al.*, 2011; Fodorová *et al.,* 2011).

LPS is typically organized into three structural domains: lipid A, a core oligosaccharide and a highly variable *O*-antigen constituted of repeating oligosaccharide units (Fig. 1.6) (Raetz and Whitfield, 2002). Lipid A is a unique glycolipid that forms the outer hydrophobic leaflet of the OM (Raetz *et al.,* 2007). The core is covalently linked to lipid A and can be further divided into inner (lipid A proximal) and outer core.

The chemical structure of the outer core is variable, whereas the inner core region tends to be quite conserved within a genus or a family. In all species so far analyzed, 3-deoxy-D-*manno*-oct-2 ulosonic acid (Kdo) is the first residue linking the inner core to lipid A, and thus Kdo is a chemical hallmark of LPS and a marker of Gram-negative bacteria (Holst, 2007).

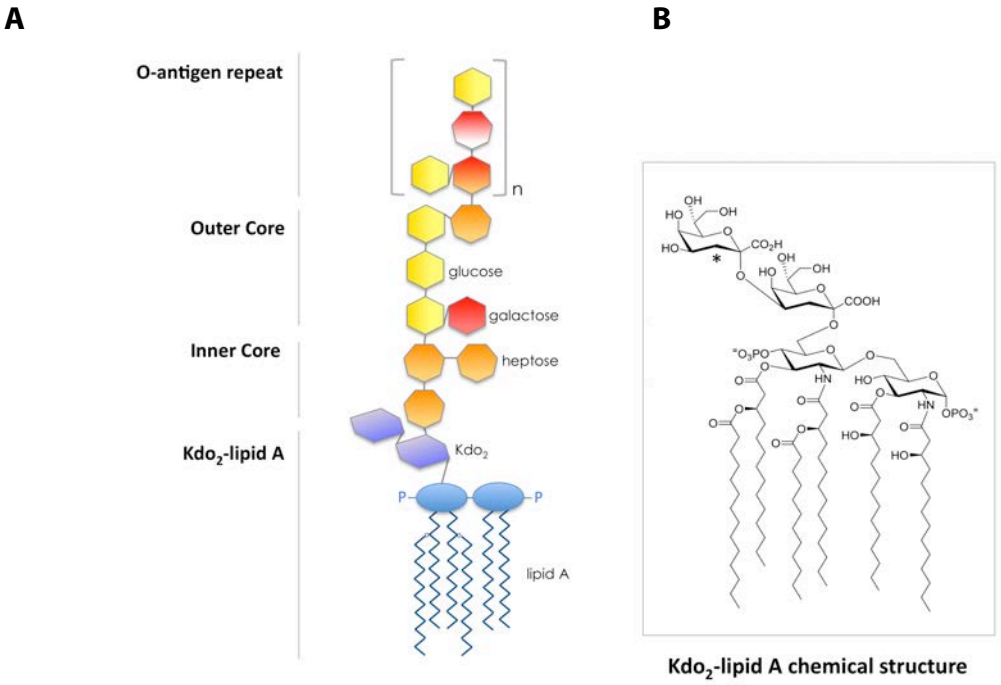

Figure 1.6 | Structure of LPS. A. General structure of LPS in Gram-negative bacteria. The Kdo_2 Lipid A moiety, the inner and outer core and the O-antigen repeat are shown. Glucosamine residues are indicated as ovals, Kdo residues as slant hexagons, heptose as heptagon, galactose and glucose as light and dark grey hexagons, respectively. A single repeating unit composing the O-antigen polisaccharide is shown. **B.** Chemical structure of Kdo_2-lipid A. The glucosamine disaccharide backbone and the Kdo disaccharide are shown. The asterisk indicates the position modified by Kdo dioxygenase to generate the Ko moiety (see text for details) (Sperandeo *et al.,* 2012 in press).

The *O*-antigen is the distal, surface exposed LPS moiety and responsible of the immunogenic properties of this macromolecule; it is the most variable portion, a feature used as a tool for strains classification based on the different serological properties (Raetz and Whitfield, 2002). In many pathogenic Gram-negatives the *O*-antigen is a virulence factor that enables the bacterium to escape killing by phagocytosis and serum complement (Raetz and Whitfield, 2002).

Although differing in sugar composition, the common structure of LPS may be seen as the core oligosaccharide and the lipid A; indeed these two structural domains are present in all LPS analyzed so far (Holst, 2007). LPS is essential in most gram-negative bacteria with the notable exception of *Neisseria meningitidis* (Steeghs *et al*., 1998); however, the LPS structural requirements for bacterial viability may vary across genera/species. In *E. coli* the minimal LPS structure required for growth has

been defined as Kdo_2-lipidA (Raetz and Whitfield, 2002), although the lethal phenotype of Kdo-deficient mutants may be overcome by several suppressor mutations (Meredith *et al*., 2006). In contrast, to be viable, *Pseudomonas aeruginosa* requires the full inner core and at least part of the outer core in addition to lipid A (Rahim *et al*., 2000; Walsh *et al*., 2000).

The structural complexity of LPS reflects the multiple functions displayed by this macromolecule. The outer hydrophilic layer of LPS leaflet in the OM represents a very effective barrier for the spontaneous diffusion of lipophilic compounds, whereas the core, together with the phospholipids of the internal leaflet, forms a hydrophobic barrier. LPS is also a potent activator of the innate immune response and lipid A (also known as endotoxin) represents the conserved molecular pattern recognized by innate immune receptors (Miller *et al.,* 2005).

Several LPS features contribute to the peculiar permeability properties exhibited by the OM:

i) in enterobacteria grown under usual laboratory conditions, the LPS fatty acids substituents are saturated and are thus thought to form a low fluidity gel-like layer (Nikaido, 2003);

ii) the core region is negatively charged due to phosphoryl substituents and sugar acids such as Kdo; in addition, a strong lateral interaction between LPS molecules occurs by the bridging action of Mg^{2+} and Ca^{2+} divalent cations that counteract the negative repulsive charges and stabilize the structure (Nikaido, 2003; Holst, 2007);

iii) finally, the strong association of LPS to OMPs such as FhuA, a ferric hydroxamate uptake receptor, offers an additional mode of interaction between neighbouring LPS molecules (Ferguson *et al.,* 2000).

LPS organization is disrupted by defects in assembly of OM components (Ruiz *et al*., 2006), in mutants producing LPS severely truncated in sugar chains ("deep rough" mutants) (Young and Silver, 1991) or by exposure to antimicrobial peptides and chelating agents such as EDTA, which displace the divalent cations that shield the repulsive charges between LPS molecules (Nikaido, 2003). In all these cases the consequence is that much of the LPS layer is shed and phospholipids from the inner leaflet migrate into the breached areas of the outer leaflet. These locally symmetric bilayer rafts are more permeable to hydrophobic molecules, which can thus gain access to the periplasm while the OM continues to retain the more polar periplasmic

contents (Nikaido, 2005). Therefore, appreciable levels of phospholipids in the outer leaflet of the OM are detrimental to the cell and thus, not surprisingly, cells have evolved systems to monitor the asymmetry of the OM and to respond either by removing phospholipids from the outer leaflet or by modifying LPS.

Two main mechanisms have been described that restore OM asymmetry by acting on phospholipids migrated into the outer leaflet: the phospholipase PldA (also known as OMPLA), which degrades the invading lipid molecules, and the Mla pathway, which removes phospholipids from the outer leaflet.

PldA normally exists as an inactive monomer in the OM. PldA phopholipase activity is modulated by a reversible dimerization mechanism triggered by events that promote the migration of glycerophospholipids into the OM outer leaflet (Dekker, 2000). Activated PldA sequesters and destroys the invading lipid substrates, thus the enzyme proposed function is to maintain lipid asymmetry of the OM under stress conditions provided that enough substrate is available to promote dimerization (Dekker, 2000).

The Mla (Maintenance of OM lipid asymmetry) proteins constitute a highly conserved ABC transport system that prevents phospholipids accumulation in the outer leaflet of the OM under non-stress conditions. Mla operates in the absence of PldA but the converse is not true; indeed, the Mla pathway inhibits the activation of phospholipases in non-stressful conditions (Malinverni and Silhavy, 2009). Based on these observations it has been proposed that the Mla proteins constitute a bacterial intermembrane phospholipid trafficking system (Malinverni and Silhavy, 2009) (Fig. 1.7). In agreement with the proposed function of the Mla system, in Polissi's lab was recently found that in cells depleted for LptC, an IM protein implicated in LPS transport to the OM (see below), MlaD is up-regulated, suggesting that LPS export to the cell surface and phospholipids removal from the OM are functionally interconnected pathways (Mauri P.L. and Polissi A., unpublished results).

An alternative response to OM asymmetry perturbation consists in LPS modification. LPS can be palmitoylated at the position 2 of lipid A by PagP, an OM β-barrel acyltransferase that utilizes phospholipids migrated in the OM as the substrate (Bishop *et al.*, 2000). The product of the PagP reaction is an hepta-acylated LPS which possesses increased hydrophobicity (Bishop, 2008) and therefore contributes to restore the permeability barrier function of the OM. The active site residues of PagP map to the extracellular surface of the outer membrane, and thus the reaction can proceed only upon phospholipids migration to the outer leaflet (Hwang *et al.*, 2002). In *Salmonella pagP* is regulated by the PhoP/PhoQ regulatory system, which senses

low Mg^{2+} concentration, a condition encountered during infection (Guo *et al.*, 1998). Moreover, it appears that Lipid A palmitoylation is also a regulated process in other human, insect, and plant pathogens (Rebeil *et al.*, 2004; Derzelle *et al.*, 2004; Fukuoka *et al.*, 2001), thus supporting the hypothesis that such LPS modification contributes to adaptation to the host.

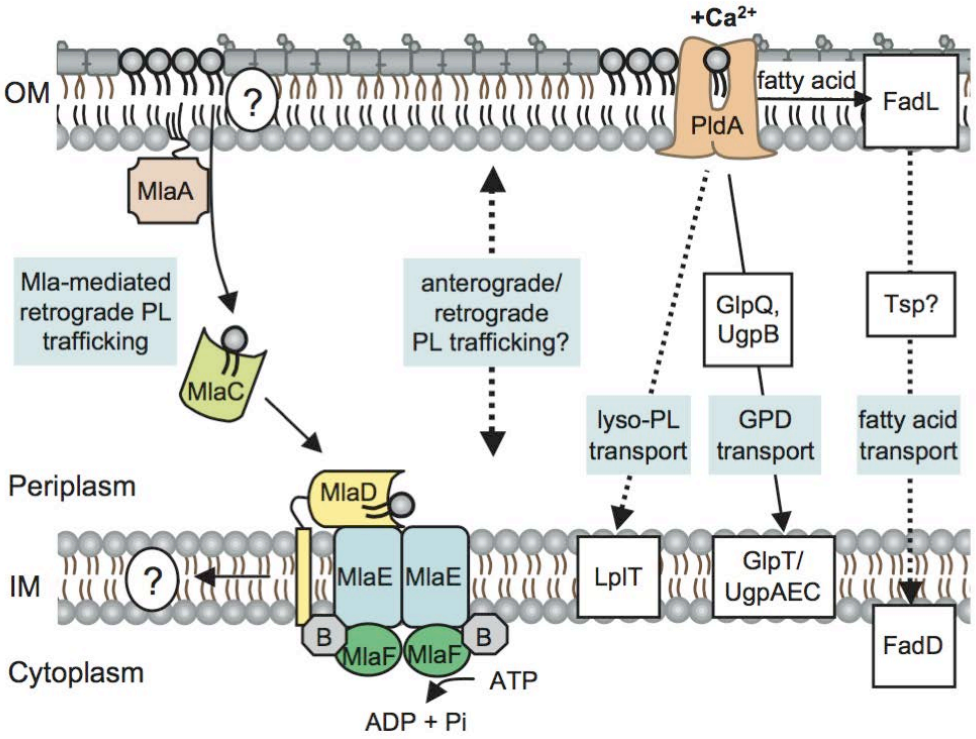

Figure 1.7 | Model of the Mla and PldA PL turnover pathways. The Mla pathway removes phospholipids (PL) from the OM (either from the inner leaflet before surface migration or directly from the outer leaflet) and delivers it to the MlaFEDB complex at the IM via the periplasmic substrate binding protein MlaC. The fate of the PL is unknown, but may be reintroduced at the IM. Other retrograde PL trafficking systems likely exist, and the mode of bulk anterograde and retrograde PL trafficking is still unknown. Increased levels of PldA suppress mutants of the Mla pathway by destroying surface exposed PL, resulting in production of free fatty acids, lyso-PLs, and glycerophosphodiesters (GPDs). Each of these molecules can be taken up from exogenous or intramembrane sources and delivered to the IM by various pathways, but it is unclear whether these same pathways are used to clear PldA breakdown products from the outer leaflet. Dashed lines represent unknown modes of transport across the periplasm, and proteins depicted in white boxes have not been directly proven to be part of the PldA turnover pathway (Malinverni and Silhavy, 2009).

1.6.1 Overview of LPS biosynthesis

The biosynthesis of LPS is a complex process requiring spatial and temporal coordination of several independent pathways that converge in an ordered assembly line to give the mature molecule (Fig. 1.8) (Raetz and Whitfield, 2002; Valvano, 2003; Samuel and Reeves, 2003). The lipid A-core domain is synthesized in the cytoplasm and at the inner leaflet of the IM and requires the convergent synthetic pathways of the lipid A moiety, the Kdo residue and the oligosaccharide core. Then the assembled lipid A-core moiety is flipped over the IM by the ABC transporter MsbA and becomes exposed in the periplasm (Polissi and Georgopoulos, 1996; Zhou *et al*., 1998). The biosynthesis of the *O*-antigen repeating units occurs at the cytoplasmic face of the IM where it is assembled on a lipid carrier and then translocated across the IM. The lipid A-core and *O*-antigen biosynthetic pathways converge with the ligation of *O*-antigen to the lipid A-core moiety at the periplasmic side of the IM mediated by the WaaL ligase to form the mature LPS molecule. The *O*-antigen domain is not essential and is missing in common laboratory *E. coli* K12 strains due to mutations in *wbbL*, a gene implicated in *O*-antigen repeat biosynthesis (Reeves *et al*., 1996; Rubires et al., 1997).

1.6.2 Biosynthesis of lipid A-core

The enzymes for lipid A biosynthesis are constitutively expressed and are located in the cytoplasm or at the inner leaflet of the IM (Raetz and Whitfield, 2002; Raetz *et al*., 2009). The first step of lipid A biosynthesis is the acylation of UDP-N-acetyglucosamine (UDP—GlcNAc) catalyzed by LpxA. The enzyme has a strict dependence for a β–hydroxymyristoyl acyl carrier protein and functions as an accurate hydrocarbon ruler that incorporates a β–hydroxymyristoyl chain two orders of magnitude faster than β-hydroxylauroyl or β-hydroxypalmytoyl chain (Anderson and Raetz, 1987; Wyckoff *et al*., 1998). The next step involves the deacetylation of UDP-3-O-acyl-GlcNAc catalyzed by LpxC a Zn^{2+} dependent enzyme (Jackman *et al*., 1999). LpxC is an attractive target for developing antibiotics inhibiting lipid A biosynthesis as it is well conserved in diverse Gram-negative bacteria and does not possess sequence similarity to other deacetylases or amidases (Onishi *et al*., 1996). Following deacetylation a second β–hydroxymyristoyl chain is added by LpxD to form UDP-2,3-diacylglucosamine (Bartling and Raetz, 2008) which is cleaved by the

pyrophosphatase LpxH to produce UMP and 2,3-diacylglucosamine-1-phosphate also known as lipid X (Babinski et al., 2002). The disaccharide synthase LpxB catalyzes the condensation of one molecule of UDP-2,3-diacylglucosamine with one molecule of lipid X to form a β-1'-6 linked disaccharide (Radika and Raetz, 1988).

LpxA, LpxC and LpxD are soluble proteins whereas LpxH and LpxB are peripheral membrane proteins (Raetz *et al.*, 2009); the homologues of such genes have been identified in other Gram-negative bacteria by sequence comparison, with the exception of LpxH, which appears to be missing in all α–*Proteobacteria* and many δ–*Proteobacteria*, although they use a similar lipid A biosynthetic pathway (Price *et al.*, 1994; Gonzalez *et al.*, 2006). Based on the notion that genes involved in the same pathway are often clustered, a gene (named LpxI) located between the *lpxA* and *lpxB* in *Caulobacter crescentus* has been shown to encode an alternative pyrophosphatase and to rescue the conditional lethal phenotype of an *lpxH*-deficient *E. coli* mutant. LpxH from *C. crescentus* catalyzes *in vitro* the hydrolysis of UDP-2,3-diacylglucosamine thus indicating that LpxH and LpxI are functional homologues (Metzger and Raetz, 2010).

An integral IM protein, LpxK, catalyzes the addition of a phosphate group to the 4'-position of the tetraacylated disaccharide 1-phosphate thus producing lipid IV_A (Garrett *et al.*, 1997). The reaction catalyzed by LpxK precedes the addition of the Kdo residues by the bifunctional enzyme WaaA. Kdo is synthesised by a separate pathway and requires four sequentially acting enzymes (Cipolla *et al.*, 2009). *E. coli* WaaA is a CMP-Kdo dependent transferase that catalyzes the sequential incorporation of two activated CMP-Kdo residues (Belunis and Raetz, 1992). WaaA homologues from different bacterial species can transfer up to four Kdo residues, thus accounting for the differences observed in the structure of lipid A-core moieties across species (Raetz and Whitfield, 2002; Holst, 2007). However, in few species such as *Yersinia pestis* and *Burkholderia cepacia* the outer Kdo residue may be replaced by the stereochemically similar sugar Ko (D-glycero-D-*talo*-oct 2-ulosonic acid) in which the axial hydrogen atom at the 3-position is replaced by an OH group (Fig. 1.6) (Isshiki *et al.*, 2003; Vinogradov *et al.*, 2002). The biosynthesis of Ko has not been elucidated yet; however, a recent study reports the identification of a unique Kdo hydrolase (KdoO) that is present in *Burkholderia ambifaria* and in *Y. pestis* that catalyzes the hydroxylation of the deoxy-sugar residue Kdo (Chung and Raetz, 2011). The biological function of Ko is not known; it has been speculated that the extra OH group in Ko may facilitate hydrogen bonding between adjacent LPS molecules and therefore provide an advantage under stress conditions (Chung and Raetz, 2011).

In *E. coli* and *Salmonella* the synthesis of the final hexaacylated lipid A (Kdo_2-lipid A) requires the two late acyltransferases LpxL and LpxM that catalyze the addition of secondary acyl chains to the distal glucosamine (Clementz *et al.*, 1996; Clementz *et al.*, 1997). However, *Pseudomonas aeruginosa* LPS biosynthesis differs in that fully acylated lipid A is required before Kdo residues addition (King *et al.*, 2009). The additional sugars composing the oligosaccharide core are then added to Kdo_2-lipid A by specific glycosyl-transferases to generate the lipid A-core structure (Raetz and Whitfield, 2002).

The enzymes for the biosynthesis of Kdo_2-lipid A are constitutively expressed. However, in *E. coli* the production of Kdo_2-lipid A is post-transcriptionally regulated by FtsH, an essential membrane bound protease belonging to the AAA family (ATPase associated with various cellular activities) that controls the turnover of LpxC (Ogura *et al.*, 1999). Mutations in *ftsH* lead to increased cellular levels of LpxC and are lethal (Ogura *et al.,* 1999). This can be explained by the fact that both lipid A and phospholipid biosynthetic pathways largely depend on the same precursor molecule, R-3–hydroxymyristoyl ACP. The increased level of LpxC may thus effectively deplete the R-3–hydroxymyristoyl ACP pool thus leading to an imbalanced phospholipid/LPS ratio in the OM (Ogura *et al.*, 1999), which is crucial for survival of most Gram-negative bacteria, as mentioned above. More recently it has been shown that FtsH also controls the turnover of WaaA, the CMP-Kdo dependent transferase that catalyzes incorporation of Kdo residues (Katz and Ron, 2008). Therefore FtsH dependent proteolysis seems to be essential for balancing the levels of two key components of the lipid A-core moiety. Control of LPS biosynthesis by FtsH mediated proteolysis, however, is not a widespread mechanism across Gram-negative bacteria but seems restricted to *Enterobacteria*; indeed the C-terminus of LpxC (where sequence specific degradation signals are located) differs significantly among species whereas the overall sequence of LpxC is highly conserved (Langklotz *et al.*, 2011). Interestingly, the turnover of LpxC in some α*–Proteobacteria* such as *Agrobacterium tumefaciens* and *Rhodobacter capsulatus* depends on the Lon protease, whereas in *P. aeruginosa* the control of LPS biosynthesis seems to be independent of proteolysis and lipid A-core biosynthesis might thus be regulated by a yet unknown mechanism (Langklotz *et al.*, 2011).

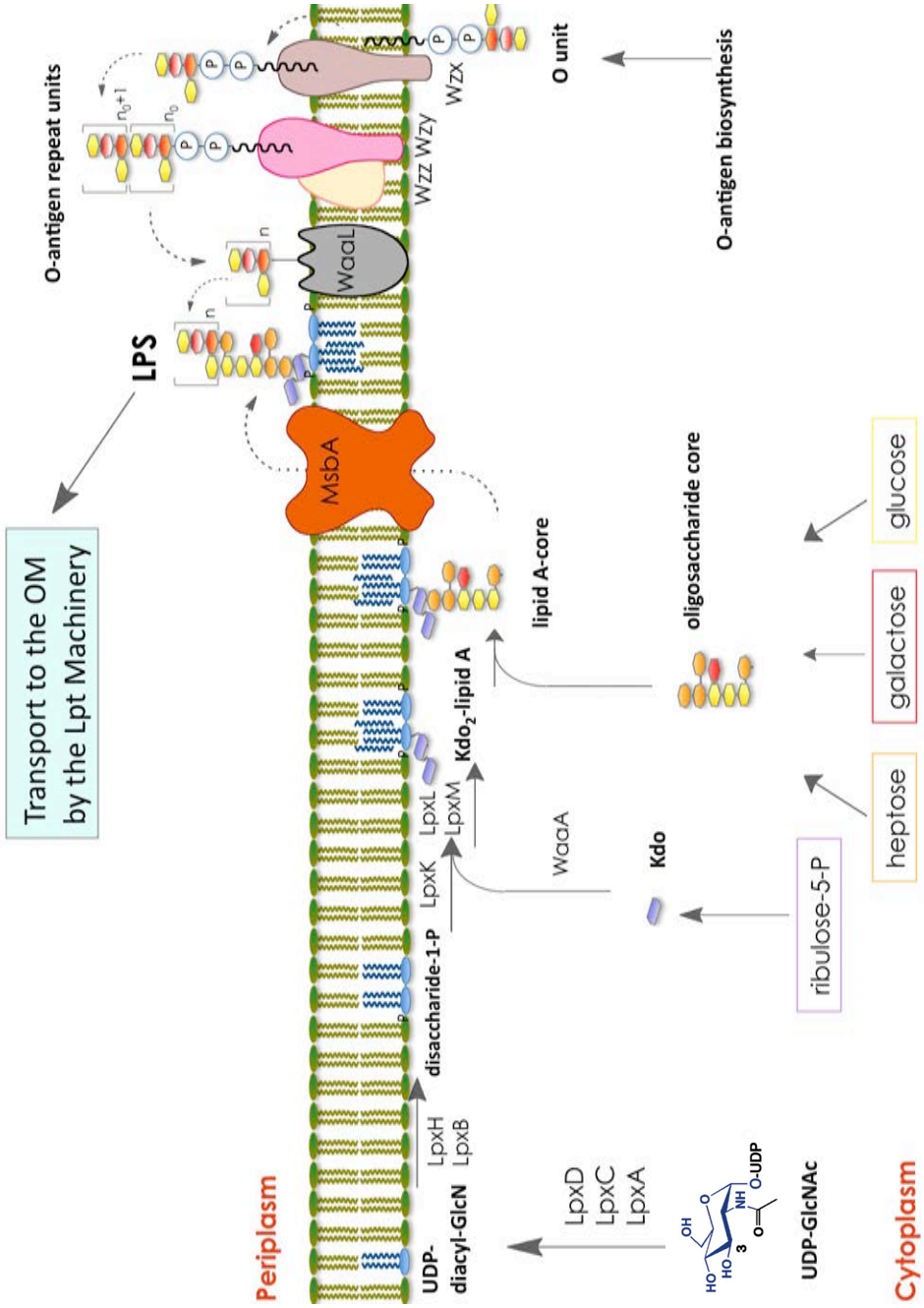

Figure 1.8 | Convergent pathways for LPS biosynthesis in *E. coli*. Starting from bottom left (cytoplasm and inner leaflet of IM): UDP-2,3-diacylglucosamine (UDP-diacyl-GlcN) is synthesized in the cytoplasm by the action of LpxA, LpxC and LpxD enzymes. The synthesis of β-1′-6 linked disaccharide (Disaccharide-1-P) requires LpxH and LpxB. The Kdo_2-lipid A is synthesized from the sequential action of LpxK, WaaA, which transfers two molecules of Kdo, and the late acyltransferases LpxL and LpxM. Core oligosaccharide is assembled on Kdo_2-lipid A via sequential glycosyl transfer of sugar precursors. Lipid A-core is translocated across the IM by the ABC transporter MsbA. Starting from bottom right (cytoplasm and inner leaflet of IM): *O*-antigen repeat units are synthesized in the cytoplasm and at the IM; they are then transported and (outer leaflet of IM) polymerized via a separated pathway (Wzx-Wzy dependent pathway). Lipid A-core ligation to O-antigen polysaccharide occurs at the periplasmic face of the IM by the action of WaaL ligase. Symbols are as shown in Figure 1.6. LPS is then delivered to the Lpt machinery (see text for details) (Sperandeo *et al*., 2012 in press).

1.7 Assembly of Mature LPS at the Outer Leaflet of IM

1.7.1 Translocation of lipid A-core across the IM

After biosynthesis, the lipid A-core is anchored to the IM with its hydrophilic moiety exposed to the cytoplasm and is then flipped across the IM by the essential ABC (ATP binding cassette) transporter MsbA (Fig. 1.8, 1.9 and 1.10) (Davidson *et al*., 2008). The 64.3 kDa peptide encoded by *msbA* is described as a "half-transporter" and the functional MsbA protein is presumed to be a homodimer. MsbA belongs to a class of ABC transporters with the transmembrane domain (composed by 6 membrane-spanning helices believed to contain the substrate-binding site) is fused to the nucleotide-binding domain (NBD) (Davidson *et al*., 2008). Substrate transport is driven by the energy provided by ATP hydrolysis.

MsbA was originally identified in *E. coli* as a multicopy suppressor of the thermosensitive phenotype of a *htrB* deletion mutant (Karow and Georgopoulos, 1993). *htrB* (now renamed *lpxL*) encodes one of the two late Kdo-dependent acyltransferases responsible for the addition of lauryl moieties to the tetraacylated Kdo_2-lipid IVA, thus forming the pentaacylated Kdo_2-lipid A (Clementz *et al*., 1996). Mutants in *htrB*/*lpxL* are not viable at temperatures above 33°C and produce underacylated LPS that is not efficiently transported to the OM (Zhou *et al*., 1998). Under non-permissive conditions, the *htrB*/*lpxL* null mutant shows alterations in cell morphology (such as formation of bulges and filaments), accumulates phospholipids (Karow *et al*., 1992) and the tetraacylated LPS precursor in the IM (Polissi and Georgopoulos, 1996; Zhou *et al*., 1998). Expression of *msbA* from a plasmid vector in the *htrB*/*lpxL* null mutant suppresses the thermosensitive growth defect and the abnormal phospholipids overproduction, and restores tetraacylated LPS precursor translocation and transport to the OM. Therefore, the higher expression of MsbA at higher temperature does not restore lipid IVA acylation to give lipid A but seems to facilitate the transport of the immature LPS form to the OM (Zhou *et al*., 1998). By contrast, MsbA depleted cells accumulate hexaacylated lipid A at the IM (Zhou *et al*., 1998), thus further implicating MsbA in LPS transport. The key role of MsbA in lipid trafficking was proposed by Doerrler and co-workers (Doerrler *et al.,* 2001) who showed that in an *E. coli* thermosensitive *msbA* mutant carrying a single amino acid substitution (A270T) in a transmembrane region of the protein, the transport of both LPS and phospholipids to the OM was inhibited at the non permissive temperature,

thus suggesting that *E. coli* MsbA is needed to export both major membrane lipids (Doerrler *et al*., 2001).

In *N. meningitidis* the *msbA* gene is not essential for cell viability as this bacterium can survive without LPS (Steeghs *et al*., 1998). *N. meningitidis msbA* mutants produce reduced amounts of LPS, a feature typical of mutants in LPS transport in this organism, but possess an OM mostly composed of phospholipids, indicating that phospholipid transport to the OM is not impaired and suggesting a difference in general lipid transport with respect to *E. coli* (Tefsen *et al.,* 2005a). In *P. aeruginosa* MsbA is essential as expected for an organism that requires the lipid A with at least part of the outer core to be viable (see above). However, *msbA* from *E. coli* cannot cross-complement *msbA* merodiploid cells of *P. aeruginosa*. Moreover, differences between the corresponding gene products are remarked by the observation that the kinetic parameters of purified and reconstituted *P. aeruginosa* MsbA considerably differ from those of *E. coli* MsbA (Ghanei *et al.,* 2007).

A topological analysis of lipids *in vivo* can be performed using as markers covalent modifications catalyzed by compartment-specific enzymes. The topology of newly synthesised lipid A in the temperature sensitive *msbA*A270T mutant was assessed in a polymyxin-resistant genetic background (Doerrler *et al*., 2004). In *E. coli* and *Salmonella* polymyxin resistance depends on enzymes acting at the periplasmic side of the IM that covalently modify lipid A with cationic substituents (Raetz *et al*., 2007). Upon MsbA inactivation at high temperature, newly synthesized lipid A was not modified, suggesting that the molecule accumulates in the IM facing the cytoplasm (Doerrler *et al*., 2004). This is consistent with a model of MsbA-mediated LPS flipping over the membrane leaflets, rather than translocation and ejection from the bilayer.

Very recently several mutations in the NBD of *E. coli* MsbA have been characterized *in vitro* by fluorescent ATP binding, radioactive ATP hydrolysis assays, and Electron Paramegnetic Resonance (EPR) spectroscopy (Schultz *et al*., 2011a; Schultz *et al*., 2011b). These studies have identified residues within the NBD domain that are either necessary for efficient ATP hydrolysis (Leu511) or for the conformational rearrangements required during flipping (Glu506, Asp512, His537).

Several *in vitro* studies have been performed to evaluate MsbA substrate specificity. The basal ATPase activity of purified MsbA reconstituted into liposomes is stimulated by hexaacylated lipid A, Kdo_2-lipidA, or LPS but not by underacylated lipid A precursors, suggesting that hexaacylated LPS is the substrate required for the transport (Doerrler and Raetz, 2002), in line with previous genetic and biochemical evidence (Zhou *et al*., 1998). This work was further expanded by functional

reconstitution of the protein into proteoliposomes of *E. coli* lipids to estimate MsbA binding affinities for nucleotides and putative transport substrates (Eckford and Sharom, 2008). Using purified labelled MsbA simultaneous high affinity binding of lipid A and daunorubicin was demonstrated (Siarheyeva and Sharom, 2009). These results indicate that MsbA contains two substrate-binding sites that communicate with both the nucleotide-binding domain and with each other. One is a high affinity-binding site for the physiological substrate, lipid A, and the other site interacts with drugs with comparable affinity. Thus, MsbA may function as both a lipid flippase and a multidrug transporter (Siarheyeva and Sharom, 2009). Early attempts to demonstrate MsbA-mediated lipid flipping *in vitro* failed (Kol *et al*., 2003). However, a direct measurement of the lipid flippase activity of purified MsbA in a reconstituted system has been recently reported (Eckford and Sharom, 2010).

The X-ray crystal structures of MsbA from the three closely related orthologues from *E. coli*, *Vibrio cholerae*, and *S. enterica* (serovar Typhimurium) in different conformations were recently reported (Ward *et al*., 2007). The overall shape and domain organization of MsbA resemble that of the 3.0-Å structure of the putative bacterial multidrug transporter Sav1866 (Dawson and Locher, 2006) and the 8-Å cryo-EM structure of Pgp (Rosenberg *et al.,* 2005). The analyses of crystal structures of MsbA trapped in different conformations indicate that this molecule may undergo large ranges of motion that may be required for substrate transport (Ward *et al*., 2007). Collectively, these results show that MsbA has the potential, at least *in vitro*, to handle a variety of substrates as expected from a protein belonging to the sub-family of drug-efflux transporters. However, *in vivo* MsbA displays a remarkable selectivity towards the LPS substrates being capable to translocate only hexaacylated but not penta or tetraacylated LPS. This observation, together with data that will be discussed in the following paragraphs, suggests that MsbA may play the role of "quality control system" for LPS export to the OM.

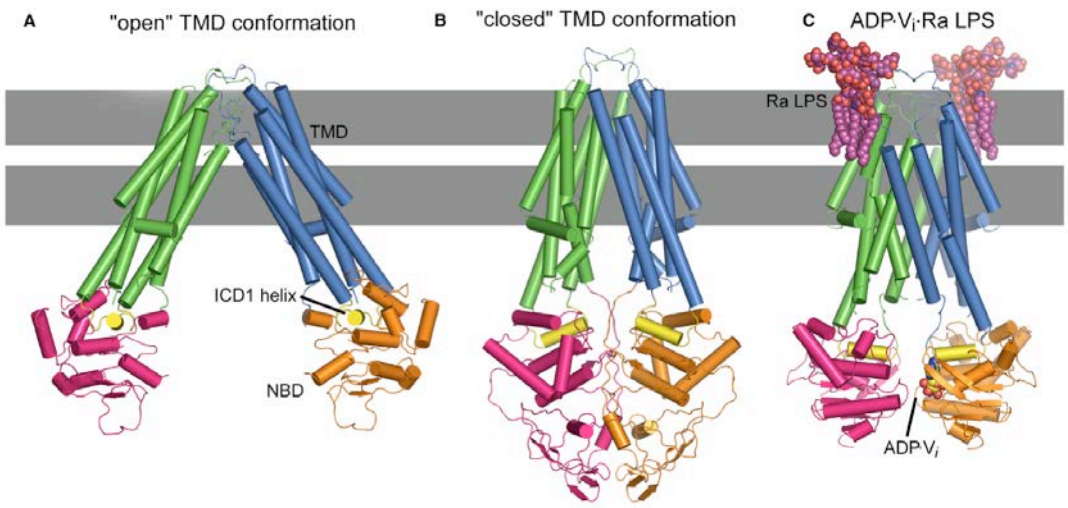

Figure 1.9 | X-ray crystal structures of MsbA. TMDs (TransMembrane Domain) are colored green and blue, NBDs (Nucleotide Binding Domain) are colored magenta and orange. ICD1 (Intracellular Domain) helix is colored yellow. **A** "Open" conformation of apo MsbA from *E. coli* (1JSQ). **B** "Closed" conformation of apo MsbA and *V. cholera* (1PF4). **C** ADP-bound structure of MsbA from *S. typhimurium* with bound Ra LPS is shown in magenta (reviewed by Reyes *et al.*, 2006).

1.7.2 Lipid A-core modification systems

Following MsbA mediated translocation, the nascent core-lipid A moiety may undergo diverse covalent modifications during its transit from the outer surface of the IM to the OM. These modifications are not essential for growth but confer an advantage to the bacterium in evading the innate immune system (Raetz *et al.*, 2007). The majority of such modifications are regulated and, in most cases, relevant only during specific phases of the bacteria life cycle. Regulation of LPS modifications has been extensively studied in *Salmonella*, where it occurs via the PhoP/PhoQ and PmrA/PmrB two component systems (Gunn, 2008).

Several bacteria such as *Rhizobium* and *Francisella* can remove the phosphate moieties from positions 1 and 4' of lipid A by two distinct inner membrane phosphatases designated LpxE and LpxF, respectively (Raetz *et al.*, 2007). Interestingly, lipid A cannot be dephosphorylated when LpxE and LpxF are expressed in a conditional *E. coli* MsbA mutant unable to transport the core-lipid A across the IM

(Wang *et al*., 2004; Wang *et al*., 2006); this is consistent with the proposed localization of their active sites at the periplasmic side of the IM.

Decoration of phosphate groups may occur in both *E. coli* and *Salmonella* by addition of L-Ara4N (4-amino-4-deoxy-L-arabinose) and PEtN (phosphoethanolamine) catalyzed by the ArnT (Trent *et al*., 2001b) and EptA (Lee *et al*., 2004) enzymes, respectively. These modifications mask phosphate groups with positively charged moieties and, when present in LPS, confer resistance to antimicrobial peptides. Expression of both enzymes is regulated by the PmrA/PmrB bacterial two-component system (Gunn, 2008).

The number of acyl chains in core-lipid A may also be modulated. Three different enzymes have been implicated in such modifications: PagP, PagL and LpxR. The OMP PagP, mentioned above, catalyzes the addition of palmitate residue at position 2 of lipid A acyl chains. According to both X-ray and NMR structures of PagP from *E. coli*, the active site of the enzyme faces the exterior of the cell (Hwang *et al*., 2002). PagL is an OM lipase regulated by the PhoP/PhoQ two component system responsible of 3-O-deacylation of lipid A (Trent *et al*., 2001a) whereas LpxR is a distinct OM lipase cleaving 3'-O-linked acyl chains (Reynolds *et al*., 2006).

Based on their sub-cellular localization and mechanism of action, lipid A modification enzymes have been extremely useful as reporters for LPS trafficking within the bacterial envelope (see below).

1.7.3 O-antigen biosynthesis, transport and ligation to the lipid A-core

The structural diversity of the *O*-antigens stems from variation in sugar composition and the sequence of sugars and linkages. The oligosaccharide units (O-units) composing the *O*-antigens are synthesised as lipid-linked intermediates and then assembled (Fig. 1.8). The lipid component is undecaprenyl phopsphate (Und-P), a C55-polyisoprenoid derivative (Whitfield, 1995; Raetz and Whitfield, 2002). The enzymes implicated in the synthesis of the O-unit are either integral membrane proteins or associated with the cytoplasmic site of the IM by ionic interaction (Raetz and Whitfield, 2002). Most of the O-units is exported and assembled by the so-called Wzx/Wzy dependent pathway (Raetz and Whitfield, 2002). At least three proteins, Wzx, Wzy and Wzz, are involved in this export pathway. Wzx is an integral membrane protein postulated as a candidate for the O-unit flippase across IM (Marolda *et al*.,

2010). The Wzy protein is required for the polymerization of Und-PP-linked O-units at the periplasmic face of the IM (McConnell *et al.*, 2001). Chain length distribution of *O*-antigen polysaccharide depends on Wzz that belongs to a family of protein called "polysaccharide co-polymerases" (Morona *et al.*, 2000). An alternative way of ttransport, consist of the ABC transporter-dependent pathway. The most significant features of this pathway are that the completion of the O-specific polysaccharide occurs at the cytosolic side of the IM and the export of the polymer across IM requires an ABC transporter (Zhang *et al.,* 1993).

Irrespective of the export and polymerization mode, the assembly of the mature LPS molecule occurs at the periplasmic face of the IM where ligation of assembled Und-PP linked *O*-antigens to the lipid A-core moiety takes place. This reaction is catalyzed by a specific glycosyltransferase, an integral membrane protein encoded by the *waaL* gene (Raetz and Whitfield, 2002). Mutant strains devoid of *waaL* are viable but cannot ligate *O*-antigen molecules to lipid A-core and thus produce LPS lacking *O*-antigen polysaccharide and accumulate membrane bound Und-PP linked *O*-antigen molecules (McGrath and Osborn, 1991). WaaL displays relaxed substrate specificity, as donor Und-PP linked glycans for the ligation reaction can originate from various biosynthesis pathways. For example colanic acid, a cell surface capsular material that is produced upon cold shock or other stress conditions and that is usually loosely associated with the bacterial cell, can be covalently linked to the lipid A-core by WaaL at the same position as the *O*-antigen (Meredith *et al.*, 2007; Sperandeo *et al.,* 2008).

Finally, the mature LPS molecule is transported to the cell surface. In the following paragraphs the advances made in the last decade in understanding the LPS export pathway downstream of MsbA-mediated translocation across the IM will be reviewed.

1.8 LPS Transport to the OM

1.8.1 The Lpt machinery: identification of the genes, structure and organization of the components across IM and OM

The mature LPS molecule assembled at the periplasmic face of the IM must then traverse the aqueous periplasmic compartment before being inserted and correctly assembled at the OM. As mentioned above the periplasm is devoid of high-energy phosphate bound molecules as ATP (Oliver, 1996), therefore the transport across the periplasm occurs in absence of an obvious energy source.

In 1972, exploiting sucrose density gradient ultracentrifugation to separate IM and OM from *S. enterica (serovar* Thyphimurium), Osborn and collaborators demonstrated for the first time that LPS transport from the site of synthesis at the IM to the OM is unidirectional (Osborn *et al*., 1972). However, it took several decades to unravel the first molecular details of this process. Unlike MsbA, whose role in LPS flipping across the IM has been clearly established during the last two decades (Doerrler *et al*., 2001; Doerrler and Raetz, 2002; Doerrler *et al*., 2004), most of the factors involved in LPS transport downstream of MsbA have been identified only in the past 5 years.

The *E. coli* Lpt (lipopolysaccharide transport) complex is composed of seven essential and variably conserved proteins (LptABCDEFG) that are located in every cellular compartment: cytoplasm, IM, periplasm and OM (Fig. 1.11). The Lpt complex provides energy for LPS extraction from the IM and mediates its transport across the aqueous periplasm, its insertion, and its assembly at the OM (Sperandeo *et al*., 2009; Ruiz *et al*., 2009).

This complex may be divided in three subassemblies: LptBCFG, LptA, and LptDE which are located at the IM, in the periplasm, and at the OM, respectively. LptBFG is an IM-associated ABC transporter that harbors an atypical subunit constituted by the bitopic IM protein LptC, whose function in the ABC transporter has not yet been clarified (Narita and Tokuda, 2009). LptB is the ATP binding domain of this transporter and is phylogenetically related to ABC proteins of hydrophobic amino acid uptake systems (Saurin *et al*., 1999). LptF and LptG are the transmembrane subunits of this ABC transporter. LptA is a periplasmic protein and is reminiscent of the

substrate binding proteins often related to importers in *E. coli* as suggested by Davidson and collegues (Davidson *et al.,* 2008). At the OM resides the LptDE complex, which is composed by the β-barrel protein LptD and the lipoprotein LptE.

The reason why this field has been left unexplored for so many years is that the identification of OM biogenesis factors has been challenged by the lack of specific phenotypes in LPS transport mutants, which often made difficult the design of genetic selections.

The long journey of LPS from the IM to the OM has been unveiled starting from its end. *lptD* (formerly designated *imp* for increased membrane permeability or *ostA* for organic solvent tolerance) was the first gene isolated in a genetic selection designed with the aim of obtaining mutations affecting OM permeability (Sampson *et al.*, 1989). In that pioneering work, a mutant lacking the maltodextrins-specific channel LamB was grown in the presence of maltodextrins larger than maltotriose as a sole energy and carbon source and mutants with altered OM permeability, which allowed the entry of these large molecules through the OM, were isolated. Two such mutants bore mutations that not only allowed growth on maltodextrins but also conferred sensitivity to several hydrophobic and hydrophilic antibiotics, thus suggesting that OM barrier integrity was impaired. These two mutations mapped into the *lptD* gene that was shown to be essential in the same work.

Interestingly, *lptD* was identified again five years later in an independent genetic screen as the responsible of increased resistance to organic solvent and designated *ostA* (Aono *et al.,* 1994), thus confirming that alterations of LptD functionality actually result in permeability defects.

LptD is an 87 kDa OM protein characterized by a C-terminal β-barrel domain (a.a. 203-784) and a periplasmic N-terminal domain (a.a. 25-202). This protein is conserved among the major classes of *Proteobateria* and its presence in different genomes correlates with the presence of the second lipid A biosynthesis enzyme LpxC (See "The Present Investigation" for details).

Initially, a role for LptD in OMPs biogenesis was proposed, based on the observation that LptD depletion results in accumulation of newly synthesized proteins and lipids in a membrane fraction with higher density than the OM in sucrose density gradient centrifugation (Braun and Silhavy, 2002). The appearance of this novel membrane fraction was attributed to the unbalanced protein/lipid ratio resulting from OMPs mislocalization. This hypothesis was further supported by the finding that *lptD* belongs to the σ^E regulon, which controls envelope biogenesis genes in response to extracytoplasmic stresses (Dartigalongue *et al.,* 2001) and by the observation that it is

genetically linked to *surA*, a gene coding for the primary chaperon involved in transit of the bulk mass of OMPs through the periplasm (Missiakas *et al*., 1996; Sklar *et al*., 2007).

However, the function of LptD was clearly demonstrated two years later by Tommassen's group by exploiting the ability of *N. meningitidis* to survive without LPS (Steeghs *et al*., 1998). The authors demonstrated that in mutants lacking the neisserial *lptD* ortholog, which are viable, LPS is not accessible to extracellularly added neuraminidase, an enzyme that modifies LPS by adding sialic acid residues, and its lipid A moiety is not deacylated by the ectopically expressed OM deacylase PagL, thus suggesting that these *lptD* mutants are unable to transport LPS to the cell surface (Bos *et al*., 2004). In addition in these mutants the LPS total content in the cell is dramatically decreased, as previously observed in an *msbA* knockout mutant that in this organism is viable (Tefsen *et al*., 2005a).

The role of *E. coli* LptD in LPS assembly to the cell surface was further confirmed by two different works showing that LptD depletion prevents newly synthesized LPS from reaching the OM (Wu *et al*., 2006; Sperandeo *et al.,* 2008).

As early observations suggested that LptD exists as a high molecular weight complex in the OM (Braun and Silhavy, 2002), Kahne and co-workers searched for additional Lpt factors by affinity purification. Using a His-tagged version of LptD the authors enriched on a Ni-NTA column the LptD-containing protein complex from solubilized OM extracts of *E. coli*. The LptD-interacting protein was subjected to tandem mass spectrometry and was identified as the essential 21.2 kDa rare lipoprotein formerly known as RlpB, and now renamed LptE (Wu *et al*., 2006). The role of LptE in LPS transport to the OM was demonstrated by assessing the occurrence of PagP-mediated lipid A modification in newly synthesized LPS extracted from LptE depleted cells. In both LptE and LptD depleted cells newly synthesized LPS fails to be modified by PagP, thus proving that both proteins are implicated in the LPS transport pathway (Wu *et al*., 2006).

Recent work by the same group has provided new insights into the structure and biogenesis of the LptDE complex. Using proteolysis experiments coupled to size exclusion chromatography, they demonstrated that the C-terminal domain of LptD strongly interacts with LptE and that the stoichiometric ratio of the two proteins in the heterodimeric complex is 1:1. The stable association revealed by proteolysis experiments suggests that LptE may be important to correctly fold the C-terminal domain of LptD, which appears to be unstable when overexpressed without LptE (Chng *et al.,* 2010b). The interaction with LptE seems to be required for the formation

of the disulphide bonds of LptD, which is essential for its function (Ruiz *et al.*, 2010). Indeed it has been shown that LptE forms a plug buried in the lumen of the mature β-barrel formed by the C-terminal domain of LptD and that the two proteins associate via an extensive interface which involves a predicted extracellularly exposed loop of LptD (Freinkman *et al.*, 2011). This strong interaction may also explain the previous observation that LptE is functional even without its N-terminal lipid anchor (Chng *et al.,* 2010b). LptE does not seem to simply play a structural role in LPS biogenesis, as it has been demonstrated to specifically bind LPS (Chng *et al.,* 2010b). Finally, in a screening for suppressor mutants of a two-codons *lptE* deletion that altered LptE interaction with LptD, suppressors were isolated that mapped not only in *lptD* but also in *bamA* (Bam complex protein that assemble OMP at the OM), revealing that LptE association has a role in LptD assembly by the Bam β-barrel assembly machinery (Chimalakonda *et al.*, 2011).

The remaining Lpt components, LptABCFG, are inserted in or associated to the IM. These factors were discovered by different approaches. *lptA*, *lptB* and *lptC* (formerly *yhbN*, *yhbG* and *yrbK* respectively) were identified by Polissi and co-workers using a genetic screen designed to identify novel essential functions in *E. coli* (Serina *et al.*, 2004). In this work a Tn5-derived minitransposon carrying the inducible *araBp* arabinose promoter oriented outward at one end was used to generate mutants that were subsequently assayed for conditional lethal phenotypes. This genetic selection led to the identification of a chromosomal locus containing novel essential functions. Along with *lptA*, *lptB* and *lptC*, this locus contains two LPS biosynthesis genes (*kdsD* and *kdsC* coding for two enzymes involved in Kdo biosynthesis (Meredith and Woodard, 2003; Wu and Woodard, 2003). The chromosomal organization of the genes at this locus is conserved among Gram-negative bacteria, especially in the *Enterobacteriaceae* (Fig. 1.10). Conservation of these gene sequences, by the way, will be discussed further in this thesis. The entire locus in *E. coli* is transcribed from a single upstream promoter, but at least two complex internal promoter regions may allow differential expression of the different genes (Sperandeo *et al.*, 2007; Martorana *et al.,* 2011).

All three *lpt* genes turned out to be essential in subsequent researches later on: this feature together with the genetic linkage with LPS biosynthesis genes strongly suggested a role in OM biogenesis and possibly in LPS transport (Sperandeo *et al.,* 2006).

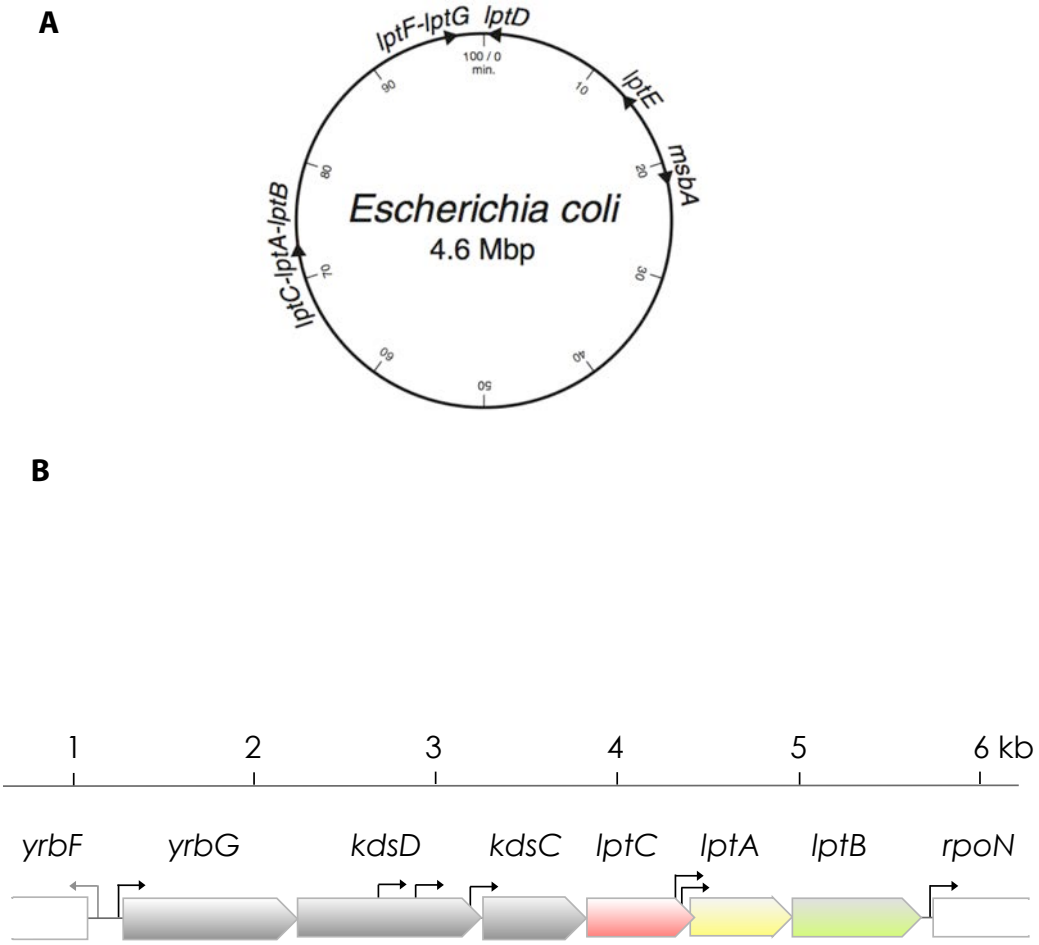

Figure 1.10 | The LPS transport genes. A Chromosomal localization of *lpt* genes and *msbA* in *E. coli* K-12 (reviewed by Narita, 2011). **B**. Map of the *E. coli yrbG-lptB* locus: genes are drawn to scale as open rectangles with arrowhead. Co-ordinates in the kb scale are obtained from *E. coli* genomic sequence (GenBank NC_000913) by subtracting 3337. Promoters are indicated by bent arrows (Martorana *et al*., 2011, redrawn).

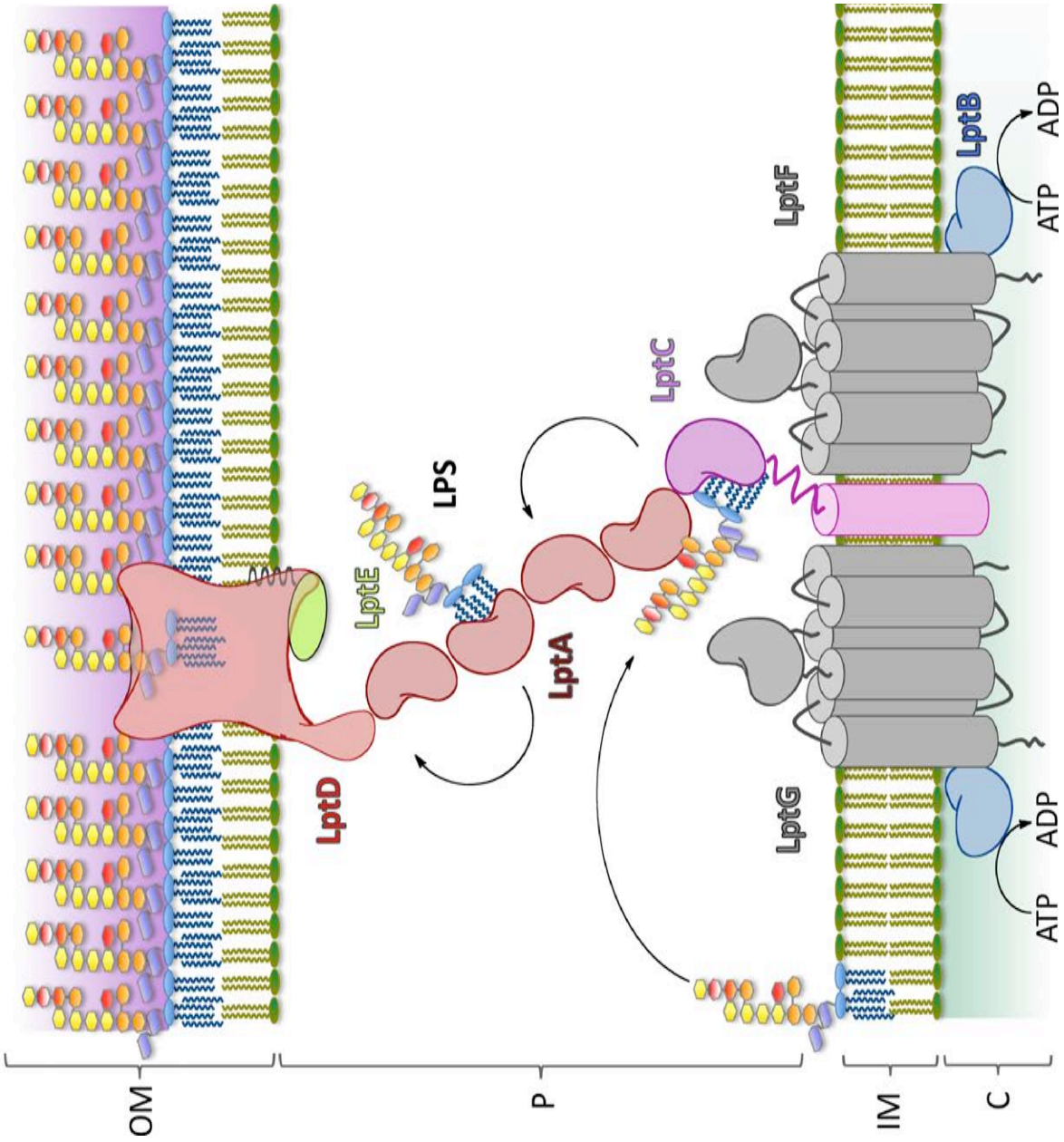

Figure 1.11 | LPS transport through the cell envelope. The flipped LPS molecule is extracted from the IM by the ABC transporter LptBCFG. According to the "trans-envelope complex" model LptA, LptE and LptD constitute a multiprotein complex with LptBCFG which spans the cell envelope by bridging IM and OM components (see text for details). The name of the specific Lpt components is indicated; the bean shape indicates the OstA_N domains present in different proteins of the complex (see text for details) (Sperandeo *et al.,* 2012 in press).

The analysis of conditional mutants in each gene allowed Polissi and collaborators to validate this hypothesis. Membrane fractionation experiments using sucrose density gradient centrifugation revealed that depletion of LptA, LptB and LptC leads to:

i) arrest of cell growth after few generations,

ii) accumulation of abnormal membrane structure in the periplasm,

iii) appearance of an anomalous LPS form (visible in tricine SDS-PAGE as a ladder-like banding of high molecular weight species), and, more importantly,

iv) block of the transport to the OM of *de novo* synthesized LPS, which accumulated in a novel membrane fraction with intermediate density between IM and OM (Sperandeo et al., 2007; Sperandeo et al., 2008).

A closer inspection of the modified LPS extracted from LptA-LptB and LptC depleted cells revealed that repeated units of colanic acid were ligated to the inner core of LPS by the *O*-antigen ligase WaaL (Sperandeo *et al*., 2008). As the active site of this enzyme is located at the periplasmic side of the IM, it was postulated that when LPS transport is impaired, newly synthesized LPS stacked in the IM could become substrate of WaaL, which has a relaxed substrate specificity. For this reason this LPS modification was suggested to be diagnostic of LPS transport impairment (Sperandeo *et al.,* 2008). Similar observations were made by Raetz and co-worker by exploiting the ectopic expression of lipid A 3-O-deacylase PagL from *Salmonella* and the lipid A 1-phosphatase LpxE from *Francisella* as OM and periplasmic markers, respectively, of LPS topology in a novel temperature sensitive LptA mutant. They demonstrated that at the non-permissive temperature, LptA inactivation leads to lipid A-core arrest at the outer side of the IM where it becomes substrate of LpxE. Interestingly, the newly synthesized lipid A-core extracted from the LptA-inactivated mutant cells is not modified by PagL, whose active site is localized at the OM. These observations confirmed that LptA is required to transfer LPS from the periplasmic side of the IM to the OM (Ma *et al*., 2008).

LptB is a 26.7 kDa protein possessing the nucleotide binding domain typical of ABC transporters. Initial evidence revealed that LptB was associated to the IM in a high molecular complex of approximately 140 kDa, although the interacting partners of LptB were not identified (Stenberg *et al*., 2005).

LptA is a 18.6 kDa periplasmic protein, with an N-terminal signal sequence that is processed in the mature form (Tran *et al*., 2008). In early works, *E. coli* LptA

versions fused to a C-terminal His tag and overexpressed from a plasmid were reported to have a periplasmic localization (Tran *et al.*, 2008; Sperandeo *et al.*, 2007); however, in a recent paper by Kahne and co-workers it has been demonstrated that physiologically expressed LptA is able to associate with both IM and OM (Chng *et al.*, 2010a). Similar observations had been already made for the neisserial LptA homologue LptH (Bos *et al.*, 2007). *lptA* and *lptB* are co-transcribed in a dicistronic operon belonging to the σ^E regulon, which is implicated in envelope stress response (Dartigalongue *et al.*, 2001). Interestingly, the σ^E-dependent *lptAp* promoter seems to be exclusively activated by an LPS specific stress, but the fine regulation of this promoter is still unknown (Martorana *et al.*, 2011).

LptC is a small bitopic 21.1 kDa protein that is anchored to the IM by an uncleaved signal sequence. This protein possesses an N-terminal transmembrane segment and a large soluble C-terminal domain exposed to the periplasm (Tran *et al.*, 2010).

In Gram-negative bacteria transmembrane components of ABC transporters are constituted either by one protein with 12 transmembrane segments or two proteins with 6 transmembrane segments each (Davidson *et al.*, 2008); for this reason it was immediately clear that LptC could not be the transmembrane partner of LptB and LptA and that some components of the Lpt transporter were missing. Ruiz and collaborators identified these by a bioinformatic approach exploiting the high degree of conservation of OM biogenesis proteins among Gram-negative bacteria, including endosymbionts whose genome is dramatically reduced. The authors selected a model organism to search for novel Lpt factors, namly the endosymbiont *Blochmannia floridanus*, an Enterobacteriacea with a reduced proteome—14% of the *E. coli* proteome—but containing most of the OM biogenesis factors identified so far in *E. coli* (Gil *et al.*, 2003). This approach led to the discovery of two essential IM proteins, LptF (40.4 kDa) and LptG (39.6 kDa) (formerly YjgP and YjgQ, respectively), as the transmembrane components of the novel Lpt ABC transporter, both possessing a 6-transmembrane domain. In *E. coli* the genes encoding LptF and LptG belong to an operon unlinked to *lptB*. The involvement of LptF and LptG in LPS transport was demonstrated using conditional expression mutants and analyzing the PagP-mediated modification of *de novo* synthesized LPS in LptF or/and LptG depleted cells. The lack of LPS modification and its accumulation at the IM upon depletion revealed that the two proteins are actually required for LPS transport downstream MsbA (Ruiz *et al.*, 2008). Recently, it has been confirmed that LptBCFG proteins physically interact and display ATPase activity (Narita and Tokuda, 2009).

Based on bioinformatic analysis it is reasonable to postulate that the proteins required for LPS transport so far identified and described in this paragraph represent the entire set of essential components of the LPS transport machine (Ruiz *et al.,* 2008). Genetic evidence suggests that the complex functions as a single device (Sperandeo *et al.*, 2008); however, the molecular mechanisms underlying the LPS transport still wait to be clarified and at the moment only models are available.

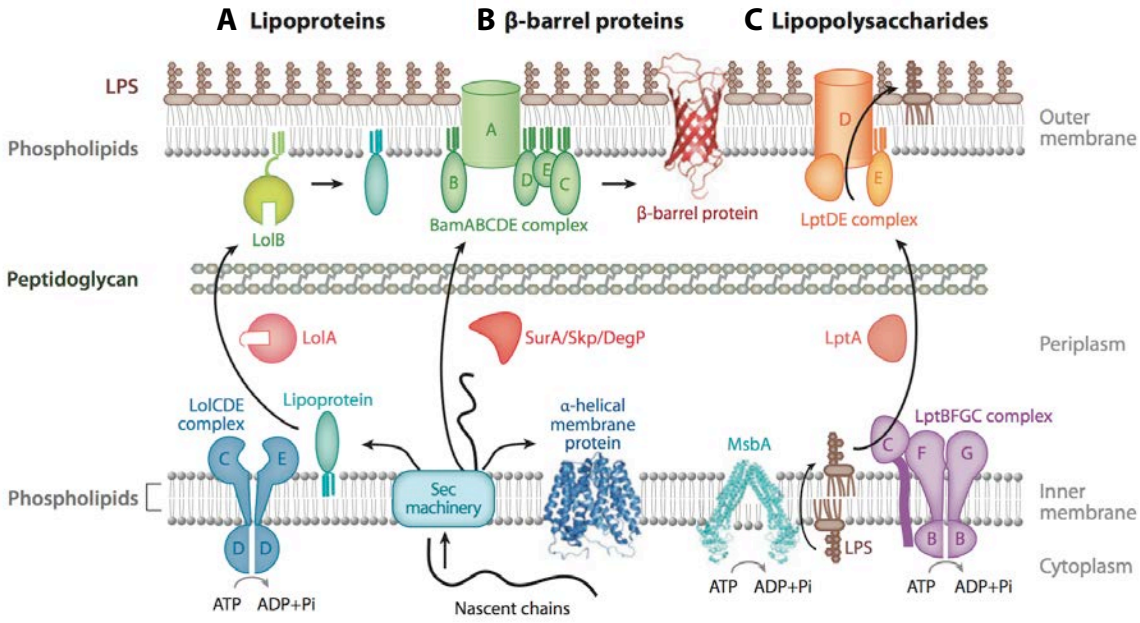

Figure 1.12 | Transport of the three OM main components in comparison: Lipoprotein, β-barrel and Lipopolysaccharide. Periplasmic and OM proteins are synthesized as precursors with a signal peptide at their N termini in the cytoplasm and are then translocated across the IM by a Sec translocon. OmpA is shown as a typical β-barrel protein in the OM. LacY is shown as a typical α-helical protein in the IM. **A** Lipoproteins are transported to the OM from the IM by the Localization of lipoproteins (Lol) system. **B** β-barrel OM proteins are inserted into the OM from the periplasm by a complex consisting of one β-barrel protein, BamA, and four lipoproteins, BamB/C/D/E. Periplasmic chaperones, SurA, Skp, and DegP, are involved in the formation of the folded β-barrel structure. **C** LPS is flipped across the IM by the ABC transporter, MsbA, and then transported from the outer leaflet of the IM to the outer leaflet of the OM by the Lpt system. The phospholipid transport mechanism to the OM remains to be clarified (Reviewed by Okuda, 2011).

1.8.2 Mechanism of LPS transport: facts and models

The body of work available so far reveals that LPS transport requires an IM associated ABC transporter, composed by LptBFG and the atypical subunit LptC with the stoichiometric ratio of 2:1:1:1 (Narita and Tokuda, 2009), a periplasmic subunit, LptA, and an OM-inserted two-component complex LptDE. However, the molecular mechanism by which this complex achieves the unidirectional LPS transport from IM to OM is far from being understood.

The main obstacle encountered in dissecting the role of each Lpt component is that depletion of any Lpt factor leads to the same phenotypes ultimately resulting in LPS accumulation in the periplasmic leaflet of the IM and no intermediate stages have been so far identified. This fact, on one hand, makes it impossible to perform epistasis experiments, on the other hand, it provides a strong evidence that the Lpt machinery operates as a single device in a step downstream of the MsbA-mediated LPS translocation across the IM (Sperandeo *et al*., 2008).

Due to its amphipatic nature, LPS transport cannot occur by simple diffusion and needs an energy transducing device to cross the aqueous periplasmic space; such a device is expected to cross the cell envelope spanning each cell compartment from the cytoplasm to the OM.

Three main models have been proposed to account for the transport mechanism: the vesicle-mediated movement, the chaperone-mediated transit across the periplasm, and the transport at IM-OM fusion sites (compatible with the so-called "Bayer bridges").

A model based on transport mediated by membrane vesicles was abandoned early because of the short space between IM and OM and the observation that the peptidoglycan layer could represent a barrier for such a bulky vehicle (Dijkstra and Keck, 1996). Moreover, vesicles have never been documented within the periplasm.

By analogy with the OM lipoprotein transport mechanism (see Fig. 1.12), the chaperone-mediated transport model implies a soluble periplasmic protein that binds LPS and shields its lipid portion, thus allowing its diffusion across the periplasm. In the lipoprotein transport system, the periplasmic protein LolA receives its substrate from the IM-associated ABC transporter LolCDE, which provides energy for the conformational changes required by LolA to accommodate the lipid moiety lipoproteins in its cavity. LolA is then responsible to deliver its cargo to an OM

associated receptor lipoprotein, LolB, which ultimately inserts it into the OM (Tokuda, 2009). According to the chaperone-mediated model, LptA could be the soluble carrier, which receives LPS from the IM ABC transporter LptBFGC, diffuses across the periplasm and delivers it to the OM complex LptDE. Consistent with this model, LptA binds LPS *in vitro* (Tran *et al.,* 2008) and, interestingly, also LptC is able to bind LPS *in vitro*; moreover, LptA can displace LPS from LptC in line with their location and their proposed placement in a unidirectional export pathway (Tran *et al.,* 2010).

However, some substantial differences exist between Lol and Lpt transporters. First of all LptC is an atypical subunit that has no counterpart in the Lol transporter. The ATPase activity displayed by LptBFG and LptBCFG exhibit the same K_m and V_{max} values, suggesting that LptC does not affect the kinetic parameter of the ATPase activity (Narita and Tokuda, 2009). Moreover, it has been demonstrated that LPS transport can occur in spheroplasts, where the periplasmic soluble content has been effectively drained, indicating that all the components required for LPS transport remain stably associated to the spheroplast; finally, no LPS carrier has been identified in periplasmic extracts using the same approach that allowed the isolation of LolA (Tefsen *et al.,* 2005b).

The third model suggests the existence of bridges connecting IM and OM and was proposed more than 40 years ago by Manfred E. Bayer (Bayer, 1968; Bayer, 1991). Whatever the nature of the bridges (proteinaceous or lipidic), it was postulated that they could facilitate the transit of hydrophobic molecules through the periplasm. Some initial evidence in *S. typhimrium* supported this model. First of all, in 1973 it was reported that newly synthesized LPS appears in zones of adhesion between IM and OM (Muhlradt *et al*., 1973). In line with this observation, Ishidate and co-workers, using sucrose density gradient centrifugation, identified a lighter OM domain (OM_L fraction) where newly synthesized LPS transiently accumulates and demonstrated that in OM_L IM and OM components were present along with murein, evoking the existence of bridges between IM and OM (Ishidate *et al*., 1986). In a very recent work by Kahne's group, the OM_L fraction was isolated and it was demonstrated that all the Lpt proteins co-fractionate in this membrane fraction. In the same paper evidences supporting the physical interaction between the seven Lpt proteins were provided, supporting the idea that Bayer bridges actually exist and are constituted by a transenvelope protein complex (Chng *et al.,* 2010a). Genetic evidence also supports the transenvelope model: as already mentioned above, depletion of any component of the Lpt machine results in a similar phenotype (i.e. LPS accumulation at the

periplasmic side of the IM) (Sperandeo *et al.*, 2008), additional biochemical data will be reported in this thesis (see papers attached).

The interaction mode between Lpt proteins and the molecular determinants of LptA, LptC, and LptE involved in LPS interaction remain to be investigated: all these questions will be addressed in this thesis.

Very recently LptA-LptC interaction has been demonstrated *in vitro* (Bowyer *et al.*, 2011): interestingly Tran and co-workers also demonstrated that LptA binds LPS with higher affinity than LptC, suggesting that LptC may deliver it to LptA (Tran *et al.*, 2010). A transport model can be proposed as follows: LptC may initially use energy provided by the ATP hydrolysis to extract LPS from the IM, after that, LPS unidirectional transit from LptC to LptA can occur by increasing affinity gradient. By the way, as previously mentioned LptC does not affect the kinetic parameter of the ATPase activity of the LptBCFG complex (Narita and Tokuda, 2009). As it has been shown that neither LPS nor lipid A are able to stimulate the ATPase activity of either LptBFG or LptBCFG (Narita and Tokuda, 2009), it is likely that in this *in vitro* assay some component was missing, for example LptA.

The crystal structure of LptA has been solved in the presence and absence of LPS (Fig. 1.13). LptA presents a novel fold consisting of 16 antiparallel β-strands folded to resemble a semiclosed β-jellyroll; the structure in not completely symmetrical and it opens slightly at the N- and C-termini. In the presence of LPS, LptA molecules associate in a head-to-tail fashion forming fibrils containing a hydrophobic groove. According to the hypothesis that LptA physically connects IM and OM, the interior cavity of LptA fibers could ultimately accommodate LPS (Suits *et al.,* 2008), eventhough new biochemical tools should be implemented to prove that LPS is at least partially buried inside LptA cavity.

Interestingly, the recently solved crystal structure of LptC revealed a similar fold to LptA with 15 antiparallel β-strands, although the two proteins share very low sequence similarity (Tran *et al.*, 2010). LptA and LptC belong to the same OstA family of the N-terminal domain of LptD, which has been recently demonstrated to be essential for LptD function *in vivo* (Bos *et al.*, 2007; Chng *et al.,* 2010b) (Figure 1.6A). It may be postulated that LptA bridges the membranes by interacting with LptC at the IM and the N-terminal domain of LptD at the OM.

LptA, LptC and LptE have been demonstrated to bind specifically LPS (Tran *et al.,* 2008; Tran *et al.,* 2010; Chng *et al.*, 2010b); however, the determinants for LPS binding are yet unknown.

LPS binding analysis performed on LptA has revealed that the Lpt complex posses relaxed substrate specificity as this protein is able to bind hexa and tetraacylated lipid A *in vitro* (Tran *et al.,* 2008). However, it is well established that the minimal essential portion of LPS required to sustain cell viability is composed of lipid A and two molecules of Kdo (Raetz and Whitfield, 2002). For this reason MsbA can work as the quality control step in LPS transport. Several lines of evidence support this notion. For example, MsbA overexpression from a multicopy plasmid can rescue mutants lacking *htrB/lpxL* acyltransferase (Karow and Georgopoulos, 1993) or defective in the first Kdo biosynthetic enzyme (KdsD and its paralogue GutQ) (Meredith *et al*., 2006) and thus unable to synthesize a complete Kdo_2-lipid A. This evidence implies that *in vivo* MsbA can flip under-acylated and non-glicosylated lipid A precursors, although with low efficiency, and that these molecules can be efficiently transported by the downstream Lpt machinery. This hypothesis has been further supported by the isolation of two classes of suppressor mutations allowing growth of a *waaA* deletion mutant unable to ligate Kdo to lipid A and accumulating lipid IV_A (Mamat *et al.,* 2008). The first class of suppressor mutations carries a single amino acid substitution in MsbA, resulting in more relaxed substrate specificity. Indeed, those mutants are viable and possess an OM composed by lipid IV_A. The second class of suppressor mutations mapped in *yhjD,* a gene coding for a conserved integral IM protein whose function is not known. The suppressor allele (*yhjD400*) consists in a single amino acid substitution in YhjD, which seems to activate an alternative transport pathway, independently by MsbA (Mamat *et al*., 2008). Indeed, in *yhjD400* genetic background *msbA* turns out to be dispensable. Finally, in line with these overall observations, Raina and co-worker have recently isolated a suppressor-free *waaC lpxL lpxM lpxP* mutant defective in heptosyltransferase I and late acyltransferase genes. This mutant is viable under slow growth condition at low temperatures, although producing a Kdo_2-lipid IV_A LPS precursor, and shows a constitutive envelope stress response. Interestingly, *waaC lpxL lpxM lpxP* growth at normal temperature can be rescued by chromosomal D498V suppressor mutation in MsbA or by wild-type MsbA overexpression (Klein *et al*., 2009).

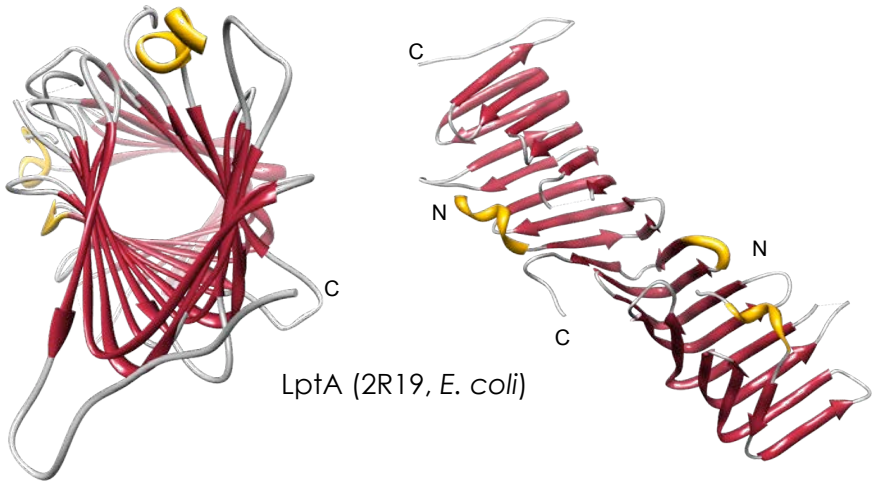

LptA (2R19, *E. coli*)

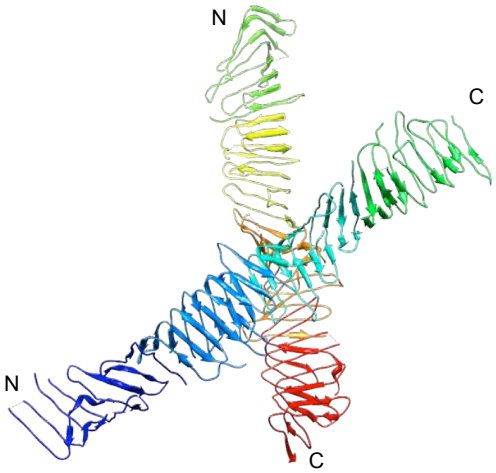

LptA (2R1A, *E. coli*)

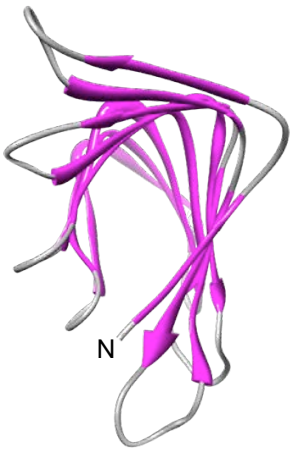

LptC (3MY2, *E. coli*)

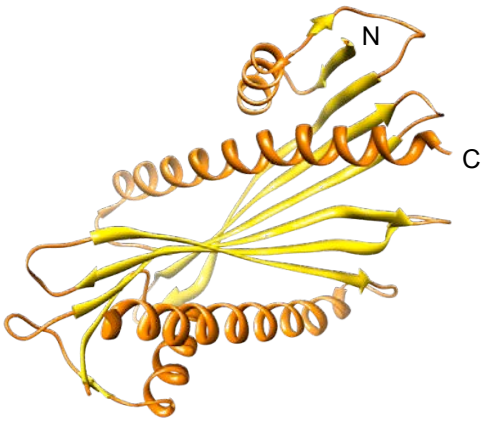

LptE (2R76, *S. oneidensis*)

Figure 1.13 | Crystal structures of Lpt proteins. The crystal structure of LptA, LptC and LptE are reported together with the respective PDB codes. LptA structures obtained in the presence (PDB: 2R1A) or in the absence of LPS (PDB: 2R19) are shown. The structure of LptE has been solved from three different *E. coli* orthologues, only the structure of LptE from *Shewanella oneidensis* is shown.

1.9 An Ancient Story of Fighting: LPS-binding Proteins in Nature

LPS is a potent immunomodulator, as it is able to activate the innate immune system, it is responsible of inflammation and septic shock at higher concentrations, causing disseminated intravascular coagulation, multiple organ failure, and often death.

At the molecular level, a prerequisite for the induction of host responses to LPS is its interaction with LPS-binding molecules.

In the last 40 years a large panel of peptides and proteins were reported to associate with LPS. Collecting information on their origin, their structure and the location of aminoacid residues involved in interaction with LPS, is extremely useful to understand the molecular basis of recognition and binding of LPS by Lpt proteins, implicated in LPS export to the cell surface in LPS-producing bacteria.

It should be pointed out that the very first LPS-binding molecule is LPS itself. Indeed, early after the development of techniques of extraction and purification, it has been recognized that because of their amphiphilic nature, LPS molecules associates together in aqueous media to form aggregates (Hirschfeld *et al*., 2000).

(1) A first group of molecules that recognize LPS are lectins directed against the O-specific polysaccharide chain or the core region of particular LPS. A notable example is the cystic fibrosis transmembrane conductance regulator (CFTR) of lung epithelial cells (Schroeder *et al*., 2002). These proteins, as well as antibodies directed against LPS O-chains, cannot be classified *sensu stricto* as LPS-binding molecules inasmuch as they interact only with a restricted group of LPS: those carrying an appropriate carbohydrate determinant.

(2) A second group of molecules that interact with LPS are enzymes involved in its degradation, such as the lysosomal phosphatase involved in LPS catabolism (Hampton and Raetz, 1991).

(3) However the most important LPS-binding molecules are those belonging to a third group of proteins that interact with the biologically active lipid A region, but do not directly degrade it. We will extensively discuss about them in the next paragraphs.

1.9.1 Bacterial LPS-binding molecules

Bacterial proteins able to interact with LPS are either constitutive proteins of Gram-negative bacteria required for their survival, or molecules produced by other competitive microorganisms such as Gram-positive bacteria. Probably as soon as the first Gram-positive bacteria had to compete with the first Gram-negative bacteria, some 3.5 billion years ago, they selected weapons against the protective coating of Gram-negative: the LPS —as suggested by Chaby (Chaby, 2004).

For example polymyxing B (PMB) is a compound produced by *Bacillus polymyxa*, a Gram-positive organism living in the soil. It is an antibiotic consisting of a cyclic and cationic decapeptide with five positive charges, and a N-linked fatty acid tail. Polymyxing binds Lipid A embedded into the OM bilayer, changes the packing order of LPS and increases the permeability of the outer membrane to a variety of molecules, including PMB itself (Daugelavicius *et al*., 2000; Vaara *et al*., 1992) (see Fig. 1.14).

It should be noted that in specific growth conditions, some strains of enterobacteria become resistant to PMB. This was shown to be due to the addition of L-4-amino- 4-deoxy-arabinopyranose (L-Arap4N) to the phosphate at position 4' of their lipid A. Therefore, this additional positive charge prevents the interaction between PMB and lipid A (Helander *et al*., 1994).

Obviously LPS is not only recognized by proteins that are recruited to detect and neutralize noxious agents; first of all, in LPS-producing bacteria, proteins implicated in its biogenesis are assumed to bind LPS, and later the rich proteome embedded in the OM lipid bilayer where LPS is finally located.

FhuA is found on the surface of *E. coli* and belongs to a family of proteins that mediates the active transport of siderophores, such as ferrichrome, into Gram-negative bacteria. It consists of a C-terminal β barrel and an N-terminal cork that fills the barrel interior. FhuA is immerse into the OM bilayer, so it is surrounded by Lipid A molecules. The protein binds LPS by both electrostatic interactions via eight positively charged residues, and numerous van der Waals contacts between hydrophobic side chains of FhuA and acyl chains of LPS (Ferguson *et al*., 2000) (Fig. 1.14).

Like FhuA, OmpT is found on the surface of *E. coli*. It is an outer-membrane protease with a 10-stranded antiparallel β-barrel structure. It contains an LPS-binding site on the exterior of the barrel (homologous to that found on FhuA), and ligation of LPS is strictly required for the enzymatic activity of OmpT (Vandeputte-Rutten *et al*.,

2001). This proteolytic activity is involved in the cleavage of antimicrobial peptides, and thus in the virulence of the bacteria [Kramer and Brandenburg, 2002; McCarter *et al*., 2004].

It has also been reported that the exotoxin of the Gram-negative bacteria *Bordetella pertussis* (pertussis toxin) can bind LPS. This interaction is mediated through the disaccharide backbone of the lipid A, and involves the S2 subunit of the pertussis toxin, which has a high degree of amino acid sequence similarity with lysozyme (Lei *et al*., 1993).

As already mentioned MsbA is a lipid flippase, which facilitates the export of lipid A (Zhou *et al*., 1998) by hydrolysis of ATP, indeed is a member of the superfamily of ABC transporters. In bacteria, ABC transporters considerably limit antibiotic effectiveness by exporting them as fast as they enter the cells, and in humans, ABC transporters export chemotherapy drugs and thus increase mortality rates in cancer patients. A possible mechanism of action of bacterial MsbA has been proposed by Chang (Chang, 2003) (Fig. 1.9): MsbA consists of two monomers forming a chamber, the inner membrane part of the chamber contains a cluster of positively charged residues allowing the binding of lipid A. This binding induces tertiary arrangements of transmembrane α-helices, triggering ATP hydrolysis. Then, the lipid A molecule flips to the distal leaflet side of the IM probably through out the chamber where it forms hydrophobic interactions, and becomes properly oriented for insertion into this leaflet. Expulsion of lipid A is the final step of the transport mechanism, and occurs when structural rearrangements triggered by the substrate flipping reposition MsbA in its original conformation (Chang, 2003).

Then lipid A linked to the rest of oligosaccharide core moiety someway has to be extracted from the IM and translocated through the aqueous compartment defined as periplasm. It has been reported that the IM anchored protein LptC is able to bind LPS *in vitro* (Tran and Dong *et al*., 2010): this protein could be the candidate that performs the energy consuming extraction coworking with the IM complex LptBFG.

The periplasmic protein LptA binds lipid A *in vitro* too, as Tran and colleagues previously demonstrated (Tran *et al*., 2008). Interestingly LptA can displace LPS from LptC (but not vice versa) in copurification experiments, consistent with their locations and their proposed placement in a unidirectional export pathway.

LptE is a lipoprotein which forms a stable complex with LptD in the OM. It is required together with LptD to translocate LPS to the outer leaflet of the OM: Kahne and Shilavy laboratories reported that it specifically binds LPS (Chng *et al*., 2010).

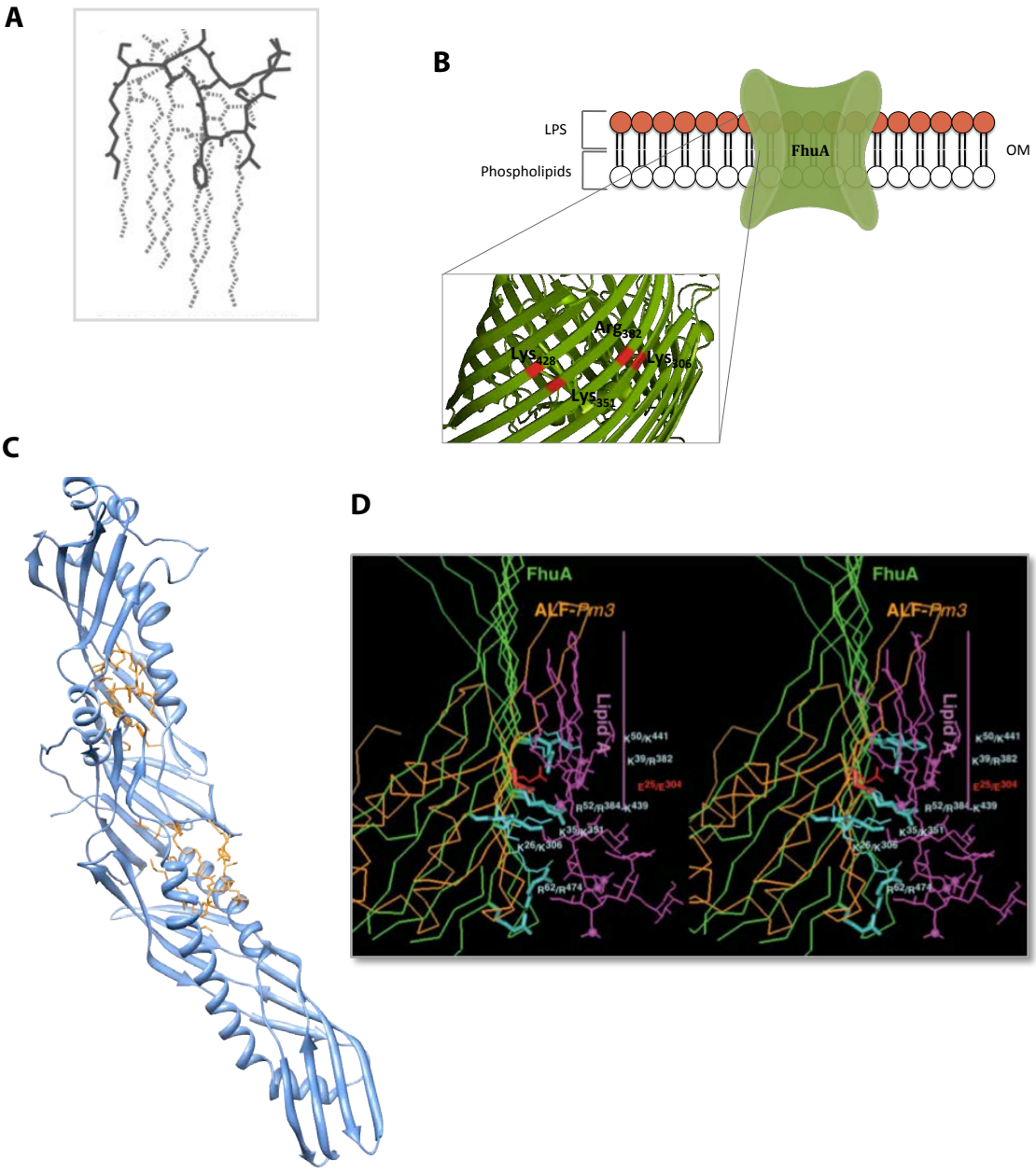

Figure 1.14. | LPS binding molecules. A PMB docked to lipid A. Lipid A is represented in dotted gray line. Modified from Pristovsek *et al.*, 1999. **B** The OM protein FhuA displays an interacation interface with membrane embedded lipid A (data from Ferguson *et al.*, 2000). **C** Human BPI protein (PDB: 1BP1) binds to and neutralizes LPS from the OM of Gram-negative bacteria. The crystal structure of BPI shows a boomerang-shaped molecule formed by two similar domains. Two apolar pockets on the concave surface of the boomerang each bind a molecule of phosphatidylcholine, primarily by interacting with their acyl chains; this suggests that the pockets may also bind the acyl chains of lipopolysaccharide (Beamer *et al.*, 1997). **D** Comparison of the FhuA/LPS interface with the proposed lipid A-binding site for ALF-Pm3. The LPS is in purple with fatty acid chains and sugars in the upper and lower parts, respectively. The lipid A moiety is labeled. Phosphorus atoms are displayed as purple spheres. The proposed binding site would be in agreement with data indicating that the synthetic β-hairpin peptide of ALF-L binds to LPS (Yang *et al.*, 2009).

1.9.2 A conserved strategy of counteracting Gram-negative infections from insects to mammals

It seems that early in the evolution, a system to counteract LPS-producing bacteria was developed, as general conserved bases of mechanism of action are found. By exploring the Tree of Life it is possible to pick representative organisms up in every phyla possessing proteins with the aim to specifically interact with LPS.

In insects, *Drosophila* produces cecropin in haemolymph (De Lucca *et al*., 1995; Bland *et al*., 2001), flesh fly produces sarcotoxin IA (Okemoto et al., 2002), melittin instead is found in bee venom (David *et al*., 1992), and attacin in silkmoth (Carlsson *et al*., 1998). Two synthetic α-helical peptides (MBI-27 and MBI-28) derived from parts of cecropin and melittin bind LPS with an affinity equivalent to that of polymyxin B (Gough *et al*., 1996). Anti-LPS peptides have also been isolated from the skin of amphibians: magainin 2 contains a basic and amphipathic α-helix motif (GKWKAQKRFLKM) with LPS-binding capacity (Matsuzaki *et al.,* 1999).

Invertebrates have developed an innate immune system that responds to surface components of potential pathogens. A very ancient arthropod on the evolutionary scale is the horseshoe crab *Limulus polyphemus*. Large granules of its hemocytes contain a factor called Limulus factor C, which is released in response to invading microbes via exocytosis. Factor C interacts with minute amounts of LPS, and this feature is used in gelation or colorimetric assays for the detection of LPS. It is a large (109 kDa) protein with an N-terminal LPS binding domain, and a C-terminal serine protease domain. The N-terminal domain contains actually three short 3.5 – 4 kDa LPS-binding consensus repeat sites, which work in cooperation for ligand interaction (Tan *et al*., 2000). In contrast, another LPS-binding protein, *Limulus* anti-LPS factor (L-ALF), is found in *Limulus* hemolymph. This is a small (11.8 kDa) basic protein, which inhibits the LPS-mediated coagulation cascade (Aketagawa *et al*., 1986). Its structure consists of three α-helices packed against a four-stranded β-sheet, with an LPS binding site in an extended amphipathic loop (residues 31 – 52)(Hoess *et al*., 1993) (Fig. 1.14).

In mammals, one of the pathological effects of LPS is the induction of disseminated intravascular coagulation (DIC). The lipid A interacts with plasma factor XII (Hageman factor) (Morrison *et al*., 1974), so that this protein becomes active and triggers the intrinsic coagulation pathway. On the other hand, the extrinsic coagulation pathway is negatively regulated by a tissue factor pathway inhibitor

(TFPI), which contains a heparin binding and LPS binding site. Therefore, in mammals as in arthropods, LPS can bind to both activators and inhibitors of the coagulation system as reviewed by Chaby in 2004.

There is an extensive list of other LPS-binding proteins in mammals, which usually transport endogenous ligands, enforcing the scavenging role of cell surface *LPS competent* receptors. Phospholipid transfer protein (PLTP) and cholesteryl ester transfer protein (CETP) are lipid transport proteins found in plasma in association with apo A1. Their role is to transfer or exchange lipids (phospholipids, cholesteryl esters, triglycerides) between plasma lipoprotein particles (Tollefson *et al*., 1998; Tall *et al*., 1993). PLTP has been reported to bind LPS, and to transfer it from Gram-negative bacterial membranes (Vesy *et al*., 2000) or LPS aggregates (Hailman *et al*., 1996) to high-density lipoprotein (HDL) particles. After its transfer to HDL, LPS is no more recognized by the *LPS signaling complex* of responsive cells (Grunfeld *et al*., 1999), but rather is cleared by phagocytices bearing HDL receptors (Maier *et al.,* 1981).

At least one type of protein constituent of lipoproteins, the apolipoprotein apoE, can directly bind LPS, possibly by its exposed hydrophilic domain involving arginine residues (Rensen *et al*., 1997).

Serum amyloid P (SAP) is a serum glycoprotein, which may play a role in clearance of cell debris at sites of acute inflammation (Gewurz *et al.,* 1995). Three LPS binding sites (27 – 39, 61 – 75 and 86 – 200) have been identified in SAP, but only the two latter are accessible on the intact SAP molecule. Corresponding synthetic peptides exihibit LPS-neutralizing activity (de Haas *et al.,* 1999).

Hemoglobin (Hb) is an oxygen-carrying globular protein located in erythrocytes. Hb is an LPS binding protein (Roth *et al.,* 1994) that enhances LPS's biological activities (Kaca *et al.,* 1994). The binding of Hb does not involve ionic interactions with the phosphate groups of lipid A, but rather hydrophobic and/or hydrogen interactions, which causes a slight rigidification of the lipid A acyl chains (Jurgens *et al.,* 2001). Hb is also a source of biologically active peptides: a C-terminal fragment of its b subunit, isolated from human placenta, was reported to exhibit LPS-binding and antibacterial activities (Liepke *et al*., 2003).

1.9.3 Lipid A *versus* the human immune system

Lipid A is the LPS conserved structure that is recognized by specific receptors on cells of the innate immune system. Innate immune receptors recognize microorganism specific motifs named PAMPs (Pathogens Associated Molecular Patterns) to trigger complex signaling cascades that lead to the release of pro-inflammatory cytokines (Miller *et al.,* 2005). Recognition of lipid A requires the TLR4-MD2 complex (Medzhitov *et al.,* 1997; Shimazu *et al.*, 1999), the accessory protein CD14 and LPB (LPS binding protein) (Miyake, 2006). LPB converts oligomeric micelles of LPS to a monomer for delivery to CD14, which in turn transfers LPS to the TLR4-MD2 receptors complex (Miyake, 2006). TLR4 and MD2 form a heterodimer and LPS binding induces the dimerization of the TLR4/MD2 complex to form the activated hetero-tetrameric complex that initiates signal transduction (Fig. 1.15). MD2, which belongs to a family of lipid binding proteins, plays a key role in initial lipid A recognition by accommodating the lipid acyl chains into its large hydrophobic pocket. The two phosphate groups of lipid A bind to the TLR4/MD2 complex by interaction with positively charged residues located on both proteins (Park *et al.,* 2009). These structural studies greatly contributed to our understanding of how lipid A is recognized and how it induces the innate immune response.

LBP, a 60 kDa glycoprotein found in plasma, it shows 24% sequence identity to PLTP and 23% to CETP respectively (Day *et al*., 1994; Schumann *et al.,* 1990), and it is one of the most extensively studied soluble proteins with LPS-binding capacity. Its serum concentration varies from 0.5 – 10 mg ml^{-1} in normal serum, to more than 200 mg ml^{-1} during the acute phase of the inflammatory response. It interacts with the lipid A region of LPS with an affinity of 10^{-9} M (Mathison *et al*., 1992). The LPS-binding activity is contained within the N-terminal half of LBP, and synthetic peptides such as CRWKVRKSFFKLQCG that mimic that region also present LPS-binding capacities (Dankesreiter *et al*., 2000). It was recently shown that LBP has a concentration-dependent dual role: at low concentrations LBP intercalates into cell membranes as a transmembrane protein which binds LPS aggregates and enhances LPS-induced responses, whereas at high concentrations (in acute phase) soluble LBP intercalates into LPS aggregates and inhibits LPS-induced stimulation (Gutsmann *et al.,* 2001). A second function of LBP is to increase the interaction of LPS with soluble CD14 (sCD14) by forming a stable trimolecular complex (Thomas *et al.,* 2002). The complex then can be transported to lipoprotein particles or to cells, which can then

respond to picomolar concentrations of LPS (Wurfel *et al*., 1995; Gegner *et al*., 1995).

In whole blood, the amount of soluble CD14 is 100 – 1000 times higher than that of membrane-bound CD14. sCD14 is a single-chain protein containing 10 leucine repeats in its carboxyl-terminal region (residues 67 – 367). Unlike the membrane form, which requires LBP, sCD14 can directly bind LPS with a dissociation constant of 74 nM (Viriyakosol *et al*., 2001). Lipoteichoic acid and phosphatidyl inositol also bind sCD14 (Gegner *et al*., 1995). The amino terminus of sCD14 contains four motifs involved in ligation of LPS (residues 9–12, 22–25, 35–39 and 59–63) (Shapiro *et al*., 1997).

The region (residues 53 – 63) which contains the fourth LPS binding motif is also the region of highest amphipathicity in sCD14, and may represent a domain analogous to the amphiphatic loops in L-ALF (residues 31– 52), LBP (residues 86 –104) and BPI (residues 86–104) that bind lipid A as early suggested by Juan and collaborators in 1995 (Juan *et al.,* 1995). It has been ipotized that sCD14-LPS complexes can activate cells that are normally deficient in membrane CD14, such as endothelial cells (Frey *et al*., 1992).

It has to be mentioned that LPS-binding molecules are also involved at different levels in the three pathways that make up the complement system (classical, lectin and alternative pathways).

Proteins produced in neutrophil granule, such as BPI, lactoferrin, heparin-binding protein and lysozyme are also known to bind LPS.

Bactericidal permeability-increasing protein (BPI) is a 57-kDa cationic antimicrobial protein that is present mainly in the azurophilic granules of polymorphonuclear leukocytes. BPI is toxic only toward Gram-negative bacteria. It has both heparin- and LPS-binding capacity, and shares ~ 44 % sequence homology with LBP. Three regions (residues 17–45, 65–99 and 142–169) have been described to cooperate for the total binding to LPS (Little *et al*., 1994) (Fig. 1.14).

Lactoferrin (Lf) is a multispecific protein, which binds iron, heparin, proteoglycan, DNA, oligodeoxyncleotides and LPS (van Berkel *et al*., 1997; Britigan *et al.*, 2001). It is released from neutrophil granules and mucosal epithelial cells in response to inflammatory stimuli (Masson *et al.,* 1969). Proteolytic digestion of human lactoferrin in vitro yields a peptide fragment called lactoferricin H, which corresponds to the helix portion of lactoferrin, in the region of LPS binding (Elass-Rochard *et al*., 1995). Actually, two LPS binding sites have been identified in Lf: the 28 – 34 loop region (89 Chaby) and an N-terminal stretch of only four arginines (residues 2 – 5) (van Berkel *et al.,* 1997).

Addition of a 12-carbon acyl chain to a lactoferricin fragment enhances ligation of LPS by up to two orders of magnitude (Majerle *et al*., 2003).

Heparin-binding protein (HBP) is another multifunctional antimicrobial protein of 37 kDa produced by human neutrophil granules (Pereira *et al.,* 1995). Adjacent to its proteoglycan/heparin-binding site, a high-affinity binding site for lipid A is located, consisting of an ionic and hydrophilic area (Asn20, Gln21 and Arg23) to bind a phosphate group, and a hydrophobic pocket (Phe25, Cys26, Cys42 and Phe43) suitable for binding the fatty acid chains of lipid A (Iversen *et al.,* 1997). A synthetic peptide corresponding to residues 20 – 44 has been shown to possess the capacity to bind lipid A (Brackett *et al*., 1997). Like LBP, HBP enhances LPS-induced tumor necrosis factor-alpha (TNF-a) release by monocytes. However, HBP cannot bind to CD14, and its capacity to increase the responses of monocytes to LPS is likely mediated by its internalization (Heinzelmann *et al*., 1998).

Lysozyme, a major cationic protein of leukocyte polymorphonuclear granules, was also found to bind LPS. Like polymyxin B, lysozyme binds first electrostatically to the phosphate groups of lipid A, whereas the carboxy-lates of the Kdo units do not play any role (Brandenburg *et al.,* 1998). This electrostatic interaction is followed by a hydrophobic interaction.

Another group of neutrophil cationic proteins able to bind LPS involves proline-rich peptides. Indolicidin, Bac5 and prophenin represent three examples of such peptides. Indolicidin is a 13-amino acid (ILPWKWPWWPWRR) proline-rich peptide present in bovine neutrophil granules, which binds LPS efficiently (Kd = 45.2 mM) (Nagpal *et al*., 2002). This is also the case of another proline-rich peptide found in ruminants, Bac5 (Shamova *et al.,* 1999). The third peptide belonging to this group is prophenin. This peptide has been isolated from leukocytes but is also detectable in preparations of lung surfactant (Wang *et al.,* 1999). It consists of a 79-residue peptide rich in proline (53 %) and phenylalanine (19 %), and contains repeating decameric elements. Its affinity for LPS is 60 times greater than that of polymyxin B (Harwig *et al*., 1995).

Polipeptides that are produced by epithelial cells, T lymphocytes and NK cells, namely SLPI, HRP and NKL of the human immunitary system bind lipid A too, so defensins and cathelicidins do (reviewed by Chaby, 2004).

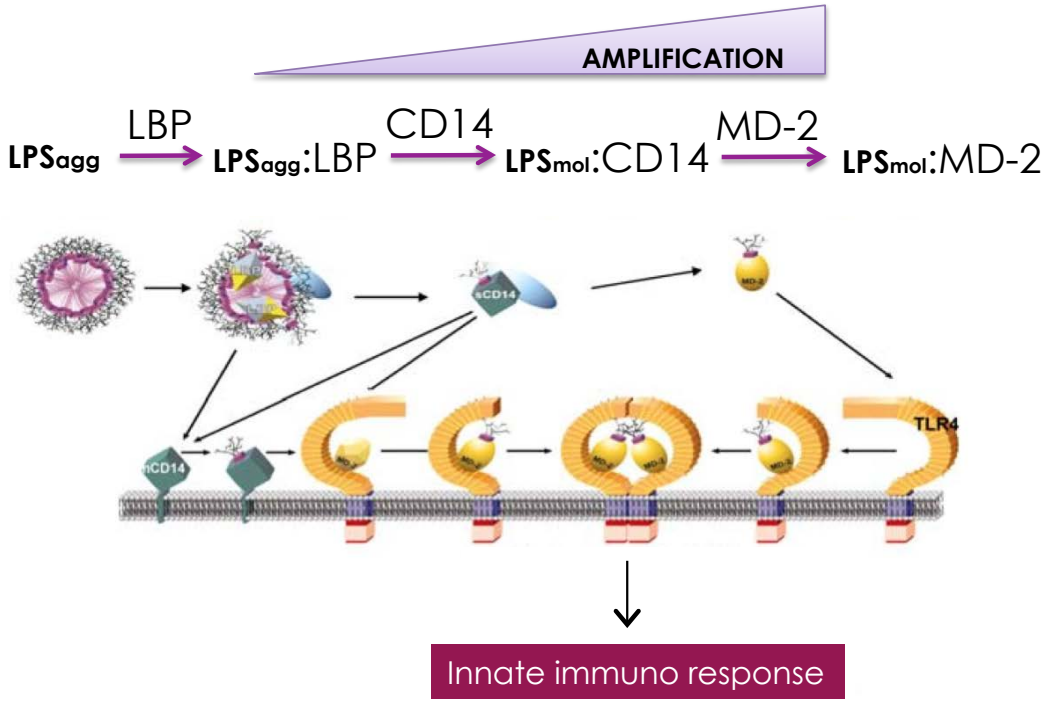

Figure 1.15. | Model for LBP/CD14/MD-2-dependent transformation of endotoxin promoting TLR4-dependent cell activation by LPS. This ordered reaction pathway reflects the fact that whereas LBP, CD14, and MD-2 are each endotoxin-binding proteins, optimal interactions of these proteins with LPS requires presentation of LPS in markedly different biochemical and physical contexts. Thus, LBP interacts most efficiently with LPS-rich interfaces (e.g., Gram-negative bacterial OM, purified endotoxin aggregates, here as "LPS aggregates"), CD14 with LBP-modified LPS-rich interfaces, and MD-2 with monomeric LPS:CD14 complex. LBP-induced changes in LPS-rich interfaces catalyze extraction and transfer of LPS monomers by CD14, yielding a monomeric LPS:CD14 complex. Once monomeric LPS:CD14 is formed, transfer of endotoxin to MD-2— either present alone or pre-associated with TLR4—is very facile, with a "Km" for transfer of endotoxin from CD14 to MD-2 (TLR4) of 100 ~ pM (from Gioannini *et al.,* 2007 modified).

THE PRESENT INVESTIGATION

This chapter is intended to discuss results and technical procedures presented in the following publications:

- **PAPER 1** — Sperandeo, P., **Villa, R.**, Martorana, A. M., Samalikova, M., Grandori, R., Deho, G., & Polissi, A. (2011). "New Insights into the Lpt Machinery for Lipopolysaccharide Transport to the Cell Surface: LptA-LptC Interaction and LptA Stability as Sensors of a Properly Assembled Transenvelope Complex. *Journal of bacteriology*, *193*(5), 1042–1053. doi:10.1128/JB.01037-10. (**see attached**)
- **PAPER 2 — Villa, R.,** Martorana, A. M., Gourlay, L. J. Sperandeo, M. Bolognesi, P., Kahne, D., & Polissi, A. (2012). Characterization of Functional Domains in LptC, a Conserved Membrane Protein Implicated in LPS Export Pathway in *Escherichia coli*. Paper draft. (**see attached**)
- **BOOK CHAPTER** — Sperandeo, P., **Villa, R.**, Deho, G., & Polissi, A. (2012). "The outer membrane of Gram-negative bacteria: lipopolysaccharide biogenesis and transport" book chapter from "Bacterial Membranes: Structural and Molecular Biology" edited by H. Remaut, R. Fronzes, Orizon/Caister Pubblication. In press.

2.1 Aim of This Study

The hallmark of Gram-negative bacteria is their cell envelope, which is composed of two membranes, the inner or cytoplasmic membrane (IM), and the outer membrane (OM), separated by a compartment (the periplasm) that contains a thin peptidoglycan layer.

Lipopolysaccharide (LPS) is the major component of the OM, and it acts as a selective barrier together with the OM proteins (OMPs), preventing the entry of many toxic molecules into the cell. Despite the structure and composition of OM have been elucidated in pivotal studies in the 50s and in the 70s, the factors required for the assembly of this organelle have only recently been identified.

The aim of this study is first to characterize by structure-function analyses, the molecular role of LptC and LptA, two key proteins involved in LPS transport to the OM, and secondly to understand how LPS is sorted to the OM.

Major results are reported below:

LptC is single-pass IM protein with a large periplasm-protruding region. LptC single mutants were obtained in this work by random-mutagenesis, and used *in vivo* and *in vitro* experiments to characterize two regions of the protein that distinctly interact with LptA and the IM protein complex LptBFG, respectively (**Paper I and Paper II**).

Chimera versions of LptC, either missing the transmembrane (TM) sequence, or with the IM anchor substituted by a heterologous sequence, were constructed and characterized to understand the role of TM region (**Paper II**).

A rapid bioinformatic tool, which has been implemented to discover the molecular determinants of LptA for the interaction with LPS, is also presented (**Ongoing work**).

The seven Lpt proteins physically interact and form a transenevlope complex (Chng *et al.*, 2010a), we demonstrated that when either LptC or other components of the LPS transport pathway are mutated or depleted, LptA is degraded: so that LptA stability can be used as a sensor of a properly assembled complex (**Paper I**).

Genetic evidences previously obtained in our laboratory together with the data presented in this thesis strongly support the LPS transport machinery model defined as the trans-envelope complex by Chng and coworkers (Chng *et al.,* 2010a). We show that LptA interacts both with the IM and the OM protein complexes (LptBCFG and LptDE respectively), bridging them together (**Paper I** and **Paper II)**.

Finally, in support of the transenvelope model, a phylogeny and structural motif conservation analysis of the Lpt components has been performed. Results suggest that the unique structural domain retained in these proteins—despite the low sequence similarity—is the key to make possible the interaction between all the Lpt components (**Book chapter**).

2.2 LptC and LptA Interaction: the Heart Inside the LPS transport Machinery

Paper I

LPS is synthesized in the cytoplasm and is flipped from the inner to the outer leaflet of the IM by the essential ABC transporter MsbA (see Introduction for further details). The mature macromolecule is then transported to the outer leaflet of the OM by a protein machine composed of seven recently discovered Lpt proteins (see introduction and Fig. 2.1) suggested to build up the so-called Lpt complex, that spans the bacterial cell envelope. Genetic evidence suggests that the Lpt complex operates as a single device, since the depletion of any component leads to similar phenotypes, namely, failure to transport newly synthesized LPS to the cell surface and its accumulation at the outer leaflet of the IM (Ma *et al.*, 2008; Ruiz *et al.*, 2009; Sperandeo *et al.,* 2008). The LPS accumulating at the outer leaflet of the IM is decorated with colanic acid residues, and therefore this modification is diagnostic of defects in transport occurring downstream of the MsbA-mediated flipping of LPS to the periplasmic face of the IM (Sperandeo *et al.,* 2008).

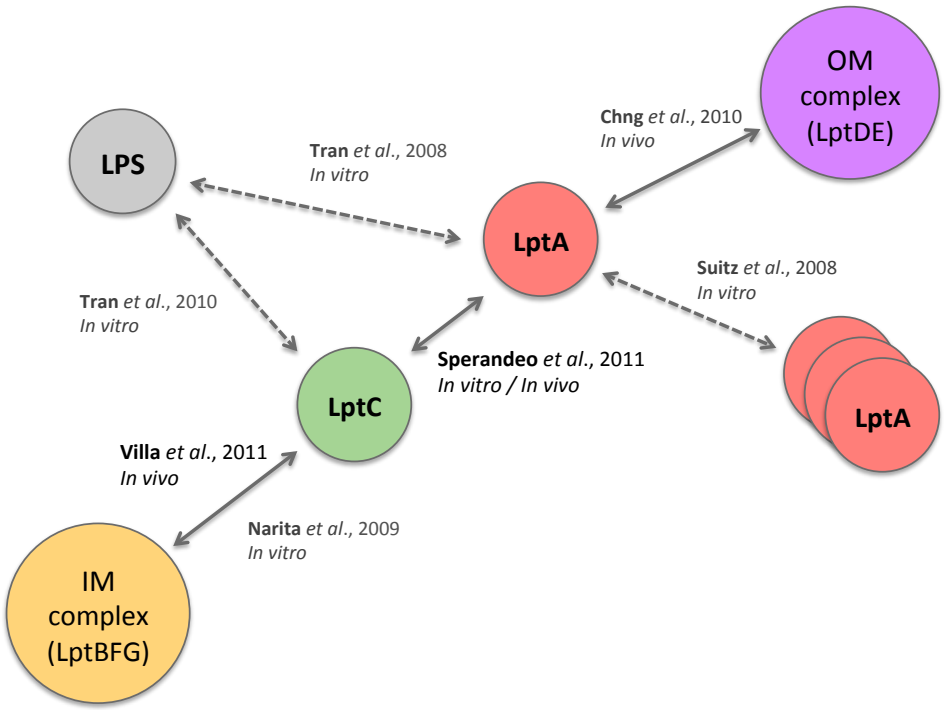

Figure 2.1 | The intricate Lpt protein interactome. LptDE constitute the OM complex which make LPS flip through the membrane and reach its final destination. Kahne and Silhavy laboratories demonstrated that LptE is necessary for the correct folding of LptD, thus both proteins are required for a proficient OM proteinaceous complex (Chng *et al.,* 2010b; Freinkman *et al.,* 2011). LptA is a periplasmic protein as demonstrated by Sperandeo and co-workers (Sperandeo *et al*., 2007), which was also co-localized at both IM and OM (Chng *et al.,* 2010b). Cristal structure of LptA was solved as monomer and multimer, indeed addition of LPS during crystallization process triggers LptA fiber formation (Suits *et al.,* 2009). Both LptA and LptC bind LPS *in vitro* (Tran *et al*., 2008, Tran *et al.,* 2010). The stoichiometry of the IM protein complex LptBCFG was solved in Tokuda's laboratory as 2:1:1:1 (Narita and Tokuda, 2009). LptC interacts with LptA as demonstrated in Sperandeo *et al*., 2011 paper, presented in this work.

Physical interaction between the several components of the machinery has been demonstrated for LptDE, which form a complex at the OM (Wu *et al*., 2006).

LptD and LptE are responsible for the LPS assembly at the cell surface; LptE stabilizes LptD by interacting with its C-terminal domain, whereas LptE binds LPS, possibly serving as a substrate recognition site at the OM (Chng *et al.,* 2010b). On the other hand, Narita and coworkers reported that both the IM spanning proteins LptF and LptG form a complex with the cytoplasmatic protein LptB. The IM protein LptC, was also included in this ABC transport complex LptBCFG in a stoichiometry of 2:1:1:1, although LptC seems not to be required for the ATPase activity of the transporter (Narita and Tokuda, 2009).

Previous work by our and other laboratories (Sperandeo *et al.*, 2007; Tran *et al.,* 2008) suggested that LptA expressed from an inducible promoter has a periplasmic localization. However, evidence of physical interaction between the seven Lpt proteins has been recently reported and LptA has been shown to associate with both IM and OM (Chng *et al.,* 2010a).

Since the bitopic IM LptC protein possesses a large C-terminal periplasmic domain (E26-P191) (Tran *et al.,* 2010), we hypothesized that LptA binding to the IM could be mediated by LptC.

To address this issue, we probed the interaction between LptA and LptC by affinity purification followed by immunoblotting. A C-terminal His tagged version of LptC (LptC-H) overexpressed ectopically in the wild-type strain AM604 was used as bait in co-purification experiments. To detect possible weak or transient interactions, *in vivo* cross-linking using dithiobis(succinimidyl) propionate (DSP) (Zgurskaya *et al.,* 2000) was also performed. As shown in Fig. 2.2, LptA co-purifies with LptC-H even when DSP was not added to the cells overexpressing LptC-H, suggesting a stable LptA-LptC interaction. When samples treated with DSP were not reverted by a reducing agent, high-molecular-weight bands appeared (Fig. 2.2, upper and lower panels, bands C1 and C2). C1 may correspond to an LptA-LptC complex, whereas the C2 band that appears only in the lower panel might correspond to an LptC-LptC complex, as inferred by the molecular weight. These data suggest that LptA and LptC interact and form a stable complex.

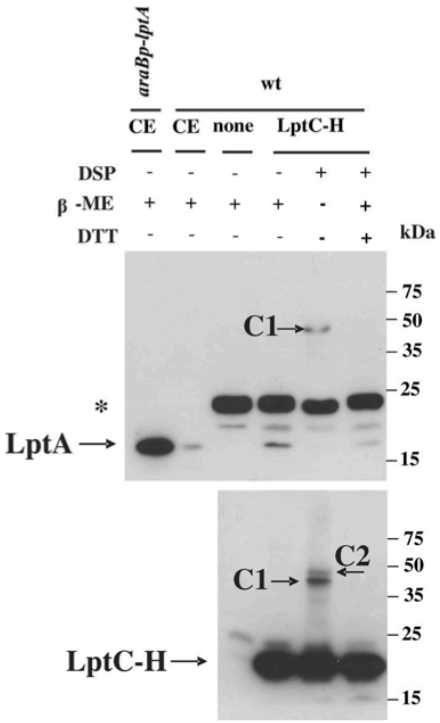

Figure 2.2 | LptA interacts with LptC *in vitro*. Affinity chromatography experiments were performed in the presence/absence of DSP in AM604/pGS108 overexpressing LptC-H (wt/LptC-H) and AM604/pRSET (wt/none) expressing the His tag element only, as a negative control. LptA and LptC were detected in Ni-NTA column-enriched fractions by Western blot analysis with anti-LptA antibody and His- Probe-HRP, respectively. LptA detected in crude cell extract (CE) of AM604 (wt) and of FL907 mutant overexpressing LptA (*araBplptA*) was used as a marker. Samples were treated with (DTT) and/or β-mercaptoethanol (β-ME) to revert the cross-linking. Equal amounts of protein were loaded into each lane. C1 and C2, high-molecular-weight complexes. The SlyD protein of 24 kDa cross-reacting with anti-LptA antibodies is labeled (*).

2.3 Discovering functional domains in LptC

Paper I /Paper II

Isolation of inactive lptC mutant alleles. To better characterize LptA-LptC interaction and to define the molecular role of LptC in LPS transport, we searched for point mutations that inactivate LptC function. Random mutations were introduced by error-prone PCR into *lptC* carried by pGS103, and the mutagenized plasmids were tested for complementation of LptC-depleted cells. Briefly, LptC depletion strain FL905 was transformed with the mutagenized plasmids in the presence of arabinose, and plasmids unable to support FL905 growth in the absence of arabinose were isolated. Of 1,664 transformants analyzed, we obtained 21 clones unable to fully complement FL905 in the non-permissive conditions. Most non-complementing clones harbored multiple mutations, as assessed by sequencing the mutant alleles.

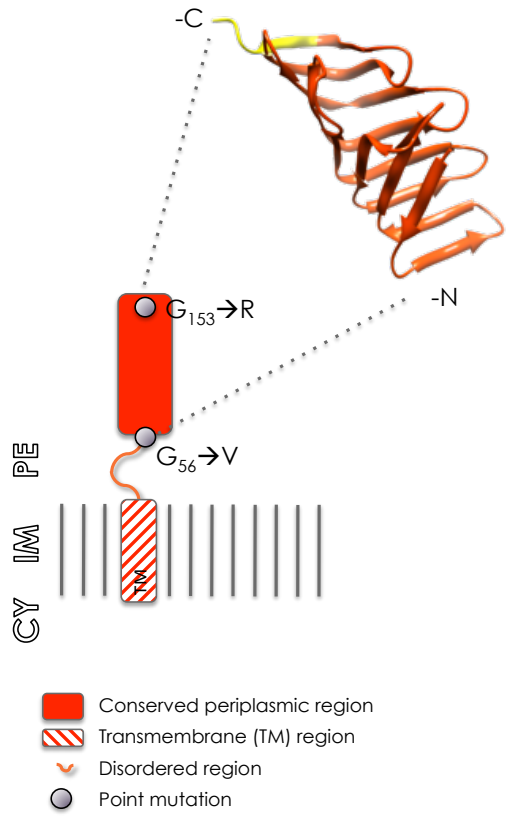

Nevertheless, three single mutations were selected: G56V, G153R, and K177Stop (which generates a truncated protein lacking the C-terminal 15 amino acids [Δ177-191]) (see table 2.1). FL905/pGS103Δ177-191 and FL905/pGS103G153R growth was completely inhibited on agar medium in the absence of arabinose, whereas FL905/pGS103$_{G56V}$ growth was severely impaired in the absence of arabinose and the mutant formed "dust-like colonies" in this condition (Fig. 2.5A).

Figure 2.3 | LptC structure and topology. LptC is a bitopic IM protein. It possesses a large C-terminal periplasmic domain (T30-P191), composed by a conserved region, which was recently crystallized (PDB 3MY2, S59-P191) (Tran *et al.*, 2919), and a disordered portion linked to a transmembrane (TM) anchor. G56V and G153R point mutations are indicated. K177stop mutation generates a truncated protein lacking the C-terminal 15 amino acids colored in yellow.

Table 2.1

Plasmid	Nucleotide change	Amino acid change
pGS103$_{G56V}$	GG^{167}G→GTG	G56V
pGS103$_{G153R}$	G^{457}GA→AGA	G153R
pGS103$\Delta_{177\text{-}191}$	A^{529}AG→TAG	K177 Stop-codon

The mutations described above fall in conserved regions of the protein as depicted in figure 2.3, and indicated by the sequence alignments of LptC orthologues from several proteobacteria (Fig 2.4).

Effects of different *lptC* alleles on LPS transport. Depletion of any Lpt protein leads to the production of LPS decorated by colanic acid; this phenotype is diagnostic of defects in LPS transport occurring downstream of the MsbA-mediated flipping of lipid A-core to the periplasmic face of the IM (Sperandeo *et al*., 2008). We therefore analyzed the LPS profile in *lptC* mutant strains. The total LPS was extracted from nondepleted and LptC-depleted FL905 strain complemented with wild-type and mutant *lptC* alleles, and the LPS profiles were analyzed as described previously (Sperandeo *et al*., 2008). As shown in Fig. 2.5C, LPS decorated with colanic acid could be detected in LptC-depleted FL905 complemented by each of the mutant alleles but not by wild-type *lptC*, indicating that each of the above LptC mutations impair LPS transport.

Stability of the LptC mutant proteins. To assay the stability of LptC mutant proteins, we examined the level of ectopically expressed LptC-H (which can be distinguished from the endogenous wild-type protein) and its mutant derivatives in the wild-type strain AM604 upon induction with IPTG, assuming that the level of *de novo*-synthesized proteins correlates with their stability. It should be noted that in these conditions the chromosomal wild-type copy of lptC is expressed from its natural promoter. Detection of the proteins using HisProbe-HRP revealed that the level of LptCG56V-H was comparable to that of LptC-H and only the basal level (before IPTG induction) of LptCG153R-H was affected, suggesting that this protein is only slightly unstable (Fig. 2.5B). On the contrary, the level of LptCΔ177-191-H protein was severely reduced under these conditions, indicating that the truncated protein is intrinsically unstable.

Figure 2.4 | Alignment of the sequences of selected LptC homologues in most representative γ-proteobacteria. Residue numbering corresponds to LptC from *Pseudomonas aeruginosa* (without gaps). Alignment was performed with MultAlin available on the web. Residues with high sequence identity or similarity are colored in red and orange, respectively. Non-conserved residues are shown as gray letters. Strains selected: *Escherichia coli*; *Salmonella enterica* (*Choleraesuis str.* SC-B67); *Pectobacterium atrosepticum* SCRI1043; *Yersinia enterocolitica subsp. Enterocolitica*; *Photorhabdus luminescens subsp. Laumondii* TT01; *Haemophilus influenzae* 86-028NP; *Actinobacillus pleuropneumoniae* L20; *Vibrio Cholerae* O1 *biovar El Tor* str. N16961; *Shewanella sp.*; *Pasteurella multocida*; *Pseudomonas aeruginosa* PAO1; *Aeromonas salmonicida salmonicida* A449; *Legionella pneumophila Corby*. Red triangles indicate G56V, G153R and K177 residues.

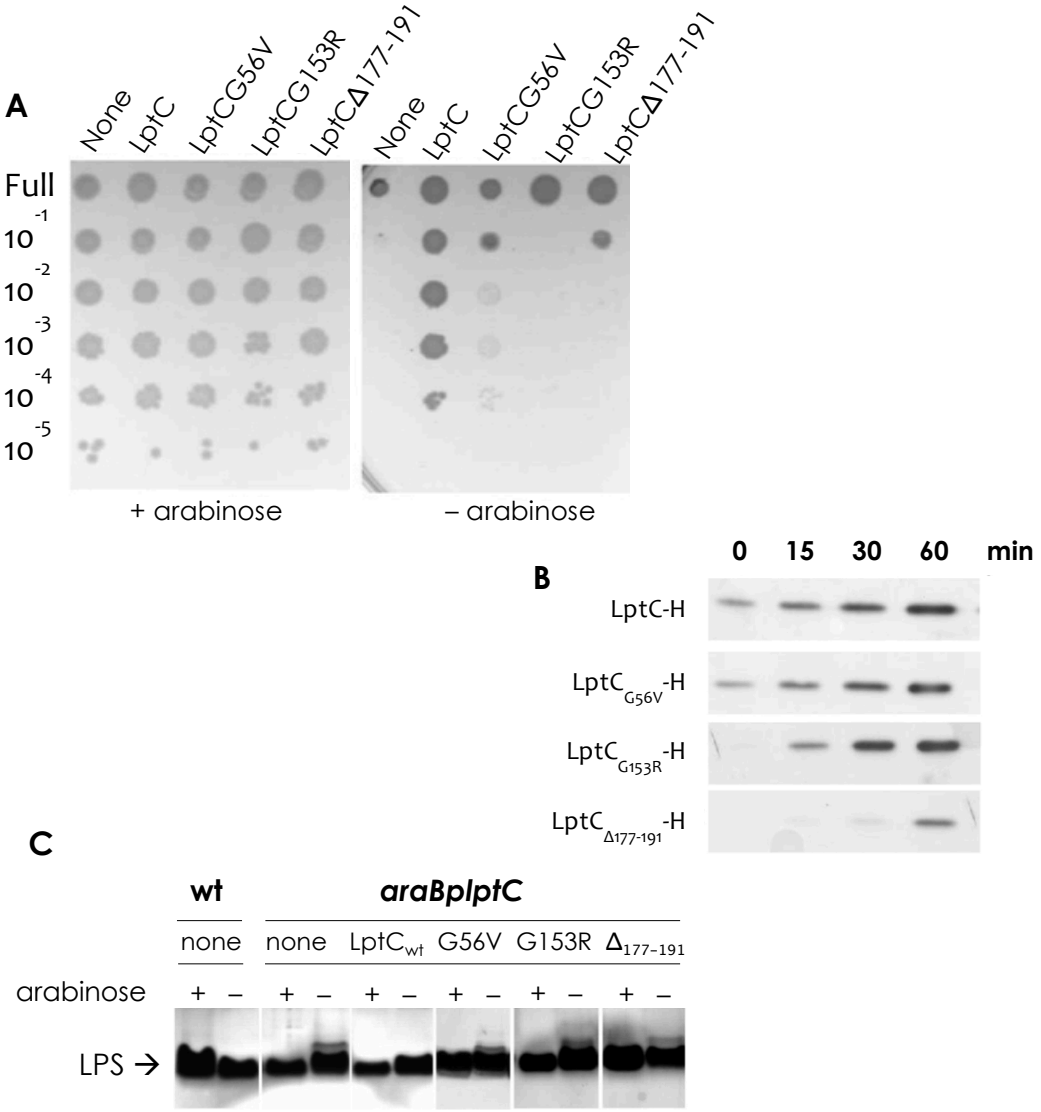

Figure 2.5 | Characterization of LptC mutants. (A) Plating efficiency of FL905 (*araBplptC*) transformed with plasmid pGS103 carrying the wild-type protein (LptC and LptC-H, respectively), or plasmids carrying the LptC mutated proteins LptCG56V, LptCΔ177-191, LptCG153R, or plasmid pGS100 (none), in agar plate containing chloranphenicol supplemented (+) or not (–) with arabinose. Serial dilutions are given on the left side of the panel. (B) LptC mutant stability *in vivo*. AM604 cells harboring pGS108 (LptC-H), pGS108G56V (LptCG56V-H), pGS108G153R (LptCG153R-H), and pGS108Δ177-191 (LptCptCΔ177-191-H) were grown to the early logarithmic phase. Expression of LptC-H or its mutant forms were induced by the addition of 0.1 mM IPTG. Samples for the protein analysis were obtained 0, 15, 30, and 60 min post-induction and analyzed using HisProbe-HRP. Equal amount of cells (0.12 OD_{600} units) was loaded into each lane. (C) cultures of AM604 (wt), FL905 (*araBplptC*) strains and FL905 carrying plasmids expressing $LptC_{wt}$, $LptC_{G56V}$, $LptC_{G153R}$, and $LptC_{\Delta177-191}$ grown exponentially in LD containing arabinose were harvested, washed, and subcultured in arabinose-supplemented (+) or arabinose-free (-) medium. Samples for LPS analyses were taken from cells grown at 240 (AM604, FL905, and FL905/p$LptC_{wt}$) or 270 min (FL905/pGS103G56V, FL905/pGS108G153R, and FL905/pGS103Δ177-191) after the shift into fresh medium. LPS extracted from cultures with a total OD_{600} of 2 were separated by Tricine-SDS-PAGE and silver stained.

Additionally, to ensure that overexpression of the mutants LptC56V and LptCG153R does not restore growth of *araBplptC* cells in non-permissive condition, FL905 strain was transformed with pGS108LptC, pGS108G56V, pGS108G153R and grown in both presence and absence of arabinose, upon induction of IPTG. Both LptCG56V and LptCG153R are not able to restore growth of LptC-depleted cells, even at the highest concentrations of IPTG, interestingly LptCG153R is toxic even when co-expressed with the chromosomal wild-type copy of LptC (permissive condition). Since LptC is part of a multiprotein complex these data suggest that different mutations cause different defects in the LPS transport, for this reason they can be further exploited in order to dissect functional domains of LptC.

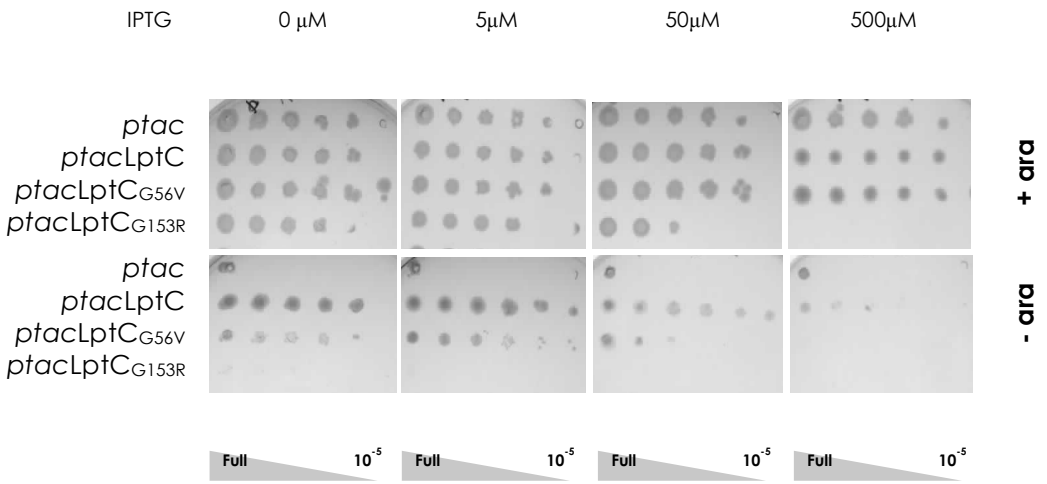

Figure 2.6 | Overexpression of LptCG56V and LptCG153R mutants could not restore the wild-type phenotype. Serial culture dilutions of *araBplptC* strain (FL905) transformed with void plasmid (ptac), ptacLptC, ptacLptCG56V, or ptacLptC153R, are replicated on agar plates supplemented with/without arabinose (+ara/-ara) and several concentrations of IPTG as indicated. Approximate dilutions are given below.

The C-terminal region of LptC is required for LptA binding. To test whether the G56V, and G153R mutations could affect LptC interaction with LptA, we compared the wild-type and the mutant proteins for their ability to co-purify LptA. Whole-cell extracts of the wild-type strain AM604 overexpressing LptC-H or the mutant His-tagged derivatives (LptCG56V-H and LptCG153R-H) were subjected to lysis, solubilization with strong synthetic zwitterionic detergent (ZW3-14), and affinity

purification. LptA and LptC-H were detected by Western blotting with anti-LptA antibodies and HisProbe-HRP, respectively.

As shown in Fig. 2.7, LptCG56V-H retained the ability to co-purify LptA, whereas the mutation in the LptC C-terminal region (G153R) severely impaired LptA-LptC complex formation.

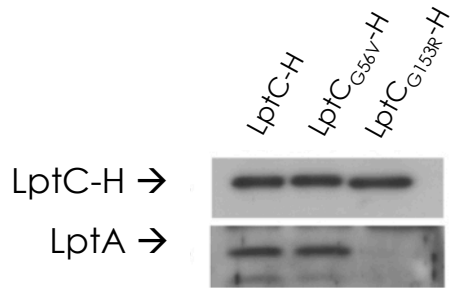

Figure 2.7 | Effect of *lptC* mutations on LptC-LptA interaction. Whole-cell extracts from AM604 cells transformed with pGS108 plasmid carrying the wild-type protein (LptC-H) or the LptC-mutated proteins LptCG56V-H and LptCG153R-H, were subjected to affinity chromatography. Equal amounts (2.5µg) of Ni-NTA column-enriched LptC-H and LptCG56VH its mutant versions were separated by SDS-12.5% PAGE and analyzed by Western blotting with anti-LptA antibody and HisProbe-HRP, respectively.

Glycin 56 is required for Lpt IM complex binding.

LptC is a component of the IM protein complex LptBFG (Narita and Tokuda, 2009), and anchored to the membrane by a single pass helix. To determine which region of the protein is involved in the interaction with LptBFG complex, LptC-H or its his-tagged mutant versions expressed by pET23/42 vector in a wild-type background (AM604) were assayed in tandem co-purification and immunoprecipitation experiments which were previously developed to demonstrate that all the Lpt proteins constitute a trans-envelope complex (Chng *et al*., 2010a). Cell lysates were French-pressed and only total membranes were collected and solubilized by an anionic surfactant (n-lauroylsarcosine). Solubilized membranes were subjected to affinity purification, and immunoblotted using LptD, LptE, LptA and LptC anti-sera (Fig. 2.8, A), or incubated with anti-his antibodies and immunoprecipitated (Fig. 2.8,B). As LptB, LptF and LptG anti-sera are not available, they were fixed and stained on PAA gels (Fig. 2.8, B) and the corresponding bands confirmed by mass analysis.

LptC mutant versions were assayed to test their ability to pull-down the other components of the Lpt trans-envelope machinery. Both LptCG56V and LptCG153R are able to co-purify the OM protein complex LptDE. Surprisingly LptGG153R is able to co-purify LptA (these apparently conflicting data are explained further on). On the other hand, only LptC G153R copurifies the IM protein complex LptBFG, whilst LptCG56V fails to interact with the other IM spanning proteins LptF and LptG, suggesting that an intact N-terminal periplasmic region of LptC is required to interact with the other IM components.

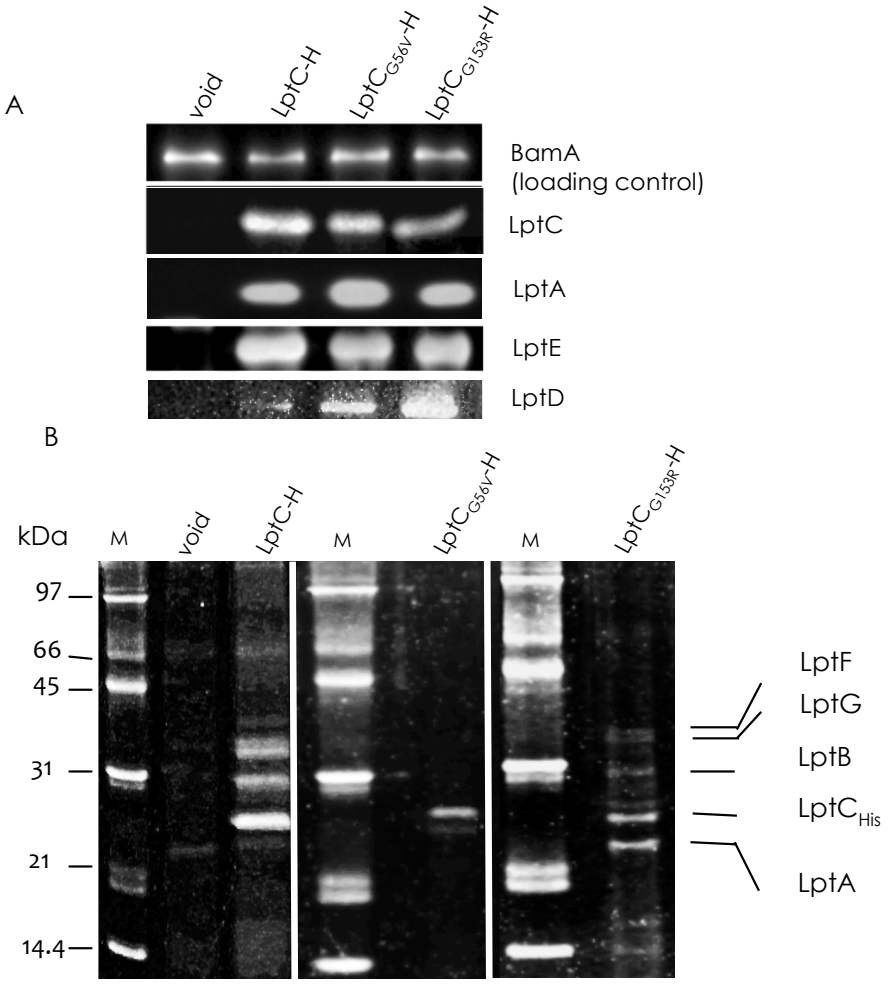

Figure 2.8 | Tandem affinity purification and immunoprecipitation of LptCG56V and LptCG153R. Membrane extracts from wild-type strain AM604 expressing his-tagged pLptC, pLptCG56V and pLptCG153R were affinity purified. Samples were then either subjected to immunoblotting with LptD, LptE, LptA and LptC anti-sera (Panel A), or incubated with anti-his antibodies and immunoprecipitated (Panel B). As LptB, LptF and LptG anti-sera are not available, proteins were fixed, stained on PAA gels (Panel B), and the identity of the corresponding bands was confirmed by mass spectrometry analysis.

Effect of LptCG153R allele on Lpt complex.

C-terminal region of LptC is required to efficiently bind LptA (Sperandeo *et al.*, 2011), despite this fact, all the Lpt machinery components are recruited when $LptC_{G153R\text{-}H}$ is used as bait in affinity purification experiments of total membranes extracts subjected to solubilization as seen in figure 2.8.

It has been recently showed that the seven Lpt proteins physically interact and constitute a trans-envelope complex (Chng *et al*., 2010a), moreover *in vivo* LptA level can be used as sensor of properly assembled machinery. For this reason we determined the steady-state level of LptA and LptE, the latter as representative of the LptDE OM complex.

The LptC depletion strain FL905 and its derivatives harboring pGS103, pGS103G56V, pGS108G153 and pGS103Δ177-191, were grown to the exponential phase and shifted into a medium lacking arabinose (non-permissive condition) to deplete the chromosomally encoded LptC wild type, while allowing expression of the mutant proteins. Samples were then taken from cultures grown in the presence or absence of arabinose for 240 min (AM604, FL905, and FL905/pGS103) or 270 min (FL905/pGS103G56V, FL905/pGS103Δ177-191, and FL905/pGS108G153R) after the shift to non-permissive conditions (Fig. 2.9) and analyzed by Western blotting with anti-LptA, anti-LptC, and anti-LptE antibodies.

The level of physiologically expressed LptC seemed very low since the protein was undetectable in the wild-type strain with our antibody preparation. However, LptC was detected when ectopically expressed from a plasmid or from the *araBp* promoter (Fig. 2.9). In FL905 cells expressing LptCG56V and LptCG153R, the level of the mutant proteins was comparable under permissive and non-permissive conditions, whereas LptCΔ177-191 was undetectable in the non-complemented strain.

In the LptC depletion strain FL905 grown in the presence of arabinose, *lptA* is expressed from the upstream *araBp* promoter, and the level of LptA is higher than in the wild-type AM604 strain, where the protein is expressed from its natural promoter (Sperandeo *et al.,* 2008). Interestingly, the level of LptA in LptC depleted cells expressing either LptCG56V or LptCG153R was similar to that observed in the positive control (FL905 complemented by wild-type LptC). The abundance of LptE did not substantially change upon depletion of LptC with or without overexpression of any mutant LptC, indicating that the steady-state level of the OM component LptE was not influenced by LptC depletion or mutations. On the contrary, in non-complemented LptC depleted cells, and in cells ectopically expressing LptCΔ177-191

LptA was undetectable. It thus appears that the absence of LptC protein caused by either depletion (non-complemented LptC depleted cells) or mutation (LptC depleted cells expressing LptCΔ177-191) induces LptA destabilization. Interestingly, LptA level seems not affected in LptC depleted cells expressing LptCG153R. This is in line with the result obtained from co-purification experiments of solubilized membranes (Fig. 2.9).

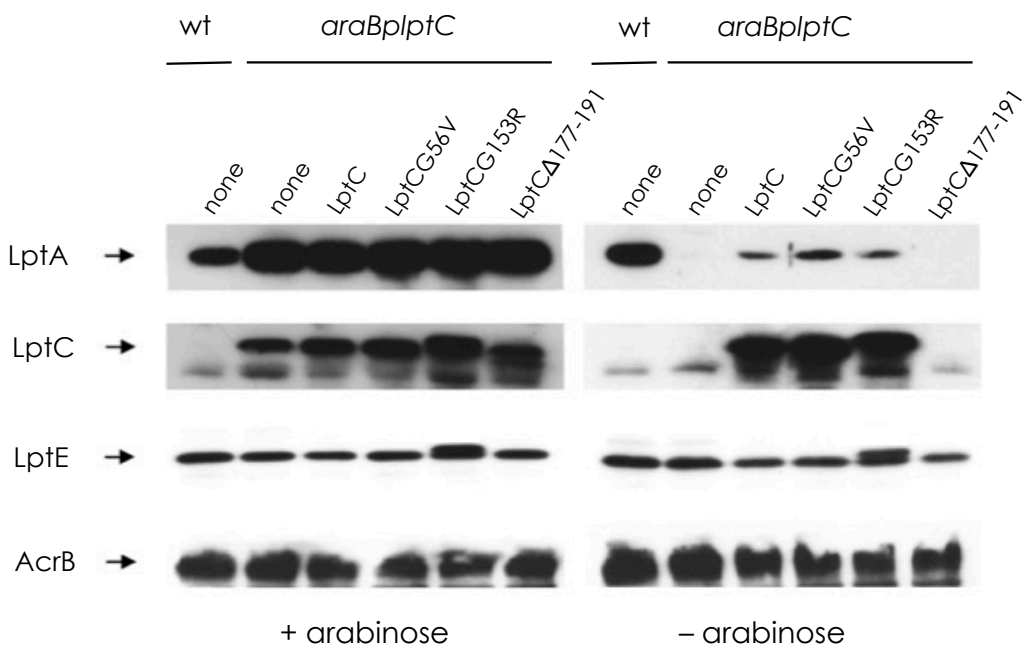

Figure 2.9 | Effect of lptC mutations on Lpt proteins complex. (A) Growth cultures of AM604 (wt), FL905 (*araBplptC*) strains and FL905 carrying plasmids expressing LptC, LptCG56V, LptCG153R, and LptCΔ177-191. Cells growing exponentially in LD containing arabinose were harvested, washed, and subcultured in arabinose-supplemented or arabinose-free medium (+ arabinose, - arabinose respectively). Growth was monitored by measuring the OD_{600}. Samples for protein analyses were taken from cells grown in the presence or absence of arabinose at 240 (wt, FL905, and FL905/pGS103LptC) or 270 min (FL905/pGS103G56V, FL905/pGS108G153R, and FL905/pGS103Δ177-191) after the shift into fresh medium. Protein samples were subjected to Western blot analysis with anti-LptA, anti-LptC, anti-LptE, and anti-AcrB (as a loading control) antibodies. Equal amounts of cells, based on the OD measurement, were loaded into each lane.

LptCG153R crystal structure retains a wild-type fold. Despite LptCG153R is defective in LPS transport, this mutant version of the protein is stable, and apparently able to efficiently pull-down the other proteins of the complex, and *in vivo* level of LptA suggests that the interaction with its partner LptA is not destabilized.

Finally, in collaboration with Professor Bolognesi's laboratory, LptCG153R crystal structure has been solved showing a wild-type tridimentional conformation (Fig. 2.10).

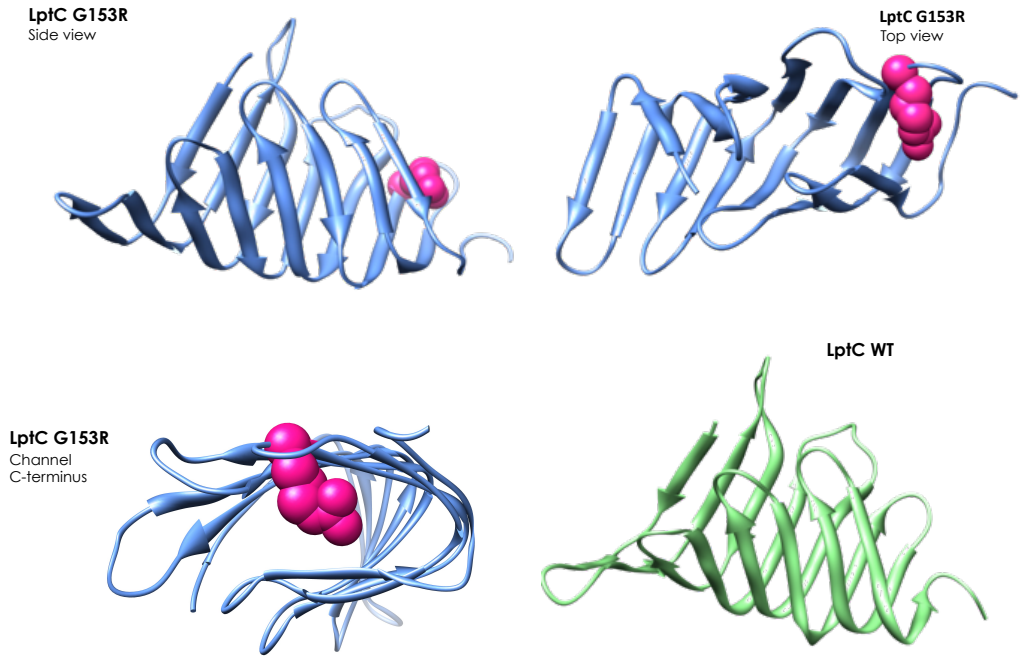

Figure 2.10 | LptCG153R crystal structure. The LptCG153R crystal structure (blue) was solved and compared to wild-type protein (green). Arginine residue is depicted in pink, considering its steric hindrance.

The presence of glycine residues may confer to a polypeptide chain a considerable degree of flexibility and internal rotation, since —wherever a glycine residue occurs, a hydrogen atom is taking the place of a more complex side chain. Accordingly, the presence of glycine residues, and their distribution along the protein backbone, may be factors influencing and determining the specific pattern of folding of polypeptide chains. The proper distribution of glycine residues would permit any combination of side chains, which otherwise, would have to be excluded because of steric hindrance. That is, another amino acid in place of glycine could determine

steric interference, like valine and arginine, which substitute Gly56 and Gly153 in selected mutants, respectively.

In particular, Gly153 is located in a short loop connecting the thirteenth and fourteenth beta-strands at the C-terminus of the protein. As protein interaction is a dynamic process, the presence of an arginine in place of a glycine might interfere in conformational change, freezing the protein in a state, which likely either disrupts any possible interaction or blocks interacting partners in a bound state. In other words, the possibility that the Lpt complex is still assembled but not functional needs be taken into account. Interestingly, LptCG153R is the only mutant toxic to the cell when expressed in presence of a wild-type copy of the protein (See Fig. 2.6 "+ara" panel).

On the contrary co-purification experiments from total cell extracts previously described, have shown that G153R substitution disrupts LptC-LptA interaction when the proteins are incubated with a strong solubilizing switterionic agent (Paper I). These apparent conflicting results could be explained as follows: LptA may not exclusively bind LptC, indeed the periplasmic protein LptA was also localized in OM fractions (Chng *et al.*, 2010a), possibly interacting with the OM LptDE complex. Interestingly, the periplasmic region of LptD is predicted to resemble an LptA-like fold (See related paragraph "The Lpt fold as a keystone of the LPS transport machinery" ahead), suggesting that LptC could also directly interact with the OM protein complex. Once the interaction between LptC and LptA is disrupted, LptD could still be recruited by LptCG153R-H in pull-down experiments.

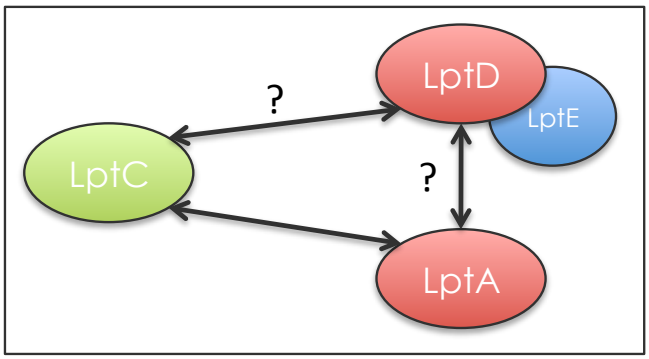

Figure 2.11 | Does LptD directly interact with LptC? We demonstrated that LptC interacts with LptA (Sperandeo *et al.,* 2011). It was also previously showed that LptA is associated to both OM and IM (Chng *et al.*, 2010b). LptA and the periplasmic region of LptD share the same structure defined as OstA domain (see PFAM repository on line an paragraph ahead), LptD could be considered as another possible interacting partner of LptC.

In addition, different procedures were used in different co-purification experiments: namely the experiments set to demonstrate LptC-LptA interaction, and pull-down of the whole trans-envelope complex. The former was performed using stronger protein extraction method, which often disrupts weak interactions as previously demonstrated (Boehning and Joseph, 2000). The latter consists in extracting and solubilizing membrane protein by an anionic detergent coupled with a disruption mechanic method by pressure, which together could preserve multi-protein complexes (Chng *et al.*, 2010a, see also Fig. 2.12).

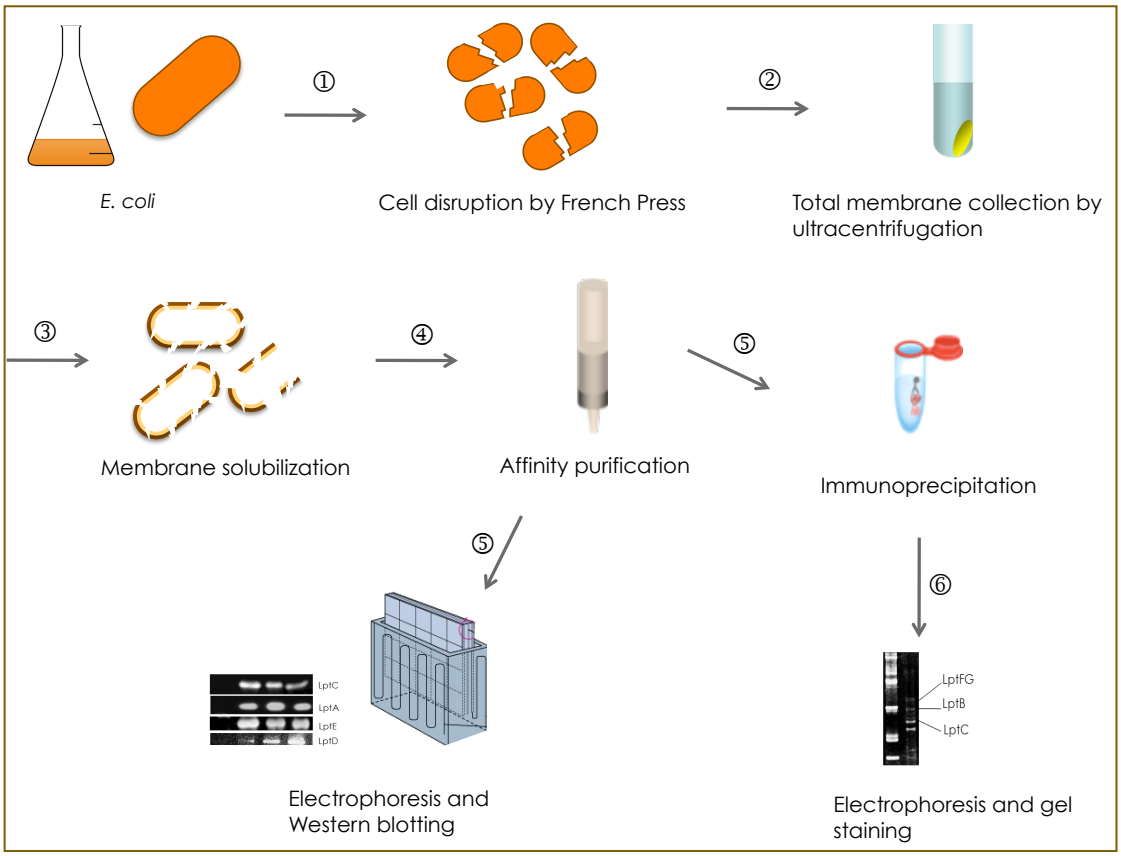

Figure 2.12 | Tandem copurification and immunoprecipitation procedure overview. AM604 (wild-type strain) and AM604 containing pET23/42LptC-H, pET23/42LptCG56V-H, pET23/42LptCG153R-H, pET23/42MalF$_{TM}$LptC-H, pET23/42MalE$_{SS}$LptC-H were processed as follows: harvested cells were lysed by a single cycle through a Cell Disrupter (French press) at 25,000 psi. Membrane pellets were then separated by ultracentrifugation and extracted at 4°C for 30 min with 1% N-Laurosylsarcosine. Solubilized membranes were subjected to affinity purification with TALON cobalt resin. Samples were then alternatively incubated with anti-his antibody and immunoprecipitated in order to detect LptB and LptFG gel bands, or immoblotted using LptA, LptC, LptD and LptE antibodies.

LptC TM region is dispensable for the interaction with Lpt complex. LptC is a bitopic protein with an IM anchor region, Narita and Tokuda demonstrated that the protein is part of the IM protein complex, LptBCFG (Narita and Tokuda., 2009). To understand the role of the IM region in LptC interactome, two chimera versions of the protein MalF$_{tm}$LptC and MalE$_{ss}$LptC, were constructed, where the IM anchor was substituted or missing, respectively. In the MalF$_{TM}$LptC construct the first TM domain of MalF is fused to the periplasmic region of LptC, in MalE$_{SS}$LptC the periplasm export sequence of MalE substitutes LptC IM anchor. MalF and MalE are an IM-spanning and a periplasmic protein, respectively, which form maltose transport system together with MalG and MalK in *E. coli* (Daus *et al.*, 2007). Chimeric genes were cloned into pGS100 vector and expressed under an IPTG inducible promoter (pGS112 and pGS114, respectively): as shown in Figure 2.13 B they are both able to complement an *araBplptC* strain (FL905) in non-permissive condition.

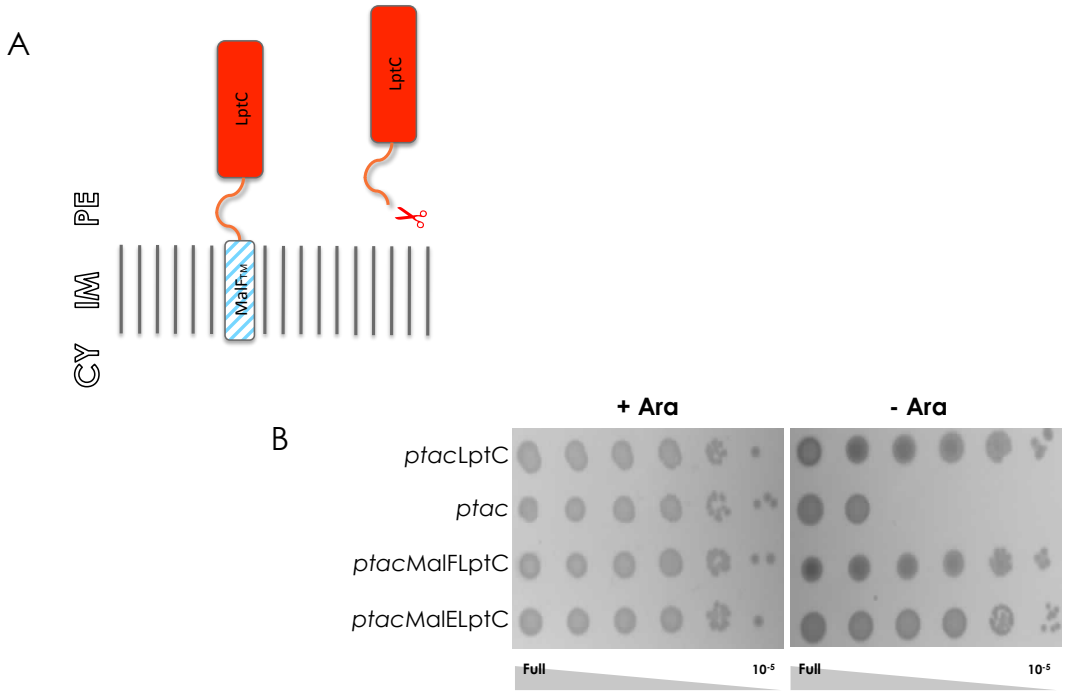

Figure 2.13 | Characterization of chimera versions of LptC. (A) MalF$_{tm}$LptC is composed by MalF TM region (aminoacids 1-36) and periplasmic region of LptC which begins from the 24th residue. MalE$_{ss}$LptC posses the MalE signal sequence for the translocation to the periplasm, composed of 26 residues, followed by the LptC periplasmic region. MalE signal sequence is not depicted as it is trimmed once the protein is translocated in the periplasm. (B) Serial culture dilutions of *araBplptC* FL905 strain transformed with void *ptac* (lane 2), ptacLptC (lane 1), *ptacMalFLptC* (lane 3), or *ptacMalELptC* (lane 4), are replicated on agar plates supplemented with/without arabinose (+Ara/-Ara). Approximate dilutions are given below.

It is known to us that *lpt* genes mutations as well as their non physiological expression could alter the OM permeability, as LPS likely fails to be correctly inserted in the outer leaflet of the membrane. (Ruiz *et al.,* 2006; Sperandeo *et al.,* 2006; Chimalakonda *et al*., 2011). To test if chimeric mutants here presented display defects in OM permeability, FL905 transformed with pGS112 and pGS114 were subjected to serial dilutions on agar plates in non permissive condition, supplemented with several hydrophobic antibiotics such as rifampicin, bacitracin or novobiocin, which have different intracellular targets but are normally blocked by a functional OM barrier formed by LPS.

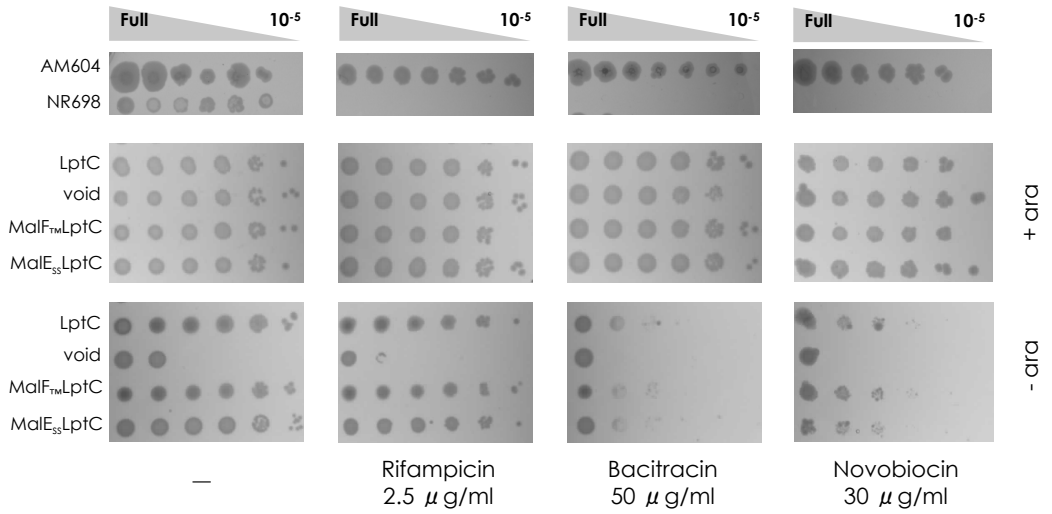

Figure 2.14 | Sensitivity analysis of $MalF_{tm}$,LptC and $MalE_{ss}$LptC chimerae in *araBplptC* strain (FL905). Serial dilutions of *araBplptC* cell cultures transformed with void ptac plasmid pGS100 (void), ptacLptC-H, ptac$MalF_{TM}$LptC-H o ptac$MalE_{SS}$LptC-H and replicated in presence (+ara = LD, 0,2% ara, 25μg/ml cam) or absence (-ara = LD, 25μg/ml cam) of arabinose. Standard conditions (—) were additionally supplemented with rifampicin, bacitracin and novobiocin as indicated. The wild-type strain AM604 is not sensitive to the toxic compounds at the concentration selected, on the contrary NR698 strain is slightly sensitive to them. *lptD* gene in NR698 has a small in frame deletion which confers a OM permeability defect to the toxic compounds (Ruiz *et al*., 2005).

As shown in Figure 2.14, both chimeric mutants do not display sensitivity to the toxic agents in non permissive conditions as the positive control, FL905 transformed with *ptaclptC* plasmid.

To investigate if the TM region of LptC is requested for a correct Lpt machinery assembly, affinity co-purification followed by immunoprecipitation experiments were performed to test the ability of chimera versions of LptC to pull-down the IM protein complex LptBFG. Total membranes from AM604 transformed with pET23/42MalF$_{TM}$LptC-H and pET23/42MalE$_{SS}$LptC-H were solubilized and purified as previously described. Neither substitution nor removal of LptC TM anchor impairs the ability of LptC to recruit LptBFG proteins as shown in Figure 2.15.

This suggests that the TM domain might be dispensable for LptC functioning, and in the presence of both chimeric proteins the LPS transport system is correctly assembled and functional.

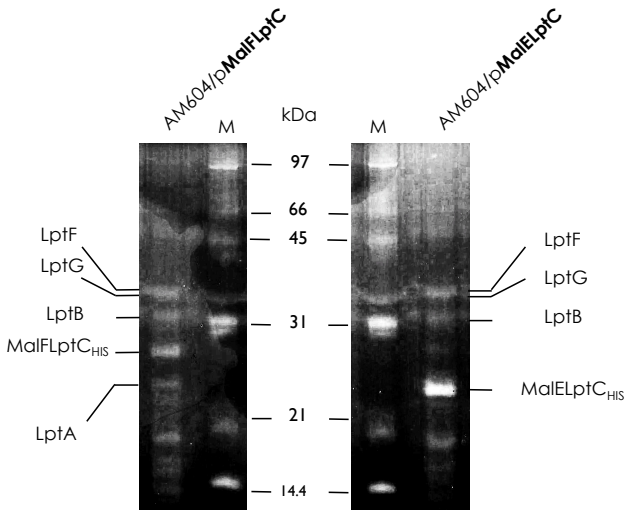

Figure 2.15 | Tandem affinity purification and IP of MalFLptC and MalELptC. Membrane extracts from wild-type strain AM604 expressing his-tagged pmalF$_{tm}$LptC, and pMalE$_{ss}$LptCG were affinity purified. Eluates were incubated with anti-his antibodies and immunoprecipitated. Samples were fixed and stained on PAA gels and then confirmed by mass analysis. M= Marker.

LptC and LptA share some properties: they have similar fold, in shape of a beta jellyroll, and bind LPS *in vitro*. Interestingly the 23 residue long anchor of LptC displays strong similarity to the signal sequence of LptA, which is trimmed once the protein correctly reaches the periplasm. *In vitro* LptA can displace LPS from LptC (but not vice versa), consistent with the location of the two proteins and their proposed

placement in a unidirectional export pathway (Tran *et al.,* 2010). LPS is flipped over the IM by the ABC transporter MsbA, LptC could then promptly bind LPS to deliver it to the other components of the Lpt machinery. Retaining a TM anchor could increase the efficiency of LptC to extract LPS from the IM, and subsequently to deliver it to the other Lpt proteins. It should be pointed out that, as inferred from *in silico* predictions, an IM anchor is not always present in LptC orthologues in Gram-negative bacteria, in line with the idea that this N-terminal peptide is not essential for LptC functioning (Fig. 2.16).

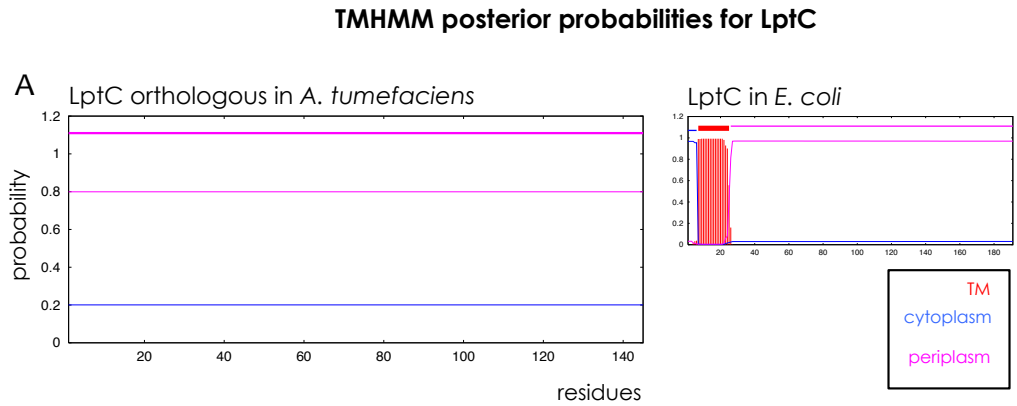

B

```
                1                                                    50
A.tumefaciens                                MMEKPAV AGRNEKGIDY SMNADRALQD
E.coli          MSKARRWVII VLSLAVLVMI GINMAEKDDT AQVVVNNNDP TYKSEHTDTL

               51                                                   100
A.tumefaciens   IANPNLMTLE KVLA--AVPV NDSVAQVIAQ EGI--FDRST NTLKMTAPFD
E.coli          VYNPEGALSY RLIAQHVEYY SDQAVSWFTQ PVLTTFDKDK IPTWSVKADK

              101                                                   150
A.tumefaciens   INLSNGIQAK FQSADVDLKA GKMSSKEPVS IKTNDGSIVA QSIDIAD---
E.coli          AKLTNDRMLY LYGHVEVNAL VPDSQLRRIT TDNAQINLVT QDVTSEDLVT

              151                                             191
A.tumefaciens   -NGKTITFSG -QVRARIAAS NIKNEGK
E.coli          LYGTTFNSSG LKMRGNLRSK NAELIEKVRT SYEIQNKQTQ P
```

Figure 2.16 | TM sequence prediction in *Escherichia coli* LptC and *Agrobacterium tumefaciens* C58 orthologous (ATU0335). (A) A Hidden Marcov Model for prediction of TM fragments (TMHMM) was applied (software available on line: www.cbs.dtu.dk/services/TMHMM/). LptC orthologous in *A. tumefaciens* seems to be anchor free. *E. coli* LptC is used as control. (B) Sequence alignment reveals that ATU0335 lacks of the first 23 residues, which constitute the IM anchor in *E. coli* LptC, as demonstrated by Tran and coworkers (Tran *et al*., 2010).

2.4 LptA as a Sensor of Lpt Machinery Properly Assembled

Paper I

As described above, the experiments reported in figure 2.9 showed that the steady-state level of LptA is affected in the absence of wild-type LptC, or by the Δ177-191 mutation, which severely impairs LptC Δ177-191 stability. It is possible that the absence of a proper IM docking site for LptA results in LptA degradation *in vivo*. Therefore, the LptA level in the cell could be diagnostic of the properly bridged IM and OM. We thus tested whether the absence of the OM LptDE complex could also exert a similar effect on LptA stability. The AM661 and AM689 strains, in which the LptD and LptE expression is driven by the inducible *araBp* promoter (Sperandeo *et al.*, 2008), were grown under permissive conditions to exponential phase and then shifted to media lacking arabinose to deplete LptD and LptE, respectively. Samples for protein analyses were taken from cultures grown in the presence or in the absence of arabinose 210 min after the shift to non permissive conditions (Fig. 2.17) and then processed for Western blot analysis with anti-LptA, anti-LptE, and anti-AcrB antibodies. As shown in Fig. 2.17 C, a lower steady-state level of LptA is observed upon LptE and LptD depletion, providing indirect evidence that LptDE complex represents the OM docking site for LptA. Overall, our data suggest that when the IM and OM docking sites are depleted, LptA is degraded. Therefore LptA abudance in the cell may be used as a marker of properly bridged IM and OM.

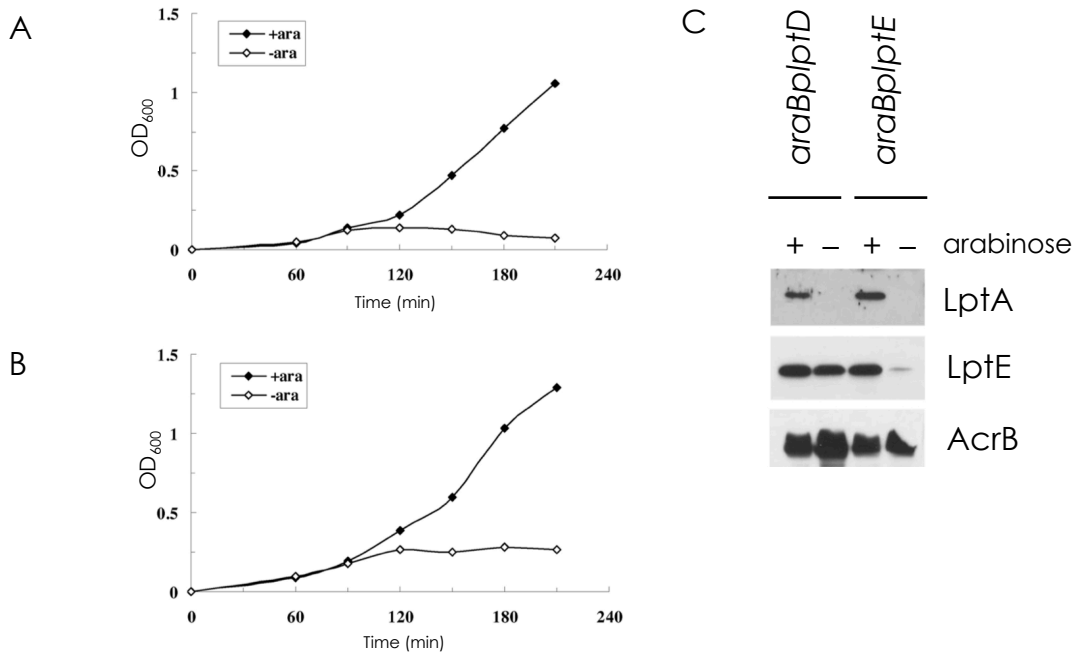

Figure 2.17 | LptA level upon LptD and LptE depletion. (A and B) Growth curves of AM661 (*araBplptD* (A)) and AM689 (*araBplptE* (B). Cells growing exponentially in LD containing arabinose were harvested, washed, and subcultured in arabinose-supplemented (+ara) or arabinose-free (-ara) medium. Growing cells were monitored by measuring the OD_{600}. (C) Steady-state levels of LptA. Samples for protein analysis taken from cells grown in the presence (+) or absence (-) of arabinose at 210 min after the shift into non permissive condition were analyzed by Western blotting with anti-LptA and anti-LptE antibodies. Equal amounts of cells (0.2 OD_{600} units) were loaded into each lane. AcrB was used as the loading control.

2.5 Searching for an *LPS-binding-domain* in Lpt Proteins

on going

LPS is a high hydrophobic macromolecule, which is never free either in the intra- or in the extra-cellular compartment (Hirschfeld *et al*., 2000). To date several proteins are known to bind LPS: they are either involved in its biogenesis, or in the innate immune response of the host, (see introduction for further details). Despite the tridimensional structure was solved for many of them, in the past years co-crystallization trials with the ligand have been figured out troublesome, due to the amphiphilic nature of lipid A —the most conserved moiety of LPS— and its tendency to aggregate.

Ferguson and collegues (Ferguson *et al*., 2000) first published the structure of the *E. coli* iron uptake receptor, FhuA, co-crystallized with LPS. This serendipity provided the very first information on a LPS-binding structural motif. It has been suggested that the LPS recognition motif consists of a geometric arrangement of four cationic residues interacting with two phosphate groups of lipid A (Fig. 2.18 and 2.19). Moreover, a search through the structural database for this motif identified a number of proteins, known to bind LPS (Ferguson *et al*., 2000).

Innate immune receptors recognize microorganism specific motifs (PAMPS) to trigger complex signaling cascades that lead to the release of pro-inflammatory cytokines (Miller *et al.,* 2005). Recognition of lipid A requires the TLR4-MD2 complex (Medzhitov *et al.,* 1997; Shimazu *et al.,* 1999), and the accessory protein CD14 (Miyake, 2006). CD14 binds LPS monomers, and transfers them to the TLR4-MD2 receptors complex (Miyake, 2006). LPS binding induces the dimerization of the TLR4/MD2 complex to form the activated hetero-tetrameric complex that initiates signal transduction (See Introduction and Fig. 2.15). MD2, which belongs to a family of lipid binding proteins, plays a key role in initial lipid A recognition by accommodating the lipid acyl chains into its large hydrophobic pocket. The two phosphate groups of lipid A bind to the TLR4/MD2 complex by interaction with positively charged residues located on both proteins (Park *et al.,* 2009).

Three components of the *E. coli* Lpt system, LptA, LptC, and LptE, bind LPS *in vitro* (Tran *et al*., 2008; Tran *et al.,* 2010; Chng *et al.,* 2010b), and the crystal structures of them (LptA, LptC), or their orthologues (LptE), have been recently solved (Suits *et al,* 2008; Tran *et al*., 2010; see also PDB ID for LptE orthologues 2JXP, 2R76 and

3BF2 from *N. europea, S. oneidensis, N. meningitides*, respectively). Intriguingly, Jia and Polissi groups suggested that LPS triggers LptA fiber formation, although no LPS-LptA complex was solved by x-ray crystallography (Suits *et al,* 2008).

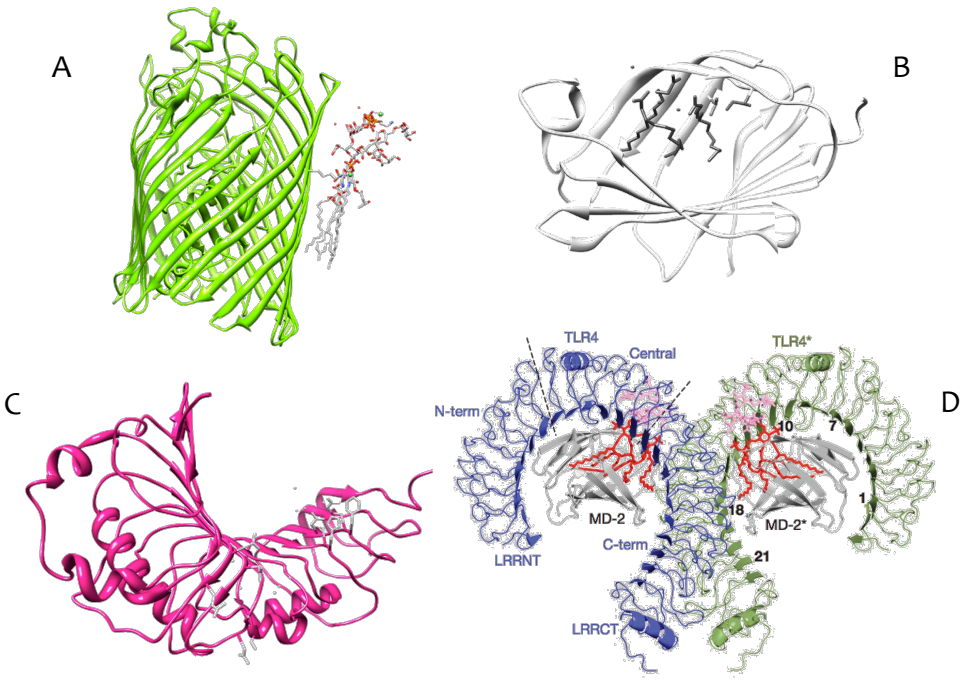

Figure 2.17 | SPASM templates. A. FhuA-lipid A crystal (PDB ID 2FCP): an additional electron density proximal to the membrane-embedded region of the barrel was modeled as a single LPS molecule. (Ferguson *et al.,* 2000). B Crystal structures of human MD-2 and its complex with the antiendotoxic tetra-acylated lipid A core of LPS have been determined at 2.0 and 2.2 Å resolutions, respectively (PDB ID 2E56, 2E59) (Ohto *et al.,* 2007). C. Crystal structure of human CD14, Previously identified regions involved in LPS binding map to the rim and bottom of the pocket indicating that the pocket is the main component of the LPS-binding site (Kim *et al.*; 2005, PDB ID 1WWL). D. crystal structure of the hetero-tetrameric complex $(TLR4\text{-}MD\text{-}2)_2$ bound to LPS. LPS interacts with a large hydrophobic pocket in MD-2 and directly bridges the two components of the multimer. (Park *et al.*, 2009, PDB ID 3FXI).

As prediction methods for small molecule binding sites have been extensively studied, an *in silico* similarity search approach was undertaken to explore the structural requirements of LptA to bind LPS, selecting proteins which respond to the following requisites as templates:

1. Crystal structure to be available
2. Structural evidence of LPS binding, or experimental data to be available, providing the existence of a determined region of interaction with LPS.

FhuA, MD-2 and CD14 posses the above mentioned properties.

SPASM (SPatial Arrangements of Side chains and Main chain) is a software of whose fast matching algorithm was developed by G. J. Kleywegt, at the Department of Cell and Molecular Biology, Uppsala University, in Sweden (Harel *et al*., 1995). SPASM can find similar arrangements of side chains and main chains (e.g., loops, turns, active sites, metal-binding sites, etc.) using protein structures as templates. Each residue selected on the template is represented by a pseudo-atom at the average position of a set of functional atoms, and it is recursively searched on target proteins through all possible residue combinations. For this reason the SPASM software was used to search for an LPS binding motif on LptA. Every template was superimposed once at time on targeted proteins (LptA and other proteins, which were selected as positive and negative controls).

The original algorithm was modified to satisfy the following criteria:

1. Main and side chain atoms of residues included in superimposition were extensively selected untill Cγ.
2. A Root Mean Squared Deviation (RMSD) value of 2 Å was used as cut-off.
3. Both the order in which template residues occur in the sequence, and the gaps between them, were not necessarily maintained.
4. In search for charged residues, interchangeable arginine/lysine superimposition was allowed.
5. In search for hydrophobic residues, interchangeable leucine/Isoleucine superimposition was allowed.

The accompanying program MKSPAZ was also compiled to generate an *ad hoc* library, which contains only the probed proteins, namely LptA and several other proteins used as control and described hereinafter (see introduction for further details).

- The crystal structure of human BPI consists of two similar, extended domains. A functional role in LPS-binding and LPS detoxification has been assigned to the distal tip of the N-terminal domain highly conserved residues. Peptides derived from residues 17–45 and

residues 65–99 of BPI inhibit the LPS-induced inflammatory response (Lamping *et al.,* 1996).

- Lactoferrin, is released from neutrophil granules during the LPS-induced inflammatory response. The tridimensional structure is composed of two related globular lobes. Synthetic peptides containing residues 28–34 of lactoferrin are bactericidal against Gram-negative bacteria (Van Berkel, *et al.,* 1997; Elass-Rochard *et al.,* 1998; Odell *et al.,* 1996).
- Lysozyme reduces the immunostimulatory activities of LPS (Brandenburg et al., 1998). Detailed information about specific LPS–lysozyme interactions is not available. The crystallographic structures of several different lysozyme types have been solved: human lysozyme (Artymiuk *et al.,* 1981), hen egg-white lysoyzme (C-type)(Blake *et al*., 1965), goose egg-white lysozyme (G-type) (Grütter *et al.,* 1983), and bacteriophage T4 lysozyme (V-type) (Matthews *et al.,* 1974). Although these proteins share a common fold, sequence comparisons between lysozyme types reveal no significant similarity.
- The Limulus anti-LPS factor (L-ALF) inhibits the LPS-induced coagulation cascade by binding LPS and neutralizing its endotoxic effects. The crystallographic structure of L-ALF contains a cluster of positively charged residues found on an amphipathic loop and on the adjacent residues of the basic face of the protein. Some of these residues have been previously proposed, but not demonstrated to be involved in LPS binding. Synthetic cyclic peptides derived from residues 36–45 of L-ALF have been shown to bind and inhibit the LPS-induced immune response (Hoess *et al.*1993; Ried *et al.,* 1996).

The proteins selected so far have already been indicated as factors carrying a possible LPS recognition motif by Ferguson and co-workers using FhuA as template in SPASM superimposition tests (Ferguson *et al.,* 2000). The 4-residue motif found was in line with the experimental data previously obtained for these proteins (see references above), for this reason we routinely used them as matching controls together with MD-2, CD14 and FhuA. Finally, the DNA-direct ω subunit of *E. coli* RNA polymerase (RpoZ, PDB 3LTI), and the satellite tobacco necrosis virus (STNV) coat protein (PDB 3RQV), were selected as negative controls: the former is rich in positively

charged residues as it interacts with DNA, the latter is an example of beta-jellyroll protein (Opalka *et al.,* 2010).

The first hit we performed using SPASM, reproduced the results previously obtained by Ferguson, using the 4-basic-residue motif of FhuA showed in Table 2.2 as template (Ferguson *et al.,* 2000). The residues identified on CD14 and MD-2, used as controls, were in agreement with experimental evidences reported in the past years.

The effect of basic residues of MD-2 for LPS binding has been analyzed before by using either synthetic peptide fragments of MD-2 or point mutations. The cumulative effect of decreasing the number of basic residues of MD-2 has been demonstrated for the residues, which formed the largest continuous stretch of basic and hydrophobic residues (Phe121–Lys132) (Visintin *et al*., 2003; Re*,* 2002; Mancek *et al*., 2002). The effect of knocking out several basic residues can be explained through the disturbance of the positive electrostatic potential, which may steer LPS toward the binding site. The electrostatic potential of MD-2 according to Gruber's model is the highest at the region, which roughly coincides with the lipid-binding sites (Gruber *et al.,* 2004).

Kim and colleagues have proposed a pocket-binding site on CD14: the main pocket contains a smaller sub-pocket at the bottom. Residues from β4 – β6 and connecting loops form this sub-pocket (Kim *et al.,* 2005), where all the residues found with SPASM fall. It is narrow and deep with dimensions 4.5 Å wide, 9.6 Å long, and 8 Å deep. Overall, the pocket including the sub-pocket has a total volume of 820 $Å^3$ and hence is large enough to accommodate at least part of the lipid chains of LPS.

Interestingly the same cationic pattern was detected in LptC and LptE with success by the algorithm applied. On the other hand, RMSD score of superimposition applied to the negative controls was lower than the one applied to LptA, showing that the LPS-binding motif proposed by Ferguson and colleagues was not sufficiently stringent (Table 2.2).

Table 2.2

SPASM, Hit 1 / template: FhuA (4 residues)						
Protein	**PDB**	**RESIDUES**				**RMSD**
FhuA	**2FCP**	**Lys306**	**Lys351**	**Arg382**	**Lys437**	
BPI	1BP1	Lys42	Arg48	Lys92	Lys99	0.88
Lactoferrin Hum N	1B1X	Arg24	Arg27	Arg2	Arg4	1.47
Lactoferrin Hum C	1B1X	Lys359	Arg356	Lys633	Lys637	1.25
Lysozyme Human	1JKC	Arg113	Arg107	Lys97	Arg21	1.34
Lysozyme C-type	135L	Lys96	Lys97	Arg61	Lys73	1.45
Lysozyme G-type	1HHL	Arg14	Lys13	Lys125	Arg121	1.43
Lysozyme V-type	145L	Arg148	Lys147	Arg137	Lys135	1.07
L-ALF	2JOB	Arg41	Arg40	Lys64	Lys47	1.43
MD-2 Human	2E56-2E59	Lys132	Lys130	Arg125	Lys55	1.89
CD-14 Murine	1WWL	Lys73	Arg74	Arg131	Arg78	1.59
RNApol ω subunit	3LU0	Arg25	Arg28	Lys45	Lys35	2.38
STNV coat protein	1VTZ	Arg18	Lys17	Lys27	Arg66	2.18
LptA	2R19-2R1A	Arg76	Lys83	Lys146	Lys118	**2.6**
LptC	3MY2	Lys170	Arg168	Lys90	Lys88	1.99
LptE	2JXP	Arg82	Arg102	Lys126	Lys130	1.95
NOTE	**4-residue motif from FhuA is not stringent**					

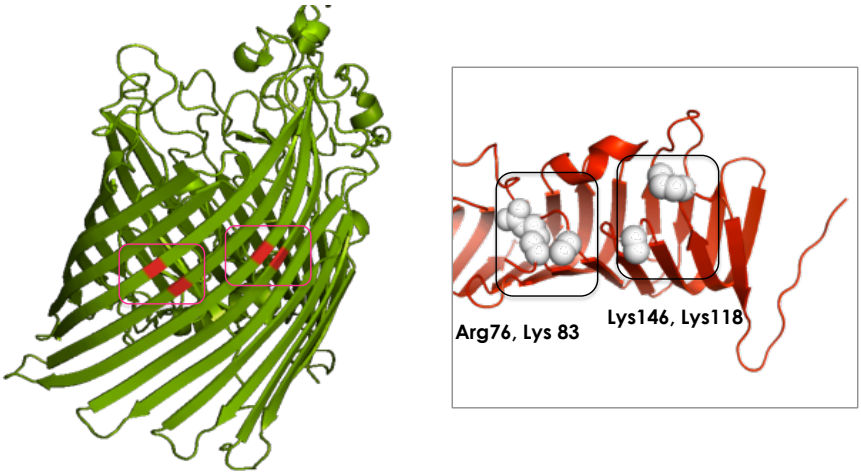

Figure 2.18 | LPS binding motif in FhuA. On the left panel Lys306-Lys351+ Arg382-Lys437 motif is depicted on the surface of FhuA. Each couple of charged residues interacts with one of the two phosphate groups flanking the GlcNs of lipid A. The same motif super-imposed by SPASM on LptA is depicted on the right.

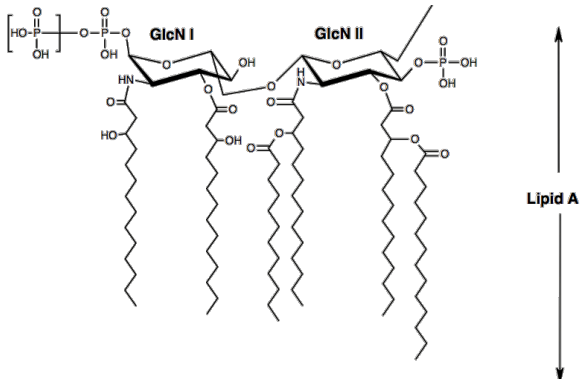

Figure 2.19 | lipid A. Enterobacterial lipid A is a phosphorylated 2-amino-2-deoxy-D-glucose (glucosamine) disaccharide. The two linked glucosamines (GlcN I and GlcN II) are bisphosphorylated at the O1-position of GlcN I and monophosphorylated at the O4′-position of GlcN II. The secondary phosphate position of the O1-diphosphate is not fully occupied (indicated with brackets). The glucosamine disaccharide is acylated (from left to right) at the 2- and 3-positions of GlcN I with 3-hydroxymyristatic [14:0(3-OH)] acid, and at the 2′- and 3′-positions of GlcN II with 14:0[3-O (C12:0)] and 14:0[3-O(C14:0)], respectively.

FhuA binds lipid A outside the barrel cavity, over a curved surface. MD-2 on the contrary sequesters LPS inside a pocket, and partially shares the ligand with TLR4 receptor. The Phe121–Lys132 region of MD-2 is involved in ligand interaction as shown in Gruber, Visintin and Re publications (Visintin *et al.*, 2003; Re *et al.,* 2003, Gruber *et al.,* 2004), the Arg/Lys components of this tract were then used in several combinations as templates in subsequent superimpositions. The best template was the tripetide Lys128-Lys130-Lys132: the results from superimposition are summarized in table 2.3. Briefly, in all the LPS-binding proteins subjected to the superimposition, a 3-basic residue motif with a RMSD score lower than negative controls RpoZ and STNV was identified. The residues found on the proteins used as positive controls are partially overlapping with the results of the first hit, however all of them fall in regions previously demonstrated or suggested to interact with lipid A. Interestingly, the triplet Arg76, Lys83 and Lys118 detected on LptA was previously outlined by the first SPASM hit, now with a RMSD of 1.10 Å.

Table 2.3

SPASM, Hit 2 / template: MD-2 (3 residues)					
Protein	**PDB**	**RESIDUES**			**RMSD**
MD-2 Human	**2E56**	**Lys128**	**Lys130**	**Lys132**	
LptA	2R19- 2R1A	Lys118	Lys83	Arg76	1.10
Lysozyme Human	1JKC	Arg115	Arg113	Lys107	1.18
CD-14 Murin	1WWL	Lys23	Arg45	Arg81	1.53
FhuA	2FCP	Lys351	Arg384	Lys437	1.14
RNApol ω subunit	3LU0	-	-	-	**>2**
STNV coat protein	1VTZ	Arg75	Arg145	Arg129	**1.58**
NOTE	**3-basic residue motif**				

MD-2 shows a deep hydrophobic cavity sandwiched by two beta sheets, in which four acyl chains of the ligand are fully confined. The phosphorylated glucosamine moieties are located at the entrance to the cavity, five of the six lipid chains of LPS are buried deep inside the pocket and the remaining chain is exposed

to the surface of MD-2, forming a hydrophobic interaction with the conserved phenylalanines of TLR4. (Park *et al.,* 2009).

Previously identified regions in CD14 involved in LPS binding, map to the rim and bottom of a pocket indicating that this region is the main component of the LPS-binding site. Mutations that interfere with LPS signaling but not with binding are also clustered in a separate area near the pocket (Kim *et al.,* 2005). The pocket is very rich in hydrophobic residues as they are required to interact with the acyl chains of lipid A.

To test if some LptA residues could delineate a pocket in order to accommodate the acyl chains of lipid A, a third superimposition test was performed, using CD14 residues, which constitute the pocket of the protein. For this reason only LPS binding proteins that rearrange a pocket or at least a cavity to accommodate the lipid A were taken into account. Moreover, only residues with side chain inside the cavity have been considered as acceptable results.

This analysis identified in LptA two pairs of isoleucines, which localize in a region between the first and the fourth beta strand of the protein (Unit A, PDB ID 2R19A). These hydrophobic amino acids are facing the pool of charged residues found in the first and second SPASM hits, outlining a pocket, where the basic residues stand at the rim, whilst the hydrophobic pattern is traced at the bottom. This residue distribution can be optimal for capturing lipid A moiety of LPS. The acyl chains might be accommodated into the pocket of the protein, while both the phosphate groups flanking the N-acetyl-glucosamine residues would be fixed at the entrance of the pocket in line with other lipid A burying cavities in CD14 and MD-2.

Table 2.4

SPASM, Hit 3 / template: CD14 (4 residues)						
Protein	**PDB**	**RESIDUES**				**RMSD**
CD14	**1WWL**	**Leu91**	**Leu94**	**Leu102**	**Leu104**	
MD-2 Human	2E56-2E59	Ile153	Ile32	Leu54	Ile124	1.36
RNApol ω subunit	3LU0	-	-	-	-	>2
LptA	2R19-2R1A	Ile67	Ile65	Ile36	Ile38	**1.54**
NOTE	**4-residue hydrophobic pattern**					

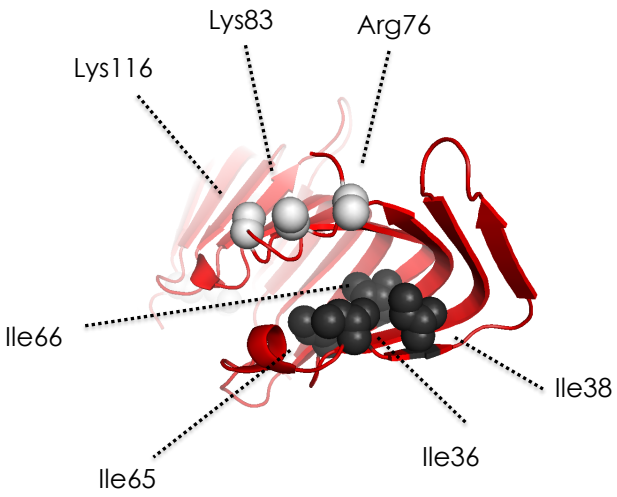

Figure 2.20 | *In silico* predicted lipid A-binding region in LptA. The residues found by SPASM superimpositions in LptA are indicated. Light and dark gray balls represent side chains of the basic and hydrophobic residue pattern, respectively.

In order to probe the putative lipid A binding pocket in LptA, 4 out of 7 residues were selected for site-directed mutagenesis. Positively charged residues Lys83 and Arg76 were substituted with the negatively charged residue aspartic acid; Ile36 and Ile38 were substituted with alanine, to reduce the steric hindrance.

The mutations were introduced alone or in different combination in lptA. The strain FL907, where the dicistronic operon *lptAB* is under the control of an arabinose inducible promoter, was transformed with a low copy number plasmid pWSK29 carrying the wild type and several mutant alleles of *lptA*. All LptA mutants are able to sustain growth in non-permissive (i.e. in absence of arabinose and in presence of glucose) conditions as shown in Fig. 2.21.

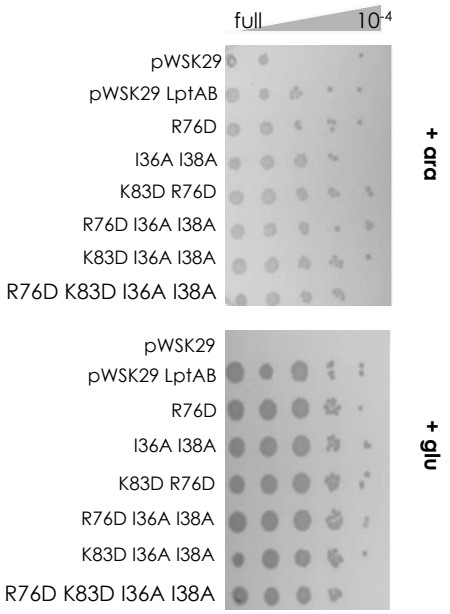

Figure 2.21 | LptA mutant phenotype. Serial culture dilutions of conditional *araBplptAB* mutant transformed with pWSK29-based plasmids expressing wild type and mutant *lptA* alleles were spotted onto permissive (+ara) or non permissive (+glu) condition at 30°C. Single or multiple *lptA* mutations are indicated; approximate dilutions are given on the top.

It is known that mutations in *lpt* genes or non physiological expression of Lpt proteins affect the OM permeability. In other words LPS fails to be correctly inserted in the outer leaflet of the OM (Ruiz *et al.,* 2006; Sperandeo *et al.,* 2006; Chimalakonda *et al.,* 2011). For example, in NR698 strain, the *lptD* gene has an in frame small deletion, which confers an increased sensitivity to specific toxic agents

(Ruiz *et al.,* 2005). To test if LptA mutants display defects in OM permeability, a strain where the *lptAB* operon is deleted (AM604Δ*lptAB*), was transformed with the low-copy number pWSK29 plasmid, carrying wild-type or *lptA* mutant alleles. The transformed AM604Δ*lptAB* cells were subjected to serial dilutions on agar plates, supplemented with hydrophobic toxic compounds used to probe OM integrity (bile salts, rifampicin, bacitracin and novobiocin). These compounds have different intracellular targets, and a functional OM barrier formed by LPS normally blocks their entrance in the cell. The results are shown in figure 2.22. Isoleucine substitutions in combination with at least one mutation that invert the charge in either arg76 or lys83, affect the OM permeability, resulting in increased sensitivity to hydrophobic toxic compounds.

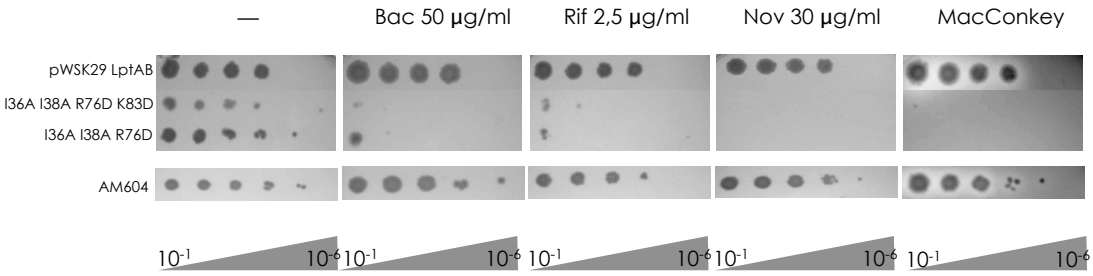

Figure 2.22 | Sensitivity analysis of LptA mutants. Serial culture dilutions of wild-type (AM604) and AM604Δ*lptAB* strain transformed with pWSK29-based plasmids expressing wild type and mutant versions of LptA (pWSK29LptAB; I36A I38A R76D K83D; I46A I38A R76D, respectively) were spotted onto LD-agar plates (—) in presence of antibiotics (Bac, bacitracine; Rif, rifampicine; Nov, novobiocine) or bile salts (McConkey). Approximate dilutions are given below.

To exclude that OM permeability might be compromised by a lower expression of LptA mutant proteins, crude cell extracts of strains expressing the wild type or the mutant versions of LptA were subjected to SDS-PAGE and immunoblot using anti-LptA antibody (Figure 2.23). The level of mutant LptA protein is comparable to that of LptA expressed from its natural promoter in AM604 wild-type strain.

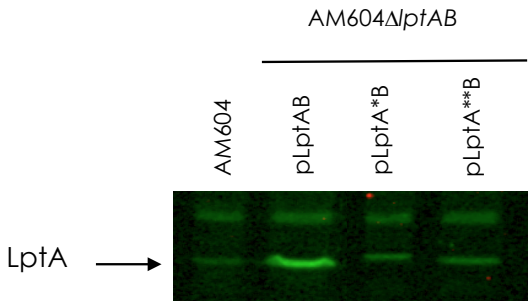

Figure 2.23 | Levels of wild-type and mutant LptA are comparable. Level of LptA in wild type (AM604), or AM604ΔlptAB strain that harbors pWSK-based plasmid carrying the wild-type copy of LptA (pLptAB) or mutant version LptAI46A-I38A-R76D (pLptA*B) and LptAI36A-I38A-R76D-K83D (pLptA**B). Crude cell extracts were subjected to SDS-PAGE and immunoblotting using anti-LptA antibodies. The antibody cross-reacts with an unknown protein with higher molecular weight used as a loading control.

Interestingly, disorder prediction of LptA structure shows that Ile36, Ile38, Arg76 and Lys83 fall in disordered clusters of residues (Fig. 2.24), it is known that many unstructured proteins undergo transitions to more ordered states upon binding to their targets. This further supports the hypothesis that the identified residues may be involved in ligand interaction.

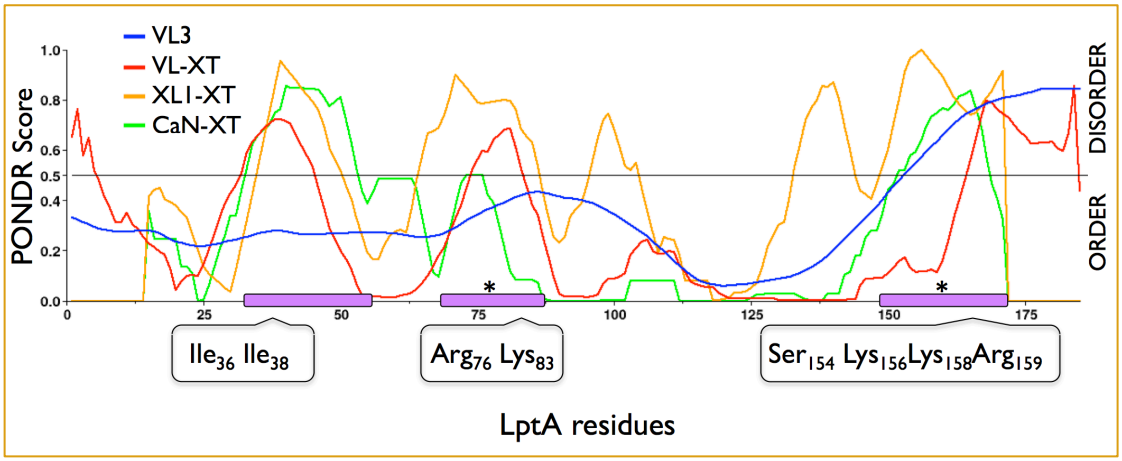

Figure 2.24 | LptA disorder prediction (Pondr.com). Purple rectangles represent disordered clusters of residues according to several prediction algorithms applied (colored lines). LptA crystallization (Suits *et al.,* 2008) failed to solve part of these regions correctly (*). Ser154 Lys156 Lys158 and Arg159 were additionally found by SPASM superimpositions hits using FhuA and MD-2 as templates, with RMSD score slightly higher than ones previously selected.

Proteins that bind and transport lipids face special challenges. Since lipids typically have low water solubility, both accessibility of the substrate to the protein and delivery to the desired destination are problematical. The amphipathic nature of LPS, and its relatively large molecular size, also means that these proteins must possess substrate-binding sites of a different nature than those designed to handle small polar molecules. A structural comparison of these LPS-binding peptides and further analyses of structure–activity relationships showed that an amphiphilic structure with a net positive charge together with a considerable hydrophobicity are a general characteristic of these molecules. Interestingly neither residues previously indicated on MD-2 (Park *et al.,* 2009) or on lysozyme are conserved, so are the amino acids detected on LptA, suggesting that more likely the spatial organization of the positive and hydrophobic moieties determines the LPS-binding than specific conserved residues (Fig. 2.25)(Iwagaki *et al.*, 2000, Mayo *et al.,* 1998, Nagaoka *et al*., 2002). It can be assumed that the positively charged amino acid residues interact with the negatively charged moieties of the LPS, such as the phosphate groups, whereas hydrophobic amino acids may bind to the fatty acid chains of LPS, and coherently the residues Ile36, Ile38, Arg76 and Lys83 could be *bona fide* considered as part of a putative LPS binding site on LptA.

Anyway we are currently setting up an *in vitro* LPS binding assay to assess LPS binding defects of LptA mutants. In case the existence of the LPS binding pocket will be directly proved, the same approach will be applied to LptC, which interestingly seems to bind LPS *in vitro* with an apparently lower affinity, as in co-purification ligand-protein experiments LptA is able to displace LPS from LptC-LPS complex, and not vice versa, suggesting a unidirectional ligand swapping (Tran *et al*., 2010).

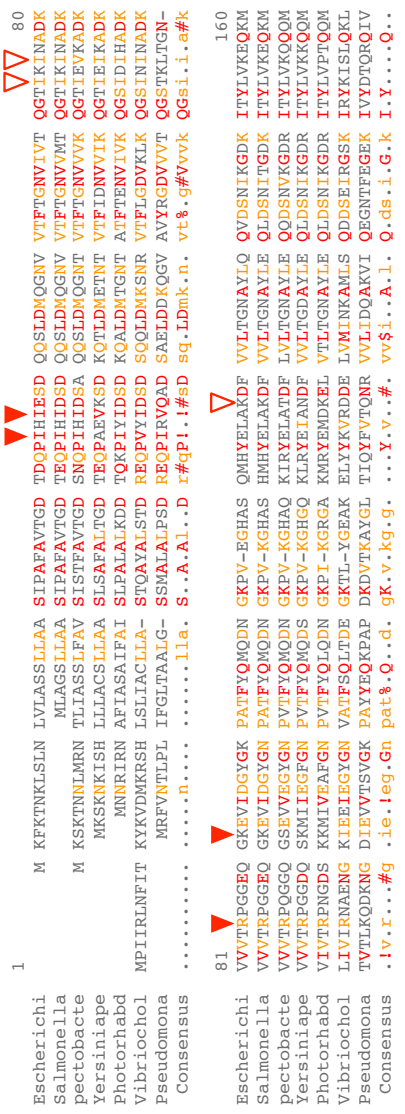

Figure 2.25 | Alignment of the sequences of selected LptA homologues in most representative γ-proteobacteria Residue numbering corresponds to LptC from *Vibrio cholera* (without gaps). Alignment was performed with MultAlin available on the web. Residues with high sequence identity or similarity are colored in red and orange, respectively. Non-conserved residues are shown as gray letters. Strains selected: *Escherichia coli*; *Salmonella enterica*; *Pectobacterium atrosepticum* SCRI1043; *Yersinia pestis Angola*; *Photorhabdus luminescens subsp. Laumondii* TT01; *Vibrio Cholerae* O1 *biovar El Tor* str. N16961; *Pseudomonas aeruginosa* PAO1. Triangles indicate the residues selected by superimposition of several structural templates; red-filled ones indicate residues subjected to mutagenesis experiments.

2.6 The Lpt fold as a keystone of the LPS transport machinery

Book chapter

As discussed in the previous chapter, the pathway of LPS translocation from IM to the OM has been characterized mainly using the *E. coli* and *N. meningitidis* model systems. A phylum level analysis of Lpt proteins conservation shows that not all the LPS-producing bacteria contain a complete set of *E. coli* Lpt proteins homologues (Sutcliffe, 2010).

However, searching Lpt orthologous proteins in LPS producing diderm bacteria by a standard BLAST analysis might be misleading. For example, Haarmaan and co-workers showed that the proteins of the Lpt complex localized within the IM (LptF and LptG) are generally present in Gram-negative bacteria, whereas the periplasmic proteins LptA, LptC and LptE result hard to be detected by BLAST analysis (Haarmaan *et al.,* 2010). This is not surprising considering that the homologues of these proteins in rather closely related strains within γ-*Proteobacteria* share a low identity level (e.g., the identity of *P. aeruginosa* and *E. coli* LptC and LptE is 19% and 21%, respectively).

For this reason, given the essential role played by the Lpt protein machinery in *E. coli*, alternative search methods are desirable to explore in greater depth the available genomic and proteomic information.

A more stringent approach could be to use the functional domains found in Lpt proteins (Fig. 2.26) to search for homologues in PFAM database (pfam.sanger.ac.uk/).

By this approach we found that the Lpt proteins are present in β- and γ-*Proteobacteria* (Table 2.5). A closer examination of the distribution at phylum level of PFAM domain PF03968 (OstA-N domain, present in both LptA and the N-terminus of LptD) in diderm bacteria reveals that LptA and LptD homologues are widely distributed, as it is possible to find PF03968 domain even in *Thermotogae*, which do not possess LPS biosynthesis genes (Plotz *et al*., 2000; Sutcliffe, 2010). Also PF03739 domain (YjgP_YjgQ domain present in both LptF and LptG) results widely distributed, as expected for an ABC transporter subunit.

On the contrary, the examination of the PF06835 and PF04390 domains (LptC and LptE, respectively) reveals a narrower distribution. LptC homologues are apparently missing in δ- and ε-*Proteobacteria*, whereas the presence of LptE homologues appears to be restricted to the β- and γ-*Proteobacteria*, with the only exception of some *Desulfuromonadales* within δ-*Proteobacteria*. Accordingly, in a recent work it has been reported that in some phyla known to produce LPS the Lpt pathway is either completely missing (e.g. in *Chlamydiae*) or lacks some components (e.g. in *Bacteroidetes*, *Chlorobi* and *Cyanobacteria*) (Sutcliffe, 2010) (Table 2.5).

However, the absence of LptC or LptE homologues in LPS producing bacteria is at odds with the essential role of these proteins in *E. coli*. Therefore, other identification criteria in addition to significant PFAM hits need to be exploited to find potential LptE and LptC-like proteins. In Gram-negative bacteria the clusters of *lpt* genes are generally conserved. Therefore, a possible strategy to detect the missing Lpt components not identified by other approaches based on sequence similarity of proteins or protein domains could be to inspect more closely the sequences flanking identified conserved homologues.

For example, in ε-*Proteobacteria* several proteins implicated in LPS synthesis and transport can be detected by the above bioinformatic methods, including the LpxC, LpxK and WaaA enzymes, the OstA_N-like proteins, and the IM protein complex components LptFG, whereas LptC and LptE appear to be missing (Table 2.5). In *H. pylori* strain 26695, the putative periplasmatic LptA homologue is coded by a gene belonging to a locus composed of three ORFs. The ORF downstream of LptA encodes a putative GTP-binding protein (HP1567), possibly an LptB functional homologue, whereas the upstream gene (HP1569) encodes a putative protein with no significant similarity with proteins of known function. However, its structural prediction (performed with I-TASSER prediction server available at http://zhanglab.ccmb.med.umich.edu/I-TASSER) indicates that HP1569 is a putative IM bitopic conserved protein of 197 residues that shows a structure similar to that of *E. coli* LptC.

It thus appears that the genetic organization of *H. pilori* putative *lptC-lptA-lptB* genes resembles the organization found in the *E. coli* genome. A similar observation can be done for LptE, which in *E. coli* is located between the housekeeping genes *holA* and *leuS*. In *H. pylori*, ORF HP1546, which is flanked by a *leuS* homologue, codes for a putative lipoprotein as suggested by *in silico* analysis using LipoP 1.0 server (http://www.cbs.dtu.dk/services/LipoP/). HP1569 and HP1546 might thus represent highly diverged LptC and LptE orthologues.

Curiously, in some species a different organization of conserved domains is observed. As an example, in *Kangiella koreensis* two PF03968 (OstA_N) domains are present in the LptA homologue whereas in *Fusebacterium nucleatum* and in *Bdellovibrio bacteriovorus* the PF03968 (OstA_N) domain is fused in a single polypeptide with one or two PF036835 (LptC) domains, thus highlighting the importance of this interaction in LPS transport pathway (Figure 2.27).

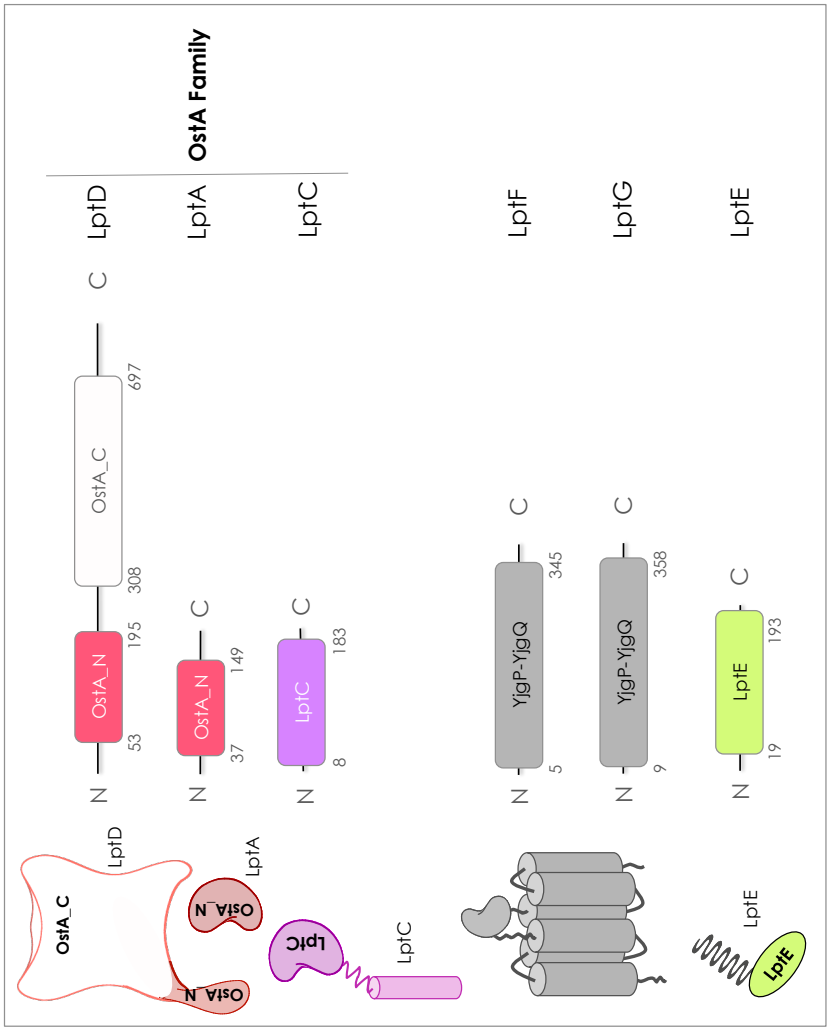

Figure 2.26 | Conserved functional domains in Lpt proteins. The OstA domain family includes the OstA_N signature in both LptD and LptA, and LptC signature in LptC. OstA_C indicates the β-barrel domain of LptD. YjgP-YjgQ domain covers the complete sequence of LptF and LptG. LptE is described by one homonymous domain.

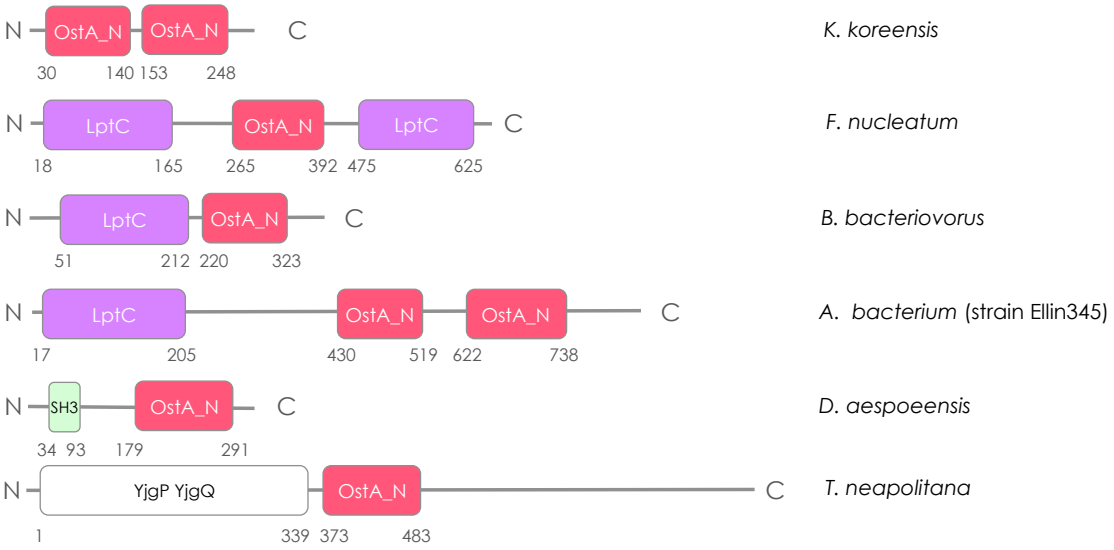

Figure 2.27 | Architecture variations in OstA-N family domains. Domain organization of PF03968 (OstA_N) and PF06835 (LptC) in selected genomes are shown. Interestingly in some specimen *lptC* and *lptA* genes are substituted by one ORF, which codes for a unique protein keeping both LptC and OstA_N domains with possibly an IM anchor sequence (e.g. *B. bacteriovorus*, Locus Names: Bd0840). A low complexity region could also be detected before and after the LptC and OstA_N domains in line with what observed at the LptC N-terminus and LptA C-terminus (Tran *et al.*, 2010; Suits *et al.*, 2008). The bacterial SH3 domain (Src homology-3) is about 60 amino acid-long, it may mediate many diverse processes such as increasing local concentration of proteins, altering their subcellular location and mediating the assembly of large multiprotein complexes (Gmeiner & Horita, 2001).

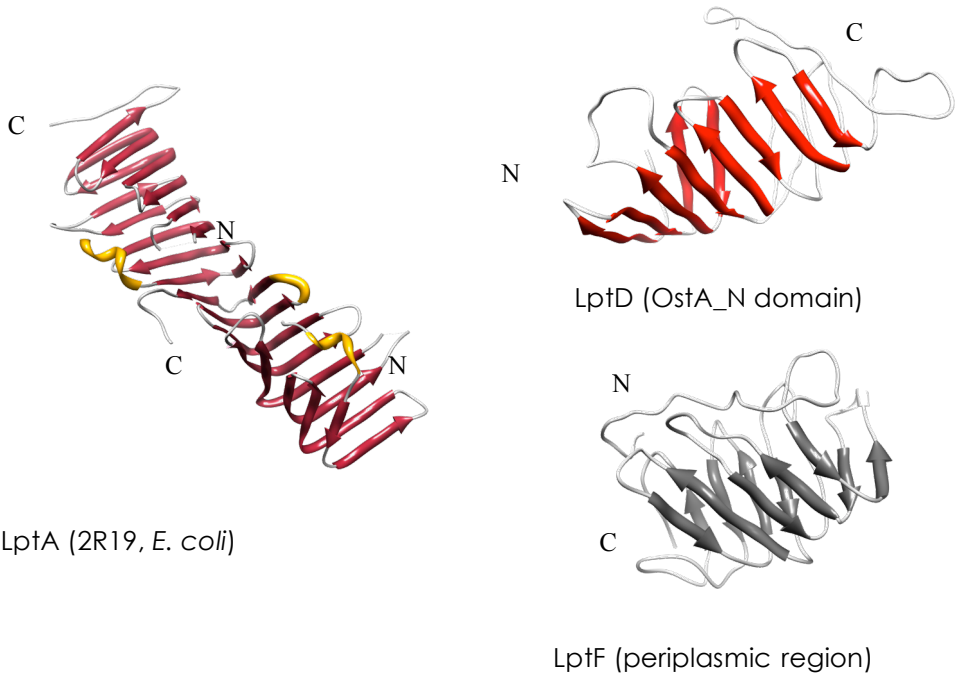

Figure 2.28 | Structural prediction of LptF and LptD. Structure prediction of periplasmic regions of LptD, LptF and LptG were performed with I-TASSER (http://zhanglab.ccmb.med.umich.edu/I-TASSER). The OstA-like fold is conserved.

Structural predictions by fold-recognition method (I-TASSER server) have also revealed that the periplasmic region of LptF, LptG and LptD share the β-jellyroll fold which was originally identified in LptA and LptC by crystallographic analysis (Suits *et al.*, 2008; Tran *et al.*, 2010). We propose that the lack of amino acid sequence conservation in proteins belonging to the Lpt pathway may reflect the mode of interaction between Lpt proteins and LPS: this Lpt fold is likely the unique functional block that is used by the Lpt proteins to interact each other and form the trans-envelope machinery. At the same time, it is possible that Lpt binding to LPS may not implicate a few specific amino acids, rather peculiar chemo-physical features extended to the whole three dimensional structure as suggested in the previous paragraph.

Intriguingly, in the non-LPS diderm phylum of *Thermotogae* (Plotz *et al.*, 2000), despite the lack of LPS biosynthetic pathway, LptA and LptC homologues have been identified (Table 2.5), suggesting that the structural motifs described for Lpt proteins are not exclusively correlated to lipid A transport and might have evolved in some genomes to transport other lipids.

Table 2.5

Distribution of protein domains functioning in LPS biogenesis[a]

Phylum	Order	LpxC[b] PF03331[c]	LpxK[b] PF02606[c]	WaaA[b] PF04413.10[c]	OstA_N[c] PF03968[c]	LptC[c] PF06835[c]	LptE[c] PF04390[c]	YjgP_YjgQ[c] PF03739[c]
α-Proteobacteria	Rickettsiales	19	21	17	15	18	0	19
	Rhizobiales	87	88	89	89	82	0	89
	Rhodospirillales	17	17	19	16	16	0	17
β-Proteobacteria	Neisseriales	32	32	32	31	32	32	32
	Burkholderiales	88	85	89	88	88	87	87
	Methylophilales	3	3	3	3	3	3	3
γ-Proteobacteria	Enterobacteriales	162	169	178	173	164	172	174
	Pasteurellales	33	32	34	33	32	33	33
	Pseudomonadales	42	41	42	43	42	42	41
δ-Proteobacteria	Desulfovibrionales	11	13	11	10	0	0	11
	Desulfuromonadales	11	11	11	11	0	3	11
	Myxococcales	6	6	6	6	0	0	6
ε-Proteobacteria	Campylobacteriales	46	46	46	46	0	0	46
Acidobacteria		3	4	3	2	3	0	3
Aquificae		9	10	10	10	7	0	10
Cyanobacteria		57	3	1	38	54	0	56
Fusobacteria		15	15	15	13	10	0	15
Thermotogae		0	0	0	7	2	0	12

a. Several diderm bacteria phyla are selected. For α, β, γ, δ, ε-proteobacteria the presence of the specific functional domains are also shown in the most representative genera. Data reported are the numbers of proteins in each phylum/genus matching the PFAM entries characteristic of the selected proteins. Data were taken from the PFAM entries for each domain, accessed at http.//pfam.sanger.ac.uk
b. Protein domains selected (LpxC, Lpxk WaaA) belong to enzymes involved in the LPS biosynthetic pathway to identify LPS producing bacteria
c. OstA_N, LptC, LptE, YjgP_YjgQ are selected domains of proteins involved in the LPS transport to the OM

2.7 Conclusions and future perspectives

The presented work made use of genetic, biochemical and bioinformatic approaches, to unveil detailed and more general mechanisms of functioning of the Lpt system, a fundamental bacterial machinery: the LPS transport system. To date it was shown that LPS transport requires an IM associated ABC transporter, composed by LptBFG and the atypical subunit LptC with the stoichiometric ratio of 2:1:1:1 (Narita and Tokuda, 2009), a periplasmic subunit, LptA (Sperandeo *et al*. 2007; Tran *et al*., 2008), and an OM-inserted two-component complex LptDE (Chng *et al*., 2010a; Freinkman *et al*., 2011). However, the molecular mechanism by which this complex achieves the unidirectional LPS transport from IM to OM is far from being understood.

At the very beginning of this work, random mutagenesis experiments did let us isolate new LptC mutants (LptCG56V and LptCG153R), which have been used in several biochemical assays to demonstrate LptC-LptA interaction first, and outline the main functional region of the protein implicated both in LptA and IM protein complex interaction. Moreover the multi-sided phenotype of LptCG153R mutant, together with *in silico* analysis, have suggested another putative partner of LptC: the OM protein LptD, envisioning an intricate network of interactions where IM and OM members of the system might directly interact, without excluding the essential role of LptA as a bridging component and sentinel of a properly assembled device.

Additional computational and phylogenetic analyses have now supported the idea that the so called Lpt fold could be the keystone of the trans-envelope complex that make the interactions among all these proteins possible as depicted in Fig. 2.29.

Co-crystallization experiments will be the ultimate approach, necessary to prove not only the tridimensional structure provided by the several predictions, but even the functional model of the whole complex. On the other hand, *in vitro* interaction assays are ongoing, testing the direct interaction between LptC and the OstA_N domain of LptD, as well as between LptC and the periplasm-protruding regions of the IM proteins LptF and LptG. Co-purifications experiments will be also extended to a mutant version of LptC, deprived of both the IM anchor and the low complexity tract which link it to the periplasmic region, to prove once and for all, that only the Lpt-folded periplasmic domain is required for the protein to interact with the other Lpt components.

By the way the TM region of LptC is reminiscent of a not-trimmed periplasm signal sequence. Once LPS is translocated through the essential flippase MsbA on the outer leaflet of the IM, the energy-consuming Lpt protein machinery undertakes this glycolipid and sorts it to its final destination. The *E. coli* bitopic LptC could have retained an IM anchor to promptly and efficiently extract the LPS, which is then released to the other system components.

Interestingly, despite the fact that this trans-envelope machinery is required to transport the LPS to the outer leaflet of the OM, it comprehends elements that constitute the prototypical elements of an import system. It is known that the bacterial cell makes use of several hybrid systems, of which proteinaceous components share functional and evolutionary properties. For example, the secretion system IV, which is necessary for intercellular exchange of polypeptides and nucleic acids, is composed of proteins that resemble structure and function of those assembling the pilus apparatus (Hayes *et al*., 2009).

LptF and LptG form the TM elements coupled to and ATP binding protein, namely LptB, of a typical binding-protein-dependent transport system. The IM component LptC could constitute one, but not the only, solute binding protein (SBP). Chimeric transport systems were isolated from both Gram-negative and Gram-positive bacteria (such as *Streptomyces coelicolor* A3, *Streptococcus pneumoniae*, and *Streptococcus pyogenes*), unvealing indeed more than one SBP fused to the TM components of the system (Van der Heide and Poolman, 2002). LptA, and the periplasmic region of LptF and LptG, could be the additional SBP together with LptC, sharing a common fold. This redundancy is explained imaging that once LPS is bound by LptC, it is in turn released to the other components in an unidirectional way, as supported by the fact that *in vitro* LptA is able to substract the ligand from LptC and not vice versa (Tran *et al*., 2010).

LptC and LptA, together with LptE, bind LPS in vitro (Tran *et al.,* 2010; Tran *et al*., 2008; Chng *et al*., 2010b), in this work we provided a fast and simple computational approach in order to find the molecular determinants of Lpt proteins required to bind lipid A. A putative four residue-motif (Arg76-Lys83-Ile36-Ile38), which interacts with both the phosphate groups and the acyl chains of lipid A, has been detected on LptA first. Sensitivity tests on LptAR76D-K83D-I36A-I38A mutant revealed an OM permeability defect typical of partial loss of function mutants previously found in other Lpt components (namely LptD and LptE, as discovered by Ruiz *et al*., 2005 and Freinkman *et al*., 2011). The selective sensitivity to bile salts together with hydrophobic antibiotics can be due to phospholipid patch formation on the outer

leaflet of the OM membrane, when LPS fails to be correctly inserted in membrane. Despite we might consider the pocket outlined on LptA, a *bona fide* lipid A binding site, this will be directly proved setting up a quantitative LPS binding assay. Subsequently, wild-type and mutant versions of LptC will be also assayed for LPS interaction.

In conclusion, LPS-binding molecules might possess potential as drugs for the treatment of sepsis and septic shock and for the generation of affinity reagents for the removal of LPS from the blood stream. Analyses of structure–activity relationships of LPS-binding site on Lpt proteins could be therefore highly relevant for the generation of optimized LPS-neutralizing agents.

In a world where multidrug resistance phenomenon is rapidly spreading, strategies for the development of new antibiotics, which target general conserved mechanism, are urgently required. The Lpt transport system is an essential device to the bacterial cell; we have here suggested that the unique Lpt-fold constitutes the building block of the entire system and that rules out all the interactions between each component, LPS included, becoming a brand new target.

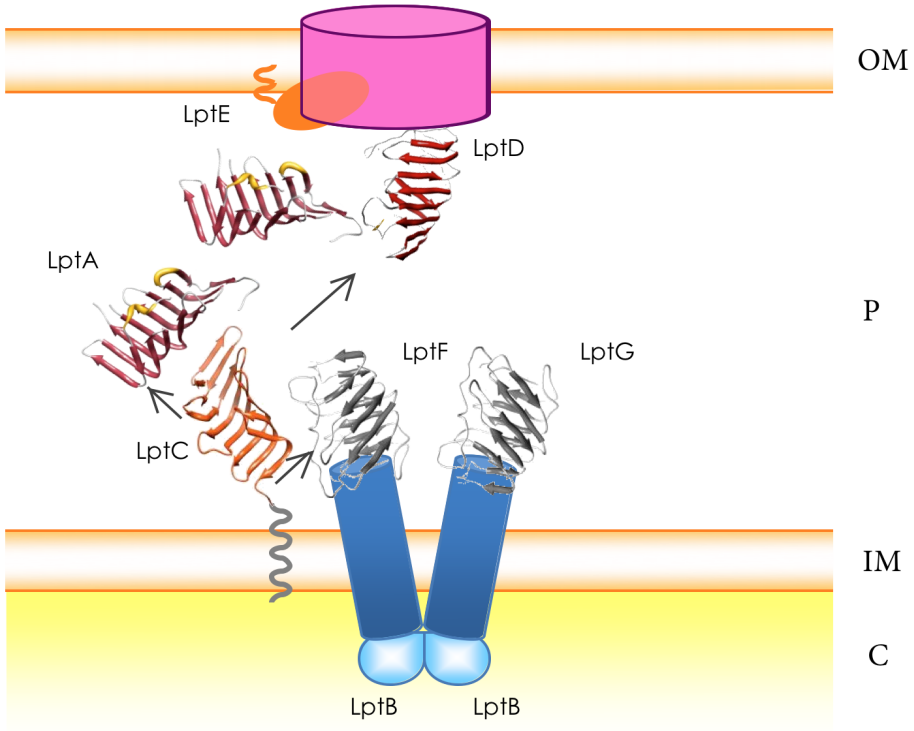

Figure 2.29 | Current model for the LPS transport system. $LptB_2CFG$ form the IM protein complex, LptB is a Nucleotide Binding Protein (NBP) with two Walker domains. LptFG are the TM components, and posses an additional periplasmic region which resemble LptA, LptC and N-terminus domain of LptD structure. LptC is a bitopic, IM-anchored protein. LptA is a periplasmic protein, which also co-localizes with both the IM and the OM complexes. Finally, LptDE form the OM complex. LPS, once is flipped through the IM by the essential ABC transporter MsbA (not shown), is presumably extracted from the membrane by LptC, which releases the ligand to the other component of the complex in a unidirectional fashion. LptC directly interact with LptA, and the IM complex component LptFG; an additional direct interaction with LptD could not be excluded (see gray narrows). Crystal structures of LptA (red and yellow, PDB code: 2R19) and LptC (orange, PDB code: 3MY2) are depicted. Periplasmic region of LptD and LpFG are represented by the tridimensional model.

REFERENCES

- Anderson,M.S. and Raetz,C.R. (1987). Biosynthesis of lipid A precursors in *Escherichia coli*. A cytoplasmic acyltransferase that converts UDP-N-acetylglucosamine to UDP-3-O-(R-3 hydroxymyristoyl)-N-acetylglucosamine. J. Biol. Chem. *262*, 5159-5169.
- Aketagawa,J., Miyata,T., Ohtsubo,S., Nakamura,T., Morita,T., Hayashida,H. , Miyata,T. and Iwanaga,S. (1986) Primary structure of limulus anti- coagulant anti-lipopolysaccharide factor. J. Biol. Chem. 261, 7357–7365.
- Aono,R., Negishi,T., Aibe,K., Inoue,A., and Horikoshi,K. (1994). Mapping of organic solvent tolerance gene *ostA* in *Escherichia coli* K-12. Biosci. Biotechnol. Biochem. *58*, 1231-1235.
- Artymiuk,P.J. and Blake,C.C.F. (1981). Refinement of human lysozyme at 1.5 A° resolution. Analysis of nonbonded and hydrogen-bond interactions. J. Mol. Biol. *152*, 733-762.
- Babinski,K.J., Ribeiro,A.A., and Raetz,C.R. (2002). The *Escherichia coli* gene encoding the UDP-2,3-diacylglucosamine pyrophosphatase of lipid A biosynthesis. J. Biol. Chem. *277*, 25937-25946.
- Bartling,C.M. and Raetz,C.R. (2008). Steady-state kinetics and mechanism of LpxD, the N-acyltransferase of lipid A biosynthesis. Biochemistry *47*, 5290-5302.
- Bayer,M.E. (1968). Areas of adhesion between wall and membrane of *Escherichia coli*. J. Gen. Microbiol. *53*, 395-404.
- Bayer,M.E. (1991). Zones of membrane adhesion in the cryofixed envelope of *Escherichia coli*. J. Struct. Biol. *107*, 268-280.
- Beamer,L.J., Carroll,S.F. and Eisenberg D. (1998) The BPI/LBP family of proteins: a structural analysis of conserved regions. Protein Sci. 7, 906–914.
- Beckmann,I., Subbaiah,T.V., and Stocker,B.A. (1964). Rough mutants of *Salmonella typhimurium*. II. Serological and chemical investigations. Nature *201*, 1299-1301.
- Belunis,C.J. and Raetz,C.R. (1992). Biosynthesis of endotoxins. Purification and catalytic properties of 3-deoxy-D-manno-octulosonic acid transferase from Escherichia coli. J. Biol. Chem. *267*, 9988-9997.
- Beveridge,T.J. (1999). Structures of gram-negative cell walls and their derived membrane vesicles. J. Bacteriol. *181*, 4725-4733.
- Beveridge,T.J. and Davies,J.A. (1983). Cellular responses of *Bacillus subtilis* and *Escherichia coli* to the Gram stain. J. Bacteriol. *156*, 846-858.
- Bielaszewska,M., Mellmann,A., Zhang,W., Köck,R., Fruth,A., Bauwens,A., Peters,G., Karch,H. (2011). Characterisation of the *Escherichia coli* strain associated with an outbreak of haemolytic uraemic syndrome in Germany, 2011: a microbiological study. Lancet Infect. Dis. 11,671–676.
- Bishop,R.E. (2008). Structural biology of membrane-intrinsic beta-barrel enzymes: sentinels of the bacterial outer membrane. Biochim. Biophys. Acta *1778*, 1881-1896.
- Bishop,R.E., Gibbons,H.S., Guina,T., Trent,M.S., Miller,S.I., and Raetz,C.R. (2000). Transfer of palmitate from phospholipids to lipid A in outer membranes of gram-negative bacteria. EMBO J. *19*, 5071-5080.
- Bladen,H.A. and Mergenhagen,S.E. (1964). Ultrastructure of Veillonella and morphological correlation of an outer membrane with particles associated with endotoxic activity. J. Bacteriol. *88*, 1482-1492.
- Blake,C.C.F., Johnson,L.N., Mair,G.A., North,A.C.T., Phillipset,D.C., and Sarma,V.R. (1965). Structure of hen egg-white lysozyme. Nature 206, 757-761.
- Bland,J.M., De Lucca,A.J., Jacks,T.J. and Vigo,C.B. (2001) All-D-cecropin B: synthesis, conformation, lipopolysaccharide binding and antibacterial activity. Mol. Cell. Biochem. 218, 105–111.
- Blattner,F.R., Plunkett,G., Bloch,C.A., Perna,N.T., Burland,V., Riley,M., Collado-Vides,J., Glasner,J.D., Rode,C.K., Mayhew,G.F., Gregor,J., Davis,N.W., Kirkpatrick,H.A., Goeden,M.A., Rose,D.J., Mau,B., and Shao,Y. (1997). The complete genome sequence of *Escherichia coli* K-12. Science. *277*, 1453-1462.
- Boehning,D., and Joseph,S.K. (2000). Direct association of ligand-binding and pore domains in homo- and heterotetrameric inositol 1,4,5-trisphosphate receptors. The EMBO J. 19, 5450–5459.
- Bos,M.P., Robert,V., and Tommassen,J. (2007). Biogenesis of the Gram-negative bacterial outer membrane. Annu. Rev. Microbiol. *61*, 191-214.
- Bos,M.P., Tefsen,B., Geurtsen,J., and Tommassen,J. (2004). Identification of an outer membrane protein required for the transport of lipopolysaccharide to the bacterial cell surface. Proc. Natl. Acad. Sci. U. S. A *101*, 9417-9422.

- Boucher,H.W., Talbot,G.H., Bradley,J.S., Edwards,J.E., Gilbert,D., Rice,L.B., Scheld,M., Spellberg,B., Bartlett,J. (2009). Bad bugs, no drugs: No ESKAPE! An update from the Infectious Diseases Society of America. Clin. Infect. Dis. 48, 1–12.
- Bowyer,A., Baardsnes,J., Ajamian,E., Zhang,L., and Cygler,M. (2011). Characterization of interactions between LPS transport proteins of the Lpt system. Biochem. Biophys. Res. Commun. *404*, 1093-1098.
- Brackett,D.J., Lerner,M.R., Lacquement,M.A., He,R. and Pereira,H.A. (1997). A synthetic lipopolysaccharide-binding peptide based on the neutrophil-derived protein CAP37 prevents endotoxin-induced responses in conscious rats. Infect. Immun. 65, 2803–2811.
- Bragonzi, A. (2010). "Fighting back: peptidomimetics as a new weapon in the battle against antibiotic resistance". Science translational medicine 2, 21-24.
- Brandenburg,K., Jurgens,G., Andra,J., Lindner,B., Koch,M.H., Blume,A. (2002). Biophysical characterization of the interaction of high-density lipoprotein (HDL) with endotoxins. Eur. J. Biochem. 269, 5972–5981.
- Braun, M. and Silhavy,T.J. (2002). Imp/OstA is required for cell envelope biogenesis in *Escherichia coli*. Mol. Microbiol. *45*, 1289-1302.
- Braun,V. (1975). Covalent lipoprotein from the outer membrane of *Escherichia coli*. Biochim. Biophys. Acta *415*, 335-377.
- Britigan,B.E., Lewis,T.S., Waldschmidt,M., McCormick,M.L. and Krieg,A.M. (2001). Lactoferrin binds CpG-containing oligonucleotides and inhibits their immunostimulatory effects on human B cells. J. Immunol. 167, 2921–2928.
- Canton,R., Coque, T.M. (2006) The CTX-M beta-lactamase pandemic. Curr Opin Microbiol. 9, 466–75.
- Carlsson,A., Nystrom,T., de Cock,H. and Bennich,H. (1998) Attacin – an insect immune protein – binds LPS and triggers the specific inhibition of bacterial outer-membrane protein synthesis. Microbiology 144, 2179–2188.
- Carillo,S., Pieretti,G., Parrilli,E., Tutino,M.L., Gemma,S., Molteni,M., Lanzetta,R., Parrilli,M., Corsaro,M.M. (2011). Structural investigation and biological activity of the lipooligosaccharide from the psychrophilic bacterium *Pseudoalteromonas haloplanktis* TAB 23 *Chemistry 17*, 7053–7060.
- Chaby,R. (2004). Lipopolysaccharide-binding molecules: transporters, blockers and sensors. Cell. Mol. Life Sci. *61*,. 1697-1713.
- Chang,G., Roth,C.B., Reyes,C.L., Pornillos,O., Chen,Y.J., and Chen,A.P. (2006). Retraction. Science *314*, 1875.
- Chimalakonda,G., Ruiz,N., Chng,S.S., Garner,R.A., Kahne,D., and Silhavy,T.J. (2011). Lipoprotein LptE is required for the assembly of LptD by the beta-barrel assembly machine in the outer membrane of *Escherichia coli*. Proc. Natl. Acad. Sci. U. S. A *108*, 2492-2497.
- Chng,S.S., Gronenberg,L.S., and Kahne,D. (2010a). Proteins required for lipopolysaccharide assembly in *Escherichia coli* form a transenvelope complex. Biochemistry *49*, 4565-4567.
- Chng,S.S., Ruiz,N., Chimalakonda,G., Silhavy,T.J., and Kahne,D. (2010b). Characterization of the two-protein complex in *Escherichia coli* responsible for lipopolysaccharide assembly at the outer membrane. Proc. Natl. Acad. Sci. U. S. A *107*, 5363-5368.
- Chung,H.S. and Raetz,C.R. (2011). Dioxygenases in *Burkholderia ambifaria* and *Yersinia pestis* that hydroxylate the outer Kdo unit of lipopolysaccharide. Proc. Natl. Acad. Sci. U. S. A *108*, 510-515.
- Cipolla,L., Polissi,A., Airoldi,C., Galliani,P., Sperandeo,P., and Nicotra,F. (2009). The Kdo biosynthetic pathway toward OM biogenesis as target in antibacterial drug design and development. Curr. Drug Discov. Technol. 6, 19-33.
- Clementz,T., Bednarski,J.J., and Raetz,C.R. (1996). Function of the *htrB* high temperature requirement gene of *Escherchia coli* in the acylation of lipid A: HtrB catalyzed incorporation of laurate. J. Biol. Chem. *271*, 12095-12102.
- Clementz,T., Zhou,Z., and Raetz,C.R. (1997). Function of the *Escherichia coli* msbB gene, a multicopy suppressor of htrB knockouts, in the acylation of lipid A. Acylation by MsbB follows laurate incorporation by HtrB. J. Biol. Chem. *272*, 10353-10360.
- Coates, A., Hu, Y., Bax, R., Page, C. (2002). The future challenges facing the development of new antimicrobial drugs. *Nat. Rev. Drug Discov.* 1, 895–910.
- Dankesreiter,S., Hoess,A., Schneider-Mergener,J., Wagner,H. and Miethke,T. (2000). Synthetic endotoxin-binding peptides block endotoxin-triggered TNF-alpha production

by macrophages in vitro and in vivo and prevent endotoxin-mediated toxic shock. J. Immunol. 164, 4804–4811.
- Dartigalongue,C., Missiakas,D., and Raina,S. (2001). Characterization of the *Escherichia coli* σ^E regulon. J. Biol. Chem. *276*, 20866-20875.
- Daugelavicius,R., Bakiene,E. and Bamford,D.H. (2000) Stages of Polymyxin B interaction with the *Escherichia coli* cell envelope. Antimicrob. Agents Chemother. 44, 2969–2978.
- Daus,M.L., Berendt,S., Wuttge,S., and Schneider,E. (2007). Maltose binding protein (MalE) interacts with periplasmic loops P2 and P1 respectively of the MalFG subunits of the maltose ATP binding cassette transporter (MalFGK(2)) from *Escherichia coli*/*Salmonella* during the transport cycle. Mol. Microbiol. 66, 1107–1122.
- David,S.A., Mathan,V.I. and Balaram,P. (1992) Interaction of melittin with endotoxic lipid A. Biochim. Biophys. Acta 1123, 269–274.
- Davidson,A.L., Dassa,E., Orelle,C., and Chen,J. (2008). Structure, function, and evolution of bacterial ATP-binding cassette systems. Microbiol. Mol. Biol. Rev. *72*, 317-64, table.
- Dawson,R.J. and Locher,K.P. (2006). Structure of a bacterial multidrug ABC transporter. Nature *443*, 180-185.
- Day,J.R., Albers,J.J., Lofton-Day,C.E., Gilbert,T.L., Ching,A.F., Grant,F.J. (1994). Complete cDNA encoding human phospholipid transfer protein from human endothelial cells. J. Biol. Chem. 269, 9388–9391.
- De Haas,C.J., van der Zee,R., Benaissa-Trouw,B., van Kessel,K.P., Verhoef,J. and van Strijp,J.A. (1999) Lipopolysaccharide (LPS)-binding synthetic peptides derived from serum amyloid P component neutralize LPS. Infect. Immun. 67: 2790–2796.
- De Lucca,A.J., Jacks,T.J. and Brogden K. A. (1995). Binding between lipopolysaccharide and cecropin A. Mol. Cell. Biochem. 151, 141–148.
- De Rosa,M., Trincone,A., Nicolaus,B., Gambacorta,A., and di Prisco G. (1991). Archeabacteria: lipids, membrane structures, and adaptation to environmental stresses. In Life under Extreme Conditions, Springer, Berlin, (Germany), pp. 61-87.
- Dekker,N. (2000). Outer-membrane phospholipase A: known structure, unknown biological function. Mol. Microbiol. *35*, 711-717.
- Derzelle,S., Turlin,E., Duchaud,E., Pages,S., Kunst,F., Givaudan,A., and Danchin,A. (2004). The PhoP-PhoQ two-component regulatory system of Photorhabdus luminescens is essential for virulence in insects. J. Bacteriol. *186*, 1270-1279.
- Desvaux,M., Hebraud,M., Talon,R., and Henderson,I.R. (2009). Secretion and subcellular localizations of bacterial proteins: a semantic awareness issue. Trends Microbiol. *17*, 139-145.
- Dijkstra,A.J. and Keck,W. (1996). Peptidoglycan as a barrier to transenvelope transport. J. Bacteriol. *178*, 5555-5562.
- DiMasi, J. A., Hansen, R. W., Grabowski, H. G. (2003). The price of innovation: New estimates of drug development costs. *J. Health Econ.* 22, 151–185.
- Doerrler,W.T., Gibbons,H.S., and Raetz,C.R. (2004). MsbA-dependent translocation of lipids across the inner membrane of *Escherichia coli*. J. Biol. Chem. *279*, 45102-45109.
- Doerrler,W.T. and Raetz,C.R. (2002). ATPase activity of the MsbA lipid flippase of *Escherichia coli*. J. Biol. Chem. *277*, 36697-36705.
- Doerrler,W.T., Reedy,M.C., and Raetz,C.R. (2001). An *Escherichia coli* mutant defective in lipid export. J. Biol. Chem. *276*, 11461-11464.
- Eckford,P.D. and Sharom,F.J. (2008). Functional characterization of *Escherichia coli* MsbA: interaction with nucleotides and substrates. J. Biol. Chem. *283*, 12840-12850.
- Eckford,P.D. and Sharom,F.J. (2010). The reconstituted *Escherichia coli* MsbA protein displays lipid flippase activity. Biochem. J. *429*, 195-203.
- Elass-Rochard,E., Roseanu,A., Legrand,D., Trif,M., Salmon,V., Motas,C. (1995). Lactoferrin-lipopolysaccharide interaction: involvement of the 28–34 loop region of human lactoferrin in the high-affinity binding to *Escherichia coli* 055B5 lipopolysaccharide. Biochem. J. 312, 839–845.
- Ellen,A.F., Zolghadr,B., Driessen,A.M., and Albers,S.V. (2010). Shaping the archaeal cell envelope. Archaea. *2010*, 608243.
- Ferguson,A.D., Welte,W., Hofmann,E., Lindner,B., Holst,O., Coulton,J.W., and Diederichs,K. (2000). A conserved structural motif for lipopolysaccharide recognition by procaryotic and eucaryotic proteins. Structure. *8*, 585-592.
- Fernandes, P.(2006).Antibacterial discovery and development—the failure of success? *Nat. Biotechnol.* 24, 1497– 1503.

- Fodorová,M., Vadovič,P., and Toman,R. (2011). Structural features of lipid A of Rickettsia typhi. *Acta Virol. 55*, 31–44.
- Freinkman,E., Chng,S.S., and Kahne,D. (2011). The complex that inserts lipopolysaccharide into the bacterial outer membrane forms a two-protein plug-and-barrel. Proc. Natl. Acad. Sci. U. S. A *108*, 2486-2491.
- Frey,E.A., Miller,D.S., Jahr,T.G., Sundan,A., Bazil,V., and Espevik T. (1992). Soluble CD14 participates in the response of cells to lipopolysaccharide. J. Exp. Med. 176, 1665–1671.
- Fukuoka,S., Brandenburg,K., Muller,M., Lindner,B., Koch,M.H., and Seydel,U. (2001). Physico-chemical analysis of lipid A fractions of lipopolysaccharide from *Erwinia carotovora* in relation to bioactivity. Biochim. Biophys. Acta *1510*, 185-197.
- Gan,L., Chen,S., and Jensen,G.J. (2008). Molecular organization of Gram-negative peptidoglycan. Proc. Natl. Acad. Sci. U. S. A *105*, 18953-18957.
- Garrett,T.A., Kadrmas,J.L., and Raetz,C.R. (1997). Identification of the gene encoding the *Escherichia coli* lipid A 4'-kinase. Facile phosphorylation of endotoxin analogs with recombinant LpxK. J. Biol. Chem. *272*, 21855-21864.
- Gegner, J.A., Ulevitch,R.J. and Tobias,P.S. (1995). Lipopolysaccharide (LPS) signal transduction and clearance. Dual roles for LPS binding protein and membrane CD14. J. Biol. Chem. 270, 5320–5325.
- Gewurz,H., Zhang,X.H. and Lint,T.F. (1995) Structure and function of the pentraxins. Curr. Opin. Immunol. 7, 54–64.
- Ghanei,H., Abeyrathne,P.D., and Lam,J.S. (2007). Biochemical characterization of MsbA from *Pseudomonas aeruginosa*. J. Biol. Chem. *282*, 26939-26947.
- Gil,R., Silva,F.J., Zientz,E., Delmotte,F., Gonzalez-Candelas,F., Latorre,A., Rausell,C., Kamerbeek,J., Gadau,J., Holldobler,B., van Ham,R.C., Gross,R., and Moya,A. (2003). The genome sequence of *Blochmannia floridanus*: comparative analysis of reduced genomes. Proc. Natl. Acad. Sci. U. S. A *100*, 9388-9393.
- Gioannini,T.L., and Weiss,J.P. (2007) Regulation of interactions of Gram-negative bacterial endotoxins with mammalian cells. Immunol,. Res. 39,249–260.
- Glauert,A.M. and Thornley,M.J. (1969). The topography of the bacterial cell wall. Annu. Rev. Microbiol. *23*, 159-198.
- Gonzalez,V., Santamaria,R.I., Bustos,P., Hernandez-Gonzalez,I., Medrano-Soto,A., Moreno-Hagelsieb,G., Janga,S.C., Ramirez,M.A., Jimenez-Jacinto,V., Collado-Vides,J., and Davila,G. (2006). The partitioned *Rhizobium etli* genome: genetic and metabolic redundancy in seven interacting replicons. Proc. Natl. Acad. Sci. U. S. A *103*, 3834-3839.
- Gough,M., Hancock,R.E. and Kelly,N.M. (1996) Antiendo- toxin activity of cationic peptide antimicrobial agents. Infect. Immun. 64, 4922–4927.
- Gruber,A., Mancek,M., Wagner,H., Kirschning,C.J., Jerala,R., 2004. Structural model of MD-2 and functional role of its basic amino acid clusters involved in cellular lipopolysaccharide recognition. J. Biol. Chem. 279, 28475–28482.
- Grunfeld,C., Marshall,M., Shigenaga,J.K., Moser,A.H., Tobias,P. and Feingold,K.R. (1999) Lipoproteins inhibit macrophage activation by lipoteichoic acid. J. Lipid Res. 40, 245–252.
- Grütter,M.G., Weaver,L.H. and Matthews, B.W. (1983). Goose lysozyme structure: an evolutionary link between hen and bacteriophage lysozymes? Nature. 303, 828-83.
- Gunn,J.S. (2000). Mechanisms of bacterial resistance and response to bile. Microbes. Infect. *2*, 907-913.
- Gunn,J.S. (2008). The *Salmonella* PmrAB regulon: lipopolysaccharide modifications, antimicrobial peptide resistance and more. Trends Microbiol. *16*, 284-290.
- Guo,L., Lim,K.B., Poduje,C.M., Daniel,M., Gunn,J.S., Hackett,M., and Miller,S.I. (1998). Lipid A acylation and bacterial resistance against vertebrate antimicrobial peptides. Cell *95*, 189-198.
- Gupta,R.S. (1998). What are archaebacteria: life's third domain or monoderm prokaryotes related to gram-positive bacteria? A new proposal for the classification of prokaryotic organisms. Mol. Microbiol. *29*, 695-707.
- Gutsmann,T., Müller,M., Carroll,S.F., MacKenzie,R.C., Wiese,A. and Seydel,U. (2001). Dual role of lipopolysaccharide (LPS)-binding protein in neutralization of LPS and enhancement of LPS-induced activation of mononuclear cells. Infect. Immun. 69, 6942–6950.
- Haarmann,R., Ibrahim,M., Stevanovic,M., Bredemeier,R., and Schleiff,E. (2010). The properties of the outer membrane localized Lipid A transporter LptD. J. Phys. Condens. Matter *22*, 454124.

- Hailman,E., Albers,J.J., Wolfbauer,G., Tu,A.Y. and Wright,S.D. (1996) Neutralization and transfer of lipopolysaccharide by phospholipid transfer protein. J. Biol. Chem. 271, 12172–12178.
- Hampton,R.Y. and Raetz,C.R. (1991). Macrophage catabolism of lipid A is regulated by endotoxin stimulation. J. Biol. Chem. 266, 19499–19509.
- Harel,M., Kleywegt,G.J., Ravelli,R.B.G., Silman,I., and Sussman,J.L. (1995). Crystal structure of an acetylcholinesterase-fasciculin complex: interaction of a three-fingered toxin from snake venom with its target. Structure. 3, 1355-1366.
- Harwig,S.S., Kokryakov,V.N., Swiderek,K.M., Aleshina,G.M., Zhao,C. and Lehrer,R.I. (1995). Prophenin-1, an exceptionally proline-rich antimicrobial peptide from porcine leukocytes. FEBS Lett. 362, 65–69.
- Hawkey, PM. (2008). Prevalence and clonality of extended-spectrum beta-lactamases in Asia. Clin. Microbiol. Infect. 14,159–165.
- Ayers,M., Sampaleanu,L.M., Tammam,S., Koo,J., Harvey,H., Howell,P.L., and Burrows,L.L. (2009). PilM/N/O/P Proteins Form an Inner Membrane Complex That Affects the Stability of the *Pseudomonas aeruginosa* Type IV Pilus Secretin. J. Mol. Biol. 394, 128–142.
- Heinzelmann,M., Mercer-Jones,M.A., Flodgaard,H. and Miller,F.N. (1998). Heparin-binding protein (CAP37) is internalized in monocytes and increases LPS-induced monocyte activation. J. Immunol. 160, 5530–5536.
- Helander,I.M., Kilpelainen,I. and Vaara,M. (1994) Increased substitution of phosphate groups in lipopolysaccharides and lipid A of the polymyxin-resistant pmrA mutants of *Salmonella typhimurium*: a 31P-NMR study. Mol. Microbiol. 11, 481–487.
- Hirschfeld,M., Ma,Y., Weis,J.H., Vogel,S.N. and Weis,J.J. (2000) Repurification of lipopolysaccharide eliminates signaling through both human and murine toll-like receptor 2. J. Immunol. 165, 618–622.
- Hoess,A., Watson,S., Siber,G.R. and Liddington R. (1993) Crystal structure of an endotoxin-neutralizing protein from the horseshoe crab, Limulus anti-LPS factor, at 1.5 A resolution. EMBO J. 12, 3351–3356.
- Holland,I.B. (2010). The extraordinary diversity of bacterial protein secretion mechanisms. Methods Mol. Biol. *619*, 1-20.
- Holst,O. (2007). The structures of core regions from enterobacterial lipopolysaccharides - an update. FEMS Microbiol. Lett. *271*, 3-11.
- Holst,O. and Molinaro,A. (2009). Core region and lipid A components of lipopolysaccharide. From "Microbial glycobiology: structures, relevance and applications" Moran,A.P., Holst,O., Brennan,P.J. ed. Elsevier.
- Hwang,P.M., Choy,W.Y., Lo,E.I., Chen,L., Forman-Kay,J.D., Raetz,C.R., Prive,G.G., Bishop,R.E., and Kay,L.E. (2002). Solution structure and dynamics of the outer membrane enzyme PagP by NMR. Proc. Natl. Acad. Sci. U. S. A 99, 13560-13565.
- Ishidate,K., Creeger,E.S., Zrike,J., Deb,S., Glauner,B., MacAlister,T.J., and Rothfield,L.I. (1986). Isolation of differentiated membrane domains from *Escherichia coli* and *Salmonella typhimurium*, including a fraction containing attachment sites between the inner and outer membranes and the murein skeleton of the cell envelope. J. Biol. Chem. *261*, 428-443.
- Isshiki,Y., Zahringer,U., and Kawahara,K. (2003). Structure of the core-oligosaccharide with a characteristic D-glycero-alpha-D-talo-oct-2-ulosylonate-(2-->4)-3-deoxy-D-manno-oct-2-ulo sonate [alpha-Ko-(2-->4)-Kdo] disaccharide in the lipopolysaccharide from *Burkholderia cepacia*. Carbohydr. Res. *338*, 2659-2666.
- Iversen,L.F., Kastrup,J.S., Bjorn,S.E., Rasmussen,P.B., Wiberg,F.C., Flodgaard, H.J. (1997). Structure of HBP, a multifunctional protein with a serine proteinase fold. Nat. Struct. Biol. 4, 265–268.
- Iwagaki,A., Porro,M., and Pollack,M. (2000). Influence of Synthetic Antiendotoxin Peptides on Lipopolysaccharide (LPS) Recognition and LPS-Induced Proinflammatory Cytokine Responses by Cells Expressing Membrane-Bound CD14. Infect. Immun. 2000, 68, 1655 – 1663.
- Jackman,J.E., Raetz,C.R., and Fierke,C.A. (1999). UDP-3-O-(R-3-hydroxymyristoyl)-N-acetylglucosamine deacetylase of *Escherichia coli* is a zinc metalloenzyme. Biochemistry *38*, 1902-1911.
- Juan,T.S., Hailman,E., Kelley,M.J., Busse,L.A., Davy,E., Empig,C.J. (1995). Identification of a lipopolysaccharide binding domain in CD14 between amino acids 57 and 64. J. Biol. Chem. 270, 5219–5224.

- Jurgens,G., Muller,M., Koch,M.H. and Brandenburg,K. (2001). Interaction of hemoglobin with enterobacterial lipopolysaccharide and lipid A. Physicochemical characterization and biological activity. Eur. J. Biochem. 268, 4233–4242.
- Kaca,W., Roth,R.I. and Levin,J. (1994). Hemoglobin, a newly recognized lipopolysaccharide (LPS)-binding protein that enhances LPS biological activity. J. Biol. Chem. 269: 25078–25084.
- Kamio,Y. and Nikaido,H. (1976). Outer membrane of *Salmonella typhimurium*: accessibility of phospholipid head groups to phospholipase c and cyanogen bromide activated dextran in the external medium. Biochemistry *15*, 2561-2570.
- Karow,M., Fayet,O., and Georgopoulos,C. (1992). The lethal phenotype caused by null mutations in the *Escherichia coli htrB* gene is suppressed by mutations in the *accBC* operon, encoding two subunits of acetyl coenzyme A carboxylase. J. Bacteriol. *174*, 7407-7418.
- Karow,M. and Georgopoulos,C. (1993). The essential *Escherichia coli msbA* gene, a multicopy suppressor of null mutations in the *htrB* gene, is related to the universally conserved family of ATP-dependent translocators. Mol. Microbiol. *7*, 69-79.
- Karuppiah,V., Berry,J.L., and Derrick,J.P. (2011). Outer membrane translocons: structural insights into channel formation. Trends Microbiol. *19*, 40-48.
- Katz,C. and Ron,E.Z. (2008). Dual role of FtsH in regulating lipopolysaccharide biosynthesis in Escherichia coli. J. Bacteriol. *190*, 7117-7122.
- Kellenberger,E. (1990). The 'Bayer bridges' confronted with results from improved electron microscopy methods. Mol. Microbiol. *4*, 697-705.
- Kim,H.M., Park,B.S., Kim,J.I., Kim,S.E., Lee,J., Oh,S.C., Enkhbayar,P., Matsushima,N., Lee,H., Yoo,O.J., and Lee,J.O. (2007). Crystal structure of the TLR4-MD-2 complex with bound endotoxin antagonist Eritoran. Cell *130*, 906-917.
- Kim,J.I., Lee,C.J., Jin,M.S., Lee,C.H., Paik,S.G., Lee,H., and Lee,J.O. (2005). Crystal structure of CD14 and its implications for lipopolysaccharide signaling. J. Biol. Chem. *280*, 11347-11351.
- King,J.D., Kocincova,D., Westman,E.L., and Lam,J.S. (2009). Review: Lipopolysaccharide biosynthesis in *Pseudomonas aeruginosa*. Innate. Immun. *15*, 261-312.
- Klein,G., Lindner,B., Brabetz,W., Brade,H., and Raina,S. (2009). *Escherichia coli* K-12 Suppressor-free Mutants Lacking Early Glycosyltransferases and Late Acyltransferases: minimal lipopolysaccharide structure and induction of envelope stress response. J. Biol. Chem. *284*, 15369-15389.
- Knowles,T.J., Scott-Tucker,A., Overduin,M., and Henderson,I.R. (2009). Membrane protein architects: the role of the BAM complex in outer membrane protein assembly. Nat. Rev. Microbiol. *7*, 206-214.
- Koch,A.L. (1998). The biophysics of the gram-negative periplasmic space. Crit Rev. Microbiol. *24*, 23-59.
- Kol,M.A., van Dalen,A., de Kroon,A.I., and de Kruijff,B. (2003). Translocation of phospholipids is facilitated by a subset of membrane-spanning proteins of the bacterial cytoplasmic membrane. J. Biol. Chem. *278*, 24586-24593.
- Kramer,R.A., Brandenburg,K., Vandeputte-Rutten,L., Werkhoven,M., Gros,P., Dekker,N., and Egmond,M.R. (2002). Lipopolysaccharide regions involved in the activation of *Escherichia coli* outer membrane protease OmpT. Eur. J. Biochem. 269, 1746–1752.
- Kumarasamy,K.K., Toleman,M.A., Walsh,T.R., Bagaria,J., Butt,F., Balakrishnan,R., Chaudhary,U., Doumith,M., Giske,C.G., Irfan,S., Krishnan,P., Kumar,A.V., Maharjan,S., Mushtaq,S., Noorie,T., Paterson,D.L, Pearson,A., Perry,C., Pike,R., Rao,B., Ray,U., Sarma,J.B, Sharma,M., Sheridan,E., Thirunarayan,M.A., Turton,J., Upadhyay,S., Warner,M., Welfare,W., Livermore,D.,M, Woodford, N. (2010). Emergence of a new antibiotic resistance mechanism in India, Pakistan, and the UK: a molecular, biological, and epidemiological study. Lancet .Infect. Dis*10*, 597–602.
- Lamping,N., Hoess,A., Yu,B., Park,T.C., Kirschning,C., Pfeil,D., Reter,D., Wright,S.D., Herrmann,F. and Schumann,R.R. (1996). Effects of site-directed mutagenesis of basic residues (Arg 94, Lys 95, Lys 99) of lipopolysaccharide (LPS)-binding protein on binding and transfer of LPS and subsequent immune cell activation. J. Immunol. 157, 4648–4656.
- Langklotz,S., Schakermann,M., and Narberhaus,F. (2011). Control of lipopolysaccharide biosynthesis by FtsH-mediated proteolysis of LpxC is conserved in enterobacteria but not in all gram-negative bacteria. J. Bacteriol. *193*, 1090-1097.

- Lee,H., Hsu,F.F., Turk,J., and Groisman,E.A. (2004). The PmrA-regulated pmrC gene mediates phosphoethanolamine modification of lipid A and polymyxin resistance in *Salmonella enterica*. J. Bacteriol. *186*, 4124-4133.
- Leeb, M. Antibiotics: A shot in the arm. (2004). *Nature* 431, 892– 893.
- Lei,M.G. and Morrison,D.C. (1993) Lipopolysaccharide interaction with S2 subunit of pertussis toxin. J. Biol. Chem. 268, 1488–1493.
- Liepke,C., Baxmann,S., Heine,C., Breithaupt,N., Standker,L. and Forssmann,W.G. (2003). Human hemoglobin-derived peptides exhibit antimicrobial activity: a class of host defense peptides. J. Chromatogr. B. Analyt .Technol. Biomed. Life Sci. 791, 345–356.
- Little,R.G., Kelner,D.N., Lim,E., Burke,D.J. and Conlon,P. J. (1994). Functional domains of recombinant bactericidal/permeability increasing protein (rBPI23). J. Biol. Chem. 269, 1865–1872.
- Livermore,D.M., Canton,R., Gniadkowski,M. (2007). CTX-M: changing the face of ESBLs in Europe. J Antimicrob Chemother. 59,165–74.
- Luederitz,O., Risse,H.J., Schulte-Holthausen,H., Strominger,J.L., Sutherland,I.W., and Westphal,O. (1965). Biochemical studies of the smooth-rough mutation in *Salmonella minneso*ta. J. Bacteriol. *89*, 343-354.
- Ma,B., Reynolds,C.M., and Raetz,C.R. (2008). Periplasmic orientation of nascent lipid A in the inner membrane of an *Escherichia coli* LptA mutant. Proc. Natl. Acad. Sci. U. S. A *105*, 13823-13828.
- Maier,R.V., Mathison,J.C. and Ulevitch,R.J. (1981) Interactions of bacterial lipopolysaccharides with tissue macrophages and plasma lipoproteins. Prog. Clin. Biol. Res. 62: 133–155.
- Majerle,A., Kidric,J. and Jerala,R. (2003). Enhancement of antibacterial and lipopolysaccharide binding activities of a human lactoferrin peptide fragment by the addition of acyl chain. J. Antimicrob. Chemother. 51, 1159–1165.
- Malinverni,J.C. and Silhavy,T.J. (2009). An ABC transport system that maintains lipid asymmetry in the gram-negative outer membrane. Proc. Natl. Acad. Sci. U. S. A *106*, 8009-8014.
- Mamat,U., Meredith,T.C., Aggarwal,P., Kuhl,A., Kirchhoff,P., Lindner,B., Hanuszkiewicz,A., Sun,J., Holst,O., and Woodard,R.W. (2008). Single amino acid substitutions in either YhjD or MsbA confer viability to 3-deoxy-d-manno-oct-2-ulosonic acid-depleted *Escherichia coli*. Mol. Microbiol. *67*, 633-648.
- Mancek,M., Pristovsek,P., Jerala,R., 2002. Identification of LPS-binding peptide fragment of MD-2, a Toll-receptor accessory protein. Biochem. Biophys. Res. Commun. 292, 880–885.
- Margolin,W. (2009). Sculpting the bacterial cell. Curr. Biol. *19*, R812-R822.
- Marolda,C.L., Li,B., Lung,M., Yang,M., Hanuszkiewicz,A., Rosales,A.R., and Valvano,M.A. (2010). Membrane topology and identification of critical amino acid residues in the Wzx O-antigen translocase from *Escherichia coli* O157:H4. J. Bacteriol. *192*, 6160-6171.
- Martorana,A.M., Sperandeo,P., Polissi,A., and Deho,G. (2011). Complex transcriptional organization regulates an *Escherichia coli* locus implicated in lipopolysaccharide biogenesis. Res. Microbiol.
- Masson,P.L., Heremans,J.F. and Schonne,E. (1969). Lactoferrin, an iron-binding protein in neutrophilic leukocytes. J. Exp. Med. 130, 643–658.
- Mathison,J.C., Tobias,P.S., Wolfson,E. and Ulevitch,R.J. (1992) Plasma lipopolysaccharide (LPS)-binding protein. A key component in macrophage recognition of gram-negative LPS. J. Immunol. 149, 200–206.
- Matsuzaki,K., Sugishita,K. and Miyajima,K. (1999). Interactions of an antimicrobial peptide, magainin 2, with lipopolysaccharide-containing liposomes as a model for outer membranes of Gram-negative bacteria. FEBS Lett. 449, 221–224.
- Matthews,B.W. and Remington,S.J. (1974). The three-dimensional structure of the lysozyme from bacteriophage T4. Proc. Natl Acad. Sci. USA 71, 4178-4182.
- Mayo,K.H., Haseman,J., Ilyina,E., and Gray,B. (1998). Designed beta-sheet-forming peptide 33mers with potent human bactericidal/permeability increasing protein-like bactericidal and endotoxin neutralizing activities. Biochim. Biophys. Acta 1425, 81–92.
- McCarter,J.D., Stephens,D., Shoemaker,K., Rosenberg,S., Kirsch,J.F., and Georgiou, G. (2004). Substrate Specificity of the *Escherichia coli* Outer Membrane Protease OmpT. J. Bacteriol. 186, 5919-5925.

- McConnell,M.R., Oakes,K.R., Patrick,A.N., and Mills,D.M. (2001). Two functional O-polysaccharide polymerase wzy (rfc) genes are present in the rfb gene cluster of Group E1 *Salmonella enterica* serovar Anatum. FEMS Microbiol. Lett. *199*, 235-240.
- McGrath,B.C. and Osborn,M.J. (1991). Localization of the terminal steps of O-antigen synthesis in Salmonella typhimurium. J. Bacteriol. *173*, 649-654.
- Medzhitov,R., Preston-Hurlburt,P., and Janeway,C.A., Jr. (1997). A human homologue of the Drosophila Toll protein signals activation of adaptive immunity. Nature *388*, 394-397.
- Meredith,T.C., Aggarwal,P., Mamat,U., Lindner,B., and Woodard,R.W. (2006). Redefining the requisite lipopolysaccharide structure in *Escherichia coli*. ACS Chem. Biol. *1*, 33-42.
- Meredith,T.C., Mamat,U., Kaczynski,Z., Lindner,B., Holst,O., and Woodard,R.W. (2007). Modification of lipopolysaccharide with colanic acid (M-antigen) repeats in *Escherichia coli*. J. Biol. Chem. *282*, 7790-7798.
- Meredith,T.C. and Woodard,R.W. (2003). *Escherichia coli* YrbH is a D-arabinose 5-phosphate isomerase. J. Biol. Chem. *278*, 32771-32777.
- Metzger,L.E. and Raetz,C.R. (2010). An alternative route for UDP-diacylglucosamine hydrolysis in bacterial lipid A biosynthesis. Biochemistry *49*, 6715-6726.
- Miller,S.I., Ernst,R.K., and Bader,M.W. (2005). LPS, TLR4 and infectious disease diversity. Nat. Rev. Microbiol. *3*, 36-46.
- Minnikin,D.E. (1991). Chemical principles in the organization of lipid components in the mycobacterial cell envelope. Res. Microbiol. *142*, 423-427.
- Missiakas,D., Betton,J.M., and Raina,S. (1996). New components of protein folding in extracytoplasmic compartments of *Escherichia coli* SurA, FkpA and Skp/OmpH. Mol. Microbiol. *21*, 871-884.
- Mistretta,N., Seguin,D., Thiébaud,J., Vialle,S., Blanc,F., Brossaud,M., Talaga,P. (2010). Genetic and structural characterization of L11 lipooligosaccharide from Neisseria meningitidis serogroup A strains. *J. Biol. Chem. 285*, 19874–19883.
- Miyake,K. (2004). Innate recognition of lipopolysaccharide by Toll-like receptor 4-MD-2. Trends Microbiol. *12*, 186-192.
- Miyake,K. (2006). Roles for accessory molecules in microbial recognition by Toll-like receptors. J. Endotoxin. Res. *12*, 195-204.
- Morona,R., Van Den,B.L., and Daniels,C. (2000). Evaluation of Wzz/MPA1/MPA2 proteins based on the presence of coiled-coil regions. Microbiology *146*, 1-4.
- Morrison, D.C. and Cochrane,C.G. (1974). Direct evidence for Hageman factor (factor XII) activation by bacterial lipopolysaccharides (endotoxins). J Exp Med. 140,797-811.
- Muhlradt,P.F. and Golecki,J.R. (1975). Asymmetrical distribution and artifactual reorientation of lipopolysaccharide in the outer membrane bilayer of *Salmonella typhimurium*. Eur. J. Biochem. *51*, 343-352.
- Muhlradt,P.F., Menzel,J., Golecki,J.R., and Speth,V. (1973). Outer membrane of *Salmonella*. Sites of export of newly synthesised lipopolysaccharide on the bacterial surface. Eur. J. Biochem. *35*, 471-481.
- Muszynski,A., Laus,M., Kijne,J.W., and Carlson,R.W. (2011). Structures of the lipopolysaccharides from Rhizobium leguminosarum RBL5523 and its UDP-glucose dehydrogenase mutant (exo5). Glycob. *21*, 55–68.
- Nagaoka,I., Hirota,S., Niyonsaba,F., Hirata,M., Adachi,Y., Tamura,H., Tanaka,S., and Heumann,D. (2002). Augmentation of the lipopolysaccharide-neutralizing activities of human cathelicidin CAP18/LL-37-derived antimicrobial peptides by replacement with hydrophobic and cationic amino acid residues. Clin. Diagn. Lab. Immunol. 9, 972–982.
- Nagpal,S., Kaur,K.J., Jain,D. and Salunke,D.M. (2002). Plasticity in structure and interactions is critical for the action of indolicidin, an antibacterial peptide of innate immune origin. Protein Sci. 11, 2158–2167.
- Nahra, R. (2008). Targeting the lipopolysaccharides: still a matter of debate? Curr. Opin. Anesthesiol. 21,98–104.
- Narita,S., (2011). ABC Transporters Involved in the Biogenesis of the Outer Membrane in Gram-Negative Bacteria. *Biosci. Biotechnol. Biochem*. *75*, 1044–1054.
- Narita,S. and Tokuda,H. (2009). Biochemical characterization of an ABC transporter LptBFGC complex required for the outer membrane sorting of lipopolysaccharides. FEBS Lett. *583*, 2160-2164.
- Niederweis,M., Danilchanka,O., Huff,J., Hoffmann,C., and Engelhardt,H. (2010). Mycobacterial outer membranes: in search of proteins. Trends Microbiol. *18*, 109-116.

- Nikaido,H. (2003). Molecular basis of bacterial outer membrane permeability revisited. Microbiol. Mol. Biol. Rev. *67*, 593-656.
- Nikaido,H. (2005). Restoring permeability barrier function to outer membrane. Chem. Biol. *12*, 507-509.
- Nikaido,H., Mikaido,K., Subbaiah,T.V., and Stocker,B.A. (1964). Rough mutants of *Salmonella typhimurium*. III. Enzymatic synthesis of nucleotide-sugar compounds. Nature *201*, 1301-1302.
- Nordmann,P., Cuzon,G., Naas,T. (2009). The real threat of *Klebsiella pneumoniae* carbapenemase-producing bacteria. Lancet Infect Dis 9, 228–36.
- Odell,E.W., Sarra,R., Foxworthy,M., Chapple,D.S. and Evans,R.W. (1996). Antibacterial activity of peptides homologous to a loop region in human lactoferrin. FEBS Lett. 382, 175-178.
- Ogura,T., Inoue,K., Tatsuta,T., Suzaki,T., Karata,K., Young,K., Su,L.H., Fierke,C.A., Jackman,J.E., Raetz,C.R., Coleman,J., Tomoyasu,T., and Matsuzawa,H. (1999). Balanced biosynthesis of major membrane components through regulated degradation of the committed enzyme of lipid A biosynthesis by the AAA protease FtsH (HflB) in *Escherichia coli*. Mol. Microbiol. *31*, 833-844.
- Okemoto,K., Nakajima,Y., Fujioka,T. and Natori,S. (2002) Participation of two N-terminal residues in LPS-neutralizing activity of sarcotoxin IA. J. Biochem. (Tokyo) 131, 277–281.
- Okuda,S., and Tokuda,H. (2011). Lipoprotein Sorting in Bacteria. Annu. Rev. Microbiol. 65, 239–259.
- Oliver,D.B. (1996). Periplasm. In *Escherichia coli* and *Salmonella* Cellular and Molecular Biology, F.C.Neidhardt, ed. ASM press, pp. 88-103.
- Onishi,H.R., Pelak,B.A., Gerckens,L.S., Silver,L.L., Kahan,F.M., Chen,M.H., Patchett,A.A., Galloway,S.M., Hyland,S.A., Anderson,M.S., and Raetz,C.R. (1996). Antibacterial agents that inhibit lipid A biosynthesis. Science *274*, 980-982.
- Opalka,N., Brown,J., Lane,W.J., Twist,K.A.F., Landick,R., Asturias,F.J., and Darst,S.A. (2010). Complete Structural Model of Escherichia coli RNA Polymerase from a Hybrid Approach. PLoS Biology. 8, e1000483.
- Osborn,M.J., Gander,J.E., and Parisi,E. (1972). Mechanism of assembly of the outer membrane of Salmonella typhimurium. Site of synthesis of lipopolysaccharide. J. Biol. Chem. *247*, 3973-3986.
- Park,B.S., Song,D.H., Kim,H.M., Choi,B.S., Lee,H., and Lee,J.O. (2009). The structural basis of lipopolysaccharide recognition by the TLR4-MD-2 complex. Nature *458*, 1191-1195.
- Payne, D. J. Gwynn, M. N., Holmes, D. J., Pompliano, D. L. (2007). Drugs for bad bugs: Confronting the challenges of anti- bacterial discovery. *Nat. Rev. Drug Discov.* 6, 29–40.
- Pereira,H.A. (1995). CAP37, a neutrophil-derived multifunctional inflammatory mediator. J. Leukoc. Biol. 57, 805–812.
- Perna,N.T., Plunkett,G., Burland,V., Mau,B., Glasner,J.D., Rose,D.J., Mayhew,G.F., Evans,P.S, Gregor,J., Kirkpatrick,H.A., Pósfai,G., Hackett,J., Klink,J.S., Boutin,A., Shao,Y., Miller,L., Grotbeck,E.J., Davis,.N.W., Lim,A., Dimalanta,E.T., Potamousis,K.D., Apodaca,J., Anantharaman,T.S., Lin,J., Yen,G., Schwartz,D.C., Welch,R.A., and Blattner,F.R. (2001). Genome sequence of enterohaemorrhagic *Escherichia coli* O157:H7. Nature. *409*, 529–533.
- Plotz,B.M., Lindner,B., Stetter,K.O., and Holst,O. (2000). Characterization of a novel lipid A containing D-galacturonic acid that replaces phosphate residues. The structure of the lipid a of the lipopolysaccharide from the hyperthermophilic bacterium Aquifex pyrophilus. J. Biol. Chem. *275*, 11222-11228.
- Polissi,A. and Georgopoulos,C. (1996). Mutational analysis and properties of the *msbA* gene of *Escherichia coli*, coding for an essential ABC family transporter. Mol. Microbiol. *20*, 1221-1233.
- Price,N.P., Kelly,T.M., Raetz,C.R., and Carlson,R.W. (1994). Biosynthesis of a structurally novel lipid A in Rhizobium leguminosarum: identification and characterization of six metabolic steps leading from UDP-GlcNAc to 3-deoxy-D-manno-2-octulosonic acid2-lipid IVA. J. Bacteriol. *176*, 4646-4655.
- Pristovsek,P. and Kidric,J. (1999) Solution structure of polymyxins B and E and effect of binding to lipopolysaccharide: an NMR and molecular modeling study. J. Med. Chem. 42, 4604–4613.
- Radika,K. and Raetz,C.R. (1988). Purification and properties of lipid A disaccharide synthase of *Escherichia coli*. J. Biol. Chem. *263*, 14859-14867.

- Raetz,C.R., Guan,Z., Ingram,B.O., Six,D.A., Song,F., Wang,X., and Zhao,J. (2009). Discovery of new biosynthetic pathways: the lipid A story. J. Lipid Res. *50 Suppl*, S103-S108.
- Raetz,C.R., Reynolds,C.M., Trent,M.S., and Bishop,R.E. (2007). Lipid A modification systems in Gram-negative bacteria. Annu. Rev. Biochem. *76*, 295-329.
- Raetz,C.R. and Whitfield,C. (2002). Lipopolysaccharide endotoxins. Annu. Rev. Biochem. *71*, 635-700.
- Rahim,R., Burrows,L.L., Monteiro,M.A., Perry,M.B., and Lam,J.S. (2000). Involvement of the rml locus in core oligosaccharide and O polysaccharide assembly in *Pseudomonas aeruginosa*. Microbiology *146 (Pt 11)*, 2803-2814.
- Rebeil,R., Ernst,R.K., Gowen,B.B., Miller,S.I., and Hinnebusch,B.J. (2004). Variation in lipid A structure in the pathogenic yersiniae. Mol. Microbiol. *52*, 1363-1373.
- Reeves,P.R., Hobbs,M., Valvano,M.A., Skurnik,M., Whitfield,C., Coplin,D., Kido,N., Klena,J., Maskell,D., Raetz,C.R., and Rick,P.D. (1996). Bacterial polysaccharide synthesis and gene nomenclature. Trends Microbiol. *4*, 495-503.
- Re, F. (2002). Monomeric Recombinant MD-2 Binds Toll-like Receptor 4 Tightly and Confers Lipopolysaccharide Responsiveness. J. Biol. Chem. 277, 23427–23432.
- Rensen,P.C., Oosten,M., Bilt,E., Eck,M., Kuiper,J. and Berkel,T.J. (1997) Human recombinant apolipoprotein E redirects lipopolysaccharide from Kupffer cells to liver parenchymal cells in rats In vivo. J. Clin. Invest. 99: 2438–2445.
- Reyes,C., Ward,A., Yu,J., and Chang,G., (2006).The structures of MsbA: Insight into ABC transporter-mediated multidrug efflux. FEBS Letters 580,1042–1048.
- Reynolds,C.M., Ribeiro,A.A., McGrath,S.C., Cotter,R.J., Raetz,C.R., and Trent,M.S. (2006). An outer membrane enzyme encoded by *Salmonella typhimurium* lpxR that removes the 3'-acyloxyacyl moiety of lipid A. J. Biol. Chem. *281*, 21974-21987.
- Ried,C., Wahl,C., Miethke,T., Wellnhofer,G., Landgraf,C., Schneider-Mergener,J., and Hoess,A. (1996). High affinity endotoxin-binding and neutralizing peptides based on the crystals structure of recombinant Limulus anti-lipopolysaccharide factor. J. Biol. Chem. 271, 28120-28127.
- Rosenberg,M.F., Callaghan,R., Modok,S., Higgins,C.F., and Ford,R.C. (2005). Three-dimensional structure of P-glycoprotein: the transmembrane regions adopt an asymmetric configuration in the nucleotide-bound state. J. Biol. Chem. *280*, 2857-2862.
- Roth,R.I., Kaca,W. and Levin,J. (1994) Hemoglobin: a newly recognized binding protein for bacterial endotoxins (LPS). Prog. Clin. Biol. Res. 388, 161–172.
- Rubires,X., Saigi,F., Pique,N., Climent,N., Merino,S., Alberti,S., Tomas,J.M., and Regue,M. (1997). A gene (wbbL) *from Serratia marcescens* N28b (O4) complements the rfb-50 mutation of Escherichia coli K-12 derivatives. J. Bacteriol. *179*, 7581-7586.
- Ruiz,N., Chng,S.S., Hiniker,A., Kahne,D., and Silhavy,T.J. (2010). Nonconsecutive disulfide bond formation in an essential integral outer membrane protein. Proc. Natl. Acad. Sci. U. S. A. *107*, 12245-12250.
- Ruiz,N., Gronenberg,L.S., Kahne,D., and Silhavy,T.J. (2008). Identification of two inner-membrane proteins required for the transport of lipopolysaccharide to the outer membrane of *Escherichia coli*. Proc. Natl. Acad. Sci. U. S. A *105*, 5537-5542.
- Ruiz,N., Kahne,D., and Silhavy,T.J. (2006). Advances in understanding bacterial outer-membrane biogenesis. Nat. Rev. Microbiol. *4*, 57-66.
- Ruiz,N., Kahne,D., and Silhavy,T.J. (2009). Transport of lipopolysaccharide across the cell envelope: the long road of discovery. Nat. Rev. Microbiol. *7*, 677-683.
- Sampson,B.A., Misra,R., and Benson,S.A. (1989). Identification and characterization of a new gene of *Escherichia coli* K-12 involved in outer membrane permeability. Genetics *122*, 491-501.
- Samuel,G. and Reeves,P. (2003). Biosynthesis of O-antigens: genes and pathways involved in nucleotide sugar precursor synthesis and O-antigen assembly. Carbohydr. Res. *338*, 2503-2519.
- Sankaran,K. and Wu,H.C. (1994). Lipid modification of bacterial prolipoprotein. Transfer of diacylglyceryl moiety from phosphatidylglycerol. J. Biol. Chem. *269*, 19701-19706.
- Saurin,W., Hofnung,M., and Dassa,E. (1999). Getting in or out: early segregation between importers and exporters in the evolution of ATP-binding cassette (ABC) transporters. J. Mol. Evol. *48*, 22-41.
- Schroeder,T.H, Lee,M.M., Yacono,P.W., Cannon, C.L., Gerceker,A.A.,Golan,D.E. and Pier,G.B. (2002). CFTR is a pattern recognition molecule that extracts Pseudomonas

aeruginosa LPS from the outer membrane into epithelial cells and activates NF-kappa B translocation. Proc. Natl. Acad. Sci. U. S. A. 99, 6907-6912.

- Schultz,K.M., Merten,J.A., and Klug,C.S. (2011a). Characterization of the E506Q and H537A Dysfunctional Mutants in the *E. coli* ABC Transporter MsbA. Biochemistry *50*, 3599-3608.
- Schultz,K.M., Merten,J.A., and Klug,C.S. (2011b). Effects of the L511P and D512G mutations on the *Escherichia coli* ABC transporter MsbA. Biochemistry *50*, 2594-2602.
- Schumann,R.R., Leong,S.R., Flaggs,G.W., Gray,P.W., Wright,S.D., Mathison,J.C. (1990) Structure and function of lipopolysaccharide binding protein. Science 249, 1429–1431.
- Serina,S., Nozza,F., Nicastro,G., Faggioni,F., Mottl,H., Dehò,G., and Polissi,A. (2004). Scanning the *Escherichia coli* chromosome by random transposon mutagenesis and multiple phenotypic screening. Res. Microbiol. *155*, 692-701.
- Shamova,O., Brogden,K.A., Zhao,C., Nguyen,T., Kokryakov,V.N. and Lehrer,R.I. (1999). Purification and properties of proline-rich antimicrobial peptides from sheep and goat leukocytes. Infect. Immun. 67, 4106–4111.
- Shapiro,R.A., Cunningham,M.D., Ratcliffe,K., Seachord,C., Blake,J., Bajorath,J. (1997). Identification of CD14 residues involved in specif ic lipopolysaccharide recognition. Infect. Immun. 65, 293–297.
- Shimazu,R., Akashi,S., Ogata,H., Nagai,Y., Fukudome,K., Miyake,K., and Kimoto,M. (1999). MD-2, a molecule that confers lipopolysaccharide responsiveness on Toll-like receptor 4. J. Exp. Med. *189*, 1777-1782.
- Siarheyeva,A. and Sharom,F.J. (2009). The ABC transporter MsbA interacts with lipid A and amphipathic drugs at different sites. Biochem. J. *419*, 317-328.
- Silhavy,T.J., Kahne,D., and Walker,S. (2010). The bacterial cell envelope. Cold Spring Harb. Perspect. Biol. *2*, a000414.
- Sklar,J.G., Wu,T., Kahne,D., and Silhavy,T.J. (2007). Defining the roles of the periplasmic chaperones SurA, Skp, and DegP in *Escherichia coli*. Genes Dev. *21*, 2473-2484.
- Spellberg, B., Powers, J. H., Brass, E. P., Miller L. G., and Edwards Jr. J. E.. (2004). Trends in antimicrobial drug development: Implications for the future. *Clin. Infect. Dis.* 38, 1279–1286.
- Sperandeo,P., Cescutti,R., Villa,R., Di Benedetto,C., Candia,D., Dehò,G., and Polissi,A. (2007). Characterization of *lptA* and *lptB*, two essential genes implicated in lipopolysaccharide transport to the outer membrane of *Escherichia coli*. J. Bacteriol. *189*, 244-253.
- Sperandeo,P., Dehò,G., and Polissi,A. (2009). The lipopolysaccharide transport system of Gram-negative bacteria. Biochim. Biophys. Acta *1791*, 594-602.
- Sperandeo,P., Lau,F.K., Carpentieri,A., De Castro,C., Molinaro,A., Dehò,G., Silhavy,T.J., and Polissi,A. (2008). Functional analysis of the protein machinery required for transport of lipopolysaccharide to the outer membrane of *Escherichia coli*. J. Bacteriol. *190*, 4460-4469.
- Sperandeo,P., Pozzi,C., Dehò,G., and Polissi,A. (2006). Non-essential KDO biosynthesis and new essential cell envelope biogenesis genes in the *Escherichia coli yrbG-yhbG* locus. Res. Microbiol. *157*, 547-558.
- Steeghs,L., den Hartog,R., den Boer,A., Zomer,B., Roholl,P., and van derLey,P. (1998). Meningitis bacterium is viable without endotoxin. Nature *392*, 449-450.
- Stenberg,F., Chovanec,P., Maslen,S.L., Robinson,C.V., Ilag,L.L., von Heijne,G., and Daley,D.O. (2005). Protein complexes of the *Escherichia coli* cell envelope. J. Biol. Chem. *280*, 34409-34419.
- Subbaiah,T.V. and Stocker,B.A. (1964). Rough mutants of *Salmonella typhimurium*. I. Genetics. Nature *201*, 1298-1299.
- Suits,M.D., Sperandeo,P., Dehò,G., Polissi,A., and Jia,Z. (2008). Novel structure of the conserved Gram-negative lipopolysaccharide transport protein A and mutagenesis analysis. J. Mol. Biol. *380*, 476-488.
- Sutcliffe,I.C. (2010). A phylum level perspective on bacterial cell envelope architecture. Trends Microbiol. *18*, 464-470.
- Sutcliffe,I.C. (2011). Cell envelope architecture in the Chloroflexi: a shifting frontline in a phylogenetic turf war. Environ. Microbiol. *13*, 279-282.
- Takase,I., Ishino,F., Wachi,M., Kamata,H., Doi,N., Asoh,S., Matsuzawa,H., Ohta,T., Matsuhashi, M. (1987) Genes encoding two lipoproteins in the leuS-dacA region of the *Escherichia coli* chromosome. J. Bacteriol. *169*, 5692-5699

- Tall,A.R. (1993) Plasma cholesteryl ester transfer protein. J. Lipid Res. 34, 1255–1274.
- Tefsen,B., Bos,M.P., Beckers,F., Tommassen,J., and de Cock,H. (2005a). MsbA is not required for phospholipid transport in *Neisseria meningitidis*. J. Biol. Chem. *280*, 35961-35966.
- Tefsen,B., Geurtsen,J., Beckers,F., Tommassen,J., and de Cock,H. (2005b). Lipopolysaccharide transport to the bacterial outer membrane in spheroplasts. J. Biol. Chem. *280*, 4504-4509.
- Thomas,C.J., Kapoor,M., Sharma,S., Bausinger,H., Zyilan,U., Lipsker,D. (2002). Evidence of a trimolecular complex involving LPS, LPS binding protein and soluble CD14 as an effector of LPS response. FEBS Lett. 531, 184–188.
- Tokuda,H. (2009). Biogenesis of outer membranes in Gram-negative bacteria. Biosci. Biotechnol. Biochem. *73*, 465-473.
- Tollefson,J.H., Ravnik,S. and Albers,J.J. (1988) Isolation and characterization of a phospholipid transfer protein (LTP-II) from human plasma. J. Lipid Res. 29, 1593–1602.
- Tran,A.X., Dong,C., and Whitfield,C. (2010). Structure and functional analysis of LptC, a conserved membrane protein involved in the lipopolysaccharide export pathway in *Escherichia coli*. J. Biol. Chem. *285*, 33529-33539.
- Tran,A.X., Trent,M.S., and Whitfield,C. (2008). The LptA protein of *Escherichia coli* is a periplasmic lipid A-binding protein involved in the lipopolysaccharide export pathway. J. Biol. Chem. *283*, 20342-20349.
- Trent,M.S., Pabich,W., Raetz,C.R., and Miller,S.I. (2001a). A PhoP/PhoQ-induced Lipase (PagL) that catalyzes 3-O-deacylation of lipid A precursors in membranes of *Salmonella typhimurium*. J. Biol. Chem. *276*, 9083-9092.
- Trent,M.S., Ribeiro,A.A., Doerrler,W.T., Lin,S., Cotter,R.J., and Raetz,C.R. (2001b). Accumulation of a polyisoprene-linked amino sugar in polymyxin-resistant Salmonella typhimurium and *Escherichia coli*: structural characterization and transfer to lipid A in the periplasm. J. Biol. Chem. *276*, 43132-43144.
- Vaara,M. (1992) Agents that increase the permeability of the outer membrane. Microbiol. Rev. 56, 395–411.
- Valvano,M.A. (2003). Export of O-specific lipopolysaccharide. Front Biosci. *8*, s452-s471.
- van Berkel,P.H., Geerts,M.E., van Veen,H.A., Mericskay,M., de Boer,H.A. and Nuijens,J.H. (1997). N-terminal stretch Arg2, Arg3, Arg4 and Arg5 of human lactoferrin is essential for binding to heparin, bacterial lipopolysaccharide, human lysozyme and DNA. Biochem. J. 328, 145–151.
- Van der Heide, T. and Poolman,B. (2002). ABC transporters: one, two or four extracytoplasmic substrate-binding sites. EMBO reports. 3, 938–943.
- Vandeputte-Rutten,L., Kramer,R.A., Kroon,J., Dekker,N., Egmond,M.R. and Gros,P. (2001) Crystal structure of the outer membrane protease OmpT from *Escherichia coli* suggests a novel catalytic site. EMBO J. 20, 5033–5039.
- Vesy,C.J., Kitchens,R.L., Wolfbauer,G., Albers,J.J. and Munford,R.S. (2000) Lipopolysaccharide-binding protein and phospholipid transfer protein release lipopolysaccharides from gram-negative bacterial membranes. Infect. Immun. 68: 2410–2417.
- Vinogradov,E.V., Lindner,B., Kocharova,N.A., Senchenkova,S.N., Shashkov,A.S., Knirel,Y.A., Holst,O., Gremyakova,T.A., Shaikhutdinova,R.Z., and Anisimov,A.P. (2002). The core structure of the lipopolysaccharide from the causative agent of plague, Yersinia pestis. Carbohydr. Res. *337*, 775-777.
- Visintin,A., Latz,E., Monks,B.G., Espevik,T., and Golenbock,D.T. (2003). Lysines 128 and 132 enable lipopolysaccharide binding to MD-2, leading to Toll-like receptor-4 aggregation and signal transduction. J. Biol. Chem. 278, 48313–48320.
- Vollmer,W. and Seligman,S.J. (2010). Architecture of peptidoglycan: more data and more models. Trends Microbiol. *18*, 59-66.
- Wachtershauser,G. (2003). From pre-cells to Eukarya--a tale of two lipids. Mol. Microbiol. *47*, 13-22.
- Walsh,A.G., Matewish,M.J., Burrows,L.L., Monteiro,M.A., Perry,M.B., and Lam,J.S. (2000). Lipopolysaccharide core phosphates are required for viability and intrinsic drug resistance in *Pseudomonas aeruginosa*. Mol. Microbiol. *35*, 718-727.
- Wang,X., Karbarz,M.J., McGrath,S.C., Cotter,R.J., and Raetz,C.R. (2004). MsbA transporter-dependent lipid A 1-dephosphorylation on the periplasmic surface of the

inner membrane: topography of *Francisella novicida* LpxE expressed in Escherichia coli. J. Biol. Chem. *279*, 49470-49478.
- Wang,X., McGrath,S.C., Cotter,R.J., and Raetz,C.R. (2006). Expression cloning and periplasmic orientation of the *Francisella novicida* lipid A 4'-phosphatase LpxF. J. Biol. Chem. *281*, 9321-9330.
- Wang,Y., Griffiths,W.J., Curstedt,T. and Johansson,J. (1999). Porcine pulmonary surfactant preparations contain the antibacterial peptide prophenin and a C-terminal 18-residue fragment thereof. FEBS Lett. 460, 257–262.
- Ward,A., Reyes,C.L., Yu,J., Roth,C.B., and Chang,G. (2007). Flexibility in the ABC transporter MsbA: Alternating access with a twist. Proc. Natl. Acad. Sci. U. S. A *104*, 19005-19010.
- Whitfield,C. (1995). Biosynthesis of lipopolysaccharide O antigens. Trends Microbiol. *3*, 178-185.
- Wu,J. and Woodard,R.W. (2003). *Escherichia coli* YrbI is 3-deoxy-D-manno-octulosonate 8-phosphate phosphatase. J. Biol. Chem. *278*, 18117-18123.
- Wu,T., McCandlish,A.C., Gronenberg,L.S., Chng,S.S., Silhavy,T.J., and Kahne,D. (2006). Identification of a protein complex that assembles lipopolysaccharide in the outer membrane of *Escherichia coli*. Proc. Natl. Acad. Sci. U. S. A *103*, 11754-11759.
- Wurfel,M.M., Hailman,E. and Wright,S.D. (1995). Soluble CD14 acts as a shuttle in the neutralization of lipopolysaccharide (LPS) by LPS-binding protein and reconstituted high density lipoprotein. J. Exp. Med. 181, 1743–1754.
- Wyckoff,T.J., Lin,S., Cotter,R.J., Dotson,G.D., and Raetz,C.R. (1998). Hydrocarbon rulers in UDP-N-acetylglucosamine acyltransferases. J. Biol. Chem. *273*, 32369-32372.
- Yang,Y., Boze,H., Chemardin,P., Padilla,A., Moulin,G., Tassanakajon,A., Pugnière,M., Roquet,F., Destoumieux-Garzón,D., Gueguen,Y., Bachère,E., and Aumelas,A. (2009). NMR structure of rALF- Pm3, an anti-lipopolysaccharide factor from shrimp: Model of the possible lipid A-binding site. *91*, 207–220.
- Yong,D., Toleman,M.A., Giske,C.G., Cho,H.S., Sundman,K., Lee,K., Walsh,T.R.(2009). Characterization of a new metallo-beta-lactamase gene, *bla*(NDM-1), and a novel erythromycin esterase gene carried on a unique genetic structure in *Klebsiella pneumoniae* sequence type 14 from India. Antimicrob. Agents Chemoter. 53,5046-5054.
- Young,K. and Silver,L.L. (1991). Leakage of periplasmic enzymes from envA1 strains of *Escherichia coli*. J. Bacteriol. *173*, 3609-3614.
- Zhang,L., al Hendy,A., Toivanen,P., and Skurnik,M. (1993). Genetic organization and sequence of the rfb gene cluster of Yersinia enterocolitica serotype O:3: similarities to the dTDP-L-rhamnose biosynthesis pathway of *Salmonella* and to the bacterial polysaccharide transport systems. Mol. Microbiol. 9, 309-321.
- Zhou,Z., White,K.A., Polissi,A., Georgopoulos,C., and Raetz,C.R. (1998). Function of *Escherichia coli MsbA*, an essential ABC family transporter, in lipid A and phospholipid biosynthesis. J. Biol. Chem. *273*, 12466-12475.
- Zuber,B., Chami,M., Houssin,C., Dubochet,J., Griffiths,G., and Daffe,M. (2008). Direct visualization of the outer membrane of mycobacteria and corynebacteria in their native state. J. Bacteriol. *190*, 5672-5680.

Reports, bulletins, and repositories available on the World Wide Web

- Antibiotic Resistance: An Ecological Perspective on an Old Problem, A REPORT FROM THE AMERICAN ACADEMY OF MICROBIOLOGY, 2008 (ttp://academy.asm.org/index.php/colloquium-program/browse-all-reports/232-antibiotic-resistance-an-ecological-perspective-on-an-old-problem-september-2009-d.)
- A public health crisis brews, 2004 (http://www.idsociety.org/ badbugsnodrugs.html).
- EcoCyc, SRI International (http://ecocyc.org/)
- *Escherichia coli* Statistics by CyberCell Database CCDB, University of Alberta (http://redpoll.pharmacy.ualberta.ca/CCDB/cgi-bin/STAT_NEW.cgi.)
- ExPASy, the new SIB Bioinformatics Resource Portal (http://expasy.org/)
- Health Protection Report (http://www.hpa.org.uk/hpr/archives/2009/news2609.htm#ndm1). Health Protection Agency, 3 July 2009

- Infectious Diseases Society of America, 2004 (www.idsociety.org/badbugsnodrugs.html)
- PubMed, NCBI (http://www.ncbi.nlm.nih.gov/pubmed/).
- Pfam 26.0, Wellcome Trust Sanger Institute (http://pfam.sanger.ac.uk/)
- WHO, world health organization — Global Burden Desease bulletins (http://www.who.int/healthinfo/en/)

Softwares

I-Tasser (http://zhanglab.ccmb.med.umich.edu/I-TASSER)
LipoP 1.0 (http://www.cbs.dtu.dk/services/LipoP/).
MultiAlin (http://bioinfo.genopole-toulouse.prd.fr/multalin/)
SPASM (http://xray.bmc.uu.se/usf/spasm.html)
TMHMM 2.0 (http://www.cbs.dtu.dk/services/TMHMM/)

JOURNAL OF BACTERIOLOGY, Mar. 2011, p. 1042–1053 Vol. 193, No. 5
0021-9193/11/$12.00 doi:10.1128/JB.01037-10

New Insights into the Lpt Machinery for Lipopolysaccharide Transport to the Cell Surface: LptA-LptC Interaction and LptA Stability as Sensors of a Properly Assembled Transenvelope Complex[▽]

Paola Sperandeo,[1] Riccardo Villa,[1] Alessandra M. Martorana,[2]† Maria Šamalikova,[1] Rita Grandori,[1] Gianni Dehò,[2] and Alessandra Polissi[1]*

Dipartimento di Biotecnologie e Bioscienze, Università di Milano-Bicocca, Milan, Italy,[1] and Dipartimento di Scienze Biomolecolari e Biotecnologie, Università degli Studi di Milano, Milan, Italy[2]

Received 31 August 2010/Accepted 10 December 2010

Lipopolysaccharide (LPS) is a major glycolipid present in the outer membrane (OM) of Gram-negative bacteria. The peculiar permeability barrier of the OM is due to the presence of LPS at the outer leaflet of this membrane that prevents many toxic compounds from entering the cell. In *Escherichia coli* LPS synthesized inside the cell is first translocated over the inner membrane (IM) by the essential MsbA flippase; then, seven essential Lpt proteins located in the IM (LptBCDF), in the periplasm (LptA), and in the OM (LptDE) are responsible for LPS transport across the periplasmic space and its assembly at the cell surface. The Lpt proteins constitute a transenvelope complex spanning IM and OM that appears to operate as a single device. We show here that *in vivo* LptA and LptC physically interact, forming a stable complex and, based on the analysis of loss-of-function mutations in LptC, we suggest that the C-terminal region of LptC is implicated in LptA binding. Moreover, we show that defects in Lpt components of either IM or OM result in LptA degradation; thus, LptA abundance in the cell appears to be a marker of properly bridged IM and OM. Collectively, our data support the recently proposed transenvelope model for LPS transport.

Lipopolysaccharide (LPS) is a complex glycolipid uniquely present in the outer layer of Gram-negative bacteria outer membrane (OM) (20, 21). LPS, also known as endotoxin, is one of the major virulence factors of Gram-negative bacteria and is responsible for the activation of the mammalian innate immune response (17). It consists of three distinct structural elements: lipid A (the hydrophobic moiety embedded in the OM), a core oligosaccharide, and the O antigen constituted of polysaccharide repeating units (21). LPS is essential in most Gram-negative bacteria, with the notable exception of *Neisseria meningitidis* (32). The lipid A-core moiety is synthesized in the cytoplasm and is flipped from the inner to the outer leaflet of the inner membrane (IM) by the essential ABC transporter MsbA (6, 19, 43). In bacterial strains producing the O antigen, ligation to the core oligosaccharide occurs at the periplasmic face of the IM, after MsbA-mediated translocation (21). Mature LPS, containing or not the O antigen, is then transported to the outer leaflet of the OM by a protein machine composed of seven recently discovered Lpt proteins (reviewed by Sperandeo et al. [28]) suggested to build up a complex (the Lpt complex) that spans the IM and OM. Indeed, these proteins are located at the IM (LptBCFG), in the periplasm (LptA), and at the OM (LptDE) (3, 23, 27, 29, 30, 33, 41). Genetic evidence suggests that the Lpt complex operates as a single device, since the depletion of any component leads to similar phenotypes, namely, failure to transport newly synthesized LPS to the cell surface and its accumulation at the outer leaflet of the IM (16, 23, 29). The LPS accumulating at the outer leaflet of the IM is decorated with colanic acid residues, and therefore this modification is diagnostic of defects in transport occurring downstream of the MsbA-mediated flipping of LPS to the periplasmic face of the IM (29).

Physical interaction between the different proteins of the machinery has been demonstrated for LptDE, which form a complex at the OM (41), and for the IM LptBCFG complex (18). LptD and LptE are responsible for the LPS assembly at the cell surface; LptE stabilizes LptD by interacting with its C-terminal domain, whereas LptE binds LPS, possibly serving as a substrate recognition site at the OM (5). LptC is an IM bitopic protein whose large soluble domain has a periplasmic localization (38). The crystal structure of LptC periplasmic domain has been recently solved and, like LptA, LptC has been shown to bind LPS *in vitro* (38). LptC physically interacts with the IM LptBFG proteins, and the LptBCFG complex is the IM ABC transporter that energizes the LPS transport (18). However, LptC seems not to be required for the ATPase activity of the transporter (18).

LptA expressed from an inducible promoter has a periplasmic localization and has been shown to bind both LPS and lipid A *in vitro* (27, 39). These data raise the possibility that LptA may act as a periplasmic chaperone for LPS transport across the periplasm. However, in *N. meningitidis* the LptA homologue was shown to be associated to the membrane fraction (2). Moreover, in the *Escherichia coli* LptA crystal structure obtained in the presence of LPS, the LptA monomers are packed as a linear filament (34), leading to the hypothesis that oligomers of LptA may be required to bridge the IM and the

* Corresponding author. Mailing address: Dipartimento di Biotecnologie e Bioscienze, Università di Milano-Bicocca, Piazza della Scienza 2, 20126 Milan, Italy. Phone: 39-02-64483431. Fax: 39-02-64483450. E-mail: alessandra.polissi@unimib.it.

† Present address: Dipartimento di Biotecnologie e Bioscienze, Università di Milano-Bicocca, Milan, Italy.

▽ Published ahead of print on 17 December 2010.

TABLE 1. Bacterial strains and plasmids

Strain or plasmid	Relevant characteristics[a]	Source or reference
Strains		
AM604	MC4100 *ara*$^+$	41
AM661	AM604 Δ*lptD*::*kan*/*araBp-lptD*	29
AM689	AM604 Δ*lptE*::*kan* Δ(λ*att-lom*)::*bla araBp-lptE*	41
DH5α	Δ(*argF-lac169*) 80d*lacZ58*(M15) *glnV44*(AS) λ$^-$ *rfbD1 gyrA96 recA1 endA1 spoT1 thi-1 hsdR17*	11
FL905	AM604 Φ(*kan araC araBp-lptC*)*1*	29
FL907	AM604 Φ(*kan araC araBp-lptA*)*1*	29
M15/pREP4	F$^-$ *lac thi mtl*/pREP4	Qiagen
Plasmids		
pRSET	T7 promoter; Ap^r	Invitrogen
pET30b	T7 promoter; Km^r	Novagen
pET30-*lptC*-lk$_{25}$-H	pET30b derivative, expresses a LptC-lk$_{25}$-His$_6$ version where lk is a 25-amino-acid linker region separating LptC residue 191 from the His$_6$ affinity tag	This study
pQE30	T5 promoter; Ap^r	Qiagen
pQEsH-*lptC*	pQE30 derivative, expresses His$_6$-LptC$_{24\text{-}191}$	This study
pGS100	pGZ119EH derivative, contains TIR sequence downstream of *Ptac*; Cm^r	30
pGS103	pGS100 *Ptac-lptC*	30
pGS103Δ$_{177\text{-}191}$	pGS103 *Ptac-lptC*Δ$_{177\text{-}191}$	This study
pGS103G56V	pGS103 *Ptac-lptC*(G56V)	This study
pGS103Y112S-G153R	pGS103 *Ptac-lptC*(Y112S-G153R)	This study
pGS103G153R	pGS103 *Ptac-lptC*(G153R)	This study
pGS108	pGS100 *Ptac-lptC*-H	30
pGS108Δ$_{177\text{-}191}$	pGS108 *Ptac-lptC*Δ$_{177\text{-}191}$-H	This study
pGS108G153R	pGS108 *Ptac-lptC*(G153R)-H	This study
pGS108G56V	pGS108 *Ptac-lptC*(G56V)-H	This study
pGS116	pGS103Δ$_{177\text{-}191}$ derivative expressing both the truncated LptCΔ$_{177\text{-}191}$ and LptC-lk$_{25}$ from pET30- *lptC*-lk$_{25}$-H plasmid	This study

[a] Cm^r, chloramphenicol resistance; Ap^r, ampicillin resistance; Km^r, kanamycin resistance.

OM, thus facilitating LPS export. The observation that LPS is still transported to the OM in spheroplasts devoid of periplasmic content (35) is consistent with this idea. In line with these data it has been recently reported that all seven Lpt proteins physically interact and form a transenvelope complex spanning IM and OM (4).

In the present study we show that *in vivo* LptA and LptC physically interact and form a stable complex, suggesting that LptC may represent a docking site for LptA to the IM. Based on analyses of loss-of-function mutations in LptC, we predict that the C-terminal region of LptC is implicated in LptA binding and that LptC may form dimers. Finally, after analyzing the relative stability of the Lpt proteins when LptC, LptD, or LptE are either depleted or not functional, we suggest that LptA connects IM and OM via LptC and the LptDE complex and that LptA abundance in the cell may be used as a marker of properly bridged IM and OM.

MATERIALS AND METHODS

Bacterial strains and media. The bacterial strains and plasmids examined here are listed in Table 1. The oligonucleotide primers are listed in Table 2.

Bacteria were grown in LD medium (24). When required, 0.2% (wt/vol) L-arabinose (as an inducer of the *araBp* promoter), 0.1 or 0.5 mM IPTG (isopropyl-β-D-thiogalactopyranoside), 100 μg of ampicillin/ml, 25 μg of chloramphenicol/ml, and 25 μg of kanamycin/ml were added. Solid media were prepared as described above with 1% agar.

Plasmid construction. Plasmid pGS108 expresses LptC with a C-terminal His$_6$ tag (LptC-H) from the IPTG-inducible *Ptac* promoter (Table 1). Plasmids pGS108G56V, pGS103G153R, and pGS108G153R expressing LptCG56V-H,

TABLE 2. Oligonucleotides

Name	Sequence (5′–3′)[a]	Use and/or description
AP24	cgactagtctagaTTAAGGCTGAGTTTGTTTG	Random mutagenesis with AP54; XbaI
AP54	cgagaggaattcaccATGAGTAAAGCCAGACGTTGGG	pGS108Δ$_{177\text{-}191}$ construction, with AP172 and random mutagenesis with AP24; EcoRI
AP149	atatacatATGAGTAAAGCCAGACGTTG	pET30-*lptC*-H construction, with AP150; NdeI
AP150	cgcgcaggtaccAGGCTGAGTTTGTTTGTTTTG	pET30-*lptC*-H construction, with AP149; KpnI
AP164	GTCTATAACCCAGAA**GTG**GCACTAAGCTATCG	pGS108G56V construction, with AP165
AP165	CGATAGCTTAGTGC**CAC**TTCTGGGTTATAGAC	pGS108G56V construction, with AP164
AP166	cgagatggatccATGGCCGAAAAAGACGATAC	pQEsH-*lptC* construction, with AP167; BamHI
AP167	cgagatctgcagTTAAGGCTGAGTTTGTTTG	pQEsH-*lptC* construction, with AP166; PstI
AP168	CTCGTCACGTTATAC**AGA**ACAACATTTAACTC	pGS108G153R and pGS103G153R construction, with AP169
AP169	GAGTTAAATGTTGT**TCT**GTATAACGTGACGAG	pGS108G153R and pGS103G153R construction, with AP168
AP172	gtgatcacatctagatcagtggtggtggtggtggtgTTCAATCAGCTCGGCGTTC	pGS108Δ$_{177\text{-}191}$ construction, with AP54; insertion of C-terminal His$_6$ tag into LptCΔ$_{177\text{-}191}$; XbaI

[a] Uppercase letters, *E. coli* genomic sequence; underlined lowercase letters, restriction sites; boldface letters, codons mutated by site-directed mutagenesis.

LptCG153R, and LptCG153R-H, respectively, were constructed by using a QuikChange site-directed mutagenesis kit (Stratagene). Codon 56 was changed from GGG to GTG by using the primer pair AP164-AP165, and codon 153 was changed from GGA to AGA by using the primer pair AP168-AP169 (Table 2). Plasmid pGS108$\Delta_{177\text{-}191}$ expressing LptC$\Delta_{177\text{-}191}$-H, truncated at residue 177, was constructed by PCR amplifying the *lptC* open reading frames from genomic MG1655 DNA with the primer pair AP54-AP172 (Table 2). The PCR product was EcoRI-XbaI digested and cloned into pGS108 cut with the same enzymes. The EcoRI-XbaI insert in pGS108$\Delta_{177\text{-}191}$, as well as the mutations in pGS108G56V, pGS108G153R, and pGS103G153R, was verified by sequencing.

Plasmid pQEsH-*lptC* expresses a soluble cytoplasmic version of LptC deprived of the transmembrane helix and with an N-terminal His_6 affinity tag (sH-LptC) (Table 1). A 507-bp DNA fragment, encoding residues 24 to 191 of LptC, was amplified from MG1655 DNA with the primers AP166 and AP167 (Table 2) and cloned into the BamHI and PstI sites of pQE30 (Qiagen). The His_6 affinity tag is separated from the first residue of $LptC_{24\text{-}191}$ by two amino acids (G-S). The BamHI-PstI insert was verified by sequencing.

Plasmid pET30-*lptC*-lk$_{25}$-H expresses a C-terminally His_6-tagged version of LptC (LptC-lk$_{25}$-H) with a 25-amino-acid linker region (GTDDDDKAMAISD PNSSSVDKLAAALE) containing the enterokinase recognition site (DDDDK) (Table 1). The *lptC* open reading frame was amplified from MG1655 DNA with the primers AP149 and AP150 (Table 2). The PCR product was NdeI-KpnI digested and cloned into the NdeI-KpnI sites of pET30b (Novagen). The NdeI-KpnI insert was verified by sequencing.

Plasmid pGS116 is a pGS103$\Delta_{177\text{-}191}$ derivative expressing LptC-lk$_{25}$, together with LptC$\Delta_{177\text{-}191}$ from the IPTG-inducible *Ptac* promoter (Table 1). The XbaI-HindIII fragment of pET30-*lptC*-lk$_{25}$-*H*, containing the ribosome binding site (RBS) region, the *lptC* gene without its stop codon and part of the plasmid multiple cloning site was inserted into the XbaI-HindIII sites of pGS103$\Delta_{177\text{-}191}$. The resulting plasmid expresses LptC (LptC-lk$_{25}$) in frame with a 27-amino-acid coding sequence (GTDDDDKAMAISDPNSSSVDKLGCFGG). In this construct the His_6 affinity tag is lost.

Random mutagenesis, screening, and genetic characterization of LptC mutants. Random mutagenesis was performed by error-prone PCR using an unbalanced deoxynucleoside triphosphates concentration in the amplification reactions, as described previously (9). pGS103 expressing *lptC* from the *Ptac* promoter was used as a template (10 ng) in 50 μl with 50 pmol each of primers AP54 and AP24 (Table 2). The PCR conditions were as follows: 95°C denaturation for 2 min; 30 cycles of 95°C for 30 s, 55°C for 30 s, and 72°C for 1 min; followed by a 5-min extension at 72°C. The products were gel purified, digested with XbaI and EcoRI, ligated into pGS100, and electroporated into FL905 cells. The transformants were plated onto LD agar with 0.2% arabinose and 25 μg of chloramphenicol/ml at 37°C. Single colonies were then inoculated into microtiter wells containing 100 μl of LD, serially diluted 10-fold, replica plated on LD-chloramphenicol agar plates supplemented with (permissive condition) or without (nonpermissive condition) 0.2% arabinose, and incubated overnight at 37°C. Plasmids unable to support FL905 growth in the absence of arabinose were identified and sequenced.

To test the effect of LptC mutant overexpression, serial dilutions of cultures grown overnight in LD-chloramphenicol were replica plated on LD-chloramphenicol agar plates supplemented or not with 0.5 mM IPTG.

***In vivo* cross-linking.** The cross-linking experiments were based on previously described methods (36) with some modifications. The cells were grown in 250 ml of LD medium supplemented with either chloramphenicol or ampicillin to an optical density at 600 nm (OD_{600}) of 0.2, induced with 0.1 mM IPTG, and grown to an OD_{600} of ~0.7. The cells were then harvested by centrifugation at 5,000 × *g* for 10 min. For treatment with DSP (di-thiobis[succinimidyl propionate]; Pierce), the cell pellet was washed with 25 ml of 20 mM potassium phosphate (pH 7.2) and 150 mM NaCl, resuspended in 25 ml of the same buffer, and then incubated for 15 min at 37°C. DSP dissolved in dimethyl sulfoxide was added to the cell suspension at a final concentration of 80 μg/ml, and the cells were incubated for 30 min at 37°C. The cross-linking reaction was quenched by the addition 1 M Tris-HCl (pH 7.4) to a final concentration of 20 mM, and the cells were harvested by centrifugation at 5,000 × *g* for 10 min.

For whole-cell extract analysis, the cells were grown in 50 ml of LD-chloramphenicol to an OD_{600} of 0.2, induced with 0.1 mM IPTG, and grown to an OD_{600} of ~0.7. DSP treatment was performed as described above using two-thirds of each culture, whereas the reminder one-third was not treated. After the addition of 20 mM Tris-HCl (pH 7.4), the cells were centrifuged and washed twice in 20 mM potassium phosphate (pH 7.2) and 150 mM NaCl. The cell pellet was resuspended in 100 μl of sodium dodecyl sulfate (SDS) sample buffer containing or not containing 5% β-mercaptoethanol and boiled for 5 min.

Affinity purification. Protein purification was performed as described previously (26). The cell pellets were resuspended in 4 ml of 50 mM potassium phosphate buffer (pH 8.0), 150 mM NaCl, 5 mM $MgCl_2$, and 1% ZW3-14 (*n*-tetradecyl-*N*,*N*-dimethyl-3-ammonio-1-propanesulfonate) containing lysozyme (50 μg/ml), DNase I (50 μg/ml), and RNase I (50 μg/ml) and then lysed by shaking for 20 min at room temperature. To remove cell debris after lysis, the mixture was then centrifuged at 10,000 × *g* for 10 min. To the cleared lysate (whole-cell extract) 20 mM imidazole (pH 8.0) was added, and the final mixture was loaded onto a 0.4-ml Ni-NTA column. The column was first washed with 8 ml of 50 mM potassium phosphate buffer (pH 8.0), 300 mM NaCl, 20 mM imidazole, 0.1% Triton X-100, and 0.1% SDS and then eluted with 4 ml of 50 mM potassium phosphate buffer (pH 8.0), 300 mM NaCl, and 200 mM imidazole. The eluate was concentrated in an ultrafiltration device (Amicon Ultra [Millipore]; molecular weight cutoff, 10,000) by centrifugation at 5,000 × *g*. The concentrated sample was used for SDS-PAGE and Western blot analysis as described above.

Purification of sH-LptC. M15/pREP4 carrying the plasmid pQEsH-*lptC* was grown at 30°C in LD containing kanamycin (25 μg/ml) and ampicillin (100 μg/ml) for 18 h. This culture was diluted 1:100 in fresh medium and grown until mid-logarithmic phase (OD_{600}, ~0.6). The expression of sH-LptC was induced overnight at 20°C by adding IPTG to a final concentration of 0.5 mM. Cells were then harvested by centrifugation (5,000 × *g*, 10 min). The cell pellet was resuspended in buffer A (50 mM NaH_2PO_4 [pH 8.0] containing 300 mM NaCl, 10 mM imidazole, and 10% glycerol), followed by incubation for 30 min at 4°C with shaking in the presence of lysozyme (0.2 mg/ml), DNase (100 μg/ml), 10 mM $MgCl_2$, and 1 mM phenylmethylsulfonyl fluoride. After 10 cycles of sonication (10-s pulses), the unbroken cells were removed by centrifugation (39,000 × *g*, 30 min). The soluble sH-LptC protein was purified from the supernatant by using Ni-NTA agarose (Qiagen). The column was washed with 10 column volumes of 4% buffer B (50 mM NaH_2PO_4 [pH 8.0] containing 300 mM NaCl, 500 mM imidazole, and 10% glycerol) in buffer A. The protein was eluted by using a stepwise gradient obtained by mixing buffer B with buffer A in 5 steps (10, 20, 50, 70, and 100% buffer B). At each step, 1 column volume was flowed through the column. Elution fractions were monitored by 12.5% polyacrylamide SDS-PAGE. The pooled fractions containing purified protein were dialyzed against 100 volumes of buffer C (50 mM NaH_2PO_4 [pH 8.0], 100 mM NaCl) for gel filtration analysis, and 100 volumes of 10 mM ammonium acetate pH 7.5 for mass spectrometry. Protein concentrations were determined by using a Coomassie (Bradford) assay kit (Pierce) with bovine serum albumin as the standard.

Mass spectrometry. Electrospray ionization-mass spectrometry (ESI-MS) experiments were performed on a hybrid quadrupole-time-of-flight mass spectrometer (QSTAR Elite; Applied Biosystems, Foster City, CA) equipped with a nano-ESI sample source. Metal-coated borosilicate capillaries (Proxeon, Odense, Denmark), with medium-length emitter tips (1-μm internal diameter), were used to infuse the samples. The instrument was calibrated using the renin inhibitor (1,757.9 Da) (Applied Biosystems) and its fragment (109.07 Da) as standards. Spectra were acquired in the 500 to 5,000 *m*/*z* range, with accumulation times of 1 s, an ion-spray voltage of 1,300 V, a declustering potential of 40 V, and an instrument interface at room temperature. Spectra were averaged over a period of at least 3 min.

Analytical gel filtration chromatography. Size-exclusion chromatography was performed on an ÄKTA purifier liquid-chromatography system (GE Healthcare, Amersham Place, Little Chalfont, United Kingdom), using a prepacked, Superdex 75HR column (30 by 1 cm; GE Healthcare, Amersham Place, Little Chalfont, United Kingdom). Chromatography was carried out at room temperature in 50 mM NaH_2PO_4 (pH 8.0)–100 mM NaCl at a flow rate of 0.5 ml/min and monitored by the eluate absorbance at 280 nm. The calibration curve was constructed by using the following standards (0.5 mg/ml): transferrin (81,000 Da), chicken ovalbumin (43,000 Da), chymotrypsin (21,500 Da), bovine cytochrome *c* (12,200 Da), and aprotinin (6,500 Da) (Sigma Aldrich, St. Louis, MO). LptC was injected at a concentration of 1 mg/ml.

Determination of LptA, LptC, and LptE levels. LptA, LptC, and LptE levels were assessed in FL905 and its derivatives expressing mutant LptC or in AM661 or AM689 strains by Western blot analysis with polyclonal antibody raised in mouse or rabbit against peptides (LptA) or whole proteins (LptE, LptC, and AcrB). Bacterial cultures grown at 37°C in LD supplemented with 0.2% arabinose and 25 μg of chloramphenicol/ml when required were harvested by centrifugation after they had reached an OD_{600} of 0.2, washed in LD, and diluted to OD_{600}s of 0.01 (AM689), 0.004 (AM661), 0.0004 (AM604, FL905/pGS103$\Delta_{177\text{-}191}$, FL905/pGS103, FL905, FL905/pGS103G56V, and FL905/pGS108G153R) in fresh media with or without 0.2% arabinose and with 25 μg of chloramphenicol/ml. Growth was monitored by measuring the OD_{600}. Samples for protein analysis were centrifuged (16,000 × *g*, 5 min), and pellets were resuspended in a volume (in ml) of SDS sample buffer equal to one-eighth of the total OD of the sample.

The samples were boiled for 5 min, and equal volumes (25 μl) were analyzed by SDS–12.5% PAGE. Proteins were transferred onto nitrocellulose membranes (GE Healthcare), and Western blot analysis was performed as previously described (27). Polyclonal sera raised against LptA (GenScript Corp.) were used as primary antibody at a dilution of 1:2,000, whereas polyclonal sera against LptC, LptE (kindly provided by D. Kahne), and AcrB (kindly provided by K. M. Pos) were used at a dilution of 1:5,000. As secondary antibodies, sheep anti-mouse immunoglobulin G–horseradish peroxidase (HRP) conjugate (GE Healthcare) and donkey anti-rabbit immunoglobulin G–HRP conjugate (GE Healthcare) were used at dilutions of 1:5,000.

Analyses of LptC-H mutant stability. The expression of LptC was induced with 0.1 mM IPTG at an OD_{600} of 0.3 to 0.4 in cultures grown in LD-chloramphenicol, and 1-ml samples were taken immediately before and 15, 30, and 60 min after induction. Samples preparation and Western blotting were performed as described above, and wild-type and mutant versions of LptC-H were visualized by using HisProbe-HRP (Pierce) according to the manufacturer's instructions.

Total LPS extraction and analysis. LPS extraction from AM604 and FL905 transformed or not with plasmids carrying wild-type or mutant LptC was performed as previously described. Samples of a total OD_{600} of 2 were taken, and LPS was extracted from cell pellets by a mini phenol-water extraction technique (22). Briefly, the cells were resuspended in water and pelleted (5 min, 10,000 × *g*) to remove the exopolysaccharides and then resuspended in 0.3 ml of potassium phosphate buffer (pH 7.0) and thoroughly vortexed; 0.3 ml of phenol equilibrated with 0.1 M Tris-HCl (pH 5.5) was added, and the suspension was vortexed. The tubes were placed in a 65°C heating block for 15 min with thorough vortexing every 5 min and then cooled on ice. After centrifugation (10,000 × *g*, 5 min), the water phase was removed, dialyzed (molecular mass cutoff, 2,000 to 4,000 Da) against phosphate buffer (pH 7.0), and lyophilized. The lyophilized material was then dissolved in 30 μl of water. LPS was separated by *N*-[2-hydroxy-1,1-bis(hydroxymethyl)ethyl]glycine–SDS-PAGE (31) and visualized by silver staining according to the Hitchcock and Brown method as described previously (27).

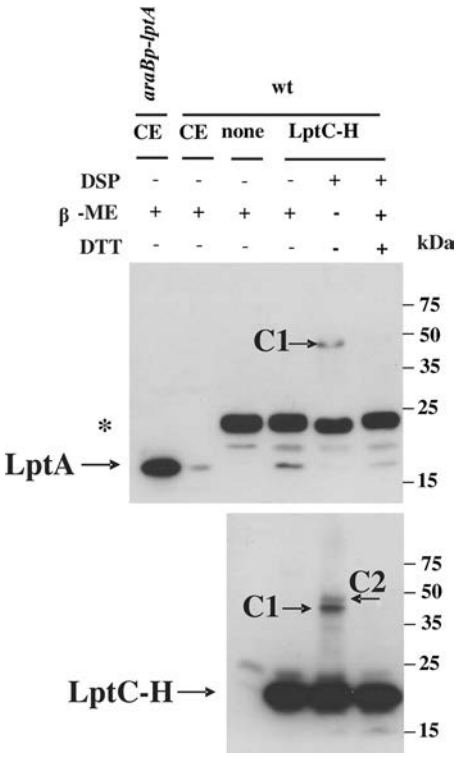

FIG. 1. LptA interacts with LptC *in vitro*. Affinity chromatography experiments were performed in the presence or absence of DSP in AM604/pGS108 overexpressing LptC-H (wt/LptC-H) and AM604/pRSET (wt/none) expressing the His tag element only, as a negative control. LptA and LptC were detected in Ni-NTA column-enriched fractions by Western blot analysis with anti-LptA antibody and His-Probe-HRP, respectively. LptA detected in crude cell extract (CE) of AM604 (wt) and of FL907 mutant overexpressing LptA (*araBp-lptA*) was used as a marker. Samples were treated with dithiothreitol (DTT) and/or β-mercaptoethanol (β-ME) to revert the cross-linking. Equal amounts of protein (2 μg) were loaded into each lane. C1 and C2, high-molecular-weight complexes. The SlyD protein of 24 kDa cross-reacting with anti-LptA antibodies is labeled (*).

RESULTS

LptC stably associates with LptA. Previous work by our and other laboratories (27, 39) suggested that LptA expressed from an inducible promoter has a periplasmic localization. However, evidence of direct physical interaction between the seven Lpt proteins has been recently reported and LptA has been shown to associate with both IM and OM (4). Since the bitopic IM LptC protein possesses a large C-terminal periplasmic domain (E26-P191) (38), we hypothesized that LptA binding to the IM could be mediated by LptC. To address this issue, we probed the interaction between LptA and LptC by affinity purification followed by immunoblotting. A C-terminal His tagged version of LptC (LptC-H) overexpressed from plasmid pGS108 in the wild-type strain AM604 was used as bait in copurification experiments. AM604 harboring the pRSET vector, which allows the basal expression of the His tag alone, was used as a negative control. To detect possible weak or transient interactions, *in vivo* cross-linking using di-thiobis(succinimidyl propionate) (DSP) (42) was also performed. As shown in Fig. 1, LptA copurified with LptC-H even when DSP was not added to the cells overexpressing LptC-H, suggesting a stable LptA-LptC interaction. When samples treated with DSP were not reverted by a reducing agent, high-molecular-weight bands appeared (Fig. 1, upper and lower panel, bands C1 and C2). C1 may correspond to an LptA-LptC complex, whereas the C2 band that appears only in the lower panel might correspond to an LptC-LptC complex, as inferred by the molecular weight. These data suggest that LptA and LptC interact and form a stable complex.

Isolation of inactive *lptC* mutant alleles. To better characterize LptA-LptC interaction and to define the molecular role of LptC in LPS transport, we searched for point mutations that inactivate LptC function. Random mutations were introduced by error-prone PCR into *lptC* carried by pGS103 (Table 1), and the mutagenized plasmids were tested for complementation of $LptC^+$-depleted cells, as described in Materials and Methods. Briefly, $LptC^+$ depletion strain FL905 was transformed with the mutagenized plasmids in the presence of arabinose, and plasmids unable to support FL905 growth in the absence of arabinose were isolated. Of 1,664 transformants analyzed, we obtained 21 clones unable to fully complement FL905 in the nonpermissive conditions. Most noncomplementing clones harbored multiple mutations, as assessed by sequencing the mutant alleles. Nevertheless, three plasmids harbored only one or two mutations in LptC (Fig. 2A), namely, G56V, K177Stop (which generates a truncated protein lacking the C-terminal 15 amino acids [$\Delta_{177\text{-}191}$]), and Y112S-G153R (a double substitution mutant in the C-terminal region). FL905/pGS103$\Delta_{177\text{-}191}$ and FL905/pGS103Y112S-G153R growth was completely inhibited on agar medium in the absence of arabinose, whereas FL905/pGS103G56V growth was severely impaired in the absence of arabinose and formed "dust-like colonies" in this condition (Fig. 2B).

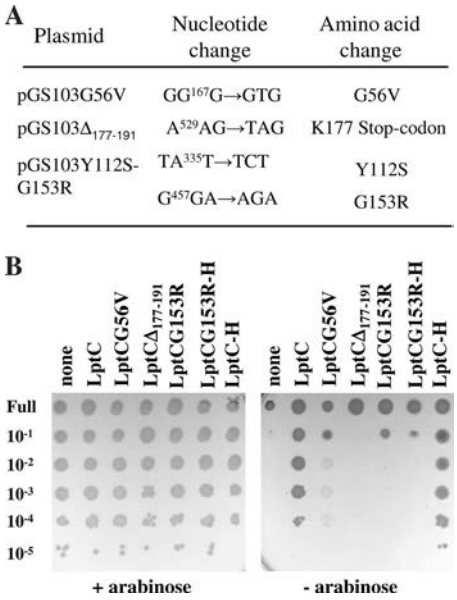

FIG. 2. Mutations affecting LptC function. (A) Mutations in the *lptC* gene in the pGS103-derived plasmids. Nucleotide coordinate numbers are based on the designation of the start codon of *lptC* as 1. The amino acid numbers are based on the predicted sequence of LptC that is 191 amino acids in length. (B) Plating efficiency of FL905 (*araBp-lptC*) transformed with plasmid pGS103 carrying the wild-type protein (LptC and LptC-H, respectively), or plasmids carrying the LptC mutated proteins LptCG56V, LptC$\Delta_{177\text{-}191}$, LptCG153R, LptCG153R-H, or plasmid pGS100 (none), in agar plate containing chloramphenicol supplemented (+) or not (−) with arabinose. Serial dilutions are given on the left side of the panel.

The G153R substitution was also found in other multiple mutants isolated in our screening associated with different amino acid substitutions, suggesting that G153R could be the residue responsible of the observed phenotype. This was confirmed by the fact that both pGS103G153R and pGS108G153R, which expresses a His_6-tagged LptCG153R mutant protein generated by site-directed mutagenesis (LptCG153R-H) (Table 1), were unable to complement FL905 (Fig. 2B). In all of the experiments described below, FL905/pGS108G153R was used. The mutations described above fall in conserved regions of the protein (see, for example, the sequence alignments of LptC orthologues from proteobacteria in reference 38).

Stability of the LptC mutant proteins. To assay the stability of LptC mutant proteins, we examined the level of ectopically expressed LptC-H (which can be distinguished from the endogenous wild-type protein) and its mutant derivatives in the wild-type strain AM604 upon induction with IPTG, assuming that the level of *de novo*-synthesized proteins correlates with their stability. It should be noted that in these conditions the chromosomal wild-type copy of *lptC* is expressed from its natural promoter. Detection of the proteins using HisProbe-HRP revealed that the level of LptCG56V-H was comparable to that of LptC-H and only the basal level (before IPTG induction) of LptCG153R-H was affected, suggesting that this protein is only slightly unstable (Fig. 3A). On the contrary, the level of the truncated LptC$\Delta_{177\text{-}191}$-H protein was severely reduced under these conditions, indicating that the truncated protein is intrinsically unstable.

We then tested the effect of LptC mutants overexpression on *E. coli* growth by plating wild-type strain AM604 harboring pGS108, pGS108G56V, pGS108$\Delta_{177\text{-}191}$, and pGS108G153R on agar medium in the absence or in the presence of IPTG. Overexpression of LptCG56V did not impair growth; on the contrary, we found that overexpression of $\Delta_{177\text{-}191}$ and G153R LptC-H mutants abolished AM604 growth (Fig. 3B). Since LptC is part of a multiprotein complex these data suggest that either the mutants may titrate a wild-type interacting Lpt factor(s) or that their toxicity may be due to the overexpression of a misfolded protein.

The C-terminal region of LptC is required for LptA binding. To test whether the G56V, $\Delta_{177\text{-}191}$, and G153R mutations could affect LptC interaction with LptA, we compared the wild-type and the mutant proteins for their ability to copurify

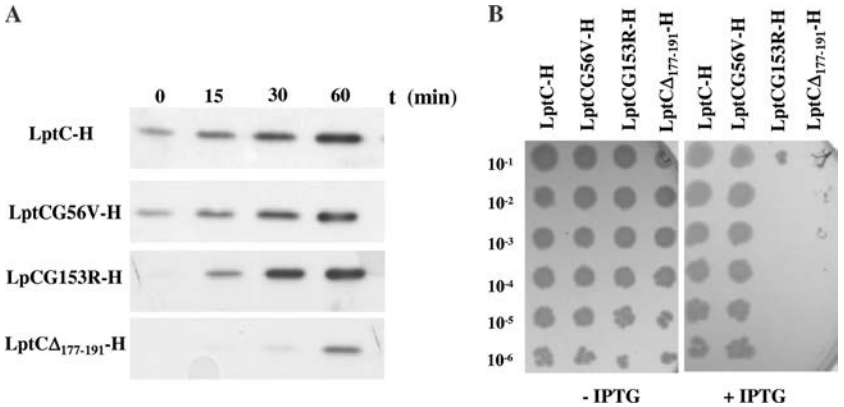

FIG. 3. LptC mutant stability *in vivo* and effects of their overexpression. (A) LptC mutant stability. AM604 cells harboring pGS108 (LptC-H), pGS108G56V (LptCG56V-H), pGS108G153R (LptCG153R-H), and pGS108$\Delta_{177\text{-}191}$ (LptC$\Delta_{177\text{-}191}$-H) were grown to the early logarithmic phase. Expression of LptC-H or its mutant forms were induced by the addition of 0.1 mM IPTG. Samples for protein analysis were obtained 0, 15, 30, and 60 min postinduction and analyzed using HisProbe-HRP. Equal amount of cells (0.12 OD_{600} units) was loaded into each lane. (B) Overexpression of LptC$\Delta_{177\text{-}191}$ and LptCG153R leads to cell lethality. Serial dilutions (indicated on the left) of overnight cultures of AM604 carrying the plasmids pGS108, pGS108G56V, pGS108$\Delta_{177\text{-}191}$, and pGS108G153R were replica plated onto agar plate supplemented (+) or not (−) with 0.5 mM IPTG and incubated overnight.

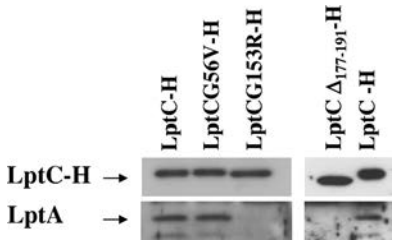

FIG. 4. Effect of *lptC* mutations on LptC-LptA interaction. Whole-cell extracts from AM604 cells transformed with plasmids pGS108 carrying the wild-type protein (LptC-H) or the LptC-mutated proteins LptCG56V-H, LptCG153R-H, and LptC$\Delta_{177\text{-}191}$-H were subjected to affinity chromatography. Equal amounts (2.5 μg) of Ni-NTA column-enriched LptC-H and its mutant versions were separated by SDS–12.5% PAGE and analyzed by Western blotting with anti-LptA antibody and HisProbe-HRP, respectively.

LptA. Whole-cell extracts of the wild-type strain AM604 overexpressing LptC-H or the mutant His-tagged derivatives (G56V, $\Delta_{177\text{-}191}$, and G153R; Table 1) were subjected to affinity purification and LptA and LptC-H detected by Western blotting with anti-LptA antibodies and HisProbe-HRP, respectively. As shown in Fig. 4, LptCG56V-H retained the ability to copurify LptA, whereas the mutations in the LptC C-terminal region (G153R and $\Delta_{177\text{-}191}$) severely impaired LptA-LptC complex formation.

Effects of different *lptC* alleles on Lpt complex and LPS transport. To gain better insights into the molecular role of LptC in the Lpt complex, we tested the effects of the three *lptC* mutant alleles on the steady-state level of LptA and LptE, the latter as a representative of the LptDE OM complex, and on LPS transport. The LptC$^+$ depletion strain FL905 and its derivatives harboring pGS103, pGS103G56V, pGS103$\Delta_{177\text{-}191}$, and pGS108G153R were grown to the exponential phase and shifted into a medium lacking arabinose (nonpermissive condition) to deplete the chromosomally encoded LptC wild type, while allowing expression of the mutant proteins. Samples were then taken from cultures grown in the presence or absence of arabinose for 240 min (AM604, FL905, and FL905/pGS103) or 270 min (FL905/pGS103G56V, FL905/pGS103$\Delta_{177\text{-}191}$, and FL905/pGS108G153R) after the shift to nonpermissive conditions (Fig. 5A) and analyzed by Western blotting with anti-LptA, anti-LptC, and anti-LptE antibodies. The level of the IM protein AcrB was used as a sample loading control.

As shown in Fig. 5B (upper part), the level of physiologically expressed LptC seemed very low since the protein was undetectable in the wild-type strain with our antibody preparation. However, LptC was detected when ectopically expressed from a plasmid or from the *araBp* promoter (Fig. 5B). In FL905 cells expressing LptCG56V and LptCG153R, the level of the mutant proteins was comparable under permissive and nonpermissive conditions, whereas LptC$\Delta_{177\text{-}191}$ was undetectable in the noncomplemented strain (see below).

In the LptC$^+$ depletion strain FL905 grown in the presence of arabinose, *lptA* is expressed from the upstream *araBp* promoter, and the level of LptA is higher than in the wild-type AM604 strain, where the protein is expressed from its natural promoter (29). The level of LptA in LptC$^+$-depleted cells expressing LptCG153R-H was similar to that observed in the positive control (FL905 complemented by wild-type LptC), whereas LptA appeared slightly more abundant in LptC$^+$-depleted cells expressing LptCG56V. On the contrary, in noncomplemented LptC$^+$-depleted cells and in cells ectopically expressing LptC$\Delta_{177\text{-}191}$ LptA was undetectable. It thus appears that the absence of LptC protein caused by either depletion (noncomplemented LptC$^+$-depleted cells) or mutation (LptC$^+$-depleted cells expressing LptC$\Delta_{177\text{-}191}$) induces LptA destabilization. The abundance of LptE did not substantially change upon depletion of LptC with or without overexpression of any mutant LptC, indicating that the steady-state level of the OM component LptE was not affected by LptC depletion or mutations (Fig. 5B, upper part). The steady-state level of LptE thus served in these experiments also as a sample loading control.

Depletion of any Lpt protein leads to the production of LPS decorated by colanic acid; this phenotype is diagnostic of defects in LPS transport occurring downstream of the MsbA-mediated flipping of lipid A-core to the periplasmic face of the IM (29). We therefore analyzed the LPS profile in *lptC* mutant strains. The total LPS was extracted from nondepleted and LptC$^+$-depleted FL905 complemented with wild-type and mutant *lptC* alleles, and the LPS profiles were analyzed as described previously (29). As shown in Fig. 5B (lower part), LPS decorated with colanic acid could be detected in LptC$^+$-depleted FL905 complemented by each of the mutant alleles but not by wild-type *lptC*, indicating that each of the above LptC mutations impair LPS transport.

Evidence for LptC oligomerization *in vivo*. As noted above, LptC$\Delta_{177\text{-}191}$ mutant protein was not detectable upon depletion of the chromosomally encoded LptC$^+$, whereas, when LptC$^+$ was coexpressed from the *araBp* promoter, the LptC$\Delta_{177\text{-}191}$ level was higher (notice that the wild-type and truncated proteins can be distinguished by their different molecular weights; Fig. 5B, upper part). On the contrary, the LptCG56V and LptCG153R mutant proteins remained abundant upon depletion of wild-type LptC. LptC$\Delta_{177\text{-}191}$ is an intrinsically unstable protein (Fig. 3A) and appears to be stabilized by overexpression of LptC$^+$, which is consistent with the idea that LptC might interact with itself to form a dimer (see also Fig. 1) or a multimer. An alternative explanation is that upon depletion envelope stress response is triggered and periplasmic proteases are induced that might degrade the unstable LptC truncated protein. To probe LptC oligomerization *in vivo*, we performed *in vivo* cross-linking experiments using the wild-type strain AM604 transformed with different LptC constructs. In DSP-treated AM604 cells expressing wild-type LptC a band of ~46 kDa was visible consistent with the formation of an LptC-LptC complex (Fig. 6, upper panel). The 46-kDa band disappeared when the DSP cross-linker was reverted with a reducing agent. When samples were analyzed by Western blotting with anti-LptA antibodies, a band of ~43 kDa was visible that possibly corresponded to an LptA-LptC complex (Fig. 6, lower panel). In DSP-treated AM604 cells expressing both LptC$\Delta_{177\text{-}191}$ and an LptC version carrying an additional 27 amino acids at the C-terminal end (LptC-lk$_{25}$), two high-molecular-mass bands with an apparent masses of approximately 46 and 52 kDa appeared, possibly corresponding to LptC-lk$_{25}$–LptC$\Delta_{177\text{-}191}$ and LptC-lk$_{25}$–LptC-lk$_{25}$ com-

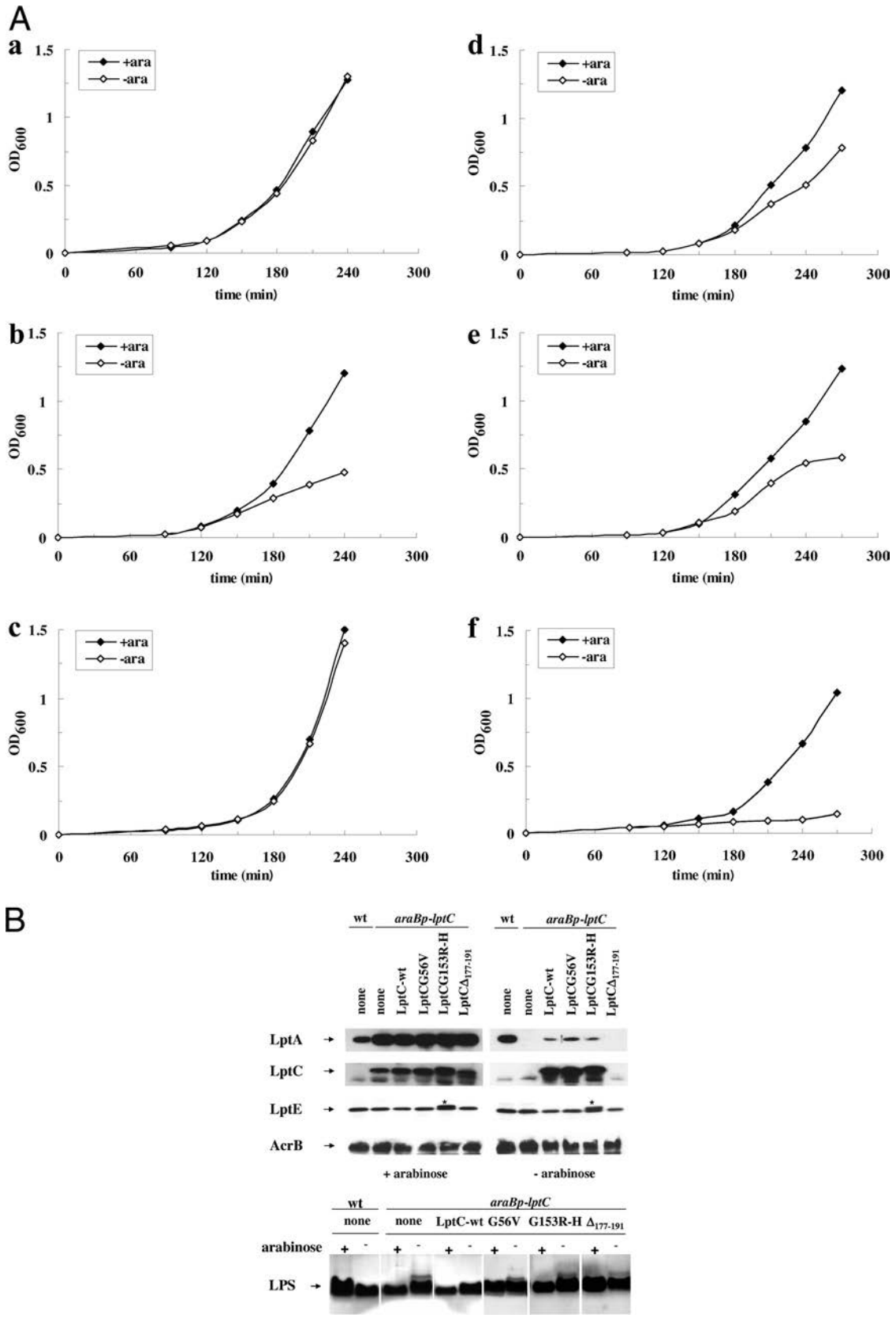

FIG. 5. Effect of *lptC* mutations on Lpt proteins complex and LPS transport. (A) Growth curves of AM604 (wt; a), FL905 (*araBp-lptC*; b) strains and FL905 carrying plasmids expressing LptC (c), LptCG56V (d), LptCG153R-H (e), and LptC$\Delta_{177\text{-}191}$ (f). Cells growing exponentially in LD containing arabinose were harvested, washed, and subcultured in arabinose-supplemented (◆) or arabinose-free (◇) medium. Growth was

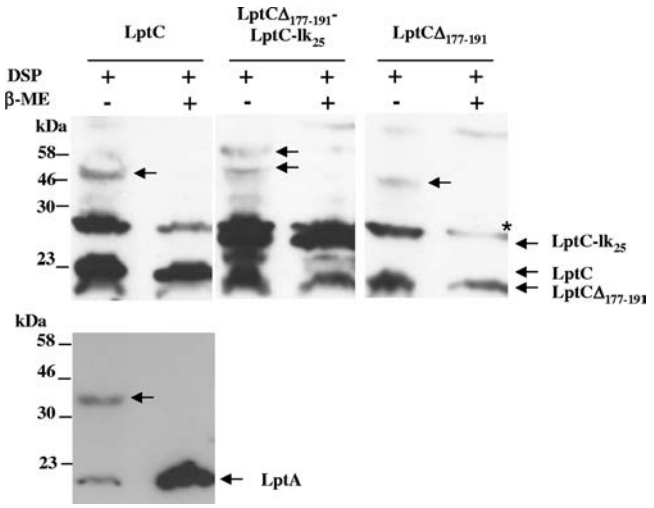

FIG. 6. LptC dimerization *in vivo*. Wild-type strain AM604 cells transformed with different LptC constructs were treated with the cross-linking DSP agent *in vivo*. Cell extracts were prepared and analyzed by Western blotting with anti-LptC and anti-LptA antibodies. Samples were treated with β-mercaptoethanol (β-ME) to revert the cross-linking. Equal amount of cells, (1.6 OD_{600} units) was loaded into each lane. An asterisk (*) labels a band that cross-reacts with the anti-LptC antibody.

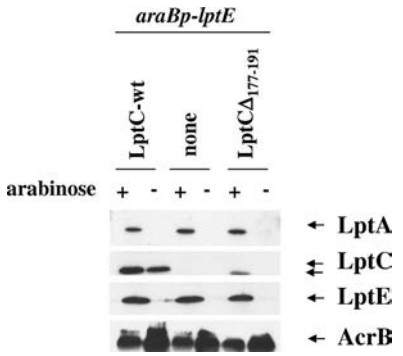

FIG. 7. Steady-state levels of LptA and LptC upon LptE depletion. Protein samples from AM689 cells transformed with various plasmids and grown in the presence (+) or absence (−) of arabinose 180 min after a shift in the nonpermissive condition were analyzed by Western blotting with anti-LptA, anti-LptC, and anti-LptE antibodies. Equal amounts of cells (0.2 OD_{600} units) were loaded into each lane. AcrB was used as a loading control.

plexes. In DSP-treated cells expressing $LptC\Delta_{177\text{-}191}$ the level of the truncated protein was low compared to the LptC wild type and LptC-lk_{25}, a finding consistent with the notion that the truncated protein is intrinsically unstable. However, an high-molecular-mass band of ~44 kDa appeared, suggesting that even the truncated protein is able to dimerize (Fig. 6, upper panel). These data suggest that LptC can form dimers *in vivo*. However, this experiment does not prove that dimerization with wild-type LptC protects the truncated $LptC\Delta_{177\text{-}191}$ protein version from degradation in the $LptC^{+}$ depletion strain FL905. Therefore, we examined the LptC levels in the *lptE* depletion strain AM689 grown under permissive and nonpermissive conditions and expressing either the wild-type or the truncated $LptC\Delta_{177\text{-}191}$ proteins. As shown in Fig. 7, $LptC\Delta_{177\text{-}191}$ was undetectable when the *lptE* depletion strain was grown in the absence of arabinose, an observation in line with the idea that $LptC\Delta_{177\text{-}191}$ is degraded by proteases induced under stress conditions.

Purified LptC is a dimer in solution. In order to probe the oligomeric state of LptC *in vitro*, the apparent molecular weight of the pure protein was tested by size-exclusion chromatography and ESI-MS under nondenaturing conditions. To do this, a preparation of the soluble version of LptC with an N-terminal His_6 tag and lacking the first 23 amino acids of the transmembrane domain was analyzed (sH-LptC [see Materials and Methods]) by size-exclusion chromatography. The protein eluted as a single, slightly asymmetric peak on a Superdex75 column (Fig. 8A, inset). The LptC elution volume corresponded to an estimated molecular mass of ~43,000 Da, relative to globular calibrants in the range 6,500 to 81,000 Da (Fig. 8A), suggesting a dimeric assembly. This conclusion was confirmed by nano-ESI-MS, which provides complementary information by direct detection and weighing of protein noncovalent complexes (13, 14). In Fig. 8B, C, and D, the spectra of pure sH-LptC preparations in the presence of ammonium acetate, which is known to favor detection of protein complexes by mass spectrometry, are reported. At 5 μM protein and 50 mM ammonium acetate (Fig. 8B), the spectrum shows signals of LptC monomers and dimers. Mass deconvolution gives a value of 20,536.8 (±0.25) Da for the monomer and 41,073.9 (±1.02) Da for the dimer which are in close agreement with the values calculated from the amino acid sequence (20,535.85 Da for the monomer and 41,071.7 Da for the dimer). Both species are characterized by conformational heterogeneity, as indicated by multimodal charge-state distributions (15), with maxima at 10+, 15+, and 23+ for the monomer and at 14+ and 21+ for the dimer. A 10-fold increase in the ionic strength results in a simpler spectrum, with only one monomeric and one dimeric species centered, respectively, on the 10+ and 14+ ions (Fig. 8C). This result suggests that the conformational heterogeneity observed at a lower ionic strength might reflect partial protein unfolding induced by the experimental conditions used. In Fig. 8D, the effect of protein concentration on the spectrum at high ionic strength is shown.

monitored by measuring the OD_{600}. Samples for protein and LPS analyses were taken from cells grown in the presence (+ara) or absence (−ara) of arabinose at 240 (wt, FL905, and FL905/pGS103) or 270 min (FL905/pGS103G56V, FL905/pGS108G153R, and FL905/pGS103$\Delta_{177\text{-}191}$) after the shift into fresh medium. (B) Steady-state levels of LptA, LptC, and LptE and LPS profile. Protein samples were subjected to Western blot analysis with anti-LptA, anti-LptC, anti-LptE, and anti-AcrB (as a loading control) antibodies. Anti-LptE antibodies cross-react with LptC-H His tag (*). Total LPS was extracted from mutant cells grown in the same conditions and at the same time points of protein analysis. LPS extracted from cultures with a total OD_{600} of 2 were separated by 18% Tricine-SDS-PAGE and silver stained. Equal amounts of cells, based on the OD measurement (0.2 OD_{600} units for protein analysis, 0.4 for LPS analysis), were loaded into each lane.

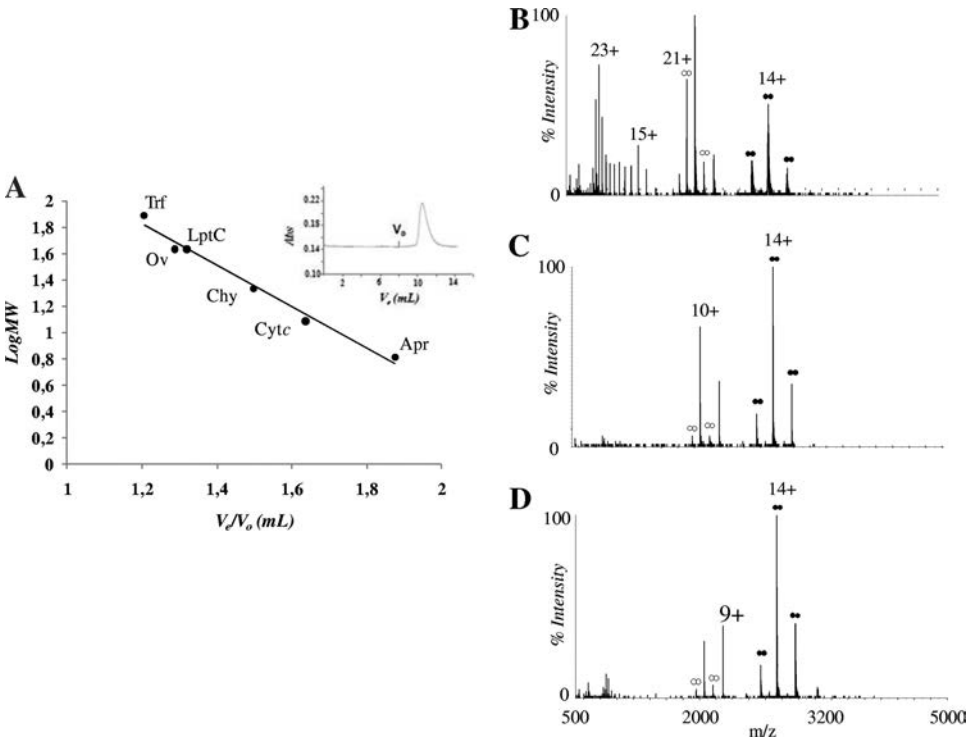

FIG. 8. LptC dimerization *in vitro*. (A) Apparent molecular weight (MW) of LptC as determined by gel filtration. The relative elution volume of sH-LptC in 50 mM sodium phosphate (pH 8.0)–100 mM NaCl was compared to that of globular standards. The chromatogram is shown in the inset. Trf, transferrin; Ov, ovalbumin; Chy, chymotrypsin; Cyt*c*, cytochrome *c*; Apr, aprotinin; V_e, elution volume; V_o, void volume; Abs, absorbance at 280 nm. (B, C, and D) Quaternary structure of LptC by mass spectrometry. The nano-ESI-MS spectra of 5 μM LptC in 50 mM ammonium acetate (pH 7.5) (B), 5 μM LptC in 500 mM ammonium acetate (pH 7.5) (C), and 20 μM LptC in 500 mM ammonium acetate (pH 7.5) (D) are shown. The main charge state of each peak envelope is labeled by the corresponding number of charges. Dimer-specific peaks are labeled by double circles. Solid symbols correspond to compact dimers, and open symbols correspond to less compact dimers.

The relative intensity of the monomer decreases as the protein concentration is increased from 5 to 20 μM, a finding consistent with a monomer-dimer equilibrium in the original liquid sample. The calculated relative amount of the dimer is ~70%. These data provide direct evidence of a predominant dimeric state of LptC in solution. However, it should be underscored that the apparent dissociation constant (in the micromolar range, according to these results) could be affected by the peculiar conditions imposed by electrospray. Overall, these data suggest that the LptC dimerizes and that the soluble portion of the protein is sufficient to promote dimerization.

Effect of LptD and LptE depletion on Lpt complex assembly. The experiments described above showed that the steady-state level of LptA is affected in the absence of wild-type LptC or by the $\Delta_{177\text{-}191}$ mutation, which severely impairs LptC$\Delta_{177\text{-}191}$ stability. It is possible that the absence of a proper IM docking structure for LptA results in LptA degradation *in vivo*. Therefore, the LptA level in the cell could be diagnostic of the properly bridged IM and OM. We thus tested whether the absence of the OM LptDE complex could also exert a similar effect on LptA stability. The AM661 and AM689 strains, in which the LptD and LptE expression is driven by the inducible *araBp* promoter (29), were grown under permissive conditions to exponential phase and then shifted to media lacking arabinose to deplete LptD and LptE, respectively. Samples for protein analyses were taken from cultures grown in the presence or in the absence of arabinose 210 min after the shift to nonpermissive conditions (Fig. 9A) and then processed for Western blot analysis with anti-LptA, anti-LptE, and anti-AcrB antibodies. As shown in Fig. 9B, a decreased steady-state level of LptA is observed upon LptE and LptD depletion. Overall, our data suggest that when the Lpt machinery is not functional for lack of either IM or OM components, LptA is destabilized, probably because it is not properly assembled in the Lpt complex.

DISCUSSION

LptA interaction with IM and OM Lpt components. The Lpt proteins constitute a machinery for LPS transport to the cell surface. Genetic and biochemical evidence indicates that the components of the machinery work in a concerted way. In fact, upon depletion of any of the seven Lpt proteins, the LPS assembly pathway is blocked in nearly the same fashion (23, 29); moreover, it has been recently shown that the seven Lpt proteins physically interact and constitute a transenvelope complex connecting IM and OM (4). However, little is known about how specific Lpt factors interact with each other. We show here by copurification experiments that *in vivo* LptA binding to IM occurs through binding to LptC, although we cannot rule out the possibility that LptA may also interact with

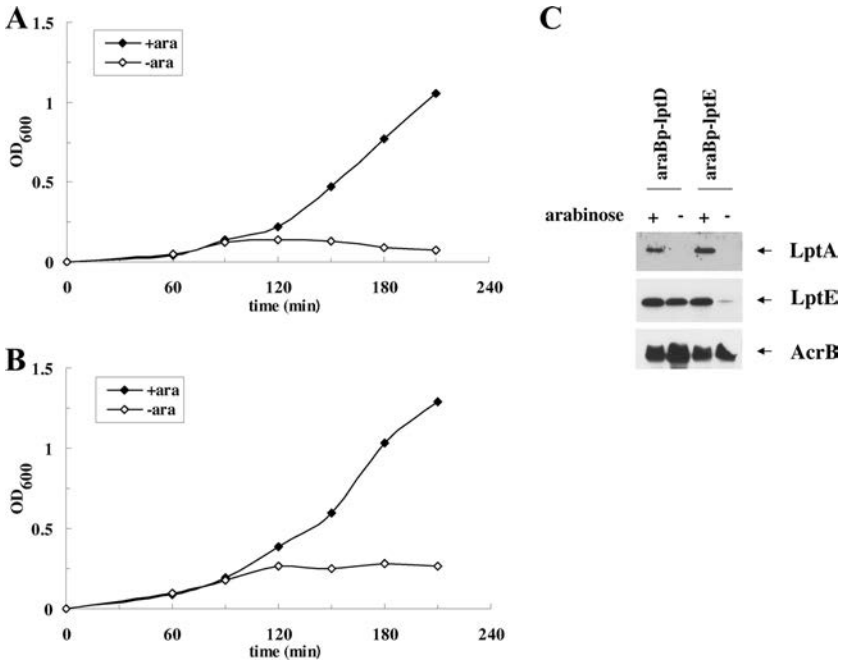

FIG. 9. LptA level upon LptD and LptE depletion. (A and B) Growth curves of AM661 (*araBp-lptD* [A]) and AM689 (*araBp-lptE* [B]). Cells growing exponentially in LD containing arabinose were harvested, washed, and subcultured in arabinose-supplemented (◆) or arabinose-free (◇) medium. Growth was monitored by measuring the OD_{600}. (C) Steady-state levels of LptA. Samples for protein analysis taken from cells grown in the presence (+) or absence (−) of arabinose at 210 min after the shift into nonpermissive condition were analyzed by Western blotting with anti-LptA and anti-LptE antibodies. Equal amounts of cells (0.2 OD_{600} units) were loaded into each lane. AcrB was used as the loading control.

other IM components such as LptFG, which possess periplasmic loops (23).

LptC depletion results in a significant decrease of LptA level. Similarly, the LptA level in the cells decreases upon LptD or LptE depletion, strongly suggesting that LptA also interacts with the LptDE complex at the OM and that in a non-properly assembled Lpt complex LptA may be degraded. It is likely that LptC and the LptDE complex play a structural role and prevent LptA degradation. Instability and/or degradation of components of protein complexes when proven or proposed interacting partners are either depleted or not functional is not unusual and provides indirect evidence of physical and functional interaction. The loss of any protein of the PilMNOP IM complex required for biogenesis of type IV pili in *Pseudomonas aeruginosa* results in instability of the other interacting partners (1); similarly, EspL and EspM, which belong to the type II secretion pathway required for cholera toxin secretion in *Vibrio cholerae*, have been shown to participate in mutual stabilization by protecting each other from proteolysis (25). Finally, Chng and coworkers demonstrated that LptD can only be overexpressed with LptE and that purified LptE is resistant to proteolytic degradation when in complex with LptD, thus indicating a structural role of LptE in stabilizing the folded state or facilitating the folding and assembly of LptD (5).

Interaction of LptA with LptC and the LptDE complex supports the model proposed by Kahne and coworkers (4), which posits that LptA interacts with both the IM and the OM. Consistent with this model are previous findings showing that in the crystals obtained in the presence of LPS, the LptA monomers are packed as a linear filament (34), suggesting that LptA oligomerization is functional to bridging the IM and OM. Since LptA consists of a conserved domain also found in the N-terminal periplasmic domain of LptD, we suggest that the latter protein may be the docking site for LptA at the OM (2, 30) and thus that LptA is anchored to the IM and OM through LptC and LptD, respectively.

LptC structure-function relationship. The analysis of loss-of-function mutations in *lptC* allowed us to further support the structural role of LptC-LptA interaction in preventing LptA degradation and to define functional regions in the LptC protein. The LptCG56V substitution falls in a stretch of relatively conserved residues and, based on the recently reported crystal structure, this residue is contained in one of the two disordered regions of the protein (residues 24 to 58) where no electron density was observed (38). The G56V amino acid substitution does not abolish interaction with LptA and in cells expressing LptCG56V the LptA level seems even higher than that observed in cells expressing wild-type LptC. However, LptCG56V impairs LPS transport, as demonstrated by the decreased viability and the appearance of LPS decorated with colanic acid in cells expressing the mutant protein only. These data suggest that this mutation does not affect IM and OM bridging by the Lpt complex, although the complex is not functional. Since LptC has been shown to bind LPS *in vitro* (38), it may be possible that the G56V mutation impairs such binding. An alternative hypothesis can be that during LPS transport LptC may undergo conformational changes, as suggested by the recently reported crystal structure analysis (38), that could be compromised by the G56V mutation.

The LptCG153R mutant protein displays a reduced affinity to LptA since it is not able to copurify LptA. As for LptCG56,

G153 also falls in a stretch of conserved residues (38). The inability of LptCG153R to copurify LptA suggests that the binding determinants are located in the C-terminal region of the protein. In cells expressing LptC$^+$ or LptCG153R, the LptA level is comparable, suggesting that the residual binding activity of LptCG153R mutant protein, overexpressed from a plasmid, is sufficient to prevent LptA degradation. Nevertheless, LptC$^+$-depleted FL905 cells expressing LptCG153R are not viable (Fig. 2B) and accumulate colanic acid decorated LPS (Fig. 5B), which indicates that transport is impaired.

LptC$\Delta_{177\text{-}191}$ is highly unstable (Fig. 3A) and fails to interact with LptA (Fig. 4), and thus the assembly of the Lpt complex is compromised. Interestingly, the C-terminal deletion of LptC$\Delta_{177\text{-}191}$ removes the second disordered region of the protein (residues 185 to 191) (38). It is well established that unfolded or only partly folded proteins in their native states fold into an ordered structure on binding a partner molecule/protein (7, 8). A well-studied example is the binding of colicins to disordered regions of their OM receptors as a key step in their translocation into the target cell (12, 37). Therefore, the intrinsically disordered region in the C-terminal end of LptC (residues 185 to 191) might be reorganized and folded upon binding to LptA.

We show here that in the Lpt machinery, LptC interacts with LptA. The recently solved crystal structure of LptC reveals a striking structural similarity to LptA despite the fact that the two proteins do not share sequence similarity (38). LptC is also part of the LptBCFG complex (18). A possible candidate for interaction in this complex is LptF since its periplasmic loop displays a structural similarity to LptC (http://zhang.bioinformatics.ku.edu/I-TASSER/). We provide evidence here that LptC, when overexpressed, is also able to dimerize *in vivo* (Fig. 6A). In addition to the *in vivo* data, size-exclusion chromatography and ESI-MS experiments showed that a soluble LptC version missing the N-terminal transmembrane domain (sH-LptC) forms dimers *in vitro* whose abundance increases with increasing protein concentration and ionic strength. In a very recent study it was reported that LptC exists as a monomer in solution (38). It is possible that this discrepancy is due to the different approaches and experimental conditions used. However, we suggest that the dimeric form is not the physiological preferred state in wild-type cells and that in the Lpt complex a single LptC molecule is present; our data suggest that LptC overexpression *in vivo* may shift the equilibrium between heterodimerization (interaction with LptA and/or LptF in the LptBFG complex) and homodimerization. It has been shown that the relative stoichiometry of the IM PilM/N/O/P proteins is crucial in promoting pilus assembly in *P. aeruginosa*. When overexpressed, PilO may form homodimers. However, the heterodimer PilN/O is the physiologically preferred state, occurring when PilO is expressed from the chromosome (1). The subunit ratio of the LptBCFG complex (LptB/LptF/LptG/LptC) has been proposed to be 2:1:1:1 (predicted molecular mass of 157.2 kDa) (18). However, the molecular mass of the LptBCFG complex determined by size-exclusion chromatography was ~330 kDa (18), which would be consistent with the ability of LptC to interact with itself, thus resulting in dimerization of LptBCFG complex.

As discussed above, the LptC$\Delta_{177\text{-}191}$ truncated protein is intrinsically unstable, since it may expose unfolded regions and become a protease substrate (40). Alternatively, LptC$\Delta_{177\text{-}191}$ could not associate with the LptBFG complex and might thus be degraded in the periplasm. In fact, it has been reported that unbalanced expression of LptB in an LptFG wild-type background results in the loss of IM association and the degradation of soluble LptB molecules in the cytoplasm (18). LptC could also be also stabilized by the interaction with LptA, the level of which does indeed increase when the LptC$^+$ depletion strain FL905 is grown with arabinose. A similar codependence has been observed for the IM divisome subcomplex FtsB/FtsL/FtsQ, where it has been shown that FtsL and FtsB are codependent for stabilization (10). However, our data (Fig. 7) suggest that the stability of LptC does not depend on LptA. In fact, upon LptE depletion LptA is undetectable since the OM docking site is missing, but the LptC level is not affected.

In conclusion, we provide evidence here that depletion of LptC, LptD, LptE, or mutations in LptC abolishing its function break the Lpt machinery by impairing either its assembly (LptC$\Delta_{177\text{-}191}$) or functionality (LptCG153R and LptCG56V). The lack of LptC (because the protein is depleted or mutated) or LptDE removes the IM and OM LptA docking sites, and the LptA level in the cell decreases. Based on these data, we suggest that the steady-state level of LptA is controlled at the protein stability level by the assembly of the Lpt complex since the inability of the protein to properly interact with IM and OM docking sites results in its degradation. Therefore, the LptA level could be used as a marker of properly bridged IM and OM components. Our genetic and biochemical data confirm that LptC plays a key role in docking LptA and other Lpt factors at the IM, in addition to a direct role in LPS transport, since the protein has also been shown to bind LPS (38). Overall, the data presented here strongly support the transenvelope complex model for LPS transport.

ACKNOWLEDGMENTS

We are grateful to Daniel Kahne for providing the LptC and LptD antibodies. We thank K. M. Pos for providing the AcrB antibodies. We also thank Chiara Raimondi for excellent technical assistance.

This study was supported in part by MIUR (Ministero dell'Istruzione Università e Ricerca) grant PRIN 200824M2HX (A.P.) and Regione Lombardia Cooperazione Scientifica e Tecnologica Internazionale grant 16876 SAL-18 (A.P.).

REFERENCES

1. **Ayers, M., et al.** 2009. PilM/N/O/P proteins form an inner membrane complex that affects the stability of the *Pseudomonas aeruginosa* type IV pilus secretin. J. Mol. Biol. **394:**128–142.
2. **Bos, M. P., V. Robert, and J. Tommassen.** 2007. Biogenesis of the Gram-negative bacterial outer membrane. Annu. Rev. Microbiol. **61:**191–214.
3. **Bos, M. P., B. Tefsen, J. Geurtsen, and J. Tommassen.** 2004. Identification of an outer membrane protein required for the transport of lipopolysaccharide to the bacterial cell surface. Proc. Natl. Acad. Sci. U. S. A. **101:**9417–9422.
4. **Chng, S. S., L. S. Gronenberg, and D. Kahne.** 2010. Proteins required for lipopolysaccharide assembly in *Escherichia coli* form a transenvelope complex. Biochemistry **49:**4565–4567.
5. **Chng, S. S., N. Ruiz, G. Chimalakonda, T. J. Silhavy, and D. Kahne.** 2010. Characterization of the two-protein complex in *Escherichia coli* responsible for lipopolysaccharide assembly at the outer membrane. Proc. Natl. Acad. Sci. U. S. A. **107:**5363–5368.
6. **Doerrler, W. T., H. S. Gibbons, and C. R. Raetz.** 2004. MsbA-dependent translocation of lipids across the inner membrane of *Escherichia coli*. J. Biol. Chem. **279:**45102–45109.
7. **Dyson, H. J., and P. E. Wright.** 2002. Coupling of folding and binding for unstructured proteins. Curr. Opin. Struct. Biol. **12:**54–60.
8. **Dyson, H. J., and P. E. Wright.** 2005. Intrinsically unstructured proteins and their functions. Nat. Rev. Mol. Cell. Biol. **6:**197–208.

9. **Eom, G. T., J. K. Song, J. H. Ahn, Y. S. Seo, and J. S. Rhee.** 2005. Enhancement of the efficiency of secretion of heterologous lipase in *Escherichia coli* by directed evolution of the ABC transporter system. Appl. Environ. Microbiol. **71:**3468–3474.
10. **Gonzalez, M. D., and J. Beckwith.** 2009. Divisome under construction: distinct domains of the small membrane protein FtsB are necessary for interaction with multiple cell division proteins. J. Bacteriol. **191:**2815–2825.
11. **Hanahan, D.** 1983. Studies on transformation of *Escherichia coli* with plasmids. J. Mol. Biol. **166:**557–580.
12. **Hecht, O., H. Ridley, J. H. Lakey, and G. R. Moore.** 2009. A common interaction for the entry of colicin N and filamentous phage into *Escherichia coli*. J. Mol. Biol. **388:**880–893.
13. **Heck, A. J., and R. H. Van Den Heuvel.** 2004. Investigation of intact protein complexes by mass spectrometry. Mass Spectrom. Rev. **23:**368–389.
14. **Invernizzi, G., A. Natalello, M. Samalikova, and R. Grandori.** 2007. Protein-protein and protein-ligand interactions studied by electrospray-ionization mass spectrometry. Protein Pept. Lett. **14:**894–902.
15. **Kaltashov, I. A., and R. R. Abzalimov.** 2008. Do ionic charges in ESI MS provide useful information on macromolecular structure? J. Am. Soc. Mass Spectrom. **19:**1239–1246.
16. **Ma, B., C. M. Reynolds, and C. R. Raetz.** 2008. Periplasmic orientation of nascent lipid A in the inner membrane of an *Escherichia coli* LptA mutant. Proc. Natl. Acad. Sci. U. S. A. **105:**13823–13828.
17. **Miyake, K.** 2004. Innate recognition of lipopolysaccharide by Toll-like receptor 4-MD-2. Trends Microbiol. **12:**186–192.
18. **Narita, S., and H. Tokuda.** 2009. Biochemical characterization of an ABC transporter LptBFGC complex required for the outer membrane sorting of lipopolysaccharides. FEBS Lett. **583:**2160–2164.
19. **Polissi, A., and C. Georgopoulos.** 1996. Mutational analysis and properties of the *msbA* gene of *Escherichia coli*, coding for an essential ABC family transporter. Mol. Microbiol. **20:**1221–1233.
20. **Raetz, C. R., et al.** 2009. Discovery of new biosynthetic pathways: the lipid A story. J. Lipid Res. **50**(Suppl.)**:**S103–S108.
21. **Raetz, C. R., and C. Whitfield.** 2002. Lipopolysaccharide endotoxins. Annu. Rev. Biochem. **71:**635–700.
22. **Reuhs, B. L., R. W. Carlson, and J. S. Kim.** 1993. *Rhizobium fredii* and *Rhizobium meliloti* produce 3-deoxy-D-manno-2-octulosonic acid-containing polysaccharides that are structurally analogous to group II K antigens (capsular polysaccharides) found in *Escherichia coli*. J. Bacteriol. **175:**3570–3580.
23. **Ruiz, N., L. S. Gronenberg, D. Kahne, and T. J. Silhavy.** 2008. Identification of two inner-membrane proteins required for the transport of lipopolysaccharide to the outer membrane of *Escherichia coli*. Proc. Natl. Acad. Sci. U. S. A. **105:**5537–5542.
24. **Sabbattini, P., F. Forti, D. Ghisotti, and G. Dehò.** 1995. Control of transcription termination by an RNA factor in bacteriophage P4 immunity: identification of the target sites. J. Bacteriol. **177:**1425–1434.
25. **Sandkvist, M., L. P. Hough, M. M. Bagdasarian, and M. Bagdasarian.** 1999. Direct interaction of the EpsL and EpsM proteins of the general secretion apparatus in *Vibrio cholerae*. J. Bacteriol. **181:**3129–3135.
26. **Sklar, J. G., T. Wu, D. Kahne, and T. J. Silhavy.** 2007. Defining the roles of the periplasmic chaperones SurA, Skp, and DegP in *Escherichia coli*. Genes Dev. **21:**2473–2484.
27. **Sperandeo, P., et al.** 2007. Characterization of *lptA* and *lptB*, two essential genes implicated in lipopolysaccharide transport to the outer membrane of *Escherichia coli*. J. Bacteriol. **189:**244–253.
28. **Sperandeo, P., G. Dehò, and A. Polissi.** 2009. The lipopolysaccharide transport system of Gram-negative bacteria. Biochim. Biophys. Acta **1791:**594–602.
29. **Sperandeo, P., et al.** 2008. Functional analysis of the protein machinery required for transport of lipopolysaccharide to the outer membrane of *Escherichia coli*. J. Bacteriol. **190:**4460–4469.
30. **Sperandeo, P., C. Pozzi, G. Dehò, and A. Polissi.** 2006. Non-essential KDO biosynthesis and new essential cell envelope biogenesis genes in the *Escherichia coli yrbG-yhbG* locus. Res. Microbiol. **157:**547–558.
31. **Sprott, G. D., G. Ferrante, and I. Ekiel.** 1994. Tetraether lipids of *Methanospirillum hungatei* with head groups consisting of phospho-*N*,*N*-dimethylaminopentanetetrol, phospho-*N*,*N*,*N*-trimethylaminopentanetetrol, and carbohydrates. Biochim. Biophys. Acta **1214:**234–242.
32. **Steeghs, L., et al.** 1998. Meningitis bacterium is viable without endotoxin. Nature **392:**449–450.
33. **Stenberg, F., et al.** 2005. Protein complexes of the *Escherichia coli* cell envelope. J. Biol. Chem. **280:**34409–34419.
34. **Suits, M. D., P. Sperandeo, G. Dehò, A. Polissi, and Z. Jia.** 2008. Novel structure of the conserved Gram-negative lipopolysaccharide transport protein A and mutagenesis analysis. J. Mol. Biol. **380:**476–488.
35. **Tefsen, B., J. Geurtsen, F. Beckers, J. Tommassen, and H. de Cock.** 2005. Lipopolysaccharide transport to the bacterial outer membrane in spheroplasts. J. Biol. Chem. **280:**4504–4509.
36. **Thanabalu, T., E. Koronakis, C. Hughes, and V. Koronakis.** 1998. Substrate-induced assembly of a contiguous channel for protein export from *Escherichia coli*: reversible bridging of an inner-membrane translocase to an outer membrane exit pore. EMBO J. **17:**6487–6496.
37. **Tozawa, K., et al.** 2005. Clusters in an intrinsically disordered protein create a protein-binding site: the TolB-binding region of colicin E9. Biochemistry **44:**11496–11507.
38. **Tran, A. X., C. Dong, and C. Whitfield.** 2010. Structure and functional analysis of LptC, a conserved membrane protein involved in the lipopolysaccharide export pathway in *Escherichia coli*. J. Biol. Chem. **285:**33529–33539.
39. **Tran, A. X., M. S. Trent, and C. Whitfield.** 2008. The LptA protein of *Escherichia coli* is a periplasmic lipid A-binding protein involved in the lipopolysaccharide export pathway. J. Biol. Chem. **283:**20342–20349.
40. **Wickner, S., M. R. Maurizi, and S. Gottesman.** 1999. Posttranslational quality control: folding, refolding, and degrading proteins. Science **286:**1888–1893.
41. **Wu, T., et al.** 2006. Identification of a protein complex that assembles lipopolysaccharide in the outer membrane of *Escherichia coli*. Proc. Natl. Acad. Sci. U. S. A. **103:**11754–11759.
42. **Zgurskaya, H. I., and H. Nikaido.** 2000. Cross-linked complex between oligomeric periplasmic lipoprotein AcrA and the inner-membrane-associated multidrug efflux pump AcrB from *Escherichia coli*. J. Bacteriol. **182:**4264–4267.
43. **Zhou, Z., K. A. White, A. Polissi, C. Georgopoulos, and C. R. Raetz.** 1998. Function of *Escherichia coli msbA*, an essential ABC family transporter, in lipid A and phospholipid biosynthesis. J. Biol. Chem. **273:**12466–12475.

Characterization of Functional Domains in LptC, a Conserved Membrane Protein Implicated in LPS Export Pathway in *Escherichia coli*.

(Paper draft)

Riccardo Villa[1], Alessandra M. Martorana[1], Louise J. Gourlay[2], Paola Sperandeo[1], Martino Bolognesi[2], Daniel Kahne[3], and Alessandra Polissi[1*].

[1]Dipartimento di Biotecnologie e Bioscienze, Università di Milano-Bicocca, Italy

[2] Dipartimento di Scienze Biomolecolari e Biotecnologie, and CIMAINA, Universita' di Milano, Italy

[3]Department of Chemistry and Chemical Biology, Harvard University, Cambridge, Massachusetts,USA; Department of Biological Chemistry and Molecular Pharmacology, Harvard Medical School, Boston, Massachusetts, USA

*Corresponding author

Alessandra Polissi

[1]Dipartimento di Biotecnologie e Bioscienze, Università di Milano-Bicocca, Italy

Piazza della Scienza 2

20126 Milano (Italy)

Phone: +39-02-64483431, Fax: +39-02-64483450

E-mail: alessandra.polissi@unimib.it

ABSTRACT

Lipopolysaccharide (LPS) is a major glycolipid present in the outer membrane (OM) of Gram-negative bacteria. The peculiar permeability barrier of the OM is due to the presence of LPS at the outer leaflet of this membrane that prevents many toxic compounds from entering the cell. In *Escherichia coli* seven essential Lpt proteins located in the inner membrane (IM) (LptBCDF), in the periplasm (LptA) and in the OM (LptDE) are responsible for LPS transport across the periplasmic space and its assembly at the cell surface. The Lpt proteins constitute a transenvelope complex spanning IM and OM that appears to operate as a single device.

LptC, a key protein in the Lpt machinery, is an essential IM-anchored protein with a large periplasm-protruding domain. LptC binds the IM LptBFG ABC transporter and also interacts with the periplasmic protein LptA.

Here we characterized two inactive *lptC* mutant alleles carrying mutation in two conserved glycines (G56 and G153) of the protein. By affinity purification experiments we found that LptCG56V fails to interact with the IM protein complex LptBFG whereas LptCG153R is able to assemble the whole Lpt complex although the assembled machinery is not functional. Moreover based on LptCG153R crystal structure and on the phenotype of the mutant protein we propose that LptC could also directly interact with the OM protein LptD. Finally we demonstrated that the TM region of LptC is not required for interaction to the IM LptBFG proteins complex suggesting that its presence might simply allow a better co-localization with LptF and LptG making LPS transport more efficient.

INTRODUCTION

Lipopolysaccharide (LPS) is a complex glycolipid uniquely present in the outer layer of Gram-negative bacteria outer membrane (OM) (Raetz and Whitfield 2002; Raetz et al., 2009).

LPS is composed of three domains: lipid A, the conserved hydrophobic moiety embedded in the OM, a central core containing non repeating oligosaccharide residues and an O-antigen constituted of polysaccharide repeating units (Raetz and Whitfield 2002). LPS at the outer leaflet of the OM contributes to a large extent to the peculiar permeability barrier properties exhibited by the OM (Nikaido 2003) enabling Gram negative bacteria to survive in harsh environments and to exclude several antibiotics effective against Gram-positive organisms. LPS biogenesis is a complex process: it involves synthesis at the inner leaflet of the inner membrane (IM), translocation across the IM, transport across the aqueous periplasmic space and insertion at the outer leaflet of the OM. The biosynthetic pathway of LPS is well understood (Raetz and Whitfield 2002) much less known is how this large amphipathic molecule is transported across the periplasm to its final destination to the cell surface. LPS flipping across the IM involves the essential ABC transporter MsbA (Doerrler et al., 2006; Polissi and Georgopoulos 1996; Zhou et al., 1998). Then seven essential Lpt (LptABCDEFG) proteins in *Escherichia coli* form a transenvelope complex that connects IM and OM (Chng et al., 2010). At the IM the LptBFG constitutes an ABC transporter that provides the energy for the transport (Narita and Tokuda 2009). LptF and LptG are the transmembrane components (Ruitz et al., 2008) whereas LptB is the IM associated ATP binding protein (Narita and Tokuda 2009). LptC is a small bitopic protein possessing a single transmembrane region and a large periplasmic domain (Tran et al., 2010). LptC binds to the IM protein complex although its association does not affect the ATPase activity of the LptBFG complex (Narita and Tokuda 2009). At the OM the β–barrel protein LptD and the lipoprotein LptE form a complex responsible for LPS translocation across the OM in the final stages of assembly (Braun and Shilavy 2002; Wu et al., 2006; Chng et al., 2010; Chimalakonda et al.,

2011; Freinkman et al., 2011). LptA is a periplasmic protein (Sperandeo et al., 2008) that physically interacts to LptC and the LptDE complex (Sperandeo et al., 2011) thus bridging IM and OM. Genetic and biochemical evidence indicate that the components of the Lpt machinery work in a concerted way. In fact upon depletion of any of the seven Lpt proteins the LPS assembly pathway is blocked in nearly the same fashion (Sperandeo et al., 2008; Ruiz et al., 2008). Moreover removal of either LptC or LptDE which are the IM and OM docking sites for LptA, respectively results in LptA degradation, further supporting the transenvelope complex model for LPS transport (Sperandeo et al., 2011).

Both LptA and LptC have been shown to bind LPS *in vitro* (Tran et al., 2008; Tran et al., 2010). Interestingly, *in vitro* LptA can displace LPS from LptC (but not vice versa) consistent with the location of the two proteins and their proposed placement in the unidirectional LPS export pathway (Tran et al., 2010).

The crystal structure of LptA and of the periplasmic domain of LptC has been solved (Suits et al., 2008; Tran et al., 2010). The overall architecture of the two proteins is remarkably similar despite they do not share sequence similarity. Both proteins show a twisted boat structure formed in LptA and LptC by 16 and 15 consecutive antiparallel β–strands, respectively (Suits et al., 2008; Tran et al., 2010). The structure of LptA has been also been solved in the presence of LPS: in these crystals LptA monomers are packed as a linear filament (Suits et al., 2008) leading to the hypothesis that oligomers of LptA may be required to bridge IM and OM.

In a previous work we isolated and partially characterized two inactive *lptC* mutant alleles carrying mutation in two conserved glycines (G56 and G153) of the protein (Sperandeo et al., 2011). This work provides a further characterization of such mutant proteins. By affinity purification experiments we found that LptCG56V fails to interact with the IM protein complex LptBFG whereas LptCG153R is able to assemble the whole Lpt complex although the assembled machinery is not

functional. Moreover based on LptCG153R crystal structure and on the phenotype of the mutant protein we propose that LptC could also directly interact with LptD.

Finally we demonstrated that the TM region of LptC is not required for interaction to the IM LptBFG proteins complex suggesting that its presence might simply allow a better co-localization with LptF and LptG making LPS transport more efficient.

RESULTS

Overexpression and subcellular localization of inactive *lptC* mutant alleles

E. coli LptC is a conserved bitopic IM protein with a single predicted N-terminal transmembrane helix (Trp7-Asp29) (Expasy, http://expasy.org/) and a large soluble (Thr30-Pro191) periplasmic domain (Tran *et al*., 2010) (Fig. 1). LptC interacts with the IM protein complex LptBFG and with LptA (Narita and Tokuda, 2009; Sperandeo *et al*., 2011).

We previously isolated and partially characterized two inactive *lptC* mutant alleles carrying the single amino acid substitutions G56V and G153R (Sperandeo et al., 2011). LptCG56V and LptCG153R expressed from a plasmid are unable to support growth of FL905 (*araBp-lptC*) conditional strain (Table 1), in which the expression of *lptC* chromosomal gene is under the control of an arabinose inducible promoter, under non permissive conditions (absence of arabinose). Both G56 and G153 fall in two clusters of conserved residues in the periplasmic region of the protein (Sperandeo et al., 2011).

To test whether the defect of LptC single mutants is due to a lower level of the proteins, LptC, LptCG56V and LptCG153R were ectopically expressed in FL905 and growth of cells was tested upon IPTG induction. Overexpression of neither LptCG56V nor of LptCG153R restores FL905 growth

under non-permissive conditions (Fig. 2). In line with previous observations LptCG153R protein is toxic for the cells even when overexpressed under permissive conditions (Sperandeo et al., 2011).

We then examined the subcellular localization of LptC mutant proteins fused to a C-terminal His_8-tag. Periplasmic, cytoplasmic, IM, and OM fractions from wild-type AM604 strain expressing pET23/42LptC-H, pET23/42LptCG56V-H, and pET23/42LptCG153R-H, were prepared and analyzed by Western blotting using anti-His_6 monoclonal antibodies. As shown in Fig. 3A, LptCG56V-H and LptCG153R-H are detectable in the IM fraction as wild-type LptC-H. A small amount of wild type and LptC mutant proteins was also detectable in the OM fraction likely due to cross-contamination during the fractionation procedure.

Assembly of the Lpt export machinery in G56V and G153R mutants

We previously probed LptCG56V and LptCG153R interaction to LptA and demonstrated that only LptCG153R lost the ability to co-purify LptA *in vitro* thus implicating the C-terminal region of the LptC in LptA binding (Sperandeo *et al.,* 2011). Moreover we showed that LptA is degraded when it fails to interact with the IM (LptC) or OM (LptDE) docking sites (Sperandeo *et al*., 2011). However, in cells expressing LptCG153R LptA is not degraded and its level is comparable to that observed in cells expressing wild type LptC suggesting that the residual binding activity of LptCG153R mutant protein, expressed from a plasmid, is sufficient to prevent LptA degradation.

To better characterize LptC mutant proteins and to explore the complex LptC interactome we performed pull-down experiment to co-purify all Lpt components by using wild type or mutant LptC proteins as baits according to the protocol recently developed by Chng and co-workers (Chng *et al.,* 2010). Total membranes were collected from wild type AM604 cells expressing pET23/42LptC-H, pET23/42LptCG56V-H or pET23/42LptCG153R-H were solubilized and subjected to tandem affinity purification. Samples eluted from the column were then incubated with anti-His_6 monoclonal

antibodies and immunoprecipitated to detect LptB, LptF and LptG by separation on SDS_PAGE gels or immunoblotted using LptA, LptC, LptD and LptE antibodies. Both LptCG56V-H and LptCG153R-H were able to co-purify LptA and the LptDE OM protein complex (Fig.4 A). LptCG56V-H was unable to co-purify LptBFG indicating that the G56V amino acid substitution impairs interaction to the IM proteins complex. These results indicate that the determinants for LptC interaction to the IM LptBFC ABC transporter are located in N-terminal region of the protein. On the contrary LptCG153R-H is able pull-down all components of the Lpt machinery (Fig.4 B). Therefore, the fully inactive LptCG153R-H mutant protein retains the ability to assemble the Lpt transenvelope complex although the assembled machinery is not functional.

Determination of the structure of the periplasmic domain of LptCG153R

Plasmid pQEsH-LptCG153R expresses a soluble cytoplasmic version of LptCG153R (23-191) missing the transmembrane helix and with an N-terminal His_6 affinity tag (sH-LptC) (Table 1).

LptCG153R is present as a dimer in the asymemetric unit, comprising two chains (A and B), each organized into a twisted boat structure formed by the sandwiching of two β–sheets (Fig.5A). The overall fold is highly identical to that of the wild type protein (*r.m.s.d*. 0.8Å and 0.5Å for chains A and B, respectively) with electron density visible for residues 58 to 182 (Chain A) and 59 to 184 (Tran et al., 2010). In agreement with the wild type structure, the N-terminus is disordered, therefore electron density is absent for the first 45 residues (9 belonging to the His-tag region), and also for the last 7 C-terminal residues (Tran et al., 2010).

The G153R mutation, located at the tip of a β-strand, projects inwards to the centre of the molecule, it is solvent-accessible and, despite the introduction of a large positive side-chain, it does not alter the overall architecture of the protein (Fig. 5B). Despite the fact that LptCG153R is fully inactive, the mutant protein is stable, and does not affect *in vivo* the level of LptA (Sperandeo *et al.,* 2011).

Therefore the structural evidence, together with the co-purification results might suggest that LptCG153R defect could not be simply due to an impairment of LptC-LptA interaction. As in proteins the positions of glycines often determines the regions of protein flexibility, it may be possible that the G153R substitution interferes with conformational changes, freezing the protein in a state, which either disrupts dynamic interactions with other Lpt partners or the LPS ligand, or blocks interacting partners in a bound state.

The TM region of LptC is dispensable

E. coli LptC is an IM anchored protein. However, sequence alignments among LptC homologues in a subset of representative Proteobacteria revealed that in some cases the anchoring sequence is missing. Therefore, to test the functional role of the first 23 residues composing the predicted transmembrane (TM) region, we constructed two LptC chimeric proteins in which either the TM region is missing or is substituted with a heterologous TM sequence. To this purpose the periplasmic region of LptC (24-191) was fused to the first TM region (1-36) of the IM spanning protein MalF protein or to the signal sequence of MalE (1-26) (Daus *et al.,* 2007) to obtain the chimeras $MalF_{TM}$LptC-H and $MalE_{SS}$LptC-H, respectively. In both constructs the C-terminal region of LptC is fused to a His_6 tag. .

To determine the subcellular localization of the LptC chimeras periplasmic, cytoplasmic, IM, and OM fractions from wild-type AM604 strain expressing pET23/42$MalF_{TM}$LptC-H and pET23/42$MalE_{ss}$LptC-H, were prepared and analyzed by Western blotting using anti-His_6 tag monoclonal antibodies. $MalF_{TM}$LptC localizes in the IM fraction, whereas $MalE_{SS}$LptC is detected only in the periplasmic fraction suggesting that the exporting signal sequence of MalE is correctly trimmed (Fig. 3B).

The chimeric *malF*$_{TM}$*lptC* and *malF*$_{TM}$*lptC* genes were cloned into pGS100 vector and expressed under an IPTG inducible promoter to give plasmids pGS112 and pGS114, respectively (Table 1). Both MalF$_{TM}$LptC and MalE$_{SS}$LptC are able to sustain growth of the conditional FL905 (*araBp-lptC*) strain under non permissive conditions even when the chimeric proteins are not induced with IPTG. To assess whether the expression of the mutant proteins missing the wild type LptC TM region affects OM integrity we tested the sensitivity of FL905 cells transformed with MalF$_{TM}$LptC and MalE$_{SS}$LptC to several toxic hydrophobic compounds. It is well known that increased sensitivity to hydrophobic antibiotics is an indicator of a disrupted barrier function at the OM permeability resulting from a partially disrupted LPS layer (Ruiz et al., 2005; Chimalakonda et al., 2011). As shown in Fig.6 FL905 LptC depleted cells (i.e. growing in the absence of arabinose) but expressing the LptC chimeras do not show sensitivity to any of the tested antibiotics, suggesting that the LptC chimeras are functional and that OM permeability barrier is intact.

To assess whether LptC chimeras are able to recruit the IM LptBFG proteins complex tandem affinity purification and immunoprecipitation were performed using MalF$_{TM}$LptC and MalE$_{SS}$LptC proteins as baits.

Both chimeras were able to efficiently co-purify the IM protein complex LptBFG (Fig. 7), suggesting that the Lpt protein machinery at the IM is correctly assembled. These results suggest that under the conditions tested the TM region of LptC is dispensable.

EXPERIMENTAL PROCEDURES

Bacterial strains and growth conditions. The bacterial strains and plasmids are listed in Table 1. The oligonucleotide primers are listed in Table 2.

Bacteria were grown in LD medium (Sabbatini et al., 1995). When required, 0.2% (wt/v) L-arabinose (as an inducer of the *araBp* promoter), 0.1 mM IPTG (isopropyl-β-D-thiogalactopyranoside),

100 μg ampicillin/ml, 25 μg chloramphenicol/ml, 25 μg kanamycin/ml, 2.5 μg rifampicin/ml, 50 μg bacitracin/ml, 30 μg novobiocin/ml, 0.5% (w/v) SDS (Sodium dodecyl sulfate), and 0.55mM EDTA (Ethylenediaminetetraacetic acid) were added. Solid media were prepared as described above with 1% (w/v) agar.

Plasmid construction. Plasmids used in this study are summarized in Table 1. The oligonucleotide primers are listed in Table 2.

Plasmids pGS112 and pGS114 express MalFTMLptC and MalEssLptC versions of LptC, respectively, from the IPTG-inducible Ptac promoter.

Briefly, MalFTMLptC is composed of the first MalF transmembrane region (amino acids 1-36) (Oldham et al.,2007) fused to the periplasmic portion of LptC, starting at amino acid 24. MalEssLptC is composed of the 26 amino acid long signal sequence of MalE (Bedouelle et al.,1980) fused to LptC starting at amino acid 24.

The *malFTMlptC* and *malEsslptC* chimerical genes were obtained by three step PCR (M.K. Chaveroche et al., 2000) using the MG1655 chromosome as template. The last PCR products were EcoRI-HindIII digested and cloned in pGS100 cut with the same enzymes. EcoRI-HindIII inserts in pGS112 and pGS114 were verified by sequencing.

Plasmids pET23/42LptCG56V-H, pET23/42LptCG153R-H, expressing LptCG56V and LptCG153R with a C-terminal His8 tag, were constructed by using a QuikChange site-directed mutagenesis kit (Stratagene) with primers listed in Table 2, as previously described (Sperandeo et al., 2011).

Plasmids pET23/42MalF$_{TM}$LptC-H and pET23/42MalE$_{SS}$lptC-H express MalF$_{TM}$LptC and MalE$_{SS}$LptC with a C-terminal His8 tag. They were constructed by cloning into NdeI-XhoI digested pET23/42 fragments obtained by PCR using pGS112 and pGS114 plasmids as template and digested

with the same enzymes. NdeI-XhoI inserts in the pET23/42MalF_{TM}LptC-H and pET23/42MalE_{SS}lptC-H were verified by sequencing.

Affinity purification and immunoprecipitation. AM604 (wild-type strain) and AM604 harbouring pET23/42LptC-H, pET23/42LptCG56V-H, pET23/42LptCG153R-H, pET23/42MalF_{TM}LptC-H, pET23/42MalE_{SS}LptC-H were used in these experiments as previously described (Chng *et al*., 2010), with following modifications. Briefly, harvested cells were resuspended in 15 ml of 20 mM Tris.HCl, pH 7.4, supplemented with 50 µg/ml DNase I, 100 µg/ml lysozyme. The cells were lysed by a single cycle through a Cell Disrupter (One Shot Model by Constant Systems LTD) at 25,000 psi as recommended by manufacturer's instructions. 1 mM phenylmethylsulfonyl fluoride (PMSF) was added soon after. The membrane pellet was extracted at 4°C for 30 min with 5 ml of 50mM Tris.HCl, pH 7.4, 10% glycerol, 5 mM $MgCl_2$ and 1% N-Laurosylsarcosine (Sigma). Affinity purification buffers were prepared as follow: the column was washed with 10 ml of 50 mM Tris.HCl, pH 7.4, 10 % glycerol, 0,05% N-Laurosylsarcosine, 5mM imidazole, and eluted with 5 ml of 50 mM Tris.HCl, pH 7.4, 10% glycerol, 0,05% N-Laurosylsarcosine, 200 mM imidazole. The eluate was concentrated using an ultrafiltration device (Amicon Ultra, Millipore, 10,000 MWCO) at 5,000 x g to a final volume of 50 µl or 1 ml. In the first case the samples were then mixed with protein sample buffer without β-mercaptoethanol, boiled and used for 10% PAGE and immunoblotting analyses as explained below. In the latter one, samples were processed for immunoprecipitation as reported by Chng *et al.* (2010). Immunoprecipitation spin columns (Sigma-Aldrich) were washed three times with 700 µl of 50 mM Tris.HCl, pH 7.4, 10% glycerol and 0,05% N-Laurosylsarcosine. The purified sample was eluted by boiling the beads in 35 µl protein sample buffer without β-mercaptoethanol. The protein samples were then separated by SDS-PAGE. Bands on the gels were excised, and proteins identified by nano-ESI-MS analyses on a hybrid Quadrupole-Time-of-Flight mass spectrometer (QSTAR ELITE, Applied

Biosystems). The indicated proteins were identified using the MASCOT software with probability scores above threshold.

Cell fractionation. Cultures of AM604 containing pET23/42LptC-H, pET23/42LptCG56V-H, pET23/42LptCG153R-H, pET23/42MalF_{TM}LptC-H, pET23/42MalE_{SS}LptC-H were grown overn night in LD. Periplasmic, cytoplasmic, inner, and outer membrane fractions were prepared as described previously (Oliver *et al.,* 1982). Equal amounts of proteins from each fraction were fractionated by 12.5% SDS-PAGE. The proteins were detected by Western blotting using the anti-LptC antibodies. Antibodies against the 55 kDa IM protein (Sperandeo *et al.*, 2008) and against the OM protein BamA (Wu T. *et al.,* 2006) were used as a control for good fractionation.

Expression and Purification of His_6-LptC(24-191). Plasmid pQEsH-LptC expresses a soluble cytoplasmic version of LptC deprived of the transmembrane helix and with an N-terminal His_6 affinity tag (sH-LptC) (Table 1) (Sperandeo *et al*., 2011). Plasmid pQEsH-LptCG153R expressing sH-LptCG153R was constructed by using a QuikChange site-directed mutagenesis kit (Agilent). Codon 153 was changed from GGA to AGA by using the primer pair AP168-AP169 (Table 2). M15/pREP4 carrying the plasmid pQEsH-LptCG153R was grown at 30°C in LD containing kanamycin (25 μg/ml) and ampicillin (100 μg/ml) for 18 h. This culture was diluted 1:100 in fresh medium and grown until mid-logarithmic phase (OD_{600}, 0.6). The expression of sH-LptCG153R was induced overnight at 20°C by adding IPTG to a final concentration of 0.5 mM. Cells were then harvested by centrifugation (5,000 x g, 10 min). The cell pellet was resuspended in buffer A (50 mM NaH2PO4 [pH 8.0] containing 300 mM NaCl, 10 mM imidazole, and 10% glycerol), followed by incubation for 30 min at 4°C with shaking in the presence of lysozyme (0.2 mg/ml), DNase (100 μg/ml), 10 mM $MgCl_2$, and 1 mM PMSF. After 10 cycles of sonication (10-s pulses), the unbroken cells were removed by centrifugation (39,000 x g, 30 min). The soluble sH-LptCG153R protein was purified from the supernatant by using Ni-NTA agarose (Qiagen). The column was washed with 10 column volumes of 4% buffer B (50 mM

NaH2PO4 [pH 8.0] containing 300 mM NaCl, 500 mM imidazole, and 10% glycerol) in buffer A. The protein was eluted by using a stepwise gradient obtained by mixing buffer B with buffer A in 5 steps (10, 20, 50, 70, and 100% buffer B). At each step, 1 column volume was flowed through the column. Elution fractions were monitored by 12.5% polyacrylamide SDS-PAGE. The pooled fractions containing purified protein were dialyzed against 10 mM HEPES [pH 7.0], 50 mM NaCl for crystallization trials. Protein concentrations were determined by using a Coomassie (Bradford) assay kit (Pierce) with bovine serum albumin as the standard.

Crystallization Conditions. Crystallization trials of LptCG153R were set up in 96-well sitting drop plates (Greiner) using the Oryx 8.0 crystallization robot (Douglas Instruments), at a protein concentration of 22.3 mg/ml. Small (approx. 50 μm) crystals, grew after one week at 20°C in a 300 nl crystallization drop containing 50 % protein and 50 % reservoir solution (Stura Footprint Screen #3.1, condition 18.2 (18% PEG 5K MME, 0.1M sodium acetate pH 5.5), Molecular Dimensions). Crystals were flash frozen in liquid nitrogen in the crystallization solution supplemented with 30% glycerol as the cryoprotectant.

Data Collection and Processing. Diffraction data were collected at a resolution of 2.8 Å at the European Synchrotron Radiation Facility (Grenoble, France; beam line ID29) and processed and scaled using XDS and SCALA (Evans, 2006; Evans, 1993; Kabsch, 2010). The orthorhombic $P2_12_12_1$ space group was assigned by POINTLESS and two LptCG153R chains were present per asymmetric unit with a solvent content estimated to be 52.5% (Table 3) (Evans, 1993).

Molecular Replacement, Model Building and Refinement. The three-dimensional structure of $LptC^{G153R}$ was solved by molecular replacement using the structure of the wildtype protein (PDB code 3MY2) as a search model (Tran et al., 2010). The structure was refined using REFMAC 5.4 and fitted to the generated electron density maps using Coot (Emsley and Cowtan, 2004; Murshudov et al., 1997). All data were refined to satisfactory final R_{factor}, R_{free} factors and geometric parameters (Table 3)

(Davis, 2007; Lovell et al., 2003). The atomic coordinates and structure factors for LptCG153R have been deposited in the Protein Data Bank, Research Collaboratory for Structural Bioinformatics, Rutgers University, New Brunswick, NJ (http://www.rcsb.org) under PDB code XXX (Berman et al.,2000).

Protein separation and visualization. Protein samples from immunoprecipitation and localization experiments were separated on 12.5 % SDS-PAGE. 10% SDS-PAGE was also employed after affinity purification experiments to better visualize LptD bands.

Fixed protein bands after immunoprecipitation were stained with Krypton IR protein stain procedure (Thermo Scientific), and visualized by the Odyssey Infrared Imaging System (LI-COR).

Affinity purification and localization samples loaded onto gels were then transferred and decorated as described below. Proteins bands were visualized by chemiluminescence using Odyssey Imaging System (LI-COR) or GE Healthcare films and Kodak reagents.

Antibodies. 5µl of a 1µg/µl working solution of Mouse Monoclonal Penta-His antibody (Quiagen) was used for immunoprecipitation. Western-blot analysis with polyclonal antibody raised in mouse or rabbit against peptides (LptA) or whole proteins (LptE, LptC, LptD, BamA and AcrB) (Sperandeo *et al*., 2010, Chng *et al*., 2010) was performed in the experiments of localizations and affinity purifications. Wild-type and mutant LptC-H were visualized in localization experiments by using HisProbe-HRP (Pierce) according to manufacturer's instructions.

DISCUSSION

The N-terminal region of LptC interacts with IM Lpt components. The Lpt machinery for LPS export to the cell surface consists of seven proteins (LptABCDEFG) located in each compartment of the cell (IM, periplasm and OM) that can be co-purified suggesting that these proteins form a continuous connection between IM and OM (Chng *et al.,* 2010a). Several reports have shown specific interactions among the Lpt proteins. At the OM the LptD β–barrel protein and the LptE lipoprotein

form a two protein pug-and-barrel architecture with LptE residing within the LptD β–barrel (Freinkman et al., 2011). LptBCFG when overexpressed from a plasmid form a stable complex with a subunit ratio $LptB_2CFG$ (Narita and Tokuda 2011). We recently showed that LptA and LptC physically interact and that the C-terminal region of LptC is implicated in LptA binding (Sperandeo et al., 2011). Several line of evidence suggest that LptA also contacts the OM. Sucrose gradient fractionation experiments show that LptA is associated at the OM (Chng *et al.,* 2010a). Moreover, in cells depleted of LptD or LptE, LptA is degraded providing indirect evidence for a functional interaction between LptA and the LptDE complex (Sperandeo et al., 2011).

Available data thus indicate a complex interactome among the Lpt proteins; moreover, the recently proposed transenvelope model for LPS transport (Chng *et al.,* 2010a) may implicate additional protein-protein interactions.

LptC is a bitopic IM protein with a single TM domain and a large periplasmic region whose structure has been recently solved (Fig1) (Tran *et al*, 2010). The role of LptC in LPS transport is unclear and, although LptC is essential for LPS transport, the ATPase activity of the LptBFG ABC transporter is not affected by LptC.

To gain deeper insights into the molecular role of LptC, two previously identified inactive LptC mutant proteins were analyzed in co-purification experiments.

The LptCG56V mutant is unable to co-purify LptBFG suggesting that the N-terminal region of the protein is implicated in interaction with the IM proteins complex. Glycine 56 is located in the linker region that connects the TM segment to the periplasmic domain (Fig 1) and is the first conserved residue in LptC. Interestingly, G56 maps at the end of one of the two disordered regions of the protein (residues 24-58) (Tran *et al*., 2010). The finding that the TM region of LptC is not implicated in LptBFG binding (see below) suggests that only the periplasmic region of LptC is essential for making the contact to the IM ABC transporter. It is not clear whether the G56V point mutation weakens the

unfolded/disordered tract of the protein and/or the C-terminal ordered structure immediately adjacent. LptFG interaction could occurs via the unstructured linker region of LptC as it is well established that unfolded or only partly folded proteins in their native states fold into an ordered structure on binding a partner molecule/protein (Dyson and Wright, 2002). Alternatively G56V mutation could interfere with the function of the C-terminal ordered structure immediately adjacent. In fact LptC might only use the structured region to take contact with LptF and/or LptG, which, according to fold-recognition predictions, possess large periplasmic regions whose structure resemble that of LptC (Sperandeo *et al*., 2011).

The LptC transmembrane region seems dispensable for LptC function. Analysis of LptC chimeras allowed us to clarify the role of the TM region of the protein.

Either a soluble periplasmic version of LptC ($MalE_{SS}$LptC) or a chimera possessing the first TM region of MalF ($MalF_{TM}$LptC) are functional as they complement an *lptC* conditional mutant and do not affect the OM permeability in LptC depleted cells. Moreover both chimeras are able to co-purify the IM proteins complex LptBFG as assessed by affinity purification experiments. Interestingly, the lipoprotein LptE is functional without its N-terminal lipid anchor and is still able to interact with LptD (Chng et al., 2010b).

Based on bioinformatic analysis, the $LptB_2$CFG complex shares several properties with canonical prokaryote ABC import systems which employ a substrate binding protein (SBP) to bind and deliver the substrate to the importer membrane bound complex (Davidson et al., 2008). The uptake system for maltose is a well characterized prokaryotic ABC importer. In this system MalE is the periplasmic maltose binding protein (SBP) interacting to the membrane-bound complex ($MalFGK_2$), that comprises the pore-forming hydrophobic subunits, MalF and MalG, and two copies of the ABC subunit, MalK (Daus *et al*., 2007). LptC represents the equivalent of SBP proteins of prokaryote importers and interestingly it possesses a TM region reminiscent of a non-trimmed periplasmic signal

sequence. Upon MsbA dependent translocation of LPS at the periplasmic face of the IM, the $LptB_2CFG$ ABC transporter undertakes this glycolipid and sorts it to its final destination. LptC could have retained an IM anchor to promptly and efficiently extract LPS, which is then released to the other components of the machinery. By the way, the TM domain is not conserved in all LPS-producing Gram-negative bacteria, as outlined by *in silico* predictions for the α-proteobacterium *Agrobacterium tumefaciens* (Fig.8).

LptC may take contact with the OM protein complex LptDE. Affinity purification experiments using LptCG153R as a bait indicate that the mutant protein is able to co-purify all Lpt components of the transenvelope machine but the assembled Lpt complex is not functional. Glycine 153 is located at the C-terminus of the LptC, within a stretch of conserved residues (Tran *et al*., 2010). The amino acid substitution G153R does not affect the overall architecture of the protein and the x-ray structure shows that the positively charged lateral chain of arginine points in the cavity of the protein. However, the G153R substitution completely abolishes the function of the protein.

We previously showed that LptC-LptA interaction *in vitro* is compromised when this residue is mutated but *in vivo* the level of LptA in cells expressing LptCG153R is comparable to that observed in cells expressing wild type LptC (Sperandeo *et al*., 2011). Indeed, our co-purification experiments demonstrate that LptCG153R is able to pull-down all the other Lpt components, LptA included. This apparent contradiction could be explained assuming that, despite the LptA-LptC interaction is disrupted or weakened other interactions could keep the protein connected to the Lpt machinery. LptC co-localizes with the OM protein complex LptDE as demonstrated by Chng and coworker (Chng *et al*., 2010a). This interaction occurs indirectly via LptA, although a direct interaction of LptC with LptD, which shares with LptA the OstA_N domain (See Pfam repository on line http://pfam.sanger.ac.uk/), cannot be excluded. While LptA-LptCG153R interaction is weakened, LptCG153R could be stacked at the OM protein complex. The perturbed LptA-LptCG153R interaction would not interfere with LptA-

LptDE direct interaction; on the contrary, it could explain the extreme toxicity of LptCG153R when expressed even in presence of a wild-type copy of LptC causing a jamming of the Lpt system (Fig.2). On the other hand, we cannot exclude that LptC153R defects could also interfere with interaction to the LPS ligand.

In the Lpt machinery an intricate network of interactions connects the seven proteins. In this work, we provide a first outline of the interactions in which LptC is involved, and map the functional domains of the protein implicated in these interactions. LptC, LptA and the periplasmic region of LptD are members of the same protein family, which is characterized by the OstA-like domain, as demonstrated for LptA and LptC by their crystal structures (Suits *et al*., 2009; Tran *et al.,* 2010), and for LptD by *in silico* evidence (Pfam, http://pfam.sanger.ac.uk/). A bioinformatic prediction of LptFG periplasmic regions by fold recognition (Sperandeo *et al*., 2011) assigned to these periplasmic loops a tertiary structure that resembles that of LptC. It thus appears that this structural motif, the "Lpt fold", is shared by every component of the Lpt machinery with the exception of LptB and LptE. Similarly, the Lol system, consisting of five proteins, LolA through LolE, catalyzes the transport of lipoproteins to the OM. LolCDE form an ABC complex at the IM, LolB is an OM protein, and LolA is a periplasmic protein which shuttles the lipoproteins from the IM to the OM. LolA and LolB, which provide consecutive lipoprotein binding steps in the pathway, also share a very similar fold despite limited similarity in their primary sequences. Lipoproteins transfer from LolA to LolB occurs in a mouth-to-mouth fashion and it has been suggested that all the components of the system could share the same structural LolA/LolB fold, envisioning that the ligand might be transferred from/to each pathway component in the same modality (Okuda and Tokuda, 2009).

Overall the data presented in this work suggest that the assembly of proteins within the Lpt transenvelope complex may occur via a common scaffold, the "Lpt fold". LptA and LptC bind LPS *in vitro* (Tran et al., 2008; Tran et al., 2010) suggesting that the "Lpt fold" in addition of providing the

structural element for protein-protein interaction may also create a continuous groove for LPS transport across the periplasm.

Table 1. Bacterial strains and plasmids

Strains/Plasmids	Characteristics[a]	References
Strains		
AM604	MC4100 ara^+	Wu *et al.,* 2006
DH5α	Δ*(argF-lac169) 80dlacZ58*(M15*) glnV44*(AS)λ^- *rfbD1 gyrA96 recA1 endA1 spoT1 thi-1 hsdR17*	Hanahan, 1983
FL905	AM604 φ (*kan araC araBp-lptC*)1	Sperandeo *et al.,* 2008
M15/pREP4	F^- *lac thi mtl*/pREP4	Qiagen
Plasmids		
pET23/42	pET23a(+) with multiple cloning sites of pET42a(+), PT7- dependent expression vector; Ap^r	Wu *et al.,* 2006
pET23/42-LptC	pET23/42 PT7-*lptC*	This study
pET23/42-LptCG56V	pET23/42 PT7-*lptC(G56V)-H*	This study
pET23/42-LptCG153R	pET23/42 PT7-*lptC(G153R)-H*	This study
pET23/42-MalEssLptCsol	pET23/42 PT7-$malE_{ss}$*lptC-H*	This study
pET23/42-MalFTMLptCsol	pET23/42 PT7-$malF_{TM}$*lptC-H*	This study
pGS100	pGZ119EH derivative, contains TIR sequence downstream of Ptac; Cm^r	Sperandeo *et al.,* 2006
pGS108	pGS100 *Ptac-lptC-H*	Sperandeo *et al.,* 2006
pGS108G56V	pGS100 *Ptac-lptC(G56V)-H*	Sperandeo *et al.,* 2011
pGS108G153R	pGS100 *Ptac-lptC(G153R)-H*	Sperandeo *et al.,* 2011
pGS100-$MalE_{ss}LptC_{sol}$	pGS100 *Ptac-*$malE_{ss}$*lptC-H*	This study
pGS100-$MalF_{TM}LptC_{sol}$	pGS100 *Ptac-*$malF_{TM}$*lptC-H*	This study
pQE30	T5 promoter; Ap^r	Qiagen
pQEsH-LptC	pQE30 derivative, expresses His_6-$LptC_{24\text{-}191}$	Sperandeo *et al.,* 2011
pQEsH-LptCG153R	pQE30 derivative, expresses His_6-$LptC_{24\text{-}191}$(G153R)	This study

a. Antibiotic resistance to ampicillin and chloramphenicol is indicated by Ap^r and Cm^r respectively.

Table 2. Oligonucleotides

Name	Sequence (5'-3') [a]	Use and/or description
AP063	gtgatcacatctagatcagtggtggtggtggtggtgAGGCTGAGTTTGTTTGTTTTG	LptC-H construction for pGS112 and pGS114; XbaI
AP204	cgagaggaattcATGGATGTCATTAAAAAGAAAC	pGS112 construction with AP063; MalFTMLptC construction by three-step PCR with 205; EcoRI
AP205	GTATCGTCTTTTTCGGCCATTGCGTACATTAAAACAAC	MalF-LptC hybrid primer for $MalF_{TM}LptC$ construction by three-step PCR, with AP204
AP206	GTTGTTTTAATGTACGCAATGGCCGAAAAAGACGATAC	MalF-LptC hybrid primer for pGS114 construction by three-step PCR, with AP063
AP210	cgagaggaattcATGAAAATAAAAACAGGTGC	pGS114 construction with AP063; $MalE_{ss}LptC$ construction by three-step PCR with 211; EcoRI
AP211	GTATCGTCTTTTTCGGCCATGGCGAGAGCCGAGGCGGAAAAC	MalE-LptC hybrid primer for pGS114 construction by three-step PCR, with AP210
AP212	GTTTTCCGCCTCGGCTCTCGCCATGGCCGAAAAAGACGATAC	MalE-LptC hybrid primer for pGS114 construction by three-step PCR, with AP211
AP225	ggaattccatAtgAAAATAAAAACAGGTGCACGC	pET23/42-$MalF_{TM}LptC$ construction with AP226; NdeI
AP226	ccgctcgagAGGCTGAGTTTGTTTGTTTTG	pET23/42-$MalF_{TM}LptC$ and pET23/42-$MalE_{ss}LptC$ constrution with AP225 and AP270; XhoI
AP270	ggaattccatAtgGATGTCATTAAAAAGAAACATTGGTGGC	pET23/42-$MalE_{ss}LptC$ construction with AP226; NdeI
AP164	GTCTATAACCCAGAA**GTG**GCACTAAGCTATCG	pET23/42-LptCG56V with AP165
AP165	CGATAGCTTAGTGC**CAC**TTCTGGGTTATAGAC	pET23/42-LptCG56V with AP164
AP168	CTCGTCACGTTATAC**AGA**ACAACATTTAACTC	pET23/42-LptCG153R and pQEsH-LptCG153R with AP168
AP169	GAGTTAAATGTTGT**TCT**GTATAACGTGACGAG	pET23/42-LptCG153R and pQEsH-LptCG153R with AP169

[a] Uppercase letters, *E. coli* genomic sequence; underlined lowercase letters, restriction sites; boldface letters, codons mutated by site-directed mutagenesis.

Table 3. Data Collection and Refinement Parameters for LptCG153R. $R_{merge} = \sum |I-(I)| / \sum I \times 100$, where I is the intensity of a reflection and *(I)* is the average intensity; R_{free} was calculated from 5 % of randomly selected data for cross-validation; R-factor = $\sum |F_o-F_c| / \sum |F_o| \times 100$. [a] The values in parentheses represent the highest resolution shell (2.8 -2.95 Å).

	G153R
Data Collection Statistics	
Space Group	$P2_12_12_1$
Unit Cell Dimensions	
a, b, c (Å)	48.9, 98.28, 123.56
α=β=γ (°)	90
No. unique reflections	12846
[a] Average I/s *(I)*	12.9 (3.2)
[a] Completeness (%)	99.5 (99.4)
[a] Redundancy	5.1 (5.4)
[a] R_{merge} (%)	0.125 (0.722)
Refinement Statistics	
Resolution Range (Å)	2.8 – 40.0
R_{gen} (%)	22.7
R_{free} (%)	28.4
No. molecules/a.u.	2
No. atoms	
Protein	2043
Water	21
Acetate	1
Glycerol	1
B-factors (Å^2)	
Protein	57.1 (A), 68.5 (B)
Water	53.9
Acetate	76.3
Glycerol	62.8
r.m.s.d. deviations	
Bond Lengths (Å)	0.005
Bond Angles (°)	0.904
Ramachandran Plot (%)	
Favoured	95.2
Allowed	100

Fig.1

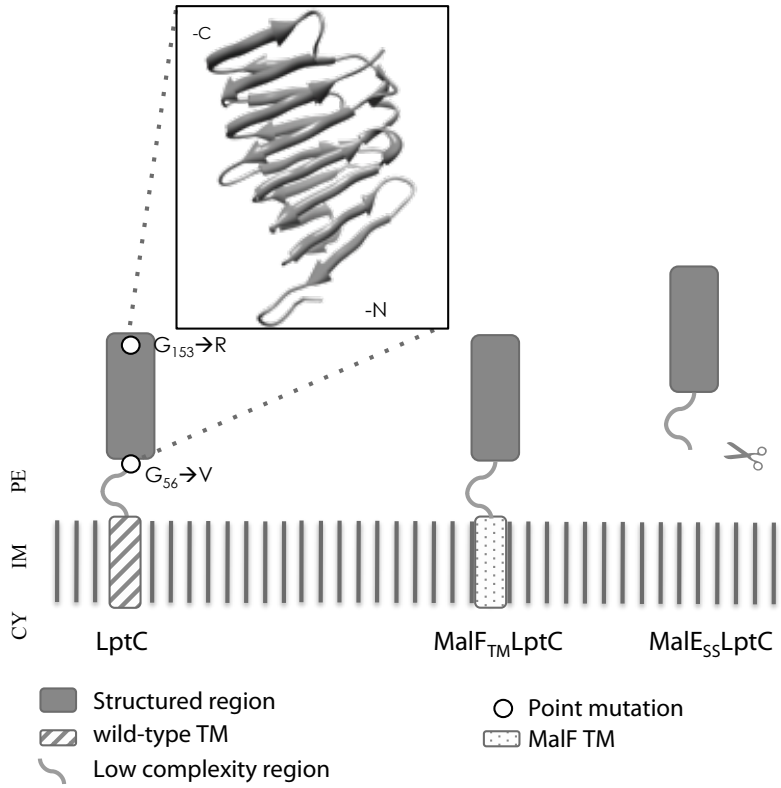

Figure 1. **Structure and topology of wild-type and chimeric LptC.** LptC is a bitopic IM protein. It possesses a large C-terminal periplasmic domain (E26-P191), composed by a conserved region, which was recently crystallized (PDB 3MY2, S59-P191, in the inset) (Tran *et al*., 2010), and a disordered portion linked to a transmembrane (wild-type TM) anchor. G56V and G153R point mutations are indicated. The $MalF_{TM}$LptC chimera is composed of the periplasmic region of LptC, fused to a MalF TM sequence (MalF TM).The $MalE_{SS}$LptC chimera (168 amino acids long) is correctly localized in the periplasm by the signal sequence of MalE, which is trimmed (as suggested by scissors icon) after translocation across IM (see also Fig 3B). CY, IM and PE: Cytoplasm, Inner Membrane and Periplasm space respectively.

Fig.2

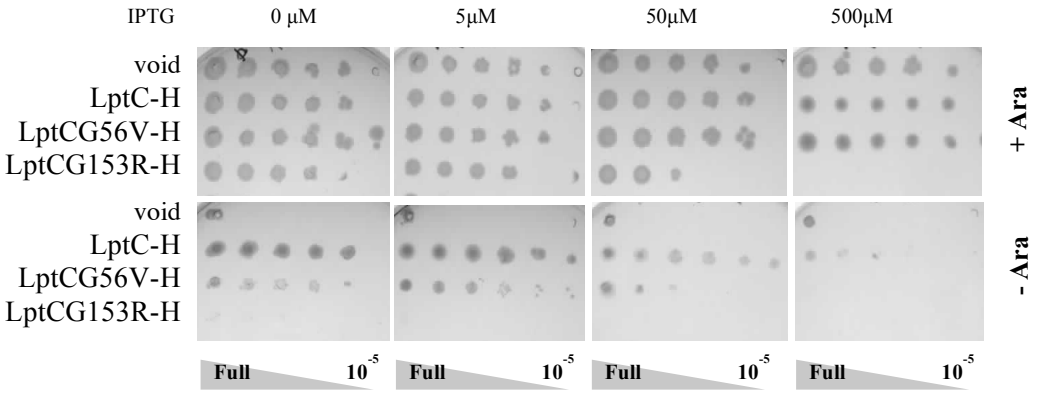

Figure 2. **Overexpression of LptCG56V and LptCG153R mutants in the *araBp-lptC* conditional strain FL905**. Tenfold serial dilutions of FL905 (*araB-plptC*) cells transformed with void plasmid (void), pGS108 (LptC-H), pGS108G56V (LptCG56V-H), or pGS108tC153R (LptCG153R-H), are replicated on agar plates supplemented with/without arabinose (+Ara/-Ara). The concentrations of IPTG used are indicated. Approximate dilutions are given below.

Fig. 3

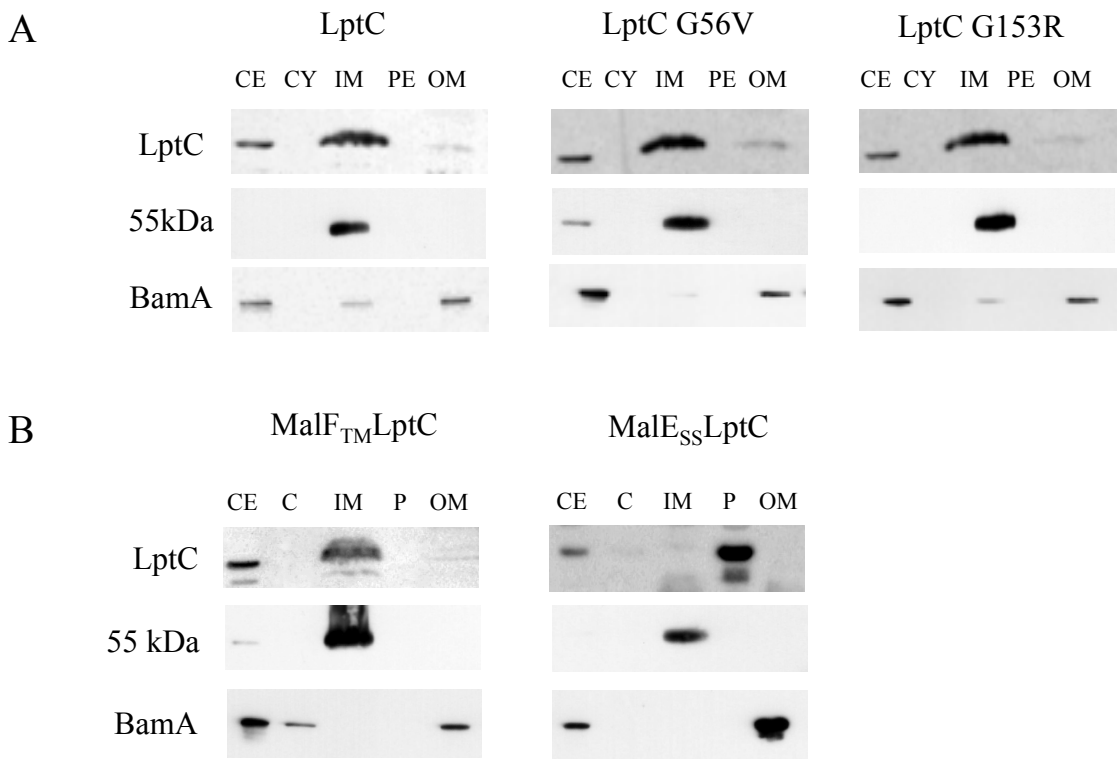

Figure 3. Subcellular localization of LptCG56V, LptCG153R, MalF$_{TM}$LptC and MalE$_{SS}$LptC mutant proteins. Crude extracts (CE), Periplasmic (PE), cytoplasmic (CY), inner (IM), and outer (OM) membrane fractions from AM604 wild-type strain expressing pET23/42LptC-H, pET23/42LptCG56V-H, pET23/42LptCG153R-H (A), pET23/42MalF$_{TM}$LptC-H and pET23/42MalE$_{SS}$LptC-H (B) were prepared and analyzed by Western blotting using monoclonal anti-his antibody. The IM 55kDa protein, which is detected by anti-LptD antibodies, and the OM BamA detected by anti-BamA antibodies are used as fractionation controls.

Fig.4

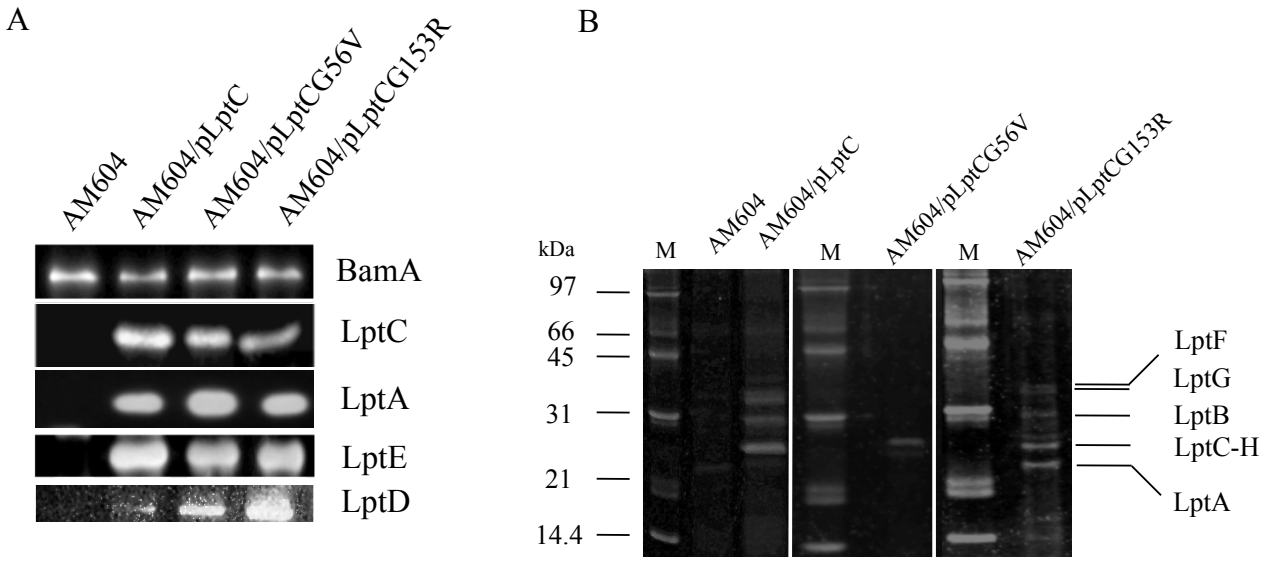

Figure 4. **Tandem affinity purification immunoprecipitation of LptCG56V and LptCG153R mutants.** Total membranes from wild type AM604 strain expressing his-tagged pET23/42LptC-H, pET23/42LptCG56V-H, and pET23/42LptCG153R-H were affinity purified. Samples were then either subjected to immunoblotting with LptD, LptE, LptA and LptC anti-sera (A), or incubated with anti-his tag antibodies and immunoprecipitated (B). As LptB, LptF and LptG anti-sera are not available, proteins were fixed and stained on PAA gels (B) and the identity of the corresponding bands was assessed by mass spectrometry analysis.

Fig.5

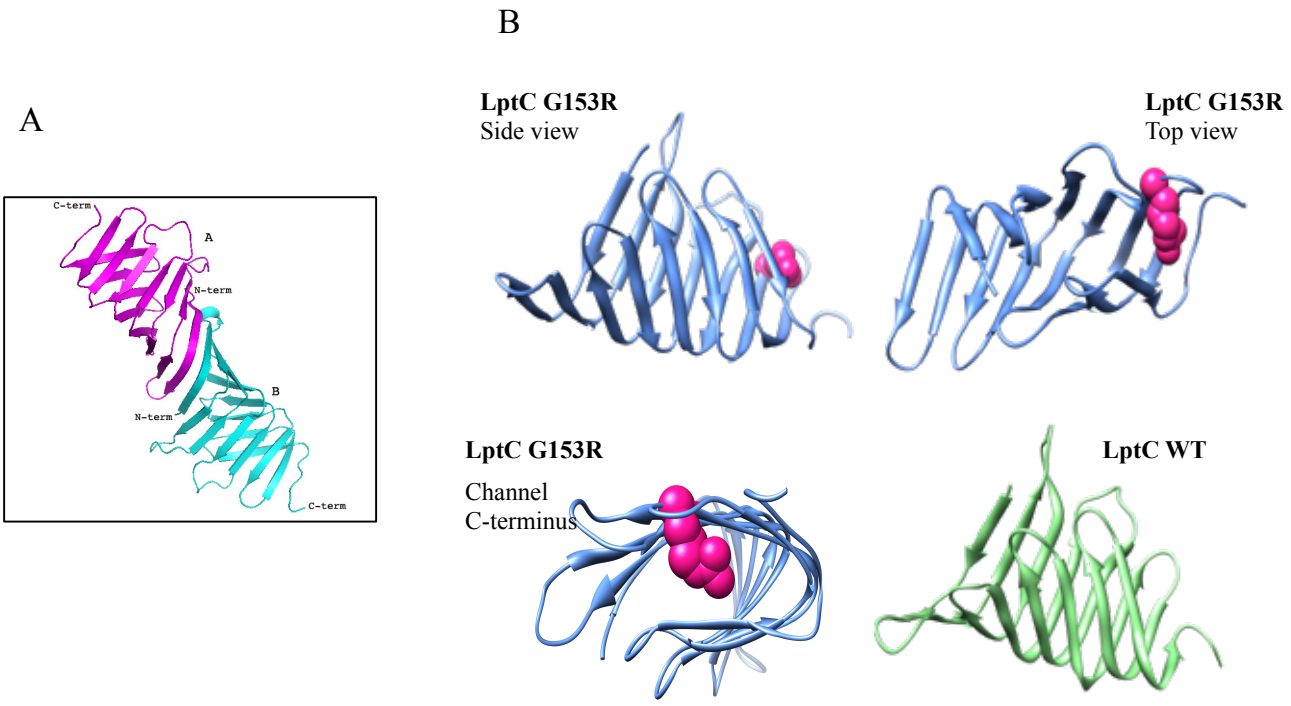

Figure 5. **Crystal structure of LptCG153R mutant protein.** (A) Ribbon representation of the 3D crystal structure of the G153R dimer present in the asymmetric unit illustrating the N- and C-termini of each monomer. (B) LptCG153R crystal structure was solved (blue) and compared to wild-type protein (green). Arginine residue is depicted in pink, considering its steric hindrance. These figures were generated using Pymol (A) and Chimera softwares (B), respectively.

Fig.6

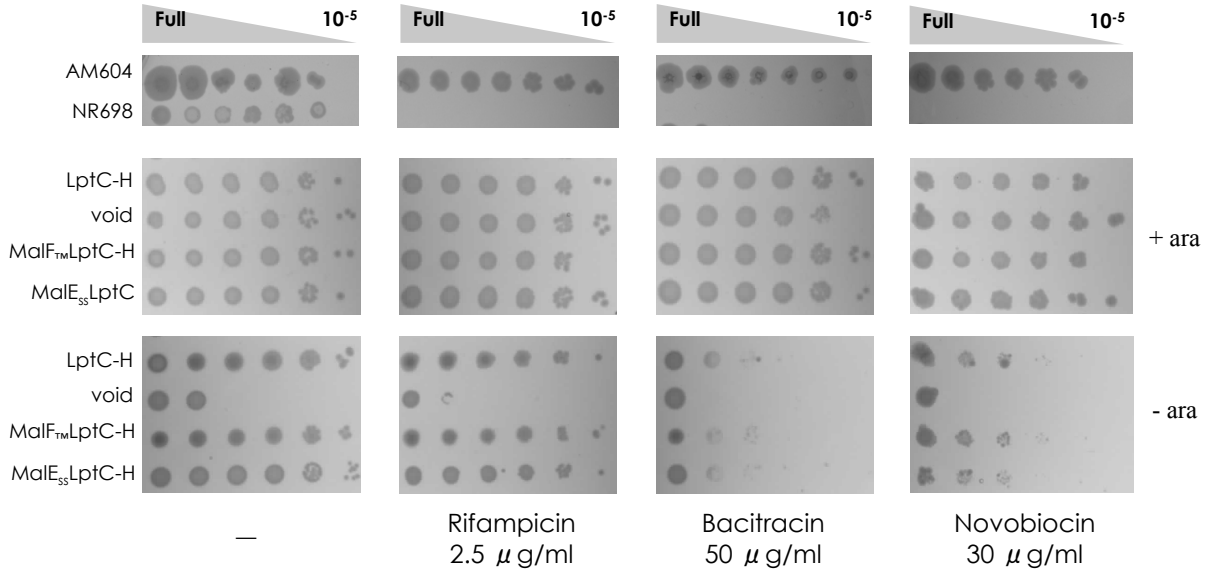

Figure 6. **Sensitivity of $MalF_{tm}LptC$ and $MalE_{ss}LptC$ to hydrophobic toxic compounds.** Serial dilutions of FL905 (*araBp-lptC*) cells were transformed with ptac plasmid pGS100 (void), pGS108 (LptC-H), pGS100-$MalF_{TM}LptC$-H ($MalF_{TM}LptC$-H) or pGS100-$MalE_{SS}LptC$-H ($MalE_{SS}LptC$-H), and replicated in presence (+ara = LD, 0,2% ara, 25μg/ml cam) or absence (-ara = LD, 25μg/ml cam) of arabinose. Plates were supplemented with rifampicin, bacitracin and novobiocin as indicated. The *lptD* gene in NR698 has a small in frame deletion (*imp4213*) which confers OM permeability defects to hydrophobic toxic compounds (Ruiz *et al*., 2005) and is used as positive control.

Fig.7

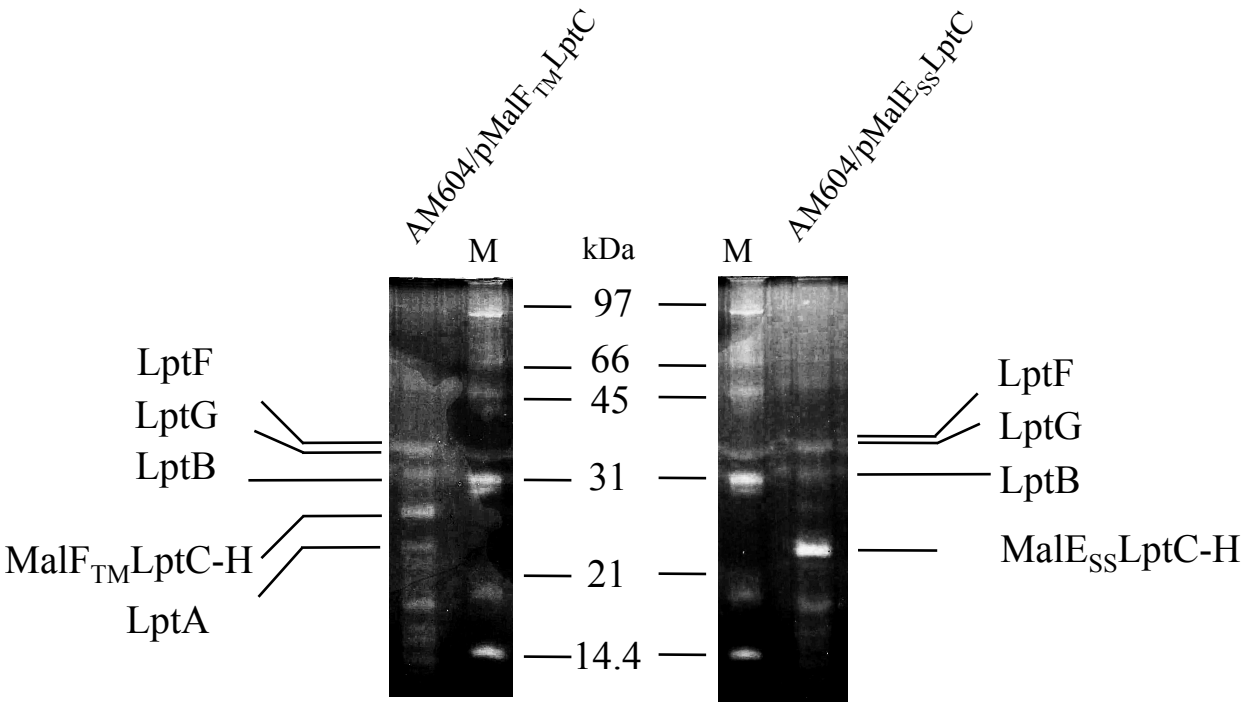

Figure 7. **Tandem affinity purification immunoprecipitation of MalF$_{tm}$LptC and MalE$_{ss}$LptC protein.** Total membranes purified from wild-type AM604 strain expressing his-tagged pET23/42MalF$_{TM}$LptC-H, and pET23/42MalE$_{SS}$LptC-H were affinity purified. Eluates were incubated with anti-his antibodies and immunoprecipitated. Samples were fixed and stained on PAA gels and the corresponding bands confirmed by mass spectrometry analysis. M= Marker. LptA was detectable as an additional band when MalF$_{TM}$LptC-H was used as bait (left part of the figure).

Fig.8

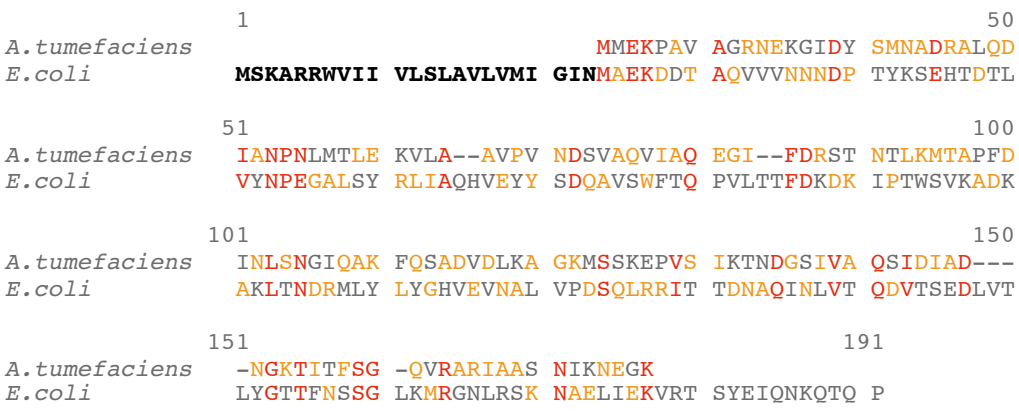

Figure 8: **alignment of *E. coli* LptC and *Agrobacterium tumefaciens* C58 orthologous protein ATU0335**. ATU0335 lacks of the first 23 residues, which constitute the IM anchor in *E. coli* LptC, as demonstrated by Tran and coworkers (Tran *et al*., 2010). A Hidden Marcov Model for prediction of TM fragments (TMHMM) was also applied (software available on line: www.cbs.dtu.dk/services/TMHMM/): LptC orthologous in *A. tumefaciens* seems to be anchor free.

REFERENCES

- Bedouelle,H., Bassford,PJ.Jr, Fowler,A.V., Zabin,I., Beckwith,J. and Hofnung,M. (1980). Mutations which alter the function of the signal sequence of the maltose binding protein of Escherichia coli. Nature. 285,78-81.
- Berman,H.M., Westbrook,J., Feng,Z., Gilliland,G., Bhat,T.N., Weissig,H., Shindyalov,I.N. and Bourne,P.E. (2000). The Protein Data Bank. Nuc. Ac. Res., 28, 235– 242.
- Braun, M. and Silhavy,T.J. (2002). Imp/OstA is required for cell envelope biogenesis in *Escherichia coli*. Mol. Microbiol. *45*, 1289-1302.
- Chimalakonda,G., Ruiz,N., Chng,S.S., Garner,R.A., Kahne,D., and Silhavy,T.J. (2011). Lipoprotein LptE is required for the assembly of LptD by the beta-barrel assembly machine in the outer membrane of *Escherichia coli*. Proc. Natl. Acad. Sci. U. S. A *108*, 2492-2497.
- Chng,S.S., Gronenberg,L.S., and Kahne,D. (2010a). Proteins required for lipopolysaccharide assembly in *Escherichia coli* form a transenvelope complex. Biochemistry *49*, 4565-4567.
- Chng,S.S., Ruiz,N., Chimalakonda,G., Silhavy,T.J., and Kahne,D. (2010b). Characterization of the two-protein complex in *Escherichia coli* responsible for lipopolysaccharide assembly at the outer membrane. Proc. Natl. Acad. Sci. U. S. A *107*, 5363-5368.
- Daus,M.L., Berendt,S., Wuttge,S., and Schneider,E. (2007). Maltose binding protein (MalE) interacts with periplasmic loops P2 and P1 respectively of the MalFG subunits of the maltose ATP binding cassette transporter (MalFGK(2)) from *Escherichia coli*/*Salmonella* during the transport cycle. Mol. Mic. 66, 1107–1122.
- Davidson,A.L., Dassa,E., Orelle,C., and Chen,J. (2008). Structure, function, and evolution of bacterial ATP-binding cassette systems. Microbiol. Mol. Biol. Rev. *72*, 317-64, table.
- Doerrler,W.T. (2006). Lipid trafficking to the outer membrane of Gram-negative bacteria. Mol. Microbiol. 60, 542–552.
- Dyson,H.J., and Wright,P.E. (2002). Coupling of folding and binding for unstructured proteins. Curr. Opin. Struct. Biol. 12, 54–60.

- Emsley,P. and Cowtan.K. (2004). Coot: model-building tools for molecular graphics. Acta Cryst. D60, 2126-2132.
- Evans,P. (2006). Scaling and assessment of data quality. Acta Cryst. D62, 72-82.
- Freinkman,E., Chng,S.S., and Kahne,D. (2011). The complex that inserts lipopolysaccharide into the bacterial outer membrane forms a two-protein plug-and-barrel. Proc. Natl. Acad. Sci. U. S. A *108*, 2486-2491.
- Kabsch,W. (2010). Integration, scaling, space-group assignment and post refinement. Acta Cryst. D66, 133-144.
- Lovell,S.C., Davis,I.W., Arendall,B., de Bakker,P.I.W., Word,J.M., Prisant,M.G., Richardson,J.S. and Richardson,D.C. (2003). Structure validation by Cα geometry: ϕ,ψ and Cβ deviation. Proteins. 50, 437-450.
- Murshudov,G.N., Vagin,A.A., and Dodson,E.J. (1997). Refinement of Macromolecular Structures by the Maximum-Likelihood method. Acta Cryst. D53, 240-255.
- Narita,S. and Tokuda,H. (2009). Biochemical characterization of an ABC transporter LptBFGC complex required for the outer membrane sorting of lipopolysaccharides. FEBS Lett. *583*, 2160-2164.
- Nikaido,H. (2003). Molecular basis of bacterial outer membrane permeability revisited. Microbiol. Mol. Biol. Rev. *67*, 593-656.
- Oldham,M.L., Khare,D., Quiocho,F.A., Davidson,A.L. and Chen,J. (2007). Crystal structure of a catalytic intermediate of the maltose transporter. Nature. 450, 515-21.
- Oliver,D.B., and Beckwith,J. (1982). Regulation of a membrane component required for protein secretion in *Escherichia coli*. Cell 30, 311–319.
- Polissi,A. and Georgopoulos,C. (1996). Mutational analysis and properties of the *msbA* gene of *Escherichia coli*, coding for an essential ABC family transporter. Mol. Microbiol. *20*, 1221-1233.
- Raetz,C.R. and Whitfield,C. (2002). Lipopolysaccharide endotoxins. Annu. Rev. Biochem. *71*, 635-700.
- Raetz,C.R., Guan,Z., Ingram,B.O., Six,D.A., Song,F., Wang,X., and Zhao,J. (2009). Discovery of new biosynthetic pathways: the lipid A story. J. Lipid Res. *50 Suppl*, S103-S108.

- Ruiz, N., & Silhavy, T. J. (2005). Sensing external stress: watchdogs of the *Escherichia coli* cell envelope. Curr. Opin. Microbiol. 8, 122–126.
- Ruiz,N., Gronenberg,L.S., Kahne,D., and Silhavy,T.J. (2008). Identification of two inner-membrane proteins required for the transport of lipopolysaccharide to the outer membrane of *Escherichia coli*. Proc. Natl. Acad. Sci. U. S. A *105*, 5537-5542.
- Sabbattini,P., Forti,F., Ghisotti,D., and G. Deho`. (1995). Control of transcription termination by an RNA factor in bacteriophage P4 immunity: identification of the target sites. J. Bacteriol. 177,1425–1434.
- Sperandeo,P., Lau,F.K., Carpentieri,A., De Castro,C., Molinaro,A., Dehò,G., Silhavy,T.J., and Polissi,A. (2008). Functional analysis of the protein machinery required for transport of lipopolysaccharide to the outer membrane of *Escherichia coli*. J. Bacteriol. *190*, 4460-4469.
- Sperandeo,P., Villa,R., Martorana,A.M., Samalikova,M., Grandori,R., Deho,G., and Polissi,A. (2011). New Insights into the Lpt Machinery for Lipopolysaccharide Transport to the Cell Surface: LptA-LptC Interaction and LptA Stability as Sensors of a Properly Assembled Transenvelope Complex. J. bacteriol. 193, 1042–1053.
- Suits,M.D., Sperandeo,P., Dehò,G., Polissi,A., and Jia,Z. (2008). Novel structure of the conserved Gram-negative lipopolysaccharide transport protein A and mutagenesis analysis. J. Mol. Biol. *380*, 476-488.
- Tran,A.X., Dong,C., and Whitfield,C. (2010). Structure and functional analysis of LptC, a conserved membrane protein involved in the lipopolysaccharide export pathway in *Escherichia coli*. J. Biol. Chem. *285*, 33529-33539.
- Tran,A.X., Trent,M.S., and Whitfield,C. (2008). The LptA protein of *Escherichia coli* is a periplasmic lipid A-binding protein involved in the lipopolysaccharide export pathway. J. Biol. Chem. *283*, 20342-20349.
- Wu,T., McCandlish,A.C., Gronenberg,L.S., Chng,S.S., Silhavy,T.J., and Kahne,D. (2006). Identification of a protein complex that assembles lipopolysaccharide in the outer membrane of *Escherichia coli*. Proc. Natl. Acad. Sci. U. S. A *103*, 11754-11759.

- Zhou,Z., White,K.A., Polissi,A., Georgopoulos,C., and Raetz,C.R. (1998). Function of *Escherichia coli MsbA*, an essential ABC family transporter, in lipid A and phospholipid biosynthesis. J. Biol. Chem. *273*, 12466-12475.